SOME ASPECTS OF ZEOLITE SYNTHESIS

BY

HELEN LAWSON COOK

PRESENTED

FOR THE DEGREE OF DOCTOR OF PHILOSOPHY

UNIVERSITY OF EDINBURGH DECEMBER 1979

DEDICATED TO MUM AND DAD FOR ALL THE HELP AND ENCOURAGEMENT THEY HAVE GIVEN ME THROUGHOUT MY EDUCATION.

ABSTRACT

This thesis describes an investigation into three aspects of zeolite synthesis; the relationships between the silica source and the products and kinetics of zeolite crystallisation, the growth of zeolites from solid/liquid slurries, and the effect of organic dyes on crystal growth.

The way in which the growth of zeolites X and P1 is related to the nature of the silica source has been investigated for a wide range of silica sources (soluble silicates and amorphous silicas covering a range of surface areas) in the presence and absence of 'active' silicates. The results which have been discussed in terms of the structure of the reactive gels provide the basis for a new interpretation of the crystallisation mechanism.

The growth of zeolites X, A, HS and P1 in solid/liquid slurries prepared from various silicates and aluminates has been investigated by x-ray diffraction and the silicate species present in the solution phase have been detected and partially identified by Si^{29} F.T. n.m.r. The latter technique has not previously been applied to this problem and its use provides new information about the relationships between the zeolites formed and the structures of the silicate species present in the solution phase.

An extensive study of the effect of organic dyes on the growth of zeolites X and P1 has been carried out. Despite previous reports that these can act as crystal growth inhibitors, positive evidence for this was not obtained. In addition to these studies the adsorption of cationic dyes on zeolites A, X, P1 and HS was studied both by the spectrophotometric determination of adsorption isotherms and by a novel method based on thin layer chromatography. The results show conclusively that dye adsorption on zeolite occurs predominantly by an ion exchange mechanism.

Declaration

I declare that this thesis, which is of my own composition is an accurate record of work which I carried out in the Department of Chemistry, University of Edinburgh and at I.C.I. Ltd., Agricultural Division, Billingham between October 1975 and July 1978. During this period I was supervised and guided by Drs. R.O. Gould, B.M. Lowe and T.V. Whittam.

In addition I attended the following lectures/courses:-

Introductory Fortran (2 weeks) - E.R.C.C. staff

Chemistry of the Atmosphere - Drs. M. Golde and R. Donovan

Nuclear Magnetic Resonance Spectroscopy - Dr. R.K. Harris

Research and Development in Industry - B.P. Research Ltd.

History of the Edinburgh University Chemistry Department - Dr. W.P. Doyle

Electrode Reactions - Drs. W.D. Cooper and A. Bellamy

Organic Chemistry of Dyes - I.C.I. Organics Division

One week CRAC course at Kings College Cambridge

Silicate Chemistry - Dr. B.M. Lowe.

ACKNOWLEDGEMENTS

It is with pleasure that I acknowledge Barrie Lowe who has given me help and encouragement throughout the period of this research. I must also acknowledge Bob Gould and Tom Whittam who have always been ready to extend words of encouragement whenever they were needed. My sincere thanks goes to all three.

I should also like to thank Professors Charles Kemball and Evelyn Ebsworth for provision of laboratory facilities and other services. The n.m.r. work described in this thesis would not have been possible without the skilled assistance of Alan Boyd whom I thank sincerely.

I should also like to thank the Science Research Council for provision of a C.A.S.E. Studentship and I.C.I. Ltd., Agricultural Division for accommodation and associated expenses during time spent at Billingham.

Last, but by no means least, I wish to thank Mrs. Marie Manson for the excellent job she has done in typing this thesis.

SOME ASPECTS OF ZEOLITE SYNTHESIS

TABLE OF CONTENTS

CHAPTER 1

INTRODUCTION

1.1 DESCRIPTION

The generic name zeolite covers a group of crystalline hydrated aluminosilicates of monovalent or polyvalent bases. Zeolites were first recognised and named as a new group of minerals consisting of hydrated aluminosilicates of the alkali and alkaline earths by Cronstedt[1] after his discovery of stilbite in 1756. As a consequence of their intumescent properties, these minerals were called zeolites (Greek; 'zeein' - to boil, 'lithos' - a stone).

The chemical composition of zeolites can be described by the formula

$$M_{2/n}O \quad Al_2O_3 \quad ySiO_2 \quad zH_2O$$

in which M represents a cation with valence n, y and z integers, and y is generally greater than 2 since AlO_4 tetrahedra are only rarely linked together.

Structurally the zeolites are framework aluminosilicates which are based on a three dimensional network of AlO_4 and SiO_4 tetrahedra linked to each other by sharing all oxygens. This gives rise to the formation of cavities of constant dimensions which are joined together by regularly arranged channels or pore systems. These cavities[2] are occupied by ions and water molecules, both of which have considerable freedom of movement, permitting ion exchange and reversible dehydration.

Ammonium and alkylammonium cations having the general formula,

$$R_n^+NH_{4-n}$$

where n is an integer, may be incorporated in synthetic zeolites. It is also possible to synthesize zeolites which contain gallium substituted for aluminium, and germanium substituted for silicon ions in the framework.

1.2 ZEOLITE MINERALS

A discussion of the zeolite minerals, their occurrence, classification, formation and properties is important to an understanding of the synthesis and properties of zeolites.

Zeolite minerals were first obtained from vesicles and fractures in igneous basaltic rocks, their formation resulting from precipitation from fluids, which permeated the basalts. In some occurrences more than one episode of zeolite crystallisation occurred, as at Sasbach, Kaiserstuhl, Germany, where faujasite lined the cavities, prior to growth of tuffs of phillipsite[3]. Hay[4] has correlated the chemical composition of the host rock, with that of the zeolite. Thus, high silica and alkali rich zeolites such as clinoptilolite and mordenite predominate in high-silica rocks, the lower silica-containing zeolites such as faujasite, phillipsite, and analcime being characteristic of the more basic or low silica rocks.

Zeolite minerals can occur in either igneous or sedimentary environments, however, although all the known natural zeolites have

been found in igneous rocks, only a few types occur in sedimentary deposits. In recent years zeolites have been found in massive amounts in sedimentary deposits. These deposits appear to have been produced by the alteration of volcanic ash, and other pyroclastic material, by the action of alkaline lake waters.

Those zeolite minerals found in igneous rocks are assumed to have crystallised in cavities and along fractures in basalt from the aqueous solutions corresponding to the last stages of magmatic activity. In most cavities successive growth of several different zeolite minerals is observed, and is usually accompanied by other hydrous minerals.

The proposed mechanism for zeolite formation in sedimentary deposits is that initially water extracts sodium and potassium from the glass by hydrolysis making the water alkaline and increasing the dissolution of silica. Comparison of the rate of solution of ordinary commercial glass suggests that glass pieces of the size range encountered in most sediments would dissolve entirely in from 30 to 3000 years. Therefore, it is likely that the zeolites are not formed from an internal devitrification process, but from the solution of the material from the glass surface and recrystallisation into crystalline zeolites. This is similar to mechanisms which have been suggested for the formation of synthetic zeolites from various amorphous substrates.

It is known that zeolites synthesised in the laboratory are formed as metastable materials under mild conditions. Zeolite minerals can also be formed as metastable materials. Most commonly, this occurs at low temperatures and pressures where kinetic factors are important in determining the particular zeolite species.

Pure zeolite minerals are colourless, however, some specimens may be coloured due to the presence of finely divided oxides of iron or similar impurities. The density of the zeolites ranges between 2 and 2.3 g cm^{-3} and depends primarily on the basic framework structure i.e. the openness and void volume. The exchange cation in the zeolite can also affect the density.

For the identification of zeolites which occur as fine grained crystals, x-ray diffraction is the primary tool. It is sometimes difficult to assign a particular x-ray diffraction pattern to a certain species because variations occur in the x-ray pattern as a result of variation in the exchange cation composition. Various other methods[5] have been suggested for identifying zeolites, however, x-ray diffraction has remained the most commonly used, and indeed, the most useful.

The three most important properties of zeolites are 1) their capacity to absorb gases and vapours i.e. molecular sieving, 2) their ability to act as catalysts and 3) their cation exchange properties. It is the industrial potential of these three properties which has led to the synthesis of zeolites on a large scale.

1.3 ZEOLITES AS MOLECULAR SIEVES

The early literature on zeolites has been summarised by McBain[6], who proposed the term molecular sieve. A more recent review on the molecular sieving properties of zeolites has been published in a monograph by Barrer[7].

On dehydration, zeolite crystals act as sieves, selectively absorbing or rejecting molecules depending on their size and other structural factors. Zeolites belong to the class of microporous

absorbents and in contrast to traditional absorbents such as silica gel and activated alumina which have very wide ranges of pore size, they have uniform pores permeating the solid. Depending on the lattice type of the zeolite, the diameters of the pores are in the range from about 300pm to 1000pm. It is the uniformity of the pore size and the resulting highly selective adsorptive characteristics which have helped the zeolites to achieve an incomparable commercial importance as absorbents.

Zeolites select polar sorbates because they are themselves very polar and can be used to remove water, ammonia, sulphur dioxide, carbon dioxide, etc., from gas or liquid streams contaminated with them. If two molecules are equally capable of entering the micropore system, the zeolite retains one preferentially to the other on the basis of polarity or other molecule-zeolite interaction effects.

In the early work by Barrer[8-10], it was established that the molecular sieving properties of a zeolite could be profoundly changed by ion exchange. For example, potassium, sodium and calcium forms of zeolite A can be formed and have been studied by Breck[11] and co-workers. These exchanged zeolites are termed 3A (the K^+ form), 4A (the Na^+ form) and 5A (the Ca^{++} form). The numbers are supposed to indicate the Van der Waals diameter in Å which must not be exceeded by the guest molecule if it is to be imbibed by the crystals. However, these figures are crude indications and should not be taken literally. Although zeolite A provides a very good example of a zeolite for which the effective pore size can be modified by ion exchange, similar behaviour is observed for most other zeolites. Consequently, ion exchange has been established as a standard method of tailoring molecular sieve zeolites to meet

the requirements of a particular separation.

From early investigations by Saha[12] it was concluded that most zeolites interesting as molecular sieve materials belong to the lowest temperature phases of Na_2O-Al_2O_3-SiO_2-H_2O. This conclusion was confirmed by an investigation by Regis[13] and co-workers.

The molecular sieve absorbents in commercial use today are primarily those based on the A,X,Y and mordenite-type structures. Chabazite- and erionite-type zeolites are also utilized to some extent.

1.4 ZEOLITES AS ION EXCHANGE MATERIALS

The cation exchange properties of zeolite minerals were first observed 100 years ago, and the ease with which they effected ion exchange in aqueous solutions led to an early interest in these materials as water-softening agents. The cation exchange behaviour of zeolites depends upon the nature of the cation species, the temperature, the concentration of the cation species in solution, the anion species associated with the cation in solution, the solvent and the structural characteristics of the particular zeolite.

Zeolite structures have unique features which lead to unusual types of cation selectivity and sieving. Recently, structural analysis of zeolites has made it possible to interpret the variable cation exchange behaviour of zeolites. A qualitative description of cation exchange behaviour has been published by Barrer[14].

The cation exchange capacity of a zeolite is dependent on its chemical composition; a higher exchange capacity is observed in zeolites of low Si/Al ratio because of the greater number of exchangeable cations. An alteration in lattice dimensions often accompanies cation exchange in zeolites as a consequence of the

different physical properties of the ions. Studies of ion exchange equilibria have supplied information about zeolites relating both to structure and to the population and distribution of cation sites.

A suspension of zeolite in water is basic[15] due to a limited amount of hydrolysis of the more loosely bound cations. If the pH of the solution is reduced below a value of about 5 (by addition of an aqueous acid), the aluminium ions are removed from the framework and the structure is destroyed. Consequently, in most cases, exchange of zeolite cations for protons cannot be achieved by acid treatment. The silica-rich zeolites, mordenite and clinoptilolite, are exceptions to this, hydrogen forms of these zeolites having been prepared by acid treatment[16,17]. However, a hydrogen form can be prepared by first exchanging the alkali metal cations with ammonium ions. Subsequent thermal treatment of the ammonium-exchanged zeolite at about 400°C liberates ammonia and leaves protons situated on oxygens in the lattice[18]. The extent to which this decationisation can occur is dependent on the Si/Al ratio of the zeolite. With zeolite X, up to 50% exchange can be tolerated, whereas with silica-rich zeolites, a crystalline zeolite completely free of cations can be obtained.

Although the ion exchange properties of zeolites were recognised very early, ion exchange processes have not been developed so extensively, in their own right, as those based on molecular sieving and catalysis. However, there are a few areas in which it has been developed and is used extensively. Clinoptilolite is one of a number of zeolites selective for strontium and caesium[20], two troublesome by-products of nuclear fission, and so this zeolite is used in the treatment of radioactive waste. Another important

environmental use of zeolites is the removal of ammonia, as ammonium ions, from waste water. Excess concentrations of ammonia in water are toxic to aquatic life and cause explosive algae growths, leading to eutrophic conditions in lakes. This process of eutrophication is also caused by phosphate ions, which are used widely in detergents. Zeolites are currently being investigated as possible replacements for these phosphates, utilising the water softening properties of the zeolites.

1.5 ZEOLITES AS CATALYSTS

Although the systematic investigation of zeolite synthesis, selective sorption, and ion exchange developed rapidly in the 1950's and 1960's, it was much later that another area of significance started to attract attention. Zeolite-based catalysis became important when it was discovered that rare earth and hydrogen forms of certain zeolites possessed cracking activity several orders of magnitude greater than that of conventional silica-alumina catalysts. This enhanced activity was explained in terms of a greater active site concentration[21], there being a greater number of highly acidic centres in zeolites, than in silica-alumina catalysts[22]. The number and strength of acid sites in zeolites depends on the extent of cation exchange and the Si/Al ratio[22,23]. The catalytic activity can also be enhanced by exchanging the cations for transition metal cations or rare earth cations.

Catalytic reactions take place within the cavities of crystalline zeolites, hence, the voids must be accessible to the reactants. The zeolites important in catalysis are usually those which have the largest pore sizes and a maximum of available void volume. Sieving effects occur in catalysis as in sorption. Not

only must the reactants be of the correct molecular dimensions to permeate the zeolite structure, but the products, likewise, must be able to exit. The zeolites also exhibit shape selectivity, and so it is not only the dimensions of the molecule which must be considered but also the shape.

Cracking catalysts based on zeolite Y were first introduced commercially in 1962 by the Mobil Company. Their performance won them rapid recognition and they have now displaced alumina-silica catalysts in almost all refineries throughout the world.

In the early 1970's, very siliceous zeolites were prepared using quaternary ammonium ions as the base. Of these siliceous zeolites, ZSM5[24] has proved to be the most important. ZSM5 is a member of a new class of shape selective catalysts with unique channel structures which differ from the large-pore faujasite and small-pore zeolites such as zeolite A and erionite. These materials possess unusual catalytic properties and have a high thermal stability. The selective conversion of methanol to high quality gasoline by ZSM5 is of major importance. Moreover, these types of zeolites have made possible the development of commercially significant petroleum and chemical processes, such as xylene isomerisation and toluene disproportionation[25].

1.6 DEHYDRATION AND STABILITY

The majority of zeolites may be dehydrated to some degree without major alteration of their crystal structure and they can be subsequently rehydrated. However, many zeolites when totally dehydrated undergo irreversible structural changes and suffer total structural collapse.

Early results of dehydration studies on zeolites tend to be inconsistent. This can be attributed to variations in the methods used to determine the dehydration curve as well as variations in mineral samples that were being studied. By using differential thermal analysis (d.t.a.) techniques, the temperature at which dehydration reactions take place, and the energy changes involved at the various stages can be determined. Thermogravimetric analysis (t.g.a.) can be used to determine the loss in weight of a zeolite as it is dehydrated by heating. Detailed discussions of the theory and techniques of thermal analysis have been published[26].

Current interpretations of the nature of water in zeolites are based on x-ray crystal structure analysis, infrared spectra, nuclear magnetic resonance measurements, and dielectric measurements, in addition to thermal analysis.

Zeolites may be classified on the basis of their dehydration behaviour into two groups a) those which show no structural change upon dehydration and which exhibit continuous dehydration curves as a function of temperature and b) those which undergo structural change and show discontinuities in their dehydration curves. The first type is characteristic of zeolites A, X, Y and chabazite, and the second type is characteristic of zeolites natrolite and scolecite. In the latter type of zeolites water molecules are arranged in groups within the structure and have different volatilities.

Differential thermal analysis techniques can be a useful tool in addition to x-ray powder diffraction for characterising zeolites. For example, two zeolites may appear to have closely related structures from their x-ray diffraction patterns, as in the case of heulandite and clinoptilolite; however, their d.t.a./t.g.a. patterns indicate that clinoptilolite is much more stable toward dehydration.

During dehydration exchangeable cations which are located in the channels and co-ordinated with water molecules may migrate to other sites even though no substantial change in the framework structure occurs.

Mikheikin[27] and co-workers have reported the migration of Cu^{2+} and Cr^{3+} ions from the large cavities of zeolite Y to the sodalite cages on the removal of water. On rehydration the cations migrate back to the large cavities. Zeolites with univalent cations normally dehydrate more readily than the multivalent forms, since, bonding in the multivalent complex is stronger. Some dehydrated zeolites exhibit a high degree of thermal stability. A temperature of about 700°C is required to decompose the crystal structure of dehydrated zeolite X, whereas structural collapse in the presence of water occurs at lower temperatures[28].

1.7 CLASSIFICATION AND STRUCTURE OF ZEOLITES

The zeolite structure is based on fundamental units in which a silicon or aluminium atom is tetrahedrally co-ordinated to four oxygen atoms. These tetrahedral units are linked in three-dimensions, via oxygen bridges, to form frameworks. According to Lowenstein[29] the alumina tetrahedra only link to silica tetrahedra so that no Al-O-Al bonding occurs and consequently the Si/Al ratio is never less than unity. Replacement of tetra-valent Si by elements of lower valency, in the case of zeolites normally Al, produces an excess of negative charge usually compensated by a cation (M^+) of low valency placed near the altervalent species. Zeolites have been synthesised in which Ge and Ga have been substituted for Si and Al respectively[30,31].

More recently phosphorus substitution in the framework has been reported, however, the evidence is conflicting[32-36]. There have also been attemp ts to incorporate boron[37] into the framework but this has met with little success.

Although the synthetic and naturally occurring zeolites have characteristic differences, they have topologically similar aluminosilicate frameworks. A structural formula of the type

$$M_{x/n}[AlO_2)x(SiO_2)y]zH_2O$$

may be used to illustrate the relationship between chemical composition and structure. M represents the metal cation and x, y, n and z are integers. For zeolite X the unit cell composition is

$$Na_{86}[(AlO_2)_{86}(SiO_2)_{106}]264\ H_2O$$

Structural classifications of the many zeolite topologies have been proposed by Smith[38], Fischer and Meier[39,40] and Breck[41]. Earlier classifications were based on morphological properties. Barrer has characterised the zeolites into five[42] classes of molecular sieve according to the size of the molecules which are sorbed by activated i.e. dehydrated crystals. In the classification proposed by Breck[41] zeolites have been divided into seven structural groups according to the presence of a common subunit of structure which is a specific array of $(Al,Si)O_4$ tetrahedra. This classification neglects the Si-Al distribution. The two simplest units are the ring of 4 tetrahedra (S_4R) and six

tetrahedra (S6R) as found in many framework aluminosilicates. These subunits have been called secondary building units (SBU) by Meier[40], the primary units being the SiO_4 and AlO_4 tetrahedra. The types of secondary building units found in zeolite frameworks are illustrated in figure 1.1. Assemblages of these secondary building units into chains, layers, and polyhedra results in the characteristic framework structures of different zeolites. The seven groups, with representative zeolite structures are listed in table 1.1.

TABLE 1.1 CLASSIFICATION OF ZEOLITES

Group	Secondary Building Unit	Examples
1	Single 4-ring, S4R	Analcime, Phillipsite, P
2	Single 6-ring, S6R	[illegible] Sodalite
3	Double 4-ring, D4R	A
4	Double 6-ring, D6R	X,Y, Faujasite, Chabazite
5	Complex 4-1, T_5O_{10} unit	Thomsonite
6	Complex 5-1, T_8O_{16} unit	Mordenite
7	Complex 4-4-1, $T_{10}O_{20}$ unit	Clinoptilolite, Stilbite

1.7.1 FAUJASITE TYPE ZEOLITES, X AND Y

The structure of the faujasite type zeolites is based on polyhedral cages of cubic or near cubic symmetry. The framework of zeolite X is a simple arrangement of truncated octahedra or β-cages in which an aluminium or silicon atom lies at each apex. These β cages are also found in sodalite and the term sodalite cage is often used. A representation of a β-cage is shown in figure 1.2..

FIG. 1.1 SECONDARY BUILDING UNITS FOUND IN ZEOLITE FRAMEWORKS

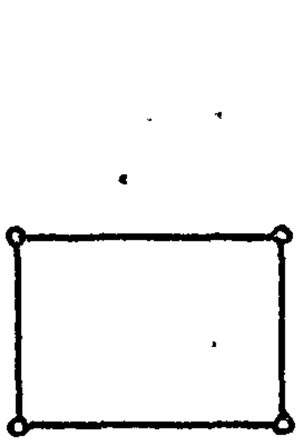

S4R

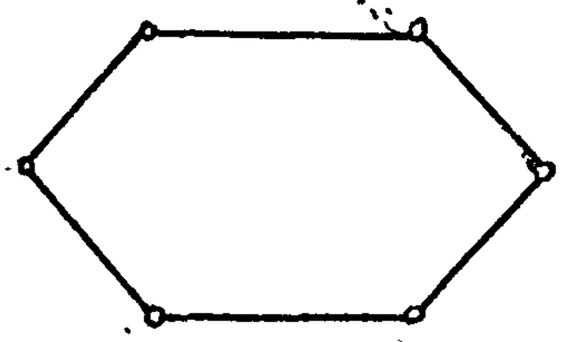

S6R

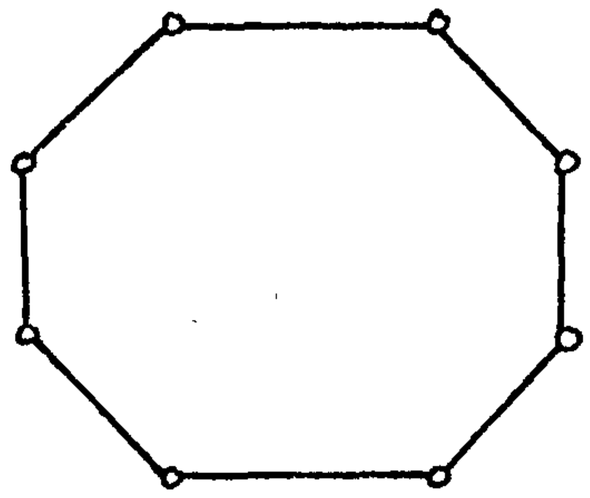

S8R

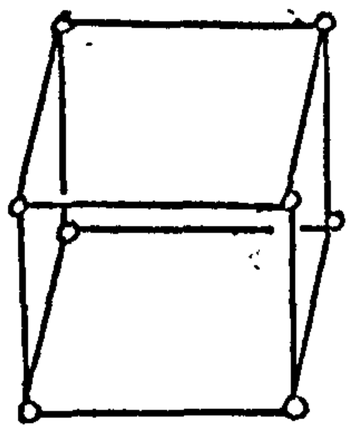

D4R

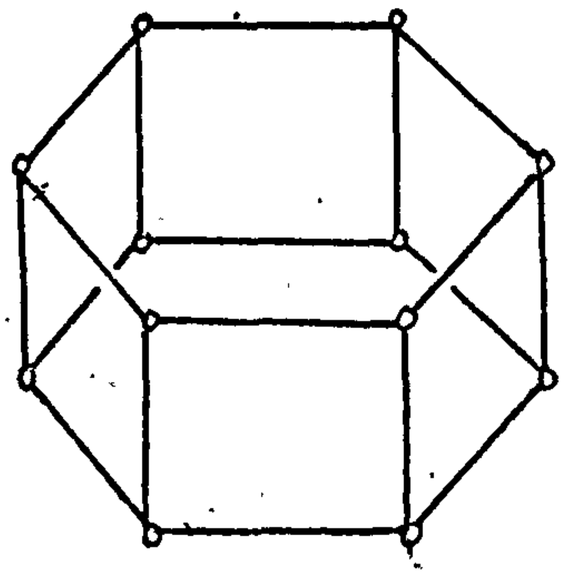

D6R

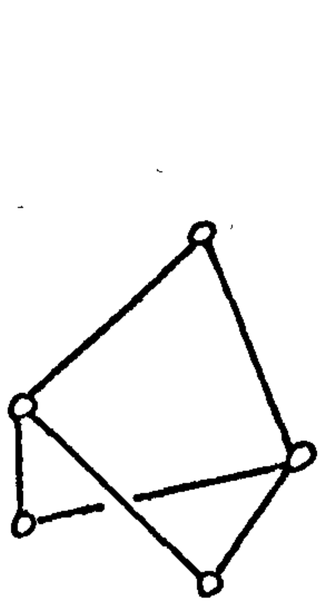

Complex 4-1

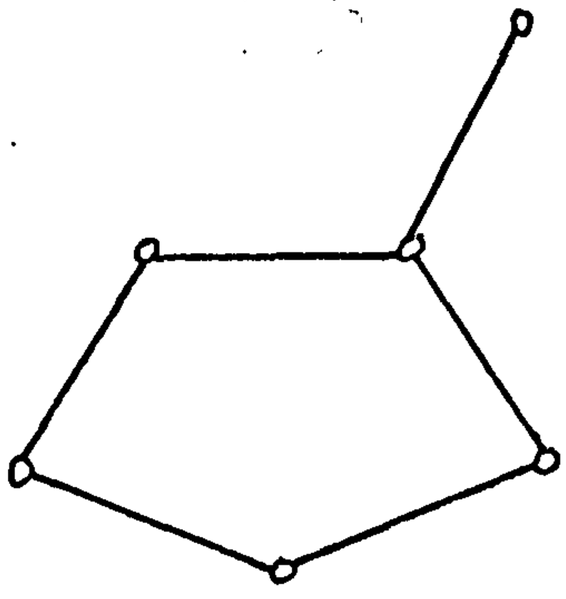

Complex 5-1

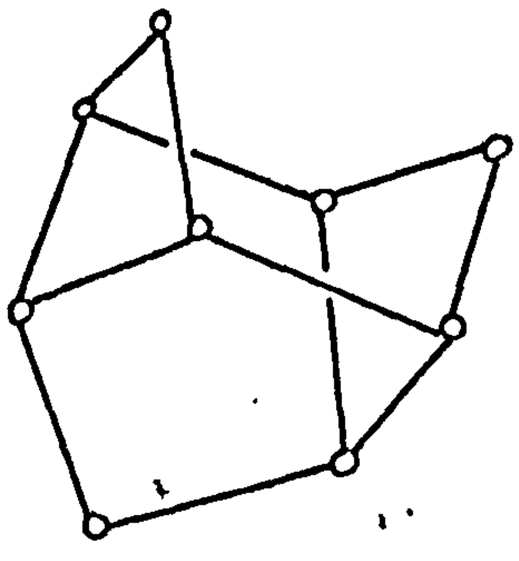

Complex 4-4-1

FIG. 1.2 THE RELATIONSHIPS OF THE SODALITE OR β-CAGE (A) TO THE STRUCTURES OF HYDROXYSODALITE (B), ZEOLITE A (C) AND FAUJASITE (D).

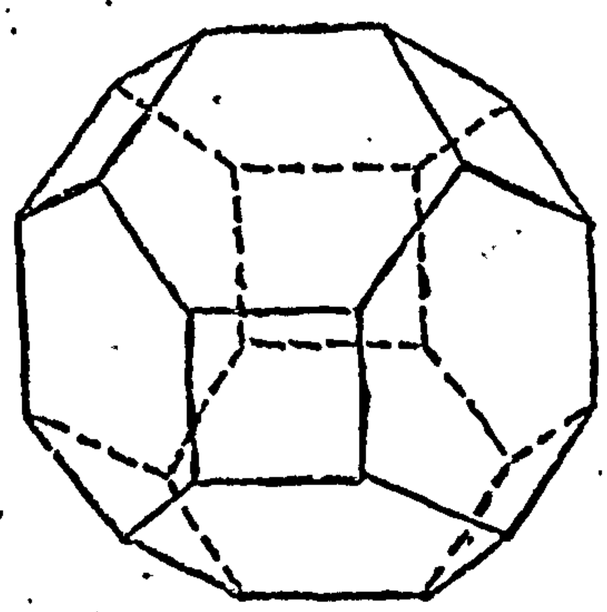

(A)

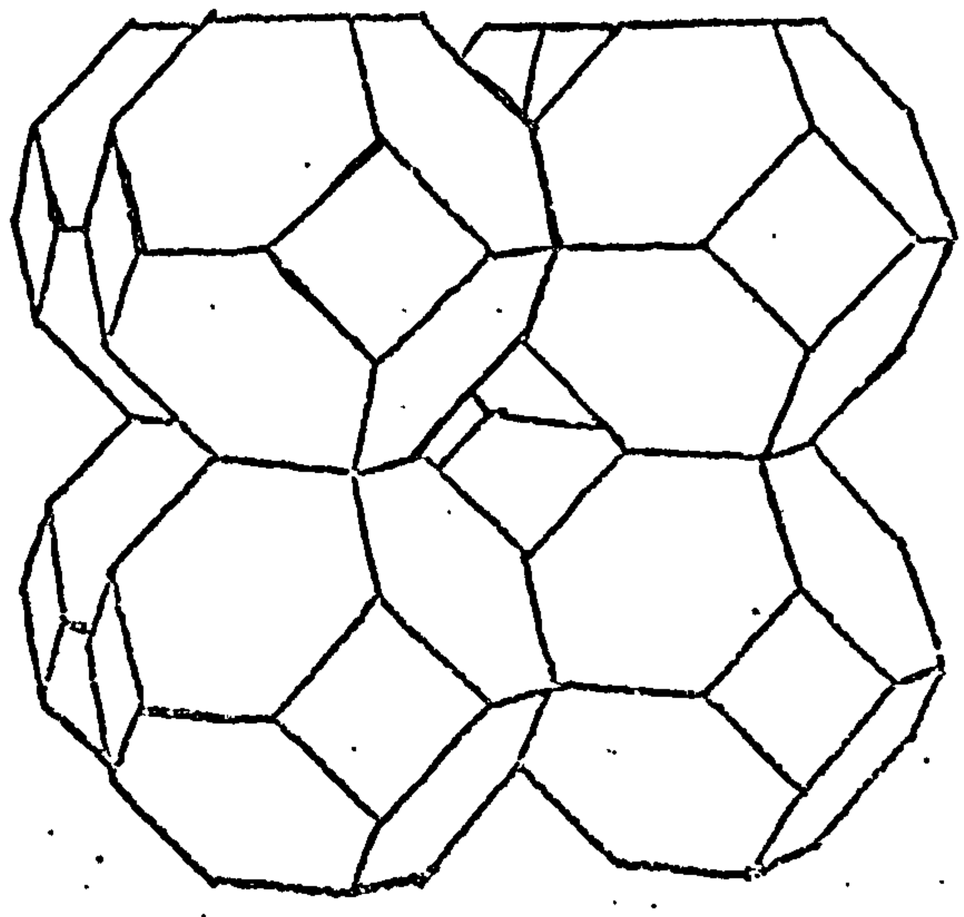

(B)

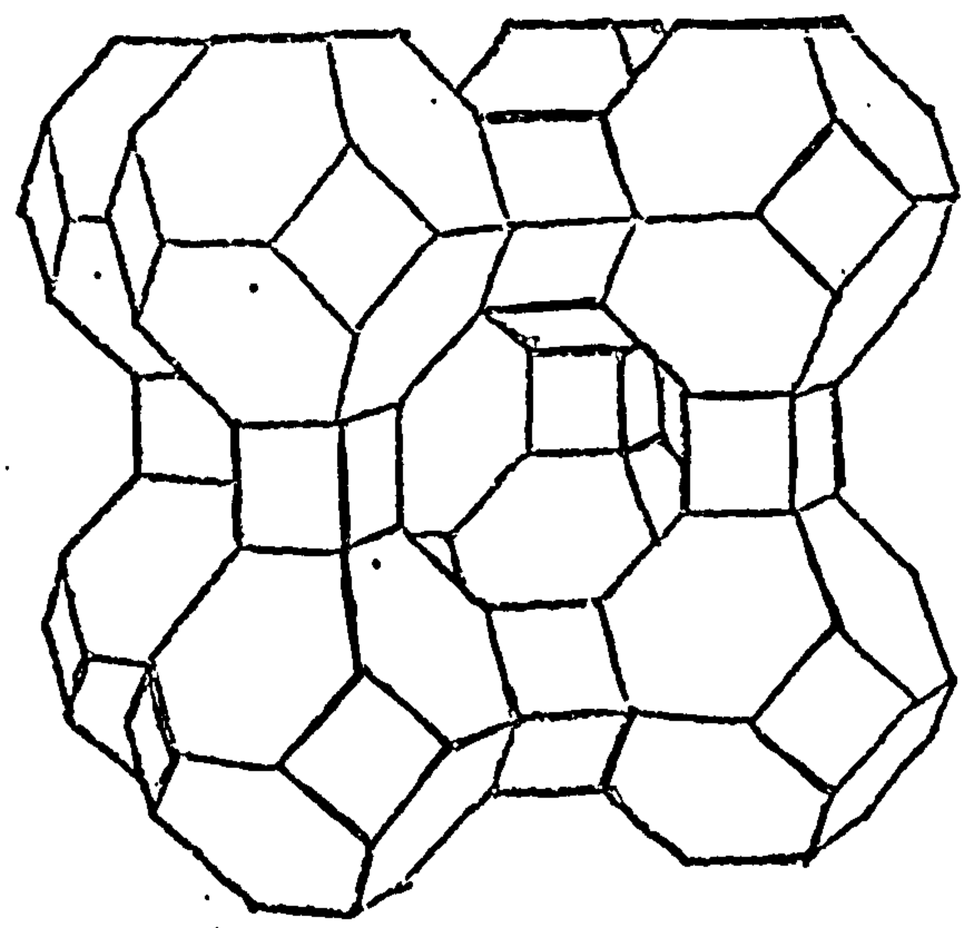

(C)

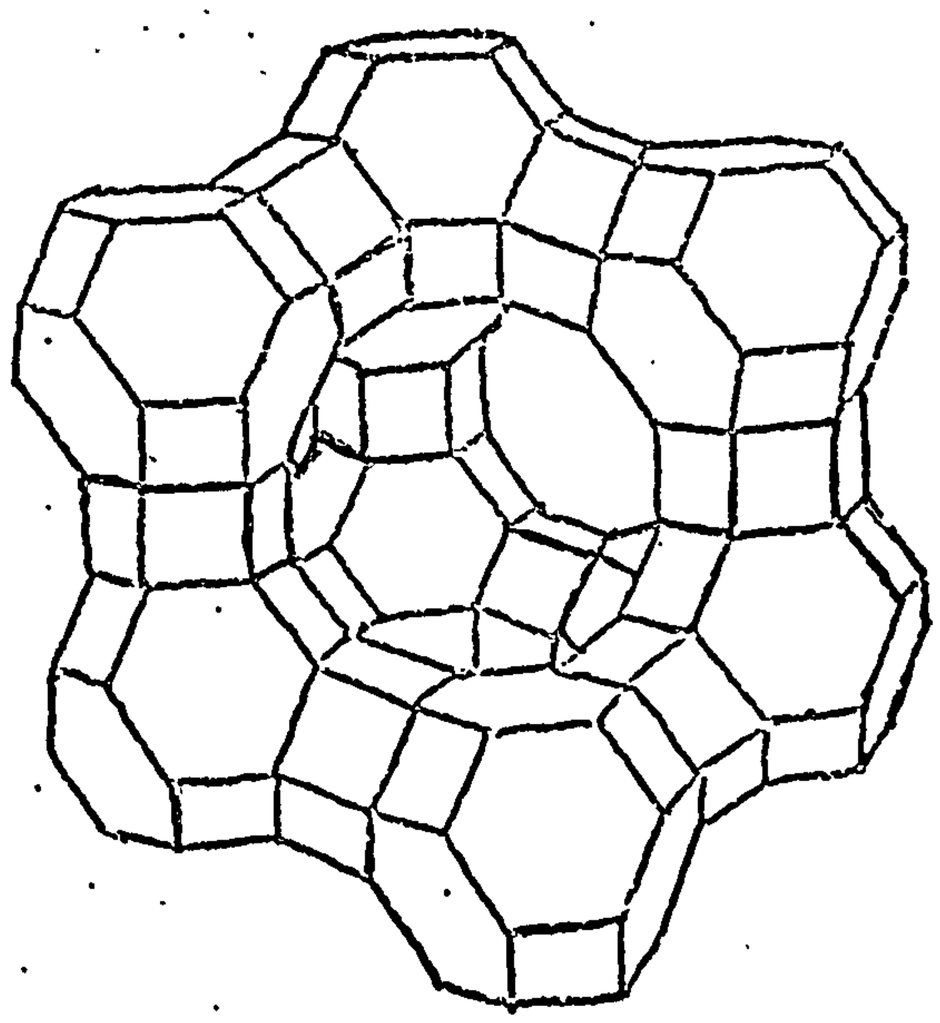

(D)

In zeolite X the β cages form a diamond type structure. The β-cages are joined tetrahedrally to one another by oxygen bridges across the six-unit rings. Thus, the linking unit is a double six-unit ring (D6R) or hexagonal prism containing twelve $(Si,Al)O_4$. The comparatively large cage, or supercage, is thereby generated. Each supercage has a free diameter of ∿13 Å and is connected to others by channels formed by distorted twelve-unit rings $[(Si,Al)O]_{12}$, with a free diameter of ∿8 Å. In contrast to the α-cage the free diameter of the β-cage is around 6 Å although the largest entrance to the six unit ring is only ∿2.2 Å in diameter. The relationship of the β-cage to the structures of hydroxysodalite, zeolite A and faujasite is shown in figure 1.2.

The unit cell of the X and Y type zeolites is cubic with a large cell dimension of nearly 25 Å and contains $192(Si,Al)O_4$ tetrahedra. These remarkably stable and rigid framework structures contain the largest void space of any known zeolites, and in dehydrated crystals this amounts to about 50% of the total volume.

1.7.2 ZEOLITE A

Zeolite A is a completely novel zeolite structure in that no structural mineral analogue has been found. Zeolite A is similar to zeolite X in that they both contain β-cages, although the arrangement of the cages in the lattice is different, as shown in figure 1.2. In the zeolite A structure, the β-cages are linked by oxygen bridges across four-unit windows, rather than across six-unit windows, as in zeolite X. This different stacking arrangement

of β-cages produces a void or α-cage analogous to the supercage in zeolite X although smaller. The free aperture into the α cage is approximately 4 Å in contrast to an aperture of ∿8 Å into the α-cage of zeolite X.

1.7.3 HYDROXYSODALITE (ZEOLITE HS)

This zeolite is closely related to the felspathoid sodalite. It is also referred to as basic sodalite or sodalite hydrate. The structure of hydroxysodalite is again based on β-cages and can be considered as built up from close packed β-cages, where the adjacent four-unit rings from six neighbouring cages have joined up to form what is, in effect, an interstitial β-cage. As a result of this fusion of the cages hydroxysodalite does not have any useful voids or channels. The structural arrangement of hydroxysodalite is shown in figure 1.2.

1.7.4 ZEOLITE P1

Zeolite P1 is one of a series of synthetic zeolite phases[43] which are referred to as the P zeolites and also as Linde type B zeolites. However, since it was first named by Barrer as zeolite P1, this nomenclature takes precedence. This zeolite has been referred to as phillipsite-like, harmotome-like, or gismondine-like, due to close similarities in the x-ray powder patterns of the synthetic zeolite with those of the minerals. Zeolite P1 is readily synthesised in the $Na_2O.Al_2O.SiO_2.H_2O$ system and is a pseudo-cubic zeolite. The structure first proposed was based upon a body-centred cubic arrangement of the D4R units of eight tetrahedra. This has been shown to be incorrect

and the framework structure has been shown to be the same as that of gismondine. The structure is dense and as a result of this zeolite P1 does not have a high sorption capacity. Zeolite P1 can be visualised as having crankshaft-like chains, built up from double four-unit rings of $[(Si,Al)O_4]$ tetrahedra joined edge to edge by oxygen bridges.

1.7.5 ZEOLITE Z-21

Zeolite Z-21 is described, in the patent literature[44], as a large pore absorbent with a cubic unit cell with $a_o = 36.7 \pm 0.3$ Å. It is suggested[44] that the structural unit of this novel zeolite, can be considered as the β-cage and that the co-ordination of these β-cages is tetrahedral as in the faujasite type zeolites. The bridging of the sodalite cage is reported to be different in each case, with the result that the scattering centres and the resulting x-ray diffraction patterns are different. Based on the structure derived from the x-ray diffraction pattern and a knowledge of the β-cage, the pore diameter has been calculated[44] to be 17 Å. However, no adsorption characterisation has been carried out. Flanigen[45] has suggested that its low water content (~12% by weight) is not consistent with an open structure with 17 Å pores.

1.7.6 ZEOLITES R AND S

Zeolites R[46] and S[47] are structurally related to the naturally occurring zeolites chabazite and gmelinite respectively. Detailed structural analysis of these zeolites has not been made although the structures of chabazite and gmelinite have been determined in detail.

The aluminosilicate framework of chabazite consists of D6R units arranged in layers in the sequence ABCABC. The D6R units are linked by tilted 4-rings. The resulting framework contains large, ellipsoidal, cavities each of which is entered by six apertures which are formed by 8-rings.

The aluminosilicate framework of gmelinite consists of the parallel stacking of hexagonal rings in the sequence AABBAABB or D6R units in the sequence ABAB. Similarly to chabazite the framework is produced by joining the D6R units at the edges through tilted 4-rings.

From gas adsorption studies on dehydrated crystals of gmelinite it has been found that the adsorptive properties are equivalent to those of chabazite. This indicates a free aperture dimension of ∿4 Å which is due to stacking faults which interrupt the large 7.0 Å channels.

Recently the synthesis of a chabazite-fault free gmelinite type zeolite has been reported[48]. However this is not synthesised in the sodium system, but involves the use of cationic polymers.

1.7.7 ZEOLITE LOSOD

Losod[49] is a sodium containing zeolite, which is not synthesised in the pure sodium system. A new framework structure is proposed for 'Losod' based on the ABAC stacking of parallel six rings and leading to two polyhedral cages, a cancrinite cage and a Losod cage. The Losod cage is a new type of tricontahedron cage containing 11 six-membered and 6 four-membered rings. It has been concluded that the organic base used in the synthesis of this material has no influence on the structure formed. The structure contains only sodium ions and thus merits a mention in this section.

1.8 ZEOLITE SYNTHESIS IN THE $Na_2O.Al_2O.SiO_2.H_2O$ SYSTEM

1.8.1 INTRODUCTION

In the preparation of synthetic zeolites, early investigators[50] attempted to duplicate what was then considered to be the process by which natural zeolite minerals were formed in basaltic rocks. Reactions were carried out at temperatures above 200°C and correspondingly elevated pressures. Although synthesis of several zeolites was reported in the subsequent years most have been discredited on the basis of improper identification. With the advent of x-ray powder diffraction techniques, positive and unambiguous identification became possible.

Following the first major demonstrations[51,52] of separations using the selective sorption properties of zeolites in the early 1940's, Barrer embarked on the first systematic hydrothermal study of zeolite synthesis. His early investigations were carried out at high temperature and lead to the synthesis of mordenite[53], analcite[54] and a barium zeolite[54,55] with molecular sieve properties similar to chabazite[56].

However, in the late 1940's a new approach to zeolite synthesis was initiated by scientists at Union Carbide. This new approach was primarily based on the use of freshly prepared, highly reactive, aluminosilicate gels or hydrogels, at low temperatures. Early successes at Union Carbide were the synthesis of zeolite A[57], a novel zeolite structure with no known mineral analogue, and zeolites X and Y[58], synthetic forms of the faujasite mineral. (At this time Barrer was in fact working towards lower temperatures and was unfortunate not to reach A, X and Y before Milton and his co-workers at Union Carbide).

Since the early work, novel zeolites have been synthesised from many varied systems which have used alkali metals, alkaline earth metals, and more recently quaternary ammonium hydroxides and binary and ternary combinations of these, as the base in the aqueous alumino-silicate gels. However, detailed discussion of these systems is beyond the scope of this thesis, which is concerned primarily with systems which contain sodium ions.

Zeolites are prepared from aqueous, alkaline reaction mixtures containing 'reactive' silicon and aluminium compounds. The reactions can be divided into three main groups depending on the source of the silica:-

1) Reaction of natural or synthetic glasses with alkali metal hydroxide solutions[59].

2) Reaction of suspensions of amorphous silicas in alkali metal aluminate solutions[60].

3) Crystallisation of gels obtained by mixing aqueous alkaline silicate and aluminate solutions.

Crystallisation from alumino-silicate gels is the most common method used for zeolite synthesis. The zeolites form, when these gels are crystallised at temperatures ranging from room temperature to 175°C at atmospheric or autogenous pressures. Typical gels are formed by mixing aqueous solutions of alkali metal aluminates and silicates or their precursors. This method is well suited for the alkali metals since they form soluble hydroxides, aluminates and silicates, and it is possible to prepare reactive and homogeneous gel mixtures[61,62]. The gel structure is produced by the polymerisation of the aluminate and silicate anions[63]. The composition and structure of this

hydrous polymer appears to be controlled by the size and structure of the polymerising species. Differences in the chemical composition of the starting gel can lead to differences in the zeolite phases which crystallise. During crystallisation of the gel, sodium ions, aluminate and silicate components apparently undergo a rearrargement into the ordered crystalline structure. A schematic diagram illustrating the hydrogel process is shown in figure 1.3. The planned crystallisation of a specific zeolite depends initially on maintaining specific ranges of concentration. This is not easy since the relative amounts of the four starting components, SiO_2, Al_2O_3, Na_2O and H_2O must be decided upon, a choice made difficult by the fact that the composition of the initial reaction mixtures may be very different from that of the crystalline zeolite which is to be prepared. However, even when the relative concentrations are properly decided upon and rigidly controlled, the particular structure which crystallises depends to a great extent on the nature of the silicate starting material. Thus it has been found possible to control which zeolite forms from a particular reaction mixture by using different silica sources. Specially reactive materials used this way include 'active' sodium metasilicate pentahydrate[64], and special silicic acid sols or silicic acid fillers[60,65].

1.8.2 SYNTHESIS PRODUCTS IN THE Na_2O-Al_2O_3-SiO_2-H_2O SYSTEM AT LOW TEMPERATURES

Eight synthetic zeolites A, X, Y, P, HS, Z21, R and S have been synthesised as pure phases from reactive sodium alumino-silicate gels at low temperatures (ca 95°C). The zeolites which

FIG. 1.3 SCHEMATIC DIAGRAM ILLUSTRATING THE HYDROXYL PROCESS

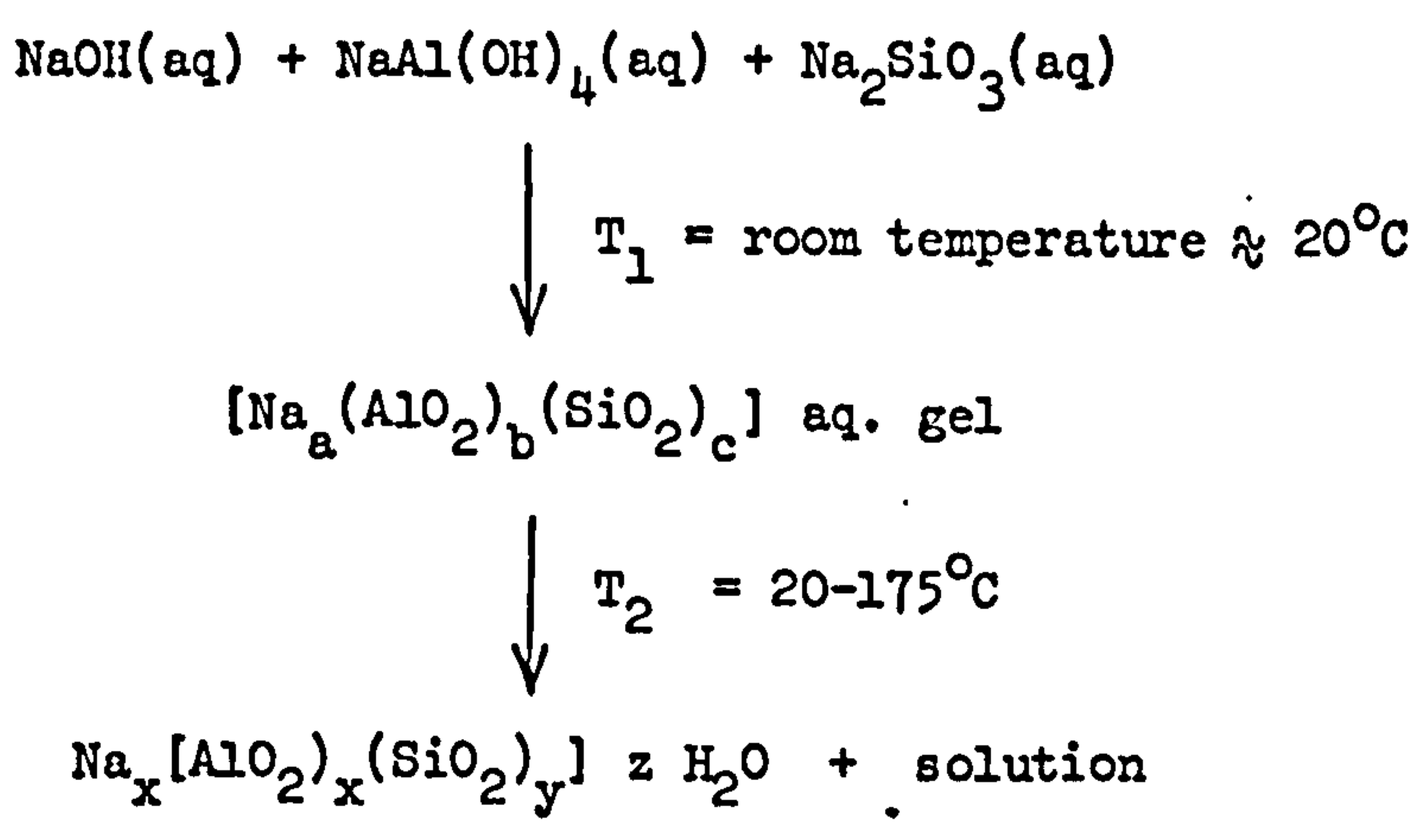

Scheme showing zeolite crystallisation from typical reactants by the hydrogel process. Parameters which must be controlled within critical limits include T_1 and T_2, the composition of the gel, the nature of the reactants, the time for each stage and the extent of agitation.

form under these conditions are usually the kinetically controlled products; zeolites in thermodynamic equilibrium with the aqueous solution phase are formed at higher temperatures, using less reactive starting materials and longer reaction times. The relative concentrations of the reacting components in the initial mixture is usually the most important factor determining the zeolite formed. Other important factors include, the temperature of crystallisation, the nature of the silica source and the gel precipitation procedure.

1.8.2.1 Zeolite A

Zeolite A was first synthesised by Milton[57]. It is crystallised from a starting gel composition which is usually high in alumina. A typical reaction mixture composition is

$$2Na_2O \quad Al_2O_3 \quad SiO_2 \quad 100H_2O$$

The SiO_2/Al_2O_3 molar ratio of the product is normally two. Silica-rich forms of zeolite A have been formed by using gels of high silica and sodium hydroxide content or, by using an organic cation e.g. tetramethylammonium (TMA), to replace part of the alkali metal. Until recently zeolite A had not been synthesised in the absence of sodium ions, which were thought to act as essential templates in its formation. However the synthesis of zeolite A has now been reported[65] in a system which contained lithium, caesium, and TMA cations only.

1.8.2.2 Zeolites X and Y

The chief difference between zeolite X and zeolite Y is that

X has a SiO_2/Al_2O_3 molar ratio (y/x) in the range $2<y/x<3$ whereas Y has $3<y/x<6$ i.e. the zeolite X framework contains more aluminium than does that of zeolite Y, and this is the reason for their differing properties. Zeolites X and Y are synthesised from starting gel compositions which are typically high in silica. A typical reaction mixture composition for the synthesis of zeolite X is

$$3.6Na_2O \quad Al_2O_3 \quad 3SiO_2 \quad 144H_2O$$

whereas zeolite Y requires a higher proportion of silica e.g.

$$8Na_2O \quad Al_2O_3 \quad 20SiO_2 \quad 320H_2O$$

The crystallisation of these zeolites is very dependent on the nature of the silica source, stirring during crystallisation and the temperature of crystallisation.

The discovery of the specially reactive silicates[64] mentioned in section 1.8.1 was a major breakthrough in facilitating the crystallisation of zeolites X and Y without the formation of zeolite P1 which is formed from reaction mixtures with the same stoichiometry as those used for zeolites X and Y. Prior to the discovery of 'active' silicates the only means of avoiding contamination of zeolites X and Y by zeolite P was to use quiescent aging steps, or non-agitated conditions throughout the reaction. This proved extremely difficult to scale up to commercial production, and consequently larger scale synthesis of zeolites X and Y usually resulted in a

product which contained significant quantities of zeolite P1. However, by using 'active' sodium silicate materials, it was possible to produce virtually pure zeolites X and Y, under agitated conditions, without a pre-aging step. These reaction conditions are relatively easy to achieve on an industrial scale.

The origin of the activity shown by some samples of sodium metasilicate hydrates is believed[67,68] to be due to a high level of aluminium which is unintentionally incorporated during the processing of these materials. However, the way in which this causes the crystallisation of faujasite structures in preference to zeolite P1 is not completely understood.

Another important factor which can influence the course of a reaction designed to give zeolite X or Y is temperature. Increasing the synthesis temperature favours the formation of zeolite P1 over zeolites X and Y. This is in accordance with the simplexity principle of Goldsmith[69] which states that low temperature favours the more complex, more easily nucleated zeolites, which in this case are zeolites X and Y.

1.8.2.3 Zeolite P1

Zeolite P1 is formed in similar composition fields to zeolite X and Y and dominates in the temperature range of 100-150°C. A typical reaction mixture for formation of zeolite P1 is

$$2Na_2O \quad Al_2O_3 \quad 3.8SiO_2 \quad 94H_2O$$

This zeolite has been successfully synthesised by many workers and is often an undesirable product of many reactions as discussed in section 1.8.2.2.

Zeolite P1 appears to be an equilibrium phase and is more thermodynamically stable than the more open structured zeolites A, X and Y. It has been reported[70] that the nucleation period for zeolite P1 is longer than for zeolite X although crystallisation proceeds at a faster rate once started.

1.8.2.4 Hydroxysodalite (zeolite HS)

Hydroxysodalite is formed in highly basic systems at ca. 95°C and, in some cases as the transformation product of zeolite A. A typical reaction composition for the formation of zeolite HS is

$$2.8Na_2O \quad Al_2O_3 \quad 3.0SiO_2 \quad 34H_2O$$

The SiO_2/Al_2O_3 ratio of the product is normally equal to two. The chief difference between these synthesis conditions and those used for the synthesis of zeolite A is that reaction mixtures for zeolite HS have a much lower water content. This is clearly related to the fact that zeolite HS has a much less open structure than zeolite A and contains much less water.

1.8.2.5 Zeolite Z-21

Zeolite Z-21 is synthesised under a very specific set of reaction conditions which includes violent agitation during mixing, very high caustic concentrations and rapid crystallisation. It is prepared from sodium aluminate and sodium silicate solutions in the presence of varying amounts of sodium hydroxide. A typical reaction mixture composition is

$$30Na_2O \quad Al_2O_3 \quad 2.0SiO_2 \quad 504H_2O$$

1.8.2.6 Zeolites R and S

Zeolite R is synthesised from gels high in silica and low in alkali in the temperature range 25 to 150°C. A typical reaction composition is

$$6Na_2O \quad Al_2O_3 \quad 6SiO_2 \quad 500H_2O$$

Zeolite S is also synthesised from gels high in silica but under much more basic conditions than zeolite R. The temperature range in which this zeolite is formed is 80 to 120°C, but preferably at 100°C. A typical reaction composition for formation of zeolite S is

$$2.4Na_2O \quad Al_2O_3 \quad 6SiO_2 \quad 80H_2O.$$

1.9 KINETICS AND MECHANISM OF ZEOLITE FORMATION

1.9.1 INTRODUCTION

Since zeolites are formed under metastable conditions, the specific zeolite phase crystallising is dependent on a large number of variables in addition to the classical ones of reactant composition, temperature and pressure found under equilibrium phase conditions. These variables include pH of starting gel, nature of reactant materials, agitation during reaction and time taken for crystallisation. Crystallisation of two or more zeolite phases from the same reaction mixture is very common, and strict reaction procedures must be adhered to if pure zeolite phases are to be synthesised. This can be exemplified in the common co-existence of zeolites A and P1. If zeolite X is to be obtained

in a pure form from an agitated reaction, then either an active silicate (section 1.8.2.2) must be used, or the gel must be aged at room temperature prior to agitation. Divergence from these procedures or ones like them normally results in zeolite P1 formation.

The types of reactions involved in zeolite crystallisation include polymerisation and depolymerisation, solution and precipitation, nucleation and crystallisation, and complex phenomena encountered in aqueous colloidal dispersions. The large number of known and hypothetical zeolite frameworks add to the complexity. The situation has been well summarised by Barrer and Cole[71] -

> *"The art of synthesising molecular sieve zeolites has developed more quickly than the chemical science, which would properly account for their formation in nature, and in the laboratory, from apparently simple aluminosilicate compositions".*

There is extensive data relating to the composition of reaction mixtures or gels, and reaction conditions such as temperature and time of reaction, to the zeolite species or phases which result. However there is only a limited amount of information dealing with the kinetics and crystallisation mechanism.

Zeolite crystallisation is an autocatalytic process in which an induction period precedes rapid crystallisation. During this induction period nuclei form and grow to a critical size, at which point crystallisation begins. The induction period can be

decreased by increasing the temperature of crystallisation, and by increasing[72] the alkali concentrations in the mixtures. It also depends on the nature of the initial aluminosilicate materials used in the synthesis. It has been suggested by Zhdanov[73] that the induction period can be associated with the dissolution of components of the solid aluminosilicate phase during the period preceding crystallisation.

For unseeded reactions the nucleation period is usually longer than the growth period, although the length of both the growth and nucleation periods are usually found to respond in the same way to changes in the reaction conditions.

The processes taking place in the growth period are better understood than those which take place during the induction period, although there are many areas which are still open to debate. For example, although most workers believe that zeolites grow by addition of alumino-silicate units which are transported from the amorphous gel via the solution phase, there are some who believe that there is evidence for a solid phase gel to zeolite transformation mechanism.

The following sections review previous work on kinetics and mechanism of crystallisation of zeolites A and X. The various discoveries are dealt with in chronological order and since many workers have dealt with both zeolites a certain amount of overlap is inevitable.

1.9.2 KINETICS AND MECHANISM OF ZEOLITE A FORMATION

Kerr[72] found that the rate of growth of zeolite A was proportional to the quantity of crystalline zeolite present in the system; in other words, the reaction was often of an autocatalytic nature i.e.

$$\frac{dZ}{dt} = KZ \qquad (1.1)$$

He suggested that the induction period which preceded crystallisation was probably the time taken for nuclei to form and found that this induction period could be eliminated by seeding the system with zeolite A crystals at the beginning of the reaction. Kerr suggested that the mechanism of formation was one in which a dissolved species, derived from the solid phase of the aluminosilicate gel, reacted in such a way that nuclei were formed and zeolite crystals grew. A kinetic expression was proposed in which the rate of growth of zeolite depended on the concentration of the active soluble species i.e.

$$\frac{dZ}{dt} = k[s] \qquad (1.2)$$

in which [s] is the concentration of the active soluble species. Hence in equation 1.1, K contains a concentration term, K = k[s]. In addition Kerr found that the rate of formation of zeolite A increased as the alkali concentration of the solution phase increased. The solution phase mechanism proposed by Kerr differed from that suggested by Breck and Flanigen[62,74]. These workers suggested a mechanism in which extensive heterogeneous nucleation occurred during formation of the highly supersaturated gel. Crystal growth in the solid phase then proceeded by a series of depolymerisation-polymerisation reactions catalysed by excess hydroxyl ion. They also stated that no significant solution of the solid phase took place during crystallisation.

Ciric[75] followed up the work of Kerr, and in searching for more evidence for zeolite A growth, via dissolution of the

amorphous gel precipitate, studied the effect of the SiO_2/Al_2O_3 ratio in the starting gel, the caustic concentration and the stirring rate on the rate of zeolite growth. He discussed the observed kinetics in terms of mass transfer of the dissolved species from the bulk solution phase to the crystal surface. From an interpretation of the effect of the reaction mixture composition on growth rate it appeared that the diffusing species contained two negative charges. He suggested, then, that this indicated that the most likely building block for zeolite A was a relatively small unit possibly an alumino-silicate dimer or cyclic tetramer. This was consistent with Barrer's[31] idea of anionic building blocks. Ciric concluded that all his observations were consistent with a diffusion mechanism of crystal growth, in agreement with that proposed by Kerr[72].

In his study of the influence of liquid and solid phases on crystallisation from alkali aluminosilicate gels, Zhdanov[76] found that the amount of silica in the solid phase of these gels is nearly always greater than that in the zeolite which crystallises from them. He considered that his experiments showed that the formation of zeolite crystals was not determined by the composition of the Si-O-Al network of the initial gel skeleton, but was regulated by the composition of the gel liquid phase. This was again in disagreement with the mechanism suggested by Breck and Flanigen[74]. According to Zhdanov, the formation of the crystalline zeolite lattice was a result of polycondensation of hydrated silicate and aluminate ions from the liquid phase. He suggested that the growth of zeolite seeds proceeded through a quasi-equilibrium concentration

of the liquid phase components, which was reached by uninterrupted dissolution of the gel skeleton. This can be represented schematically as follows:-

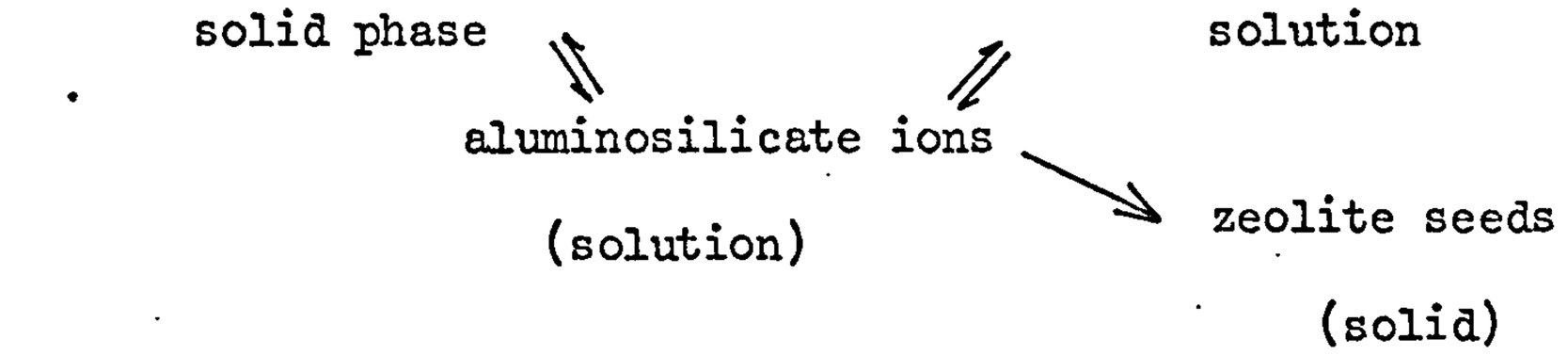

In a later review, Zhdanov[73] disputes the generally held opinion that the induction period is the time required for growth of nuclei to a critical size and states that the induction period is the time required for providing the conditions suitable for formation of nuclei. On the basis of the crystal size of zeolite A formed in a reaction at 90°C, assuming only that the linear rate of crystal growth is independent of its size, Zhdanov suggests the formation of nuclei takes place during the entire process of crystallisation. However, the rate of nucleation is increasing only during its first period. He concludes that this is what leads to the autocatalysis of zeolite crystallisation.

In their contribution to the work on the mechanism of zeolite crystallisation, Aiello, Barrer and Kerr[77] studied the stages of aggregation from alkaline aluminosilicate solutions. They observed the formation of solid amorphous lamellae, which, on prolonged heating of the system, evolve into larger particles and are finally replaced by zeolites. They concluded that nucleation of zeolites under these conditions was a heterogeneous

process. The sequence of processes observed was consistent with Ostwald's law of successive transformations and in part with Goldsmith's[69] simplexity principle. However, it was stated that the possible independent formation of lamellae and zeolite could not be excluded. The zeolites formed from this system were zeolite P1 and hydroxysodalite.

Zeolite formation from synthetic and natural glasses was investigated by Aiello, Colella and Sersale[78]. Zeolites such as zeolite A, P1, analcite, HS and faujasite were obtained. The kinetics of zeolite formation were followed and the chemical composition of the mother liquors at different reaction times was determined. Two rates of reaction were observed for zeolite X formation, both nearly linear: a slower rate up to 30% crystallisation and a faster rate from about 30-70%. (This is in contrast to the rates of crystallisation observed by Zhdanov[73], who observed faster rates for zeolite A crystallisation in the initial stage of the reaction). These authors also report the existence of a gel as an intermediate stage of the glass to zeolite transformation.

Schwochow and Heinze[79] investigated the changes in concentration with time in the solid and liquid phases of gels before crystallisation started. They also investigated zeolite formation in the mother liquors separated from the solid phases. They found that the zeolite which crystallised from the liquid phase was dependent on temperature and stirring time prior to the solid-liquid separation. Phases poor in silica e.g. zeolite A, were obtained from liquid phases rich in aluminate whereas silica rich phases e.g. zeolite X, were obtained from liquid phases rich in silicate.

In addition Schwochow and Heinze found that the zeolite phase which crystallised was dependent on the size of the silicate anion, and for zeolite X synthesis it was necessary that the dissolved silica was present in a predominantly monomeric state. Higher molecular weight anions promoted the formation of a 'phillipsite-type' phase (presumed to mean zeolite P1) in preference to faujasite material. They also found that during the nucleation period, the composition of the liquid phase had to correspond to a very high SiO_2/Al_2O_3 ratio (>20) if faujasite was to crystallise.

Migal and Nelyubov[80] have reported on the effect on zeolite crystallite size of the rate and order of mixing during gel formation. They found that larger crystals (35-40 μm) resulted from silicate to aluminate mixing, than from the reverse order. Aluminate to silicate mixing resulted in gels of higher silica content. In agreement with the mechanism suggested by Breck and Flanigen[74], they concluded that crystallisation of zeolites proceeded in the solid phase of the gel.

McNicol[81,82] and co-workers also subscribed to the idea of a solid-state mechanism of zeolite formation. They used phosphorescence and Raman spectroscopy to study the crystallisation of zeolites A and X from alkaline aluminosilicate gels. They observed from phosphorescence spectra that no zeolite cages existed in the solid phase of the gel during the induction period. At the onset of crystallisation phosphorescence spectral changes were observed which were interpreted to be a consequence of the condensation of the hydroxylated tetrahedra to non-hydroxylated tetrahedra in the zeolite crystals. Raman spectra of the liquid

phase of the gel system showed the presence of a solution of $Al(OH)_4^-$, $SiO_2(OH)_2^{2-}$, Na^+ and OH^- ions, whose concentrations did not change significantly during induction and crystallisation. No evidence was found for the existence of any soluble aluminosilicate anions. From these results, they concluded that zeolite crystallisation occurred in the solid phase of gel via condensation between hydroxylated tetrahedral aluminosilicate species.

Beard[83] carried out infra-red studies of aqueous silicate solutions in an attempt to determine the size and structure of silicate species in solution in relation to zeolite crystallisation. Despite the fact that this difficult technique was shown to be capable of characterising silicate solutions, Beard was unable to relate the nature of the silicate anions to their role in zeolite crystallisation.

Meise and Schwochow[84] followed up the work by Zhdanov, in which he described the zeolite A reaction quantitatively, by investigating crystal size, and also formulated detailed hypotheses on the chemistry of zeolite formulation. They[84] describe the influence of the alkalinity, silica source, K^+ ions and temperature on the progress of the reactions, and the particle size spectrum of the product zeolite A. Variations in temperature were found to affect both nucleation and crystal growth, whereas alkalinity, SiO_2 source, and the K^+ ion content of the reaction mixture were found to affect nucleation more than crystal growth. Temperature was found to have little effect on particle size distribution. However, an increase in the alkali concentration of the liquid phase or in the Carman surface of the SiO_2 source, increased both the speed of the

reaction, and the amount of fine particles in the crystalline product. In contrast to this it was found that even small amounts of K^+ ions added at the beginning of the reaction retarded the reaction and led to formation of coarse particles. However, if the K^+ ions were added when gel precipitation was complete, they had no influence on the nucleation. This effect was interpreted in terms of steric factors, in that the large K^+ ions were not as suitable as Na^+ ions for forming the aluminosilicate building blocks which served as nuclei. Meise and Schwochow derived equations for nucleation and crystal growth which described, to a fairly good approximation, the experimentally observed relationship between yield and time and the corresponding particle size spectrum. These workers considered that evaluation of their kinetic investigations permitted predictions about nucleation and crystal growth which were not restricted to the formation of zeolite A.

Culfaz and Sand[85] studied the mechanism of transformation of gels under autoclaving conditions. Their study showed that the crystallisation processes for mordenite, zeolite X and zeolite A were similar. They found that addition of seed crystals did not affect the nucleation period and conversion rate for zeolite X. This is in contrast to the findings of other workers[86] and suggested to Culfaz and Sand that reactions in the gel and liquid phases take place before conversion to zeolite X begins. They suggested that similar reactions preceded zeolite A crystallisation; however, since the zeolite A induction period is shorter, this initial step was not as significant for zeolite A as it was for zeolite X. The conversion rate to zeolite A was increased by the use of seed crystals.

Culfaz and Sand concluded that their data supported the hypothesis of crystal growth from the solution phase, with the crystal-liquid surface enhancing the nucleation process in seeded systems. No conclusion was reached concerning the precise mechanism in unseeded systems.

In an attempt to resolve the conflict concerning the type of crystallisation mechanism (either a solid phase transformation or a solution transport mechanism) which occurred during zeolite synthesis, Angell and Flank[87] applied a variety of techniques to the study of the zeolite A synthesis system as a function of time. The characterisation techniques used were chemical analysis, Raman x-ray diffraction, sorption and particle size measurements. The evidence discussed in their work supports a synthesis reaction mechanism involving formation and subsequent dissolution of an amorphous sodium aluminosilicate intermediate, with solution transport from the gel to the growth surface of the nucleated zeolite crystallite. They discuss the possibility of ordered moieties which could represent nucleation centres. They state, however, that this would be difficult to determine because of the overlap of the several reaction steps involved during crystallisation. It is suggested that weak bands observed in the Raman spectra for the liquid phase could be attributable to this type of species i.e. the dimer or cyclic tetramers, postulated by Ciric[75].

Culfaz and Orbey[88] have studied the kinetics of crystallisation of zeolite A in a stirred tank reactor. The fractional conversion of silica to zeolite A was varied, by varying the rate at which reactants were fed to the reactor. They found that the reaction was catalysed by the external surface area of the zeolite A

crystals which had already formed. They suggest that the catalysing nature of the product zeolite A is in supplying nucleation sites on its surface and the growth of zeolite A crystals is brought about by the diffusion of amorphous material to the nucleation sites at the solid-liquid interface. The proposal of an interface diffusion mechanism is in agreement with earlier work carried out by Culfaz and Sand[85].

1.9.3 KINETICS AND MECHANISM OF ZEOLITE X AND Y FORMATION

The growth of zeolites X and Y has not been studied as thoroughly as that of zeolite A. Kerr[70] studied the factors affecting the formation of zeolite X and P1. These two zeolites can be prepared from reaction mixtures which have the same stoichiometry but subtle changes in the preparation of the reaction mixture and in the way in which the crystallisation is performed determine which zeolite crystallises. He[70] found that the rates of formation of zeolites X and P1 followed the same law as for zeolite A[72],

$$\frac{dZ}{dt} = KZ$$

He also showed that zeolite X nucleates more readily than zeolite P1, but grows at a much slower rate. It was suggested that this observation may account for the predominance of phillipsite (a zeolite closely related to zeolite P1) in natural deposits of faujasite, (natural zeolite X).

The role of the crystal surface in the mechanism and the kinetics of the crystallisation of zeolite X has been studied by Mirskii and Pirozhkov[86]. By seeding gels from which zeolite X was

synthesised, they found a decrease in both the induction period and time for total crystallisation. This is in direct contrast with the findings of Culfaz and Sand[85] who observed no differences in either nucleation or crystal growth on the addition of seeds. Mirskii and Pirozkov concluded that the rate of crystallisation was a function of the external surface area of the seed crystal added to the gel. Their rate curves for increased amount of seed show an interesting evolution of the typical sigmoid shape into curves with two distinct linear portions: an initial slower rate presumably related to seeded growth, and a later faster portion related to unseeded growth.

Polak and Cichocki[89] have studied the changes in chemical composition occurring during aging and after crystallisation of aluminosilicate hydrogels used to synthesise zeolites X and Y. They observed that during the aging step of zeolite X synthesis, changes in both the solid and liquid phases of the hydrogel took place. However, these changes were small if the aging period was short and zeolite X was not formed after one hour but after 24 hours of aging. They suggested that this may be due to hydrolysis of the existing bonds in the silicates with subsequent formation of new bonds with other partners, thus leading to a new arrangement of aluminium and silicon tetrahedra, facilitating the formation of zeolite X crystals.

In a series of papers, Polak and Stobiecka[90-92], have published the results of their studies on the mechanism of zeolite Y formation. They have investigated the influence of the time of hydrogel aging, Na^+ concentration and SiO_2 concentration on zeolite Y formation. Their findings are similar to those of Polak and Cichocki[89], however they observed that reactions were

still taking place in the hydrogel even after 60 days and that this was still able to crystallise to zeolite Y whereas this did not occur with the hydrogels used for zeolite X synthesis. They also found that increasing SiO_2 concentration in the reactant mixtures was not favourable for zeolite Y crystallisation.

Borowiak and Berak[93] have studied the effect of the alkali content of hydrogels on zeolite Y crystallisation. They conclude that the rise in nuclei concentration is directly related to the concentration and nature of the anion. Also, they dispute Breck and Flanigen's view on the mechanism of crystallisation and conclude that nucleation occurs not only in the precipitation step but also in subsequent zeolite crystallisation steps. This is in agreement with ideas put forward by Zhdanov[73].

Kacirek and Lechert[94] have carried out detailed investigations on the growth of zeolite Y. Their reactions were seeded with varying amounts of zeolite X crystallites covering a range of particle sizes. They found that addition of these crystallites to the reaction mixtures, increased the yield of faujasite and that their amount and size are of central importance in the synthesis. In addition they found that under wide ranges of crystallisation conditions, the growth of faujasite is possible in concentration ranges where nucleation of this or other species are negligible and that over a wide range of crystallisation conditions the growth obeys a kinetics law of the order 2/3. They conclude, in agreement with Kerr[70,72], that the zeolite growth only occurs at the crystal/solution interface and that a direct transition of the gel into the crystalline state, as suggested by Breck and Flanigen must be excluded.

Rates of crystallisation of faujasitic zeolites have also been studied by Kacirek and Lechert[95]. The time taken for crystallisation was studied in some detail and the activation energy for zeolite growth was calculated. They found a linear rate of crystallisation which was proportional to the concentration of the silicate in the solution phase for final products of equal Si/Al ratios. The crystallisation rate was found to vary over three orders of magnitude as the composition was changed from that for zeolite X (Si/Al = 1.4) to that for zeolite Y (Si/Al = 3.4) and there was a consequent increase in the apparent activation energy. A model for the crystallisation process based on these results was developed.

A further study of the kinetics of growth of faujasite and Na-A type zeolites has been carried out by Kacirek and Lechert[96]. They have compared the results of kinetic studies of faujasite growth with those of the growth of the zeolite Na-A in a TMA/Na system. From this they have developed a model of crystallisation and deduced methods of preparation based on Na-A zeolites.

A comprehensive investigation of the mechanism of crystallisation of zeolite X has been carried out by Freund[68]. He found that crystallisation of zeolite X was possible from clear solutions and was similar to crystallisation from gels. Hence he concluded that crystallisation in the gels occurred either in the mother liquor or at the interface between the amorphous aluminosilicate and the mother liquor. The interfacial reaction has also been suggested by Sand[85].

Freund arrived at the following results for zeolite X crystallisation and its competition with zeolite P1, by studying

the effects of silica source, stirring and the maturation period. Firstly, nucleation of zeolite X may proceed according to two different mechanisms. One which involves no impurity is observed for all reactants, and is better at room temperature where crystal growth is very slow and does not hinder nucleation, i.e. formation of nuclei from dissolved species. The second mechanism involves aluminium impurities included in the silica source. This mechanism was also elucidated by McGilp[67]. It is believed that the presence of aluminium in the sodium silicate can promote the formation of aluminosilicate seed particles which aid the crystallisation of zeolite X. The structure of these particles is unknown.

Freund also found that the nucleation of zeolite P1 is much slower than the nucleation of zeolite X at room temperature, the converse being the case at 80°C, he further concluded that the effect of stirring was to provoke secondary nucleation by collision breeding. Finally, he suggested that the crystallisation of both zeolites X and P1 occurred in the mother liquor, the concentration of which was kept constant by the dissolution of amorphous aluminosilicate. The selectivity between zeolite X and P1 depended on the number of zeolite X nuclei present in the system before crystallisation and on stirring during crystallisation.

Work carried out by Whittam[97] on the competitive crystallisation of zeolite X and P1, suggested that the incorporation of certain basic organic dyes could influence the reaction in favour of zeolite X. It was suggested that the dye molecule adsorbed on to the surface of zeolite P1 nuclei and therefore allowed the growth of zeolite X to take place. This work is reviewed in more detail in chapter 5.

1.10 THE AIM OF THIS WORK

The principal aim of this work was to obtain information which would be useful in elucidating the mechanism of zeolite X formation, a difficult problem which had been investigated by many other workers as discussed in the previous sections. In an attempt to achieve this, several aspects of the zeolite synthesis reaction in the Na_2O Al_2O_3 SiO_2 H_2O system were investigated. In particular, the influence of the silica source on the products formed and, the kinetics of zeolite X formation has been studied in some detail and the work carried out is described in chapters 2 and 3.

A very interesting study of zeolite crystallite formation from solid/liquid slurries has been carried out by McGilp[67]. This method of studying the growth of zeolite X and other zeolites in the Na-field appeared to be an attractive prospect and a detailed investigation of zeolite growth based on solid/liquid slurries was carried out, and this is described in chapter 4.

The addition of organic molecules, in particular dye molecules, to reaction mixtures had yielded some very interesting results[97] and it was considered that further work in this area might provide mechanistic information. This work is described in chapter 5. In order to make proper use of the information gained from investigations of dye addition to zeolite reactions, it was necessary to investigate the nature of dye adsorption on solid surfaces present in the zeolite reaction mixtures and the work carried out in this area is described in chapters 6 and 7.

CHAPTER 2

SYNTHESIS OF SODIUM ZEOLITES FROM AMORPHOUS SILICAS

2.1 INTRODUCTION

The basic method used to prepare synthetic zeolites is described in chapter 1, section 1.8.1. In order to obtain zeolite X as the major product, it is necessary to allow a quiescent aging step or alternatively in a stirred system an 'active' silicate[64] must be used. However, Schwochow[98] and co-workers have recently claimed that it is possible to synthesise zeolite X with a particularly low Si/Al ratio, from a stirred system, without the use of active metasilicates, provided a silica with a high surface area is used as the chief source of silica. In particular they claimed that by using a silica sol or an amorphous silica with a surface area in the range 150 to 250 $m^2\ g^{-1}$ (as determined by the B.E.T. method) it was possible to produce zeolite X in a stirred reaction at 100°C in 6 hours.

The possibility of synthesising zeolite X from stirred reaction mixtures without the addition of 'active' metasilicate could have a significant commercial advantage since it is not easy to find a reliable and reproducible source of 'active' metasilicate. Different batches of commercial sodium metasilicate pentahydrate are 'active' to different extents, and their activity tends to increase and then decay with age. The possibility that certain amorphous silicas can direct the reaction towards the formation of zeolite X may imply a different crystallisation mechanism, or alternatively it could indicate that commercially available amorphous silicas can exhibit the same sort

of behaviour as that shown by 'active' metasilicate. For these reasons it was felt that the use of high surface area silicas as an alternative to active metasilicate was of sufficient interest to warrant further investigation. These studies form the basis of this chapter.

2.2 EXPERIMENTAL DETAILS

2.2.1 MATERIALS

The four amorphous silicas used for this work were (1) a precipitated silica, (2) a colloidal silica powder low in iron (in all that follows this material will be referred to as coll. SiO_2), (3) a fumed silica CAB-O-SIL M5 (all of which were supplied by BDH Ltd.) and (4) a precipitated silica KS300 manufactured by Akzo Ltd. and supplied by I.C.I. Ltd. The surface areas determined by the B.E.T. method and some analytical data for these materials are shown below in table 2.1.

TABLE 2.1 SOME ANALYTICAL DATA[a] FOR THE AMORPHOUS SILICAS

SiO_2	Surface Area $m^2 g^{-1}$	% Na_2O	% Al_2O_3	% loss at 1000°C
Precipitated SiO_2	74	0.84	0.4	13.5
KS300	135	-	0.28	9.8
Colloidal SiO_2	181	8 ppm	ND[b]	3.6
CAB-O-SIL M5	208	<5 ppm	ND	3.4

[a] Data obtained by I.C.I. Ltd. Agricultural Division Analytical Services

[b] Not detected.

Syton 30X, a 30% silica sol supplied by Monsanto Ltd. was also used. The specific surface area of the silica in this sol was not measured. Two forms of Kieselguhr (a silica which contains alumina as an impurity) supplied by BDH Ltd. were used. One was purified with acid and the other was called white Kieselguhr. Both forms of Kieselguhr had been calcined. Solid dry sodium aluminate, supplied by BDH Ltd., was used as the alumina source. The analysis of this sodium aluminate gave 1.2 $Na_2O.Al_2O_3$, and this excess sodium was taken into account when preparing reaction mixtures. The sodium hydroxide was technical grade reagent supplied by BDH Ltd. All reactions were made up with pure distilled water.

2.2.2 APPARATUS USED IN ZEOLITE SYNTHESIS

Reaction mixtures were prepared in a 600 cm^3 stainless steel or pyrex beaker and the resulting gel was homogenised by an electrically driven 5 cm diameter stainless steel paddle. The mixture was placed in a reactor which consisted of a 500 cm^3 three necked, round bottomed Quickfit flask type FR500/35/22P fitted with a reflux condenser and agitated by an electric stirrer with a teflon paddle. The stirrer gland, supplied by Jencons Ltd., was a simple precision bore glass sleeve within which the stirrer rod fitted. The bearing surfaces were lubricated with vaseline but tended to wear particularly when in contact with zeolite product, but this was not a serious problem.

The apparatus was partly immersed in a water thermostat bath which maintained the temperature at 95±2°C. Two types of bath equipped with constant level devices were used. These were a

Grant Instruments type SB3S with polypropylene spheres to reduce heat loss, and a small conventional water bath supplied by Towers and equipped with a Jumo type GKT15 relay.

A 15 cm Buchner filter funnel fitted with Whatman No. 1 paper was used for filtration and washing of the zeolite product.

2.2.3 X-RAY POWDER DIFFRACTION ANALYSIS

Product analysis was carried out using x-ray phase analysis. A Guinier-Hägg camera (Type XDC700) using CuKα, radiation (λ = 1.5443 Å) was used for qualitative analysis. The Guinier camera is a focussing camera and is extremely sensitive to weak reflections; it was very useful for identifying minor zeolite phases and trace quantities.

Quantitative analysis was carried out using a Phillips vertical diffractometer type PW1051 using CuKα radiation (λ = 1.5418 Å) operating at 1° per minute with a receiver slit of 0.2 min. The reference samples used were Linde 13X, Linde 4A and a pure zeolite P1, synthesised in the laboratory. Quantitative measurements were based on the diffraction lines at 2θ = 23.4° (d = 3.808 Å) and 2θ = 26.7° (d = 3.253 Å) for zeolite X, 2θ = 24.6° (d = 3.714 Å) and 2θ = 27.0° (d = 3.293 Å) for zeolite A and 2θ = 28.2° (d = 3.16 Å) for zeolite P1.

Before samples were submitted to x-ray analysis it was important that they were properly equilibrated with the atmosphere. It was found that insufficient equilibration time led to peak heights which were too high, (see figure 2.1).

2.2.4 PROCEDURE

The overall reaction composition used in this work was

$$5.15Na_2O \cdot Al_2O_3 \cdot 4SiO_2 \cdot 240H_2O$$

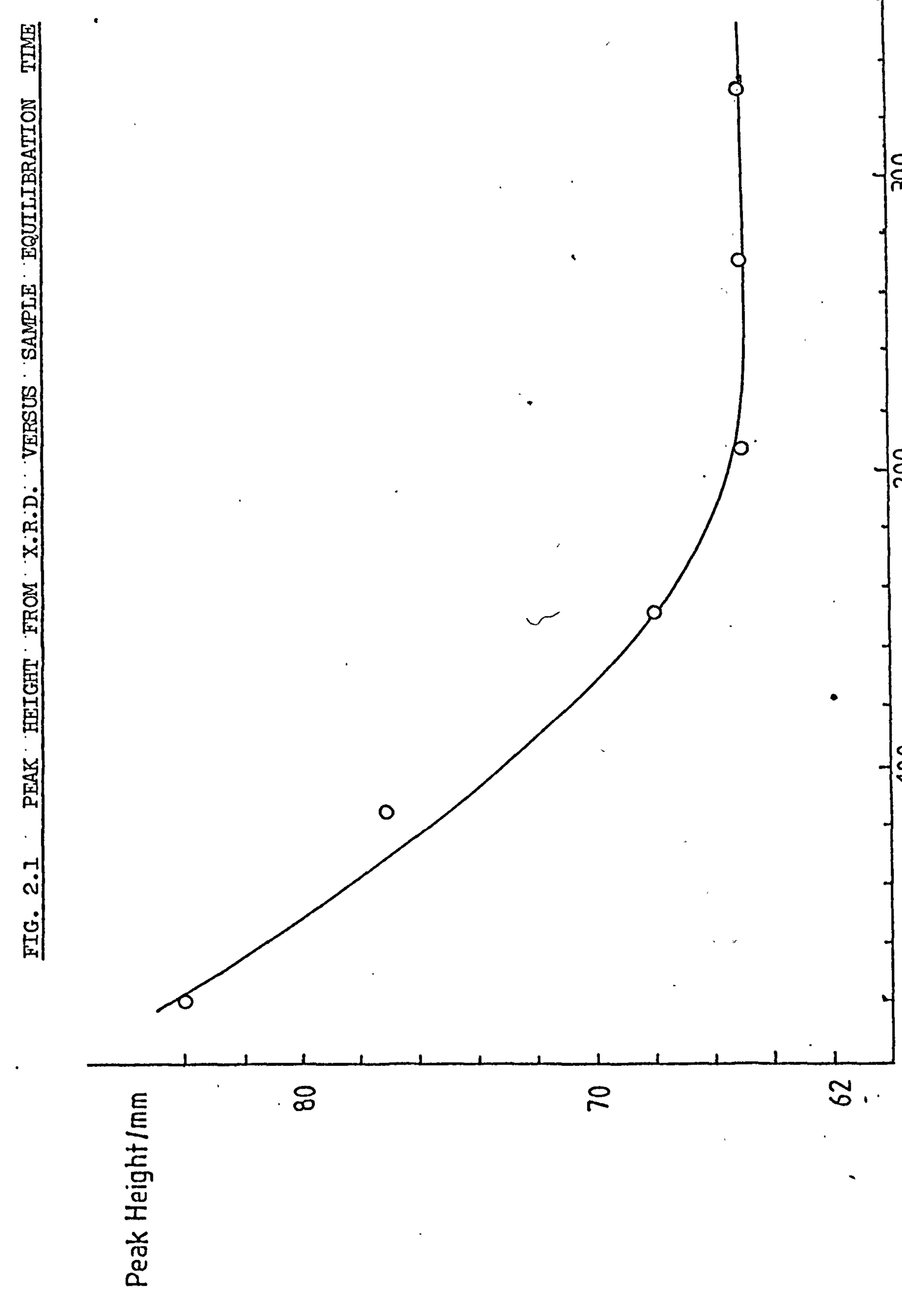

FIG. 2.1 PEAK HEIGHT FROM X.R.D. VERSUS SAMPLE EQUILIBRATION TIME

in which the molar component ratios agree well with those recommended (shown in brackets):-[64]

SiO_2/Al_2O_3 = 4.0(3.85); Na_2O/SiO_2 = 1.30(1.34); H_2O/Na_2O = 46.6(47.0)

The reaction was set up in the following way. Sodium aluminate (8.8 g) was dissolved in distilled water (100 g) with heating; it was allowed to cool and the lost water replaced. Sodium hydroxide (15.8 g) was then dissolved in distilled water (100 g). If the silica (12.0 g) was to be dissolved it was heated with the sodium hydroxide solution until a clear solution was obtained. The aluminate solution was then added to the silicate solution, with the remaining water, and stirred until a white homogeneous gel was obtained. In those reactions in which the silica was not dissolved prior to addition to the aluminate solution, it was added to the cold sodium hydroxide solution, and the aluminate solution together with the remaining water was added quickly. The mixture was stirred, but in this case no gel was formed. After the mixtures were formed, they were placed in the reactor, and stirred under reflux at 95°C. Samples were taken after 3, 4, 5 and 6 hours.

In those reactions carried out using silica sol it was observed that on addition to sodium hydroxide, the silica was precipitated and it was necessary to heat this mixture to dissolve the silica. Kieselguhr was only slightly soluble in sodium hydroxide and therefore those reaction mixtures which contained this material were prepared as those containing undissolved silica.

2.3 RESULTS

The results of the reactions with amorphous silica as the only SiO_2-source are shown in table 2.2 The results fall into two

TABLE 2.2 PRODUCTS OF REACTIONS WITH AMORPHOUS SILICAS AS THE SOLE SiO_2 SOURCE

Run No.	SiO_2 source	Dissolved (D) or undissolved (U)	PRODUCTS: Dissolved SiO_2 3h	Dissolved SiO_2 4h	Dissolved SiO_2 5h	Undissolved SiO_2 3h	Undissolved SiO_2 4h	Undissolved SiO_2 5h	Undissolved SiO_2 24h
2.1	Ppt SiO_2	U	-	-	-	Pl	Pl	Pl	
2.2	"	D	Pl	Pl	Pl	-	-	-	
2.3	KS300	U	-	-	-	Am	X		X+Pl
2.4	"	D	Pl+sl.tr.X	Pl+sl.tr.X	Pl+sl.tr.X	-	-	-	
2.5	"	D	-	Pl+sl.tr.X	-	-	-	-	
2.6	"	U	-	-	-	Am	X		
2.7	"	D[a]	-	Pl	-	-	-	-	
2.8	"	D[b]	Pl	Pl	Pl	-	-	-	
2.9	Coll. SiO_2	U	-	-	-	X+tr.Pl	X+Pl	X+Pl	X+Pl
2.10		D	Pl	Pl	Pl	-	-	-	
2.11	CAB-O-SIL M5	U	-	-	-	X+tr.Pl	X+tr.Pl	X+Pl	
2.12	"	D	Pl	Pl	Pl				
2.13	SYTON 30X	U	-	-	-	X+Pl	X+Pl	-	
2.14	"	D	Pl	Pl	-				
2.15[c]	KS300	D	Pl	Pl	Pl				

[a] Aged 14 h at room temperature. [b] Aged 2d at room temperature. [c] See text for details.

categories; those for runs in which the silica source was dissolved in sodium hydroxide solution before making up the reaction mixture, and those for runs in which the silica was not dissolved prior to making up the mixture. In the former case a gel was produced on addition of the aluminate solution, whereas in the latter case no gel was formed.

2.3.1 REACTIONS WITH DISSOLVED SILICAS

For those reactions in which the amorphous silica was dissolved, the major product was invariably zeolite P1. However, in reactions 2.4 and 2.5 in which the silica source was KS300, a slight trace of zeolite X was formed. This was not produced when the sodium silicate solution was aged for 14 hours at room temperature (reaction 2.7). It seemed possible that the formation of some zeolite X in reactions 2.4 and 2.5 reflected a latent ability of KS300 to direct the reaction towards the formation of this zeolite, but that this had been impaired by the high temperature used to dissolve the silica in the sodium hydroxide solution. To test this, the KS300 was dissolved in cold sodium hydroxide solution at room temperature, (a slow reaction which took 2 days) before being used in the reaction. In this case (reaction 2.8) the product was pure zeolite P1 and it was therefore concluded that the dissolved KS300 did not have the ability to exert a directing influence such that the product of the reaction was zeolite X.

2.3.2 REACTIONS WITH UNDISSOLVED AMORPHOUS SILICAS

In those reactions in which the amorphous silica was not dissolved, the product was either pure zeolite P1, pure zeolite X.

or a mixture of these two zeolites. In reaction 2.1 in which the silica source was precipitated silica the product was pure zeolite P1. For those reactions, 2.3 and 2.6, in which the silica source was KS300, the products were zeolite X and amorphous aluminosilicate. For those reactions, 2.9, 2.11 and 2.13, in which the silica sources were coll. SiO_2, CAB-O-SIL M5, and syton 30X respectively the products were mixtures of zeolite X and zeolite P1.

Since for all these reactions with undissolved silica no gel was formed at room temperature it seemed possible that the formation of zeolite X could be associated with gel formation at elevated temperatures. To test this reaction 2.15 was carried out: a sodium silicate solution, prepared with KS300 and sodium hydroxide solution was placed in the reaction vessel and heated to 95°C, the sodium aluminate solution also at 95°C was then added. The product of this reaction was pure zeolite P1. It was therefore concluded that the temperature of gel formation did not influence the formation of zeolite X.

It was observed that as the surface area of the amorphous silica increased, the formation of zeolite X in this system became possible. Several possible reasons for this behaviour can be put forward. Since formation of significant amounts of zeolite X only takes place when solid silica is present, it is possible that the silica surface may provide a nucleating surface on which zeolite X can grow. This seems unlikely though, as the surface of the precipitated silica and KS300, which is also a precipitated silica, are almost certainly very similar and reactions with the former material yield zeolite P1 whereas reactions with KS300 yield zeolite X. It was considered that the rate of solubility of the silica may be important since it had been shown by Cournoyer[99] et al,

using only quartz as the silica source, that the rate controlling step in zeolite HS formation was the rate of supply of silica in solution, rather than its diffusion to nucleation sites or crystal growth sites. However, it was found that at 95°C CAB-O-SIL M5 (surface area 208 m^2 g^{-1}) dissolved into sodium hydroxide solution within 20 seconds and that precipitated silica (surface area 74 m^2 g^{-1}) dissolved within 60 seconds. It was considered that this difference in the rate of solubility could not be significant.

Another possible explanation for the formation of zeolite X in systems containing solid silica is that the type of silicate species initially present in solution may depend on the type of silica dissolved. The silicate species present in solutions of CAB-O-SIL M5 and precipitated SiO_2 in sodium hydroxide (1:1; SiO_2:Na_2O, C = 1.0 mol dm^{-3}) were determined by ^{29}Si Fourier Transform n.m.r. The same silicate species, chiefly monomers, dimers and other oligomers were found to be present in both solutions in similar amounts (see figure 2.2). However, comparison of line widths shows that the lines observed for the precipitated silica are significantly broader (20 Hz) than those observed for the CAB-O-SIL M5 (5 Hz). The broad lines suggest the presence of colloidal particles[100]. Since the reaction with solid precipitated silica yielded only pure zeolite P1, it is reasonable to infer that the presence of colloidal particles in solution promotes the formation of zeolite P1. The suggestion that colloidal particles promote formation of zeolite P1 has been put forward by McGilp[67] and these results support that theory. Therefore, if, colloidal silica particles are desirable as nucleating species for zeolite P1 formation then their absence

will make the formation of this zeolite less likely. However the formation of zeolite X cannot be entirely due to the absence of colloidal silica in the silicate solution since zeolite X was not formed in those systems in which the silica was dissolved prior to gelation.

The explanation for the formation of zeolite X probably lies, at least partly, in the mechanism by which the gel forms. When an amorphous silica is completely dissolved in sodium hydroxide, the solution contains a variety of silicate polymers (see figure 2.2) which on addition of sodium aluminate will become joined in a disordered fashion, giving no ordered gel structure. (Although this is similar to what happens when 'active' sodium metasilicate is used, in this case there are already nuclei present which can act as templates for zeolite X formation.) However, if the amorphous silica is dissolved in a solution of sodium aluminate and sodium hydroxide (i.e. is added as a solid to the reaction mixture) the silicate species trapped in the gel framework will depend on the species first formed as the silica dissolved. If the silica dissolves initially as monomeric fragments, the gel formed initially will have an alumino-silicate structure with alternating silicate units and this highly ordered gel will be more likely to form zeolite X. When the silica dissolves to give colloidal particles, in addition to monomeric species, as for low surface area silicas, the gel must incorporate these particles into its structure and this will promote the formation of zeolite P1 in preference to zeolite X. These mechanisms are presented schematically in figure 2.3.

It appears from this work that the formation of zeolite X, in systems containing amorphous silica as the silica source can be roughly correlated with the surface area of the silica, as suggested by Schwochow et al[98].

FIG. 2.2 ^{29}Si n.m.r. FOR SOLUTIONS OF CAB-O-SIL AND PRECIPITATED SILICA

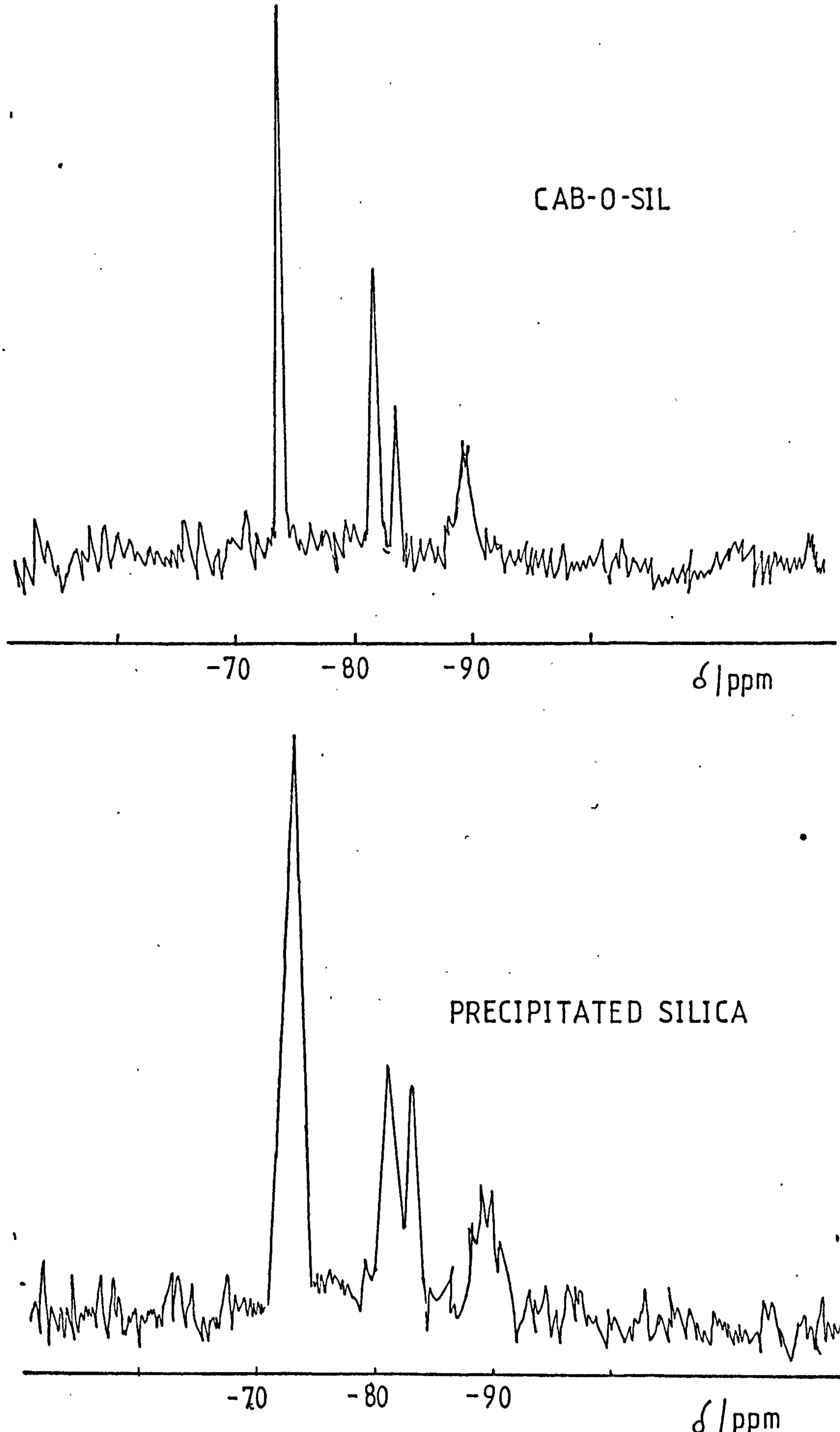

FIG. 2.3 SCHEMATIC DRAWING OF MECHANISMS OF ZEOLITE X AND P1 FORMATION

UNDISSOLVED SILICAS

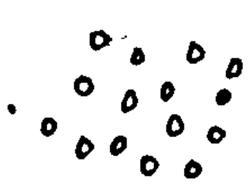

very small silica particles/high surface area materials

NaOH

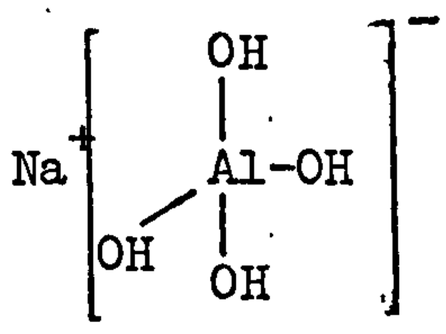

Aluminate ions

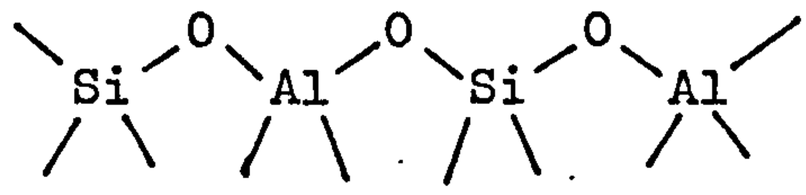

highly ordered gel structure

zeolite X

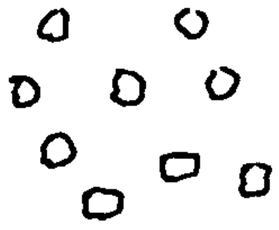

large silica particles/low surface area materials

NaOH

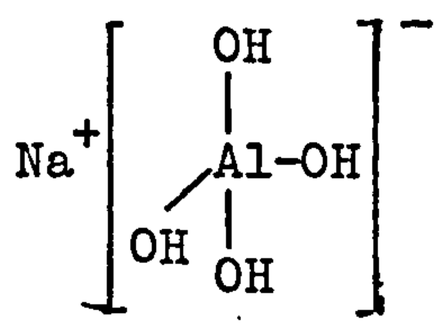

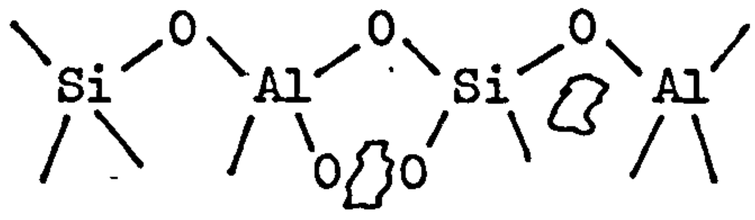

small colloidal silica particles trapped in the gel - either as undissolved solids or possibly chemically linked

zeolite P1

DISSOLVED SILICAS

either high or low surface area silica

NaOH

sodium silicate solution containing silicate monomers, dimers and higher polymers

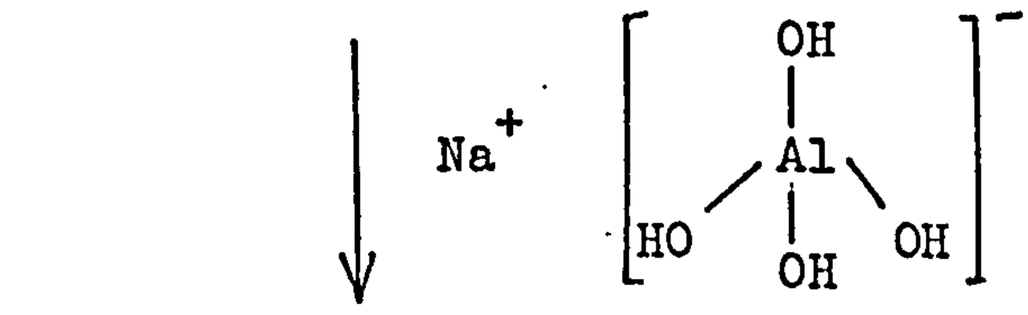

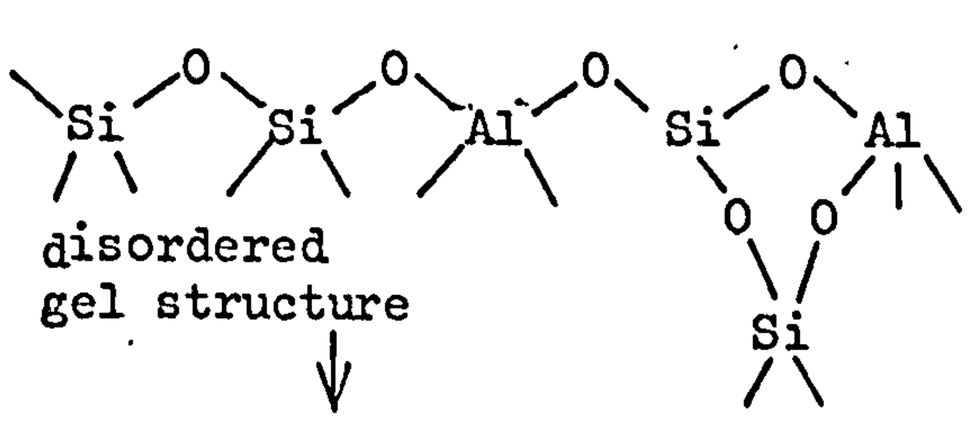

disordered gel structure

zeolite P1

2.3.3 REACTIONS WITH MIXTURES OF AMORPHOUS SILICAS

To be certain that there is a correlation between surface area of undissolved silica and the product of the reaction a series of identical silicas with different surface areas might be investigated. An alternative method of finding out if there is a correlation is to use a mixture of silicas. The four amorphous silicas of known surface area were combined in 50-50 mixtures giving six possible combinations. All of these silica mixtures were added to the reaction mixtures undissolved and the synthesis carried out as described for pure silicas. The results are shown in table 2.3. The overall surface area was taken as the arithmetic mean of the surface areas of the component silicas. In those reactions in which the surface area was less than or equal to 100 $m^2\ g^{-1}$ the product obtained in 4 hours was zeolite P1. However, as the surface area was increased the formation of significant amounts of zeolite X was observed.

In reactions 2.20 and 2.18 in which the silica source was a mixture of CAB-O-SIL M5 and precipitated silica and CAB-O-SIL M5 and KS300 respectively the zeolites formed were, in fact, zeolite Y. This crystallisation of zeolite Y from systems containing amorphous silica has been reported by Breck and Flanigen[62].

These results give further evidence to suggest that the formation of faujasite type zeolites can be roughly correlated with the surface area of an amorphous silica. They are consistent with the mechanism suggested in the previous section in that the system which contained only precipitated silicas i.e. reaction 2.16 gave only zeolite P1 whereas when higher surface area silicas i.e.

TABLE 2.3 PRODUCTS OF REACTIONS WITH MIXTURE OF UNDISSOLVED SILICAS

Run No.	Silica Materials	Surface Area[a]/m^2 g^{-1}	Products		
			4h[b]	5h	6h
2.16	ppt.SiO_2 + KS300	104	P1(100)		
2.17	ppt.SiO_2 + coll.SiO_2	127	X(24)	X	X+tr.C.
2.18	ppt.SiO_2 + CAB-O-SIL M5	141	Y(47)	Y+tr.P1	Y+P1
2.19	KS300 + coll.SiO_2	158	X(53)	X	X+tr.C.
2.20	KS300 + CAB-O-SIL M5	171	Y(28)	Y	Y+tr.P.
2.21	Coll.SiO_2 + CAB-O-SIL M5	194	X(38)	X+P1	X+P1

[a] See text.

[b] Figures in brackets are percentages based on intensities measured from Guinier-Hagg films using a Joyce microdensitometer. All quantities are relative to a reference Linde 13X or a laboratory synthesised zeolite P1.

CAB-O-SIL M5 or coll. SiO_2 were present the product was predominantly a faujasite type zeolite. Presumably the formation of the reactive ordered gels described previously has a greater influence on the reaction than the incorporation of the colloidal particles in the gel.

2.3.4 CONCLUSIONS

The results reported here are not entirely in agreement with those in the patent literature[60,65] in which it is claimed that only amorphous silicas with a surface area greater than 150 $m^2\ g^{-1}$ will react to give pure zeolite X since it was found that a silica with surface area 135 $m^2\ g^{-1}$ also gave zeolite X. However, this is not surprising, since the surface area is not the essential cause of zeolite X formation in these systems. As already stated, the prime reason for zeolite P1 formation by the low surface area silica used in this work is probably the presence of colloidal materials which nucleate this zeolite in preference to zeolite X, whilst the high surface area silicas form the reactive ordered gels which promote zeolite X formation. The way in which the amorphous silica dissolves and the type of gel formed are more important than the surface area of the amorphous silica which only gives a rough indication of the type of behaviour to be expected.

2.4 REACTIONS WITH KIESELGUHR

In addition to various high surface area silicas Schowchow et al[98] investigated the use of Kieselguhr as a silica source for the zeolite X synthesis. Kieselguhr is the impure silica (contains ~5% Al_2O_3) made from the skeletons of

diatomaceous earth. The material is very finely divided and in its uncalcined form it is very reactive. Schowchow and his co-workers[98] found that uncalcined Kieselguhr gave zeolite P1 in a typical zeolite X reaction.

Unfortunately this synthesis[98] could not be repeated as part of the present investigation as only calcined Kieselguhr was available. Syntheses were however attempted with two different forms of calcined Kieselguhr (see experimental section 2.2.4) and both give a similar mixture of products. The results are shown in table 2.5. For reaction 2.22 in which the silica source was Kieselguhr purified with acid, the zeolitic products after 5 hours were zeolite A and a zeolite which appears to be closely related to Losod. The peaks observed are listed in appendix 1.

TABLE 2.5 PRODUCTS OF REACTIONS WITH CALCINED KIESELGUHR

Run No.	Type of Kieselguhr	Product	
		3h	5h
2.22	Purified with acid	A+Kieselguhr	A+Losod type+ Kieselguhr
2.23	White Kieselguhr	-	A+HS+Losod type+ Kieselguhr

An attempt was made to relate the lines observed to those in hydroxysodalite but none of the observed lines match up with those in hydroxysodalite. Although there are lines in Losod which do not appear in the material obtained in this work, the strong lines are present which strongly indicates that this material is Losod or at least a closely related material.

For reaction 2.23 the zeolite products were zeolite A, hydroxysodalite and the Losod-type material. The peaks observed are listed in appendix 1 and although agreement of the observed lines with those reported is not quite as good as for reaction 2.22, it is obvious that the product is a mixture of zeolite A, hydroxysodalite, and the Losod-type material. The lines for hydroxysodalite and the Losod-type material overlap to some extent, but the line at d = 11.03 Å is convincing evidence that the Losod-type material is present.

The formation of zeolites A and hydroxysodalite in these Kieselguhr systems is not surprising since the slow dissolution of Kieselguhr means that the crystallisation occurs from an aluminate rich solution phase and this normally yields zeolite A or hydroxysodalite. However, the formation of the Losod-type material was unexpected. Losod is a sodium zeolite, the only previous reported synthesis of which occurred in a mixed base system containing sodium and, for example, bispyrrolidinium, $C_8H_{16}N^+$, although no organic cations were incorporated. The workers[49] who first synthesised this material concluded that the organic base served only as a source of hydroxyl ions. Assuming that their interpretation of the observed result is correct it is reasonable to assume that the systems with Kieselguhr must be extremely alkaline. This is possible since in reaction 2.22 once zeolite A has formed much of the aluminate will have been used up leaving a system which will be very alkaline and thus permit the formation of the Losod-type material. This result is worth more detailed investigation as it is the first reported synthesis of a Losod-type material in a pure sodium system.

CHAPTER 3

ZEOLITE SYNTHESIS WITH 'ACTIVE' SODIUM METASILICATES

3.1 INTRODUCTION

The use of 'active' sodium metasilicates in zeolite X and Y synthesis reactions to provide a directing influence on the product of the reaction is well known and has been discussed in chapter 1, section 1.8.2.2. In this chapter the kinetics of reactions in which part of the silica was supplied by an 'active' sodium metasilicate have been investigated in some detail, while varying the complementary silica source.

This type of study has not been carried out by any other workers in the field and it was believed that it would give a valuable insight into the influence of the different silica-sources on not only the product of the reaction but also the rate of reaction and the mechanism of zeolite X formation.

3.2 EXPERIMENTAL DETAILS

3.2.1 MATERIALS

A 3 kg sample of sodium metasilicate pentahydrate was tested and shown to be 'active'. This was then used as the source of 'active' metasilicate in all the experiments, except where otherwise stated. Three different types of commercial sodium silicate waterglasses were used: type C100 ($Na_2O.2.05SiO_2.14.27H_2O$), type Q79 ($Na_2O.3.39SiO_2.23.9H_2O$) both supplied by I.C.I. Ltd. (Mond Division) and BDH waterglass ($Na_2O.2.5SiO_2.13.5H_2O$). The amorphous silicas and silica sol were the same as these used for the work described in chapter 2.

The sodium hydroxide was BDH Ltd. AnalaR grade reagent and the alumina trihydrate was BDH Ltd. technical grade. All reaction mixtures were prepared with laboratory distilled water.

3.2.2 PROCEDURE

3.2.2.1 Reaction procedure with active sodium metasilicate

The overall reaction composition used for the synthesis of zeolite X in this work was

$$5.15Na_2O\ Al_2O_3\ 3.98SiO_2\ 240H_2O^{a}$$

The active metasilicate in the reaction mixture only contributed 1/9 of the total silica requirement, the balance being supplied by either an inactive sodium silicate solution with $SiO_2/Na_2O > 2$, an amorphous silica or a silica sol.

A typical reaction mixture was set up in the following way: Pure sodium hydroxide (11.9 g) was dissolved in distilled water (11.9 g) and alumina trihydrate (7.8 g) was added. The mixture was boiled until a clear solution was obtained, allowed to cool to room temperature and the lost water was then replaced. Sodium metasilicate pentahydrate (4.7 g) was dissolved in distilled water (50 g) at a temperature below 35°C. Sodium disilicate waterglass type C100 (38.4 g); or the molar equivalent amount of another inactive silicate was added to the metasilicate solution and mixed thoroughly using an electric mixer. The previously prepared sodium aluminate solution was added slowly with stirring to form a thick white gel. Distilled water (126.2 g) was then added and the

[a] unless otherwise stated

mixture was stirred until completely homogeneous. This mixture was then placed in the reaction vessel and stirred under reflux at 95°C for at least three hours.

For those reactions in which the additional silica source was an amorphous silica or a silica sol the procedure for setting up the reaction was as described in chapter 2. In this work all the reactions were set up adding the amorphous silicas as solids, unless otherwise stated.

3.3 USE OF VAPOUR ABSORPTION TO STUDY THE KINETICS OF ZEOLITE FORMATION

3.3.1 GENERAL OUTLINE OF METHOD

The method of vapour absorption to study the kinetics of zeolite formation is based on the fact that it is possible to determine the amount of zeolite in a sample, knowing the amount of vapour which the sample absorbs. Zeolite X can absorb water vapour and also much larger molecules such as cyclohexane. For zeolite X analysis it is preferable to use cyclohexane, as it is not significantly absorbed by the amorphous aluminosilicate gel formed at the beginning of the reaction, or by other zeolites such as P1 or A which could be present as impurities. Since zeolites P1 and A do, of course, absorb water vapour, it is possible to analyse mixtures of zeolite X with either zeolite A or zeolite P1 by measuring their uptake of cyclohexane and water.

3.3.2 ABSORPTION METHOD: PRELIMINARY INVESTIGATION

An absorption method was designed to measure the extent of water absorption of pure samples of zeolite X. Approximately 1 g of zeolite was weighed accurately in a sample

bottle of known weight. The zeolite sample was then dried in a furnace at 350°C for a period of from 1 hour to 3 hours and then allowed to cool over P_2O_5 for 16 hours. The dry weight of the sample was then determined. It was important to ensure that the lid of the sample bottle was fitted securely when weighing in order to prevent absorption of water vapour from the atmosphere. The samples and bottles were then placed in a metal block in which eight circular recesses had been machined. Samples were placed in six of the recesses whilst the remaining ones held bottles containing saturated solutions of calcium nitrate. A saturated aqueous solution of calcium nitrate has a vapour pressure of 12 mmHg at 25°C, and the samples were thus equilibrated with water vapour at this pressure. The block was placed in a 25 cm, type 4, Jencons "Dry Seal" desiccator. The complete apparatus could be evacuated by connection to a water pump. The rate of pumping was reduced to an acceptable level by use of a 13 cm length of 1 mm internal diameter glass tubing as the connecting link between the apparatus and the pump. The desiccator was then placed in a thermostat bath at 25°C. The samples were weighed at 24 hour time intervals until the weight was constant. The results for samples of pure zeolite X (Linde 13X) are shown in table 3.1 and those for pure zeolite P1 (a laboratory synthesised sample) are shown in table 3.2. In addition, samples were taken from a reaction and using the method described above were equilibrated with water vapour for 8 days and sorption capacities measured. The amount of water absorbed was plotted against time at which the sample was taken and a zeolite growth curve for zeolite P1 is shown in figure 3.1.

Although this method worked very well, as shown by the results obtained, it was not ideal. The length of time of equilibration was

TABLE 3.1 WEIGHT OF WATER ABSORBED BY LINDE ZEOLITE 13X g/g

Sample	Time in furnace/h	Equilibration Time/h 24	72	96	120	144	168
A	1	0.298	-	0.313	0.310	0.309	0.309
B	1	0.296	-	0.311	0.308	0.307	0.307
C	2	-	0.297	0.295	0.307	0.301	0.299
D	2	-	0.298	0.296	0.306	0.301	0.298
E	65	0.289	0.298	0.296	-	-	0.298
F	65	0.293	0.303	0.303	-	-	0.306
G	3	0.308	0.311	0.309	-	-	0.310
H	3	0.304	0.307	0.305	-	-	0.306

TABLE 3.2 WEIGHT OF WATER ABSORBED BY ZEOLITE P1 g/g

Sample	Time in furnace/h	Equilibration time/h 24	48	72
K	1	0.202	0.199	0.199
L	1	0.203	0.200	0.201
M	3	0.197	0.198	0.198
N	3	0.198	0.197	0.198

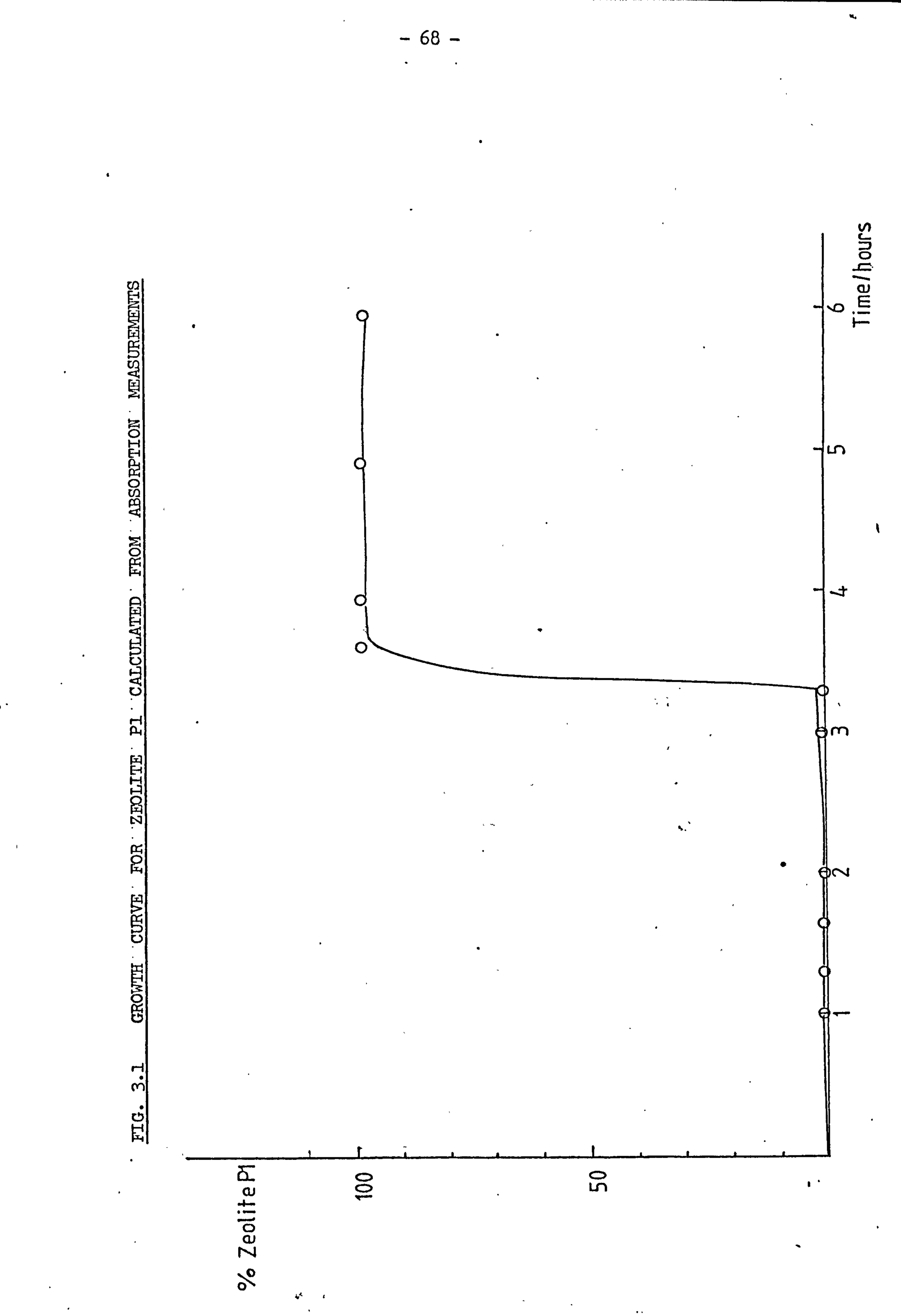

FIG. 3.1 GROWTH CURVE FOR ZEOLITE PI CALCULATED FROM ABSORPTION MEASUREMENTS

in excess of 2 days in most cases, and this was considered unacceptable. In addition, for analysis of mixtures of zeolites it was necessary to use cyclohexane, and it was found that this substance reacted with the high vacuum grease on the desiccator tap. In view of these problems it was decided that a more sophisticated method should be used.

3.3.3 ABSORPTION METHOD: FINAL FORM OF APPARATUS

The final apparatus used for absorption measurements was based on a design by Landolt[101]. A schematic diagram of the apparatus is shown in figure 3.2. It consisted of a glass absorption chamber, which was a 25 cm, type 4, Jencons desiccator sealed with an O-ring. This chamber was capable of holding 20 zeolite samples in 10 cm^3 glass weighing bottles. The absorption chamber was connected by a common manifold and solenoid valve to three separate absorbate reservoirs. The absorbate pressure was controlled by mercury manometers with preset contact points which operated a solenoid valve (Edwards High Vacuum Ltd., type D11103) by means of a relay. The manometer contacts were nominally set to give absorbate pressures of 10 and 20 mm Hg. The complete range of absorbate pressures could be measured by means of a Zimmerli gauge.

Since it was intended that the system should be used with organic solvents, greased joints and taps were avoided. All the taps were of the Rotaflo type, and the absorbate reservoirs were connected to the line with teflon sleeves (Fisons Ltd., type FVS/1). Although it was not possible to obtain a very high vacuum ($<10^{-2}$ mm) in this completely grease free system, it was considerably less trouble to operate with e.g. cyclohexane than a greased system. Also for kinetic

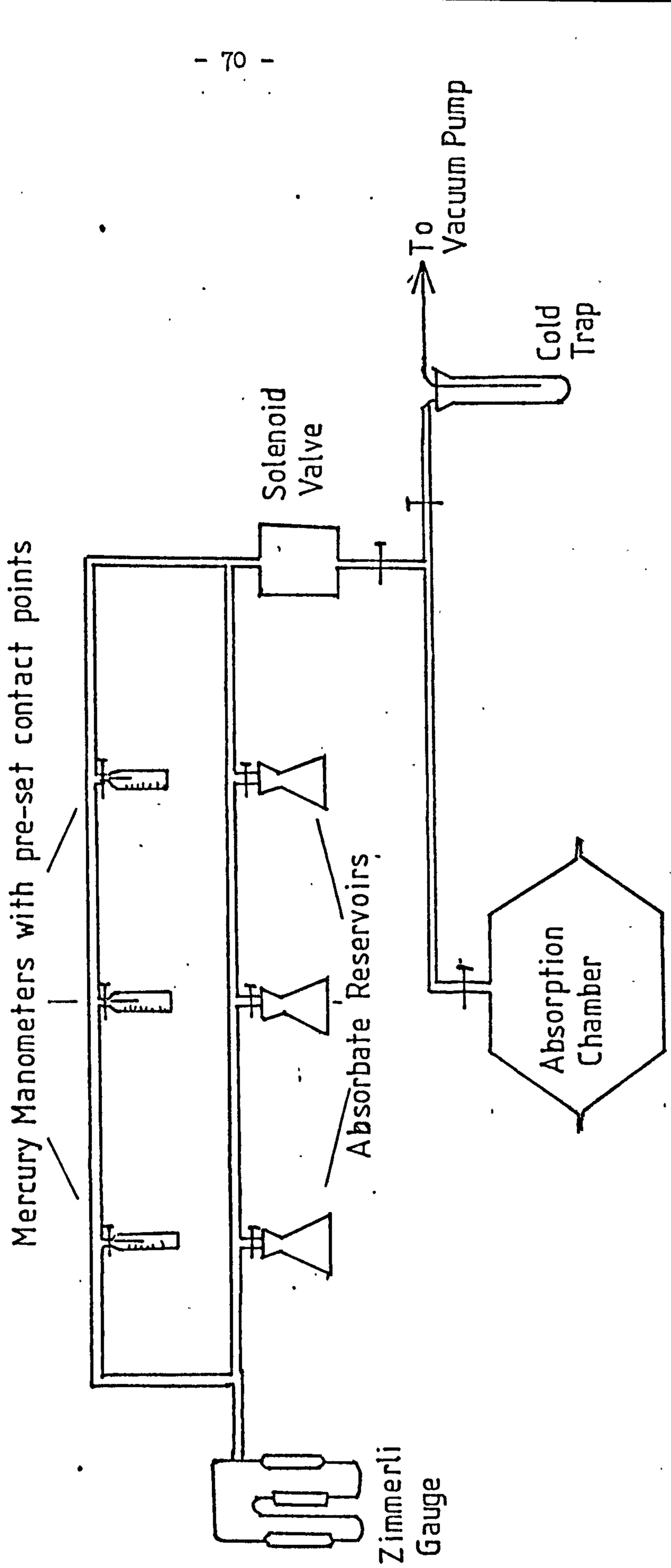

FIG. 3.2 SCHEMATIC DIAGRAM OF APPARATUS USED FOR ABSORPTION MEASUREMENTS

measurements, relative rather than absolute absorptions are important, and so failure to obtain a really high vacuum was not significant.

The system was evacuated by a rotary vacuum oil pump, protected by a cold trap filled with solid carbon dioxide.

3.3.4 PROCEDURE

When the apparatus described in section 3.3.3 was used to obtain zeolite growth curves, the following procedure was adopted. The dried samples which had been taken during the reaction were placed in pre-weighed 10 cm^3 weighing bottles. These samples, together with standard reference samples of zeolites 13X and P1, were placed together in a 15 cm diameter pyrex crystallising dish. All samples were then activated in a vacuum oven at $180^{\circ}C \pm 2^{\circ}C$ for at least 4 hours. After which they were removed, placed in a desiccator and cooled, in vacuo to room temperature, over P_2O_5. The lid was then removed from the desiccator and the sample bottle lids replaced rapidly to minimise exposure of the samples to the air. The bottles were then weighed. They were then placed in the sorption chamber and the lids removed rapidly prior to closing the chamber. After the activation step it was crucial to the experiment that the samples were not exposed to the air more than was necessary, as any water picked up at this stage could affect the final result.

The system was evacuated to 10^{-2} mm Hg, and the desired sorbate was then admitted and its pressure maintained at the pre-set value. The pressure was set at about half the room temperature vapour pressure of the liquid absorbate so that direct condensation of liquid on the sample or its container was completely avoided. Normally the time required to reach equilibrium

was about one hour for cyclohexane and two hours for water. It was usually considered that equilibrium had been achieved when the relay switch remained in the off position for at least fifteen minutes. The bottles were then removed, lids replaced and re-weighed. The amount sorbed was determined by difference.

3.3.5 METHOD OF OBTAINING PER CENT CONVERSION VALUES FROM SORPTION DATA

In general, the samples studied by the absorption method contained zeolites X and P1 and amorphous gel. All three components absorb water but only zeolite X absorbs significant amounts of cyclohexane. Thus, dried amorphous gel was found to absorb ∿0.01 g/g of dry material, pure zeolite P1 absorbed ∿0.005 g/g of dry activated material whereas zeolite X absorbs ∿0.14 g/g of dry zeolite, for 20 mm Hg pressure of cyclohexane. Since the internal channels of zeolite P1 and the amorphous material are too small to absorb cyclohexane, the absorption must be related to the external surface area of the particles. The pore size of zeolite A, which was formed in a few reaction mixtures, is also too small to absorb cyclohexane. For samples which contained only zeolite X and amorphous material, the amount of zeolite X was determined by cyclohexane absorption. For samples which contained mixtures of zeolite X and P1 water vapour absorption measurements were also made and the relative amounts calculated (see chapter 5).

3.3.6 CALCULATION OF COMPOSITIONS OF MIXTURES OF ZEOLITE X AND AMORPHOUS GEL

For samples which contained only zeolite X and amorphous material the amount of zeolite X was determined by cyclohexane

absorption. For each sample the weight of cyclohexane absorbed per dry weight of sample was calculated as

$$A = \frac{WBSC - WBS}{WBS - WB} \qquad (3.1)$$

in which WBSC - weight of bottle + sample + adsorbed cyclohexane

WBS - weight of bottle + sample

WB - weight of bottle.

The values of A obtained for amorphous samples decreased slightly during a run as the structure of the amorphous gel changed and the lowest value of absorption on the amorphous material was taken as the absorption capacity of the amorphous gel, A_{Am}. If the absorption of cyclohexane on the standard sample of zeolite 13X calculated by equation (3.1) is denoted by A_X then the absorption capacity of any sample can be written as,

$$A = x_X A_X + x_{Am} A_{Am} \qquad (3.2)$$

where x_X and x_{Am} are the fractional amounts by weight of zeolite X and amorphous material present in the sample.

If A_X and A_{Am} stay constant throughout the run, and a percentage change in the amount of gel always gives a corresponding change in the amount of zeolite X then equation (3.2) holds.

This equation is derived as follows:- consider a sample of weight w made up of W_X and W_{Am} grams of zeolite X and amorphous gel respectively. Then -

$$wA = W_X A_X + W_{Am} A_{Am}$$

$$A = \frac{W_X}{w} A_X + \frac{W_{Am}}{w} A_{Am}$$

$$A = x_X A_X + x_{Am} A_{Am} \qquad (3.2)$$

Also since $w = W_X + W_{Am}$

$$1 = \frac{W_X}{w} + \frac{W_{Am}}{w} = x_X + x_{Am}$$

$$\text{i.e.} \quad x_X + x_{Am} = 1 \qquad (3.3)$$

It is important to note that the assumption that A_X and A_{Am} stay constant throughout the run is not necessarily true. It is known that A_{Am} steadily decreases up until the start of formation of zeolite X and it may continue to do so. In addition, it is possible that as zeolite X grows, A_X may change as the particle size and structure changes during synthesis, i.e. initial tiny particles may have better absorption. In summary then, it is possible that A_{Am} decreases during zeolite formation and A_X could also decrease during zeolite formation. Unfortunately, there is no simple way of taking these possibilities into account, but it is important to realise they exist.

Combination of equations (3.2) and (3.3) gives

$$x_X = \frac{A - A_{Am}}{A_X - A_{Am}} \qquad (3.4)$$

the weight fraction of zeolite X in the sample. The amount of amorphous material was calculated using equation (3.3).

A computer program written in FORTRAN was used to carry out the calculations.

3.3.7 ANOMALOUS BEHAVIOUR OF SYNTHESISED ZEOLITE X VERSUS LINDE 13X

If A_X is obtained by measurements on zeolite 13X, a pure zeolite X analysed by the absorption method will have a value of $x_X = 1.0$, provided its absorption characteristics are the same as those of zeolite 13X.

However, the absorption capacity of pure synthetic samples of zeolite X was often greater than that of standard 13X and consequently the value calculated for x_X was greater than unity. This was found for most zeolite X synthesis which had gone to completion; the zeolite X produced in the laboratory reaction mixtures was invariably a better absorber than zeolite 13X. Similar results were obtained by Kerr[70]. Therefore, to obtain sensible measures of the amount of zeolite X formed during a reaction it was necessary to introduce a correction factor f such that

$$A_X = A_{13X}.f.$$

Since it was possible for f to vary for each zeolite formed it was decided to take the run which gave the maximum value of A_X and use the f calculated from this. Therefore, it was necessary to modify equation (3.4) to the form

$$x_X = \frac{A - A_{Am}}{A_{13X}f - A_{Am}} \qquad (3.5)$$

3.4 COMPARISON OF X.r.d. AND SORPTION DATA

3.4.1 INTRODUCTION

A comparison of the percentage of zeolite X calculated from sorption data was made with the percentage zeolite X calculated from x-ray diffraction intensities and this is shown in figure 3.3. For both X.r.d. and sorption studies the reference sample was Linde 13X.

It was found that the samples of zeolite X synthesised in this work absorbed more water and cyclohexane than Linde 13X. However, in contrast, it was found that the synthesised samples had smaller X.r.d. peaks than Linde 13X. Using both X.r.d. and scanning electron microscopy, no impurities were observed either in the Linde 13X or the best synthesised sample of zeolite X. Kerr also found that laboratory synthesised zeolite X absorbed more than Linde 13X, but in contrast to the present observations he found that his materials had higher X.r.d. peak heights than zeolite 13X.

A possible explanation of this anomalous situation can be developed by considering the particle size of the zeolite. From scanning electron micrographs for the best samples of zeolite X obtained in this work and Linde 13X, it was observed that the crystals of the synthesised sample were much smaller and better formed than those of Linde 13X. Since these crystals were smaller than those of Linde 13X, there is less likelihood of defects and therefore they are likely to be better absorbers. In addition, the surface area of the synthesised sample is much greater than that of Linde 13X and therefore may make a significant contribution to the adsorption. Furthermore, the observation that X.r.d. peak heights were always smaller for synthesised samples than for Linde 13X can be explained in terms of crystallite size differences since it is well known that broadening of lines in an x-ray powder diffraction

FIG. 3.3 COMPARISON OF X.r.d. AND SORPTION DATA

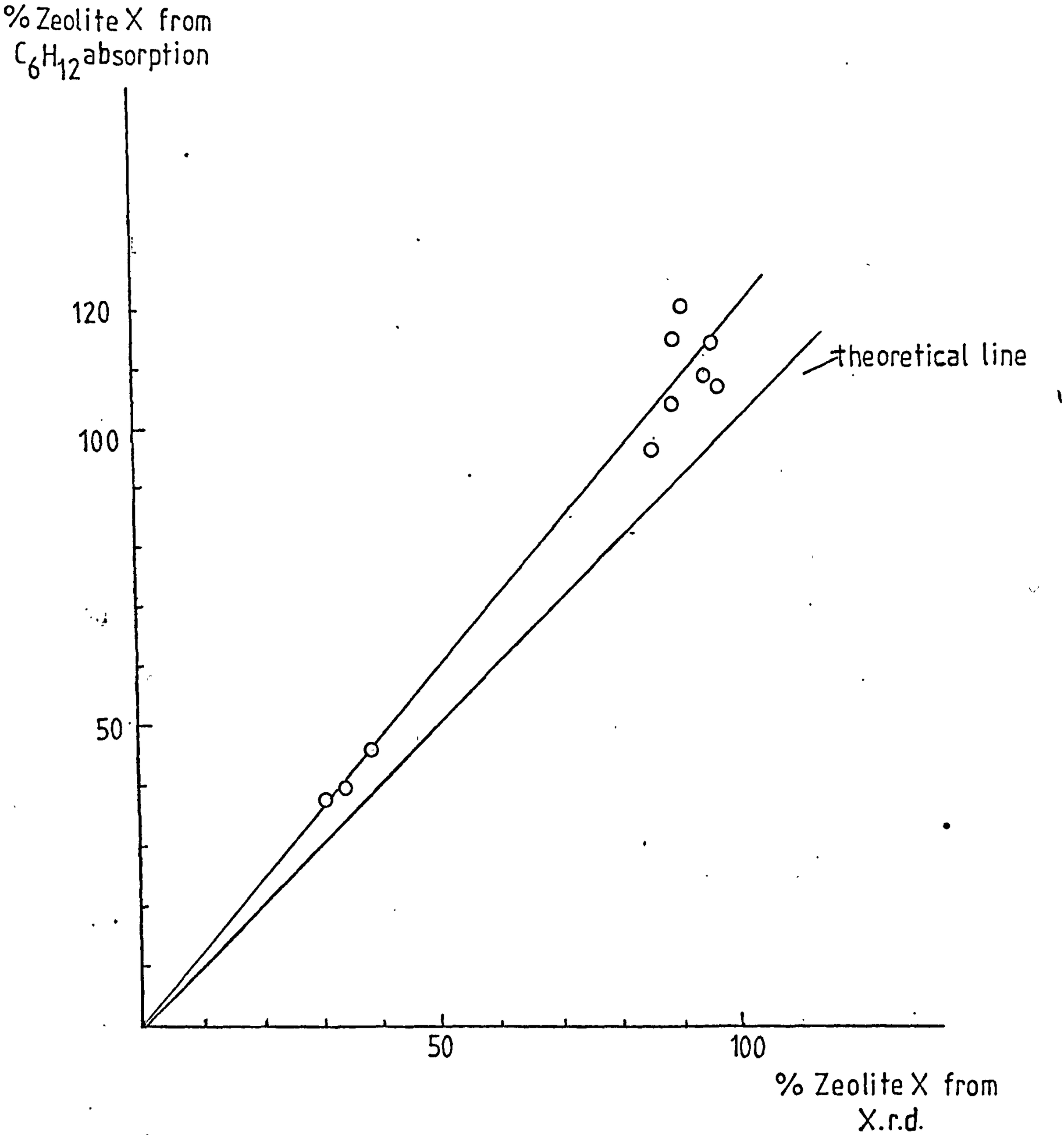

pattern occurs when the crystals become small and that in consequence the peak heights appear smaller.

This section gives a detailed analysis of the effect of particle and crystallite size on sorption capacity and X.r.d. peak heights respectively.

3.4.2 EFFECT OF PARTICLE SIZE ON SORPTION CAPACITY

Particle size distributions (figure 3.4) for Linde 13X and zeolite X from reaction 3.10 were obtained by counting particles from the scanning electron micrographs,(see plates 1 and 2). An average particle diameter was calculated by a summation process

$$\bar{D} = \frac{D_1\Delta n_1 + D_2\Delta n_2 + D_3\Delta n_3 + -D_x\Delta n_x}{N_T}$$

where $\bar{D}$ = average particle diameter, D_x is the mid point of the block, Δn_x is the number of particles in the block and N_T is the total number of particles.

For reaction 3.10 $\bar{D} = 0.74\times10^{-6}$ m

and

for Linde 13X $\bar{D} = 2.51\times10^{-6}$ m

Knowing these values it was possible to calculate the surface area per gram of dry zeolite.

The area of a sphere, i.e. one particle, is

$$A = \pi D^2$$

and the volume is

$$V = \frac{\pi D^3}{6}$$

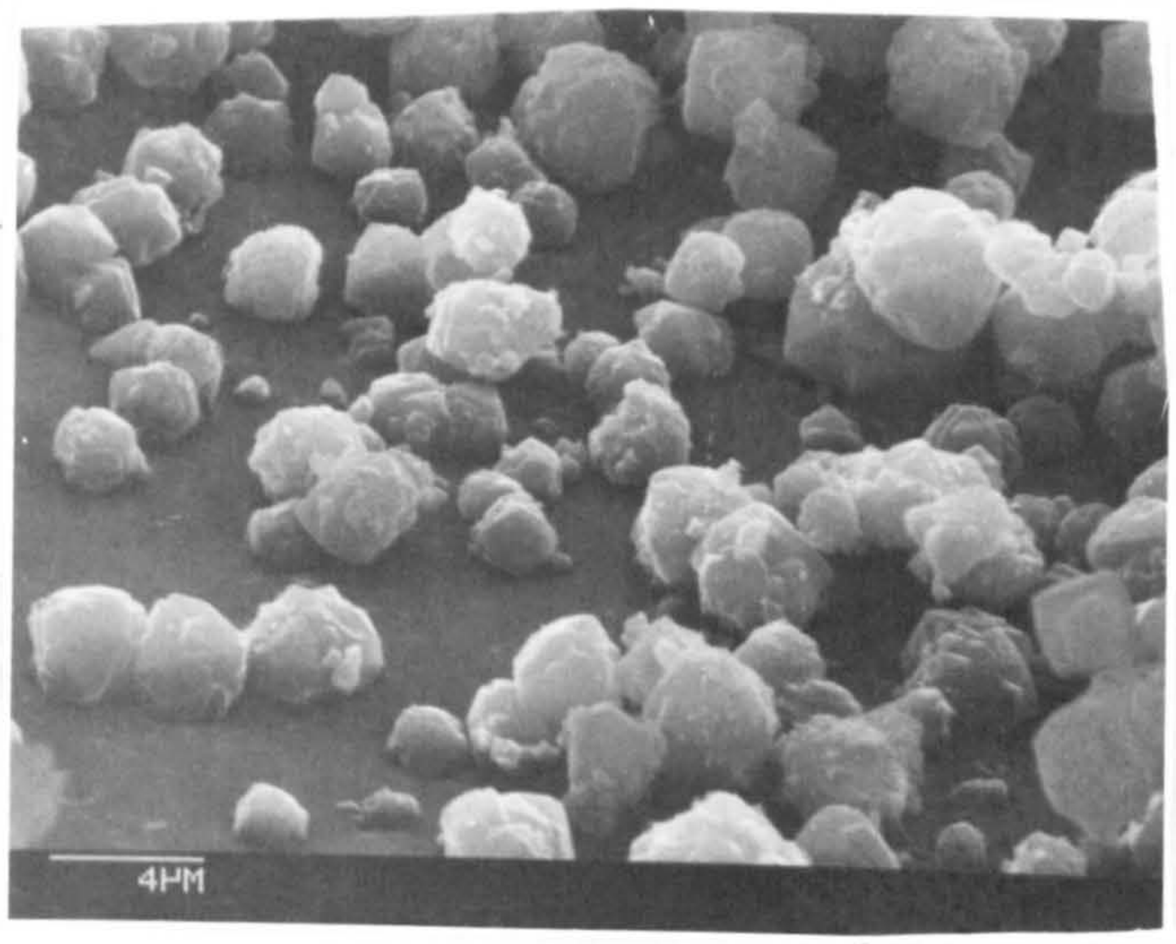

PLATE 1 —
LINDE 13X.

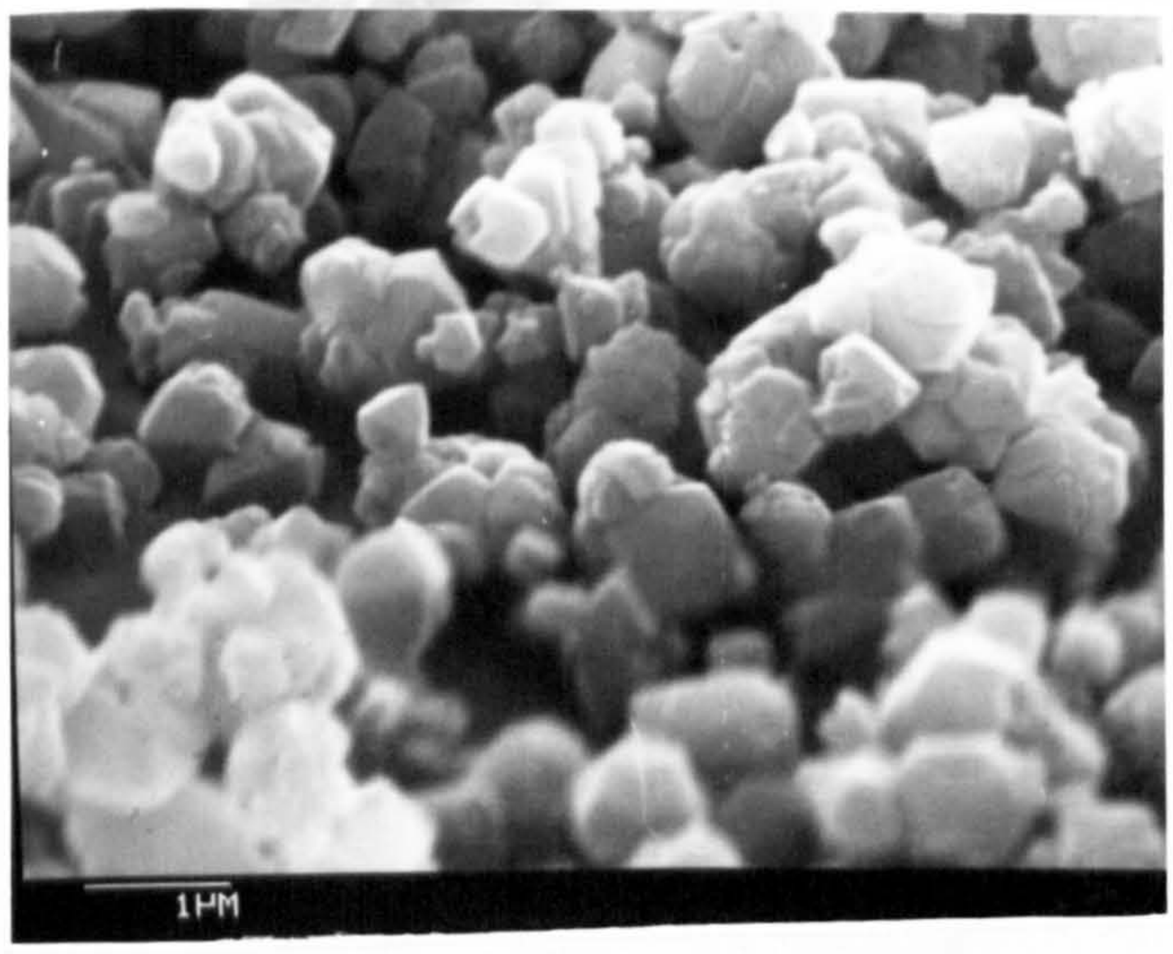

PLATE 2 —
Zeolite X from
reaction 3.10.

PLATE 3 —
Zeolite X from
reaction 3.15.

FIG. 3.4 PARTICLE SIZE DISTRIBUTIONS FOR LINDE 13X AND ZEOLITE X FROM REACTION 3.10

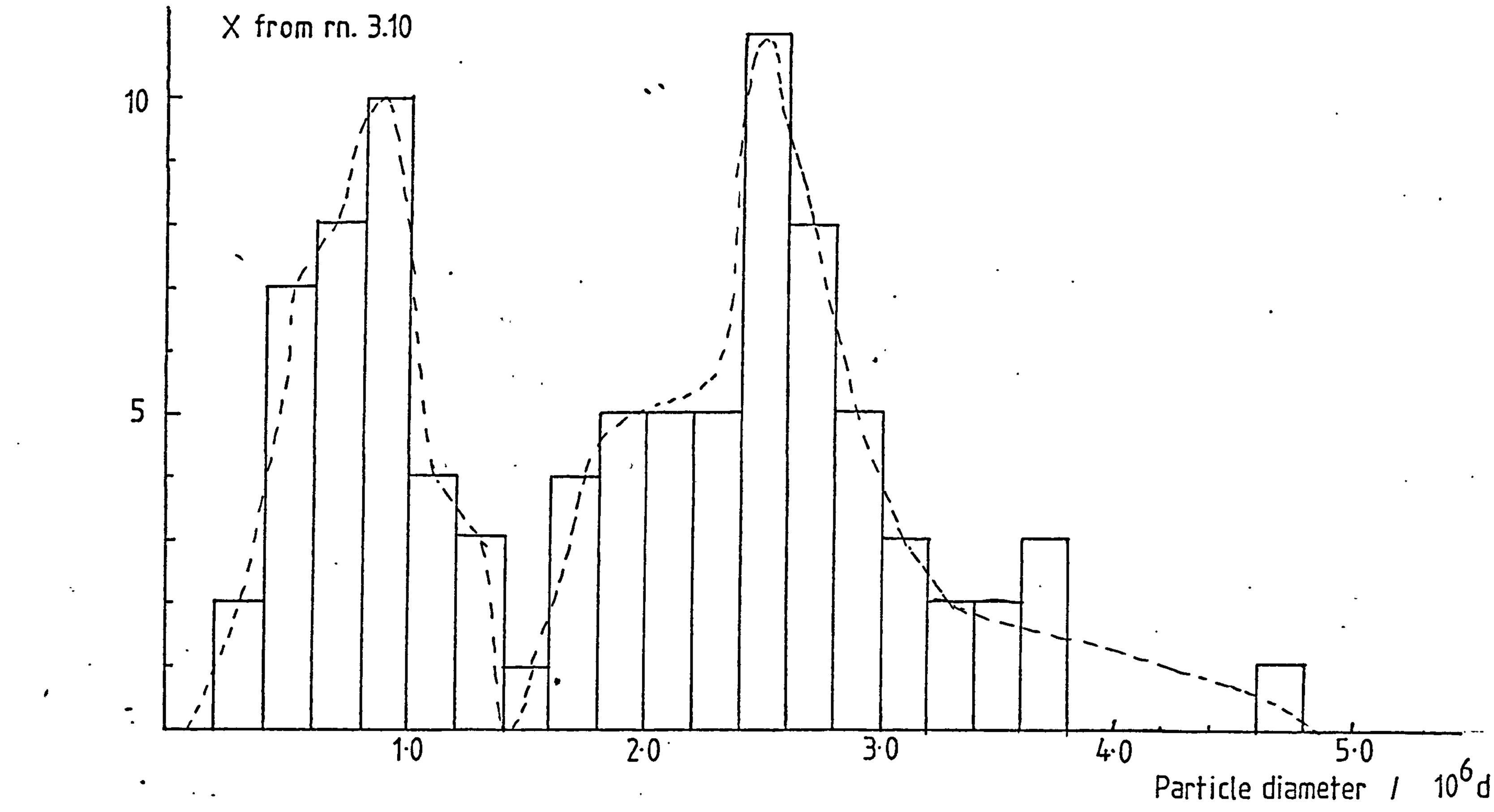

Now the number of particles per kilogram dry material is

$$No = \frac{1/d}{V}$$

where d is the density of the dehydrated material

$$\text{so} \qquad No = \frac{6}{d\pi D^3}$$

It follows then that surface area per kilogram is

$$S = \frac{6}{dD}$$

Using this equation the external surface areas for the synthesised zeolite X and Linde 13X were calculated to be

$4.54 \ m^2 \ g^{-1}$ for zeolite X from reaction 3.10

and

$1.46 \ m^2 \ g^{-1}$ for Linde 13X

(these are in good agreement with the surface areas determined by dye adsorption (see chapter 6)).

The maximum weight of cyclohexane and water which could be adsorbed on the external surface per kilogram of zeolite is given by

$$W = \frac{6}{dDA} = \frac{M}{N}$$

where A is the cross sectional area of the adsorbing molecule, M is its molecular weight and N is Avogadro's number.

If the approximate cross-sectional area[102] of cyclohexane is taken to be $44 \times 10^{-20} \ m^2$ and that for water is taken as $12 \times 10^{-20} \ m^2$ then

for zeolite X from reaction 3.10 $W_C = 1.43 \times 10^{-3}$ g and $W_H = 1.13 \times 10^{-3}$ g per gram of dry zeolite.

for Linde 13X $W_C = 0.46 \times 10^{-3}$ g and

$W_H = 0.36 \times 10^{-3}$ g per gram of dry zeolite.

The difference in cyclohexane adsorption between the synthesised zeolite X and Linde 13X, due to the difference in surface area, is therefore 0.97×10^{-3} g/g and for water adsorption is 0.77×10^{-3} g/g. These differences are small and can only account for approximately 25% of the difference in absorption observed for these zeolite X samples of approximately 4×10^{-3} g/g. It is likely that the remainder of the difference in absorption capacity is due to defects in the crystallites. The larger crystallites of Linde 13X are more likely to be subject to defects which will decrease the absorption capacity relative to the smaller and better formed crystallites of the synthesised zeolite X.

3.4.2 EFFECT OF PARTICLE SIZE ON X.r.d. PEAK HEIGHT

Measurements of half peak breadth B (i.e. the distance between the two points at which the intensity is half the maximum) for Linde 13X and zeolite X from reactions 3.2, 3.10 and 3.11, all pure zeolite X samples which exhibited anomalous behaviour, were carried out for the diffraction line at $2\theta = 23.4$. The results are shown in table 3.3. As can be seen from this table the laboratory synthesised zeolites have diffraction lines which are broader than those of zeolite 13X. In an ideal case this broadening should be related to particle size of the two zeolites by an equation[103] of the form,

$$B_1 - B_2 = \frac{\lambda}{\cos\theta}\left(\frac{1}{D_1} - \frac{1}{D_2}\right)$$

TABLE 3.3 PEAK WIDTH (B) AT HALF PEAK HEIGHT FOR ZEOLITE X SAMPLES

Source of Sample[a]	2B/°	Average value of 2B/°	Peak area (wt/g)[b]
Linde 13X	0.32)) 0.32)) 0.33)) 0.31)	0.31±0.01	0.0295±0.003
reaction 3.10	0.37)) 0.35)) 0.37)	0.36±0.01	0.0284±0.003
reaction 3.11	0.35)) 0.39)) 0.36)	0.37±0.02	0.0333±0.003
reaction 3.2	0.33)) 0.37)) 0.35)	0.35±0.02	0.0282±0.003

[a] At least 3 x-ray diffraction patterns were run on each sample

[b] The diffraction peaks were cut out and weighed as this was considered to be more accurate than measuring the area of the peak

in which λ is the wavelength of the radiation and θ is the angle of the diffraction line. Using the values of the crystal diameters D_1 and D_2 obtained from SEM for the sample from reaction 3.10 and for Linde 13X respectively, the line broadening $B_1 - B_2$ is calculated to be 0.01° which is somewhat less than the observed value of $0.07 \pm 0.01^{\circ}$. This poor agreement is probably because the particles are so large that true line broadening is only just detectable.

The area of the peaks for Linde 13X and zeolite X from reactions 3.2, 3.10 and 3.11 have been measured and were all found to be approximately equal (see table 3.3), as line broadening is accompanied by decrease in peak height. Thus the difference in behaviour of Linde 13X and the laboratory synthesised zeolites, summarised in figure 3.3 can be accounted for, at least in part, by the difference in their crystallite sizes. The smaller crystals of the synthetic zeolite give x-ray diffraction peaks which, because of line broadening, are not as high as those of Linde 13X, and since they have a larger surface area their absorption capacity is the higher. These two effects account for most of the observed behaviour (figure 3.3), but it should be noted that crystal defects in the larger Linde 13X crystals, causing a lower absorption capacity, could also contribute to the effect.

3.5 TREATMENT OF RESULTS

The results were analysed using the relationship found by Kerr[70,72] for the autocatalytic formation of zeolites A and X:-

$$\frac{dZ}{dt} = kZ \qquad (3.6)$$

in which Z = wt % of zeolite in the solid phase at time t and k is a rate constant.

Integration of equation (3.6) gives

$$\ln Z = kt + \ln Z_o \qquad (3.7)$$

where $Z_o = Z$ at $t = o$.

For all the reactions described in this chapter, the growth curves, % zeolite versus time, were plotted and the relation given in equation 3.7 was also plotted. The rate constant, k, was calculated from the slope of the straight line given by equation (3.7). The induction period was estimated by extrapolation of this straight line, and the growth period was taken as the time when crystallisation was complete as measured by absorption capacity minus the length of the induction period.

3.5.1 ERRORS

The errors involved in measuring the absorption capacity of the zeolite were estimated to be ±1%, giving an error in the percentage zeolite X calculated as approximately 5%. However, since a correction factor was applied to account for the anomalous behaviour of the synthesised zeolite X and the standard sample, Linde 13X, the error in the percentage zeolite X was approximately ±10%.

3.6 RESULTS

In the following sections the reactions described all contained 'active' sodium metasilicate as the minor part (1/9) of the total silica used in the reaction. The major part of the silica source

was provided by either amorphous silicas or sodium silicates with SiO_2/Na_2O greater than 2. The reactions carried out were all followed kinetically using the absorption method described in section 3.3.2.

3.6.1 REACTIONS WITH SILICATE SOLUTIONS AS THE MAJOR SILICA SOURCE

The products, induction period, growth period and rate constants for reactions 3.1, 3.2, 3.3 and 3.4 are shown in table 3.4. The growth curves are shown in figure 3.5. The product of reactions 3.1 and 3.2, in which the major silica source was C100, was pure zeolite X. For reactions in which the silica source was waterglass or Q79 respectively, i.e. 3.3 and 3.4, the product was major zeolite X with traces of zeolite P1. A correlation was found to exist between the SiO_2/Na_2O ratio of the silica source and the traces of zeolite P1 formed as shown in table 3.5. It can be seen that for SiO_2/Na_2O ratios greater than 2.5 no monomeric species are observed in the n.m.r. spectra of the sodium silicate. It appears then that the absence or low abundance of monomer species in the solution of the major silicate component is conducive to zeolite P1 formation. This is in agreement with the results of Schwochow and Heinze[79] who found that it was necessary to have a high monomer concentration in the silicate solution for zeolite X formation to be favoured. This finding is also consistent with the mechanisms suggested in chapter 2.

For all the reactions the induction period was 30±6 minutes. The growth period for reactions 3.2, 3.3 and 3.4 was 64±4 minutes, and for reaction 3.1 it was 46±8 minutes. This

TABLE 3.4 REACTIONS WITH SILICATE SOLUTIONS $SiO_2/Na_2O > 2$ AS THE MAJOR SiO_2 SOURCE

Run No.	SiO_2 Source	PRODUCT %X	PRODUCT %P1	Rate constant k/min^{-1}	Growth Period/min	Induction Period/min
3.1	C100[a]	96	-	0.105±0.018	46±8	32±4
3.2	C100	92	-	0.077±0.009	62±8	36±4
3.3	Na_2O $2.5SiO_2$ $13.5H_2O$[b]	88	5.4	0.074±0.004	64±4	24±2
3.4	Q79	84	11.7	0.070±0.016	66±16	28±8

[a] In this reaction the active metasilicate was supplied by J. Crosfield in all others it was supplied by BDH Ltd.

[b] Waterglass supplied by BDH Ltd.

TABLE 3.5 CORRELATION OF SiO_2/Na_2O RATIO AND ZEOLITE P1 FORMATION

Run No.	SiO_2/Na_2O	Material	% zeolite P1	Silicate anion distribution in starting material[a]
3.1	2.05	C100	0	A, B, C, D
3.2	2.05	C100	0	A. B, C, D
3.3	2.5	Na_2O $2.5SiO_2$ $13.5H_2O$	5.4	B, C, D
3.4	3.39	Q79	11.7	B, C, D, F

[a] Determined[67] from ^{29}Si n.m.r. spectroscopy

A - monomeric silicates

B - end groups e.g. dimers

C - chain or cyclic species

D - branched silicons - one silicon linked to three silicons • cyclic

F - one silicon bonded to three other silicons - non cyclic

Assignment of resonances to silicate species is discussed in detail in chapter 4.

FIG. 3.5 GROWTH CURVES FOR REACTIONS WITH SILICATE SOLUTIONS AS THE MAJOR SILICA SOURCE

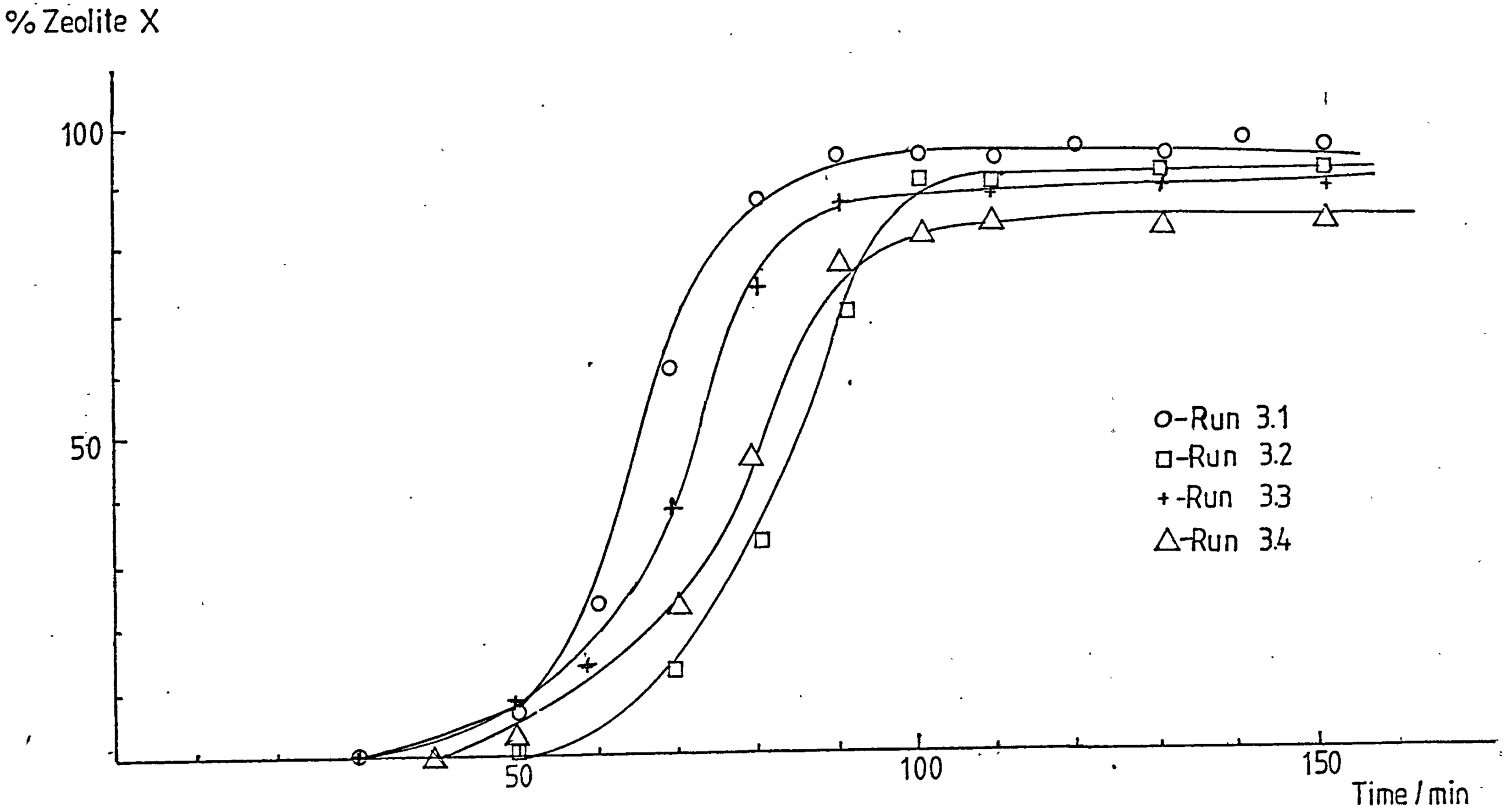

shorter growth period for reaction 3.1 is due to the fact that a different sodium metasilicate was used in this case. It is likely that the number and size of the nucleation centres will be different, therefore giving a different rate of reaction, as shown by Kacirek and Lechert[94].

3.6.2 REACTIONS WITH AMORPHOUS SILICAS AND SILICA SOL AS THE MAJOR SILICA SOURCE

The products, induction period, growth periods and rate constants for reactions 3.5 - 3.12 are shown in table 3.6. The growth curves are shown in figure 3.6. It is clear that although these reactions had identical stoichiometry, the nature of the products, and their rate of formation and induction periods show a strong correlation with the nature of the major silica source. For example, when the silica source is a silica of high surface area, i.e. colloidal silica powder or CAB-O-SIL M5 (reactions 3.10 and 3.11) the product is pure zeolite X. However, for the silica sources of lower surface area (reactions 3.6, 3.7 and 3.8) the product contained zeolites P1 and A in addition to zeolite X.

The correlation found between the surface area of the silica and the amount of zeolite P1 formed in reaction mixtures is tabulated in table 3.7. It can be seen that the amount of zeolite P1 formed increases as the surface area of the silica decreases.

This is in agreement with the findings in chapter 2. However, in these reactions with 'active' metasilicate, it is interesting that the driving force of the active material to give zeolite X is to some extent cancelled by the driving force of the colloidal silica particles to give zeolite P1, resulting in a final product

FIG. 3.6 GROWTH CURVES FOR REACTIONS WITH AMORPHOUS SILICA AND SILICA SOL AS THE MAJOR SILICA SOURCE

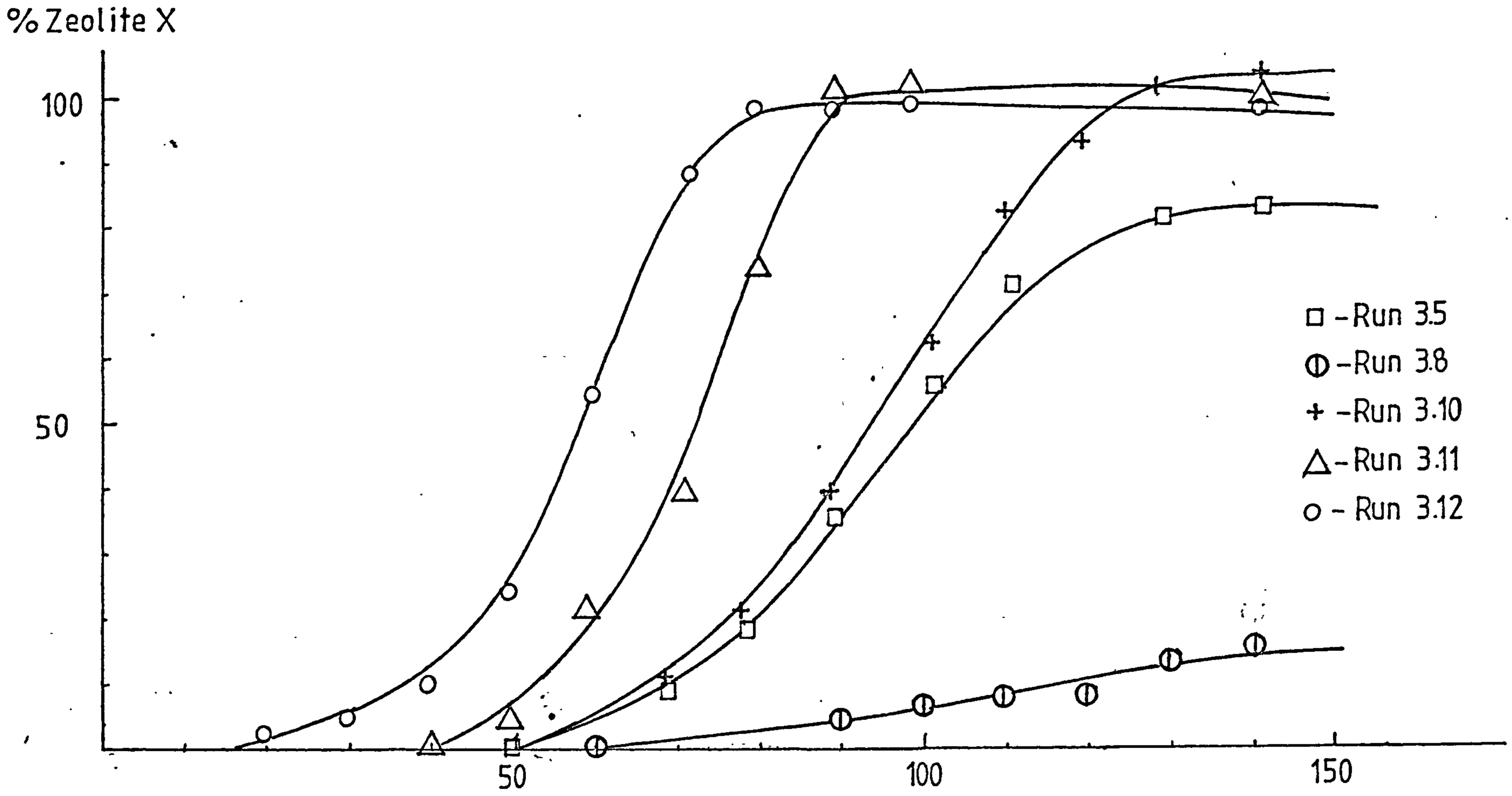

TABLE 3.6 REACTIONS WITH AMORPHOUS SILICAS AND SILICA SOL AS THE MAJOR SiO_2 SOURCE

Run No.	SiO_2 Source	%X	%P1	%A	Rate constant k min^{-1}	Growth period min	Induction period/min
3.5	Syton 30X	78	10	7	0.065±0.007	68±8	36±4
3.6	ppt SiO_2	-	80	-	0.033±[d]	90±	32±
3.7	"	8	70	-			
3.8	KS300	30	66	nd[a]	0.023±0.008[c]	150±20	30±18
3.9	"	33	67	nd	0.033±0.003[c]	110±10	50±10
3.10	Coll. SiO_2	96	-	-	0.056±0.008	84±12	28±8
3.11	CAB-O-SIL M5	92	-	-	0.071±0.004	66±4	20±4
3.12[b]	ppt SiO_2	96	-	nd	0.077±0.007	60±6	10±6

[a] nd - not detected by quantitative phase analyses with diffractometer however Guinier film showed traces of this material

[b] ppt SiO_2 was dissolved in NaOH prior to gelation

[c] growth rate for zeolite X only measured

[d] zeolite P1 growth rate.

TABLE 3.7 CORRELATION BETWEEN SURFACE AREA OF SILICA AND ZEOLITE P1 FORMATION

Run No.	Silica	Surface Area/m^2 g^{-1}	% zeolite P1
3.6	ppt. SiO_2	74	80
3.7	ppt. SiO_2	74	70
3.8	KS300	134	66
3.9	KS300	134	67
3.10	coll. SiO_2	181	-
3.11	CAB-O-SIL M5	201	-

containing a mixture of the two zeolites. The relative composition of zeolite X and P1 appears to be determined by the surface area or perhaps the type i.e. precipitated or colloidal of the amorphous silica.

The induction periods observed for reactions 3.8 - 3.11 were approximately 30±10 minutes. This is similar to that observed for those reactions discussed in section 3.6.1 and can probably be attributed to the fact that for each reaction the same amount of active material, from the same batch, was added. The growth periods, however, depend on the type of amorphous silica used (cf. 3.8 and 3.11). This is most likely related to the way in which the silica dissolves and the degree of ordering of the amorphous gel formed. This has been discussed in chapter 2.

For reaction 3.12, the induction period was 10±6 minutes. In this reaction, the silica was a precipitated silica and was dissolved in sodium hydroxide (C = 1.75 mol dm^{-3}), prior to addition to the aluminate solution. The ^{29}Si n.m.r. spectrum of this silicate solution, (see figure 2.1), shows that it contains a range of silicate anions similar to the range of species found in a sodium metasilicate solution. In both cases the monomeric species is predominant. Reaction 3.12 was the only one in which the major silica source contained a significant concentration of monomeric silicate anions prior to gel formation. It therefore appears that a high concentration of monomeric silicate species in the starting material will speed up the formation of nuclei, but does not affect the overall rate of growth. The active metasilicate present in this reaction provides the directing influence for zeolite X formation. In the absence of this material zeolite P1 would have been the product (reaction 2.1).

In reaction 3.5 the major silica source was a silica sol (syton 30X). The product of this reaction was a mixture of zeolite X, zeolite P1 and zeolite A. The induction period and growth period for zeolite X were similar to those observed for reactions with silica sources in which $SiO_2/Na_2O > 2$. The formation of zeolite A in this mixture was surprising since this zeolite normally forms from aluminate-rich solution phases, and the molar composition of this reaction gave a silicate rich-solution phase. However, it is possible that in the initial stages of the reaction, the system may in fact have been rich in aluminate, since on addition to sodium hydroxide, there was some precipitation of the silica sol.

For reactions 3.6 and 3.7 in which no zeolite X was formed an induction period and a growth period for zeolite P1 were measured. In both cases the observed induction period was short, in comparison to those observed by Kerr[70] for zeolite P1 growth.

3.6.3 EFFECT OF DILUTION ON REACTIONS WITH C100 AS THE MAJOR SILICA SOURCE

Figure 3.7 shows the effect of increasing the water content of the reaction mixture on the growth of zeolite X. For all these reactions in which C100 was the major silica source the product was pure zeolite X. The induction period, growth periods and rate constants for each reaction are shown in table 3.8. As the water content increased, with consequent decrease in the sodium hydroxide concentration, the rate of formation of zeolite X decreased. For reactions 3.2, 3.13 and 3.14 the induction period was about the same (35±5 minutes), which was expected since all

FIG. 3.7 - EFFECT OF INCREASING THE WATER CONTENT IN REACTIONS WITH C100 AS THE MAJOR SILICA SOURCE

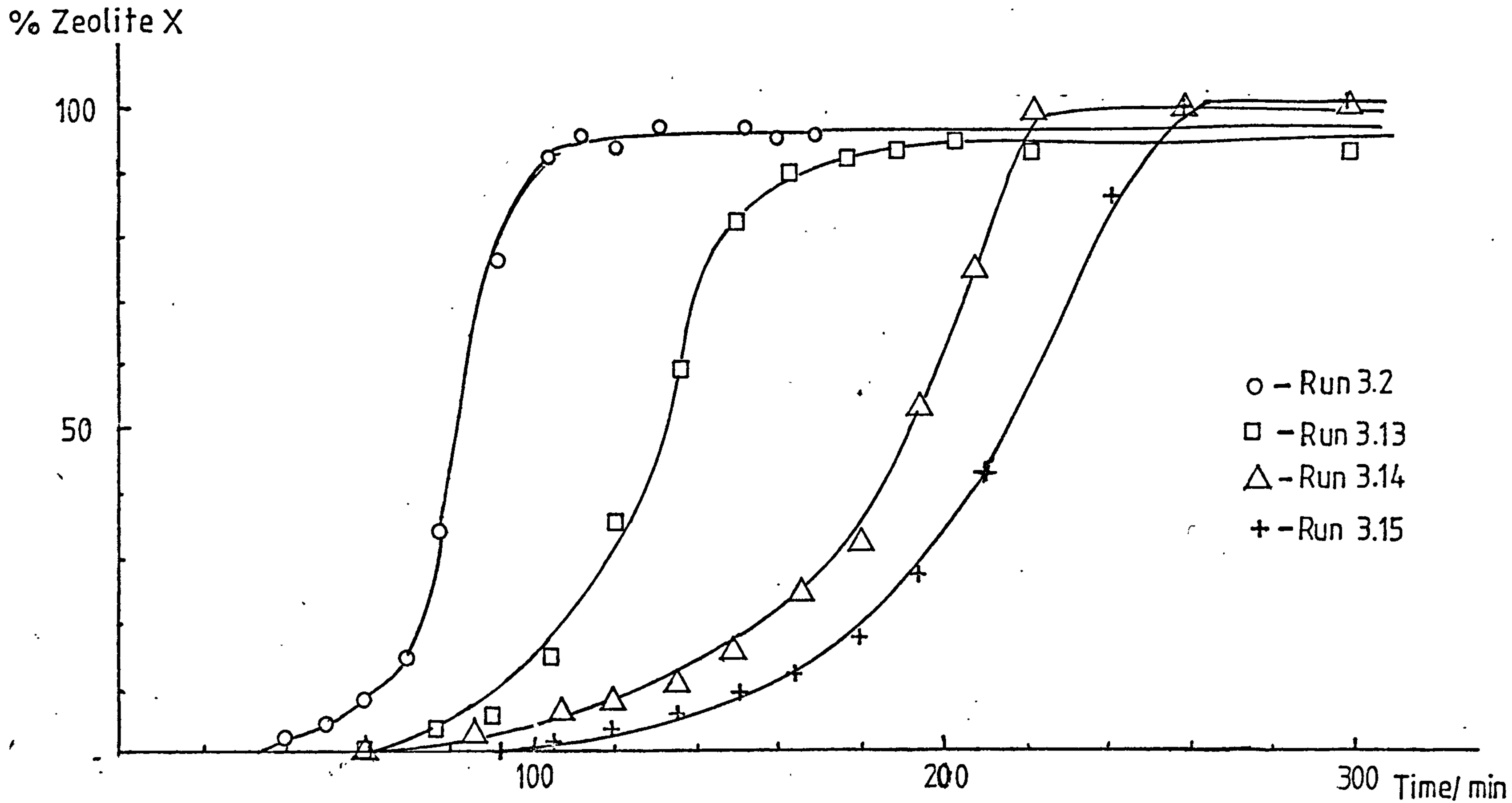

TABLE 3.8 EFFECT OF DILUTION ON REACTIONS WITH C100 AS THE MAJOR SiO_2 SOURCE

Overall Reaction Composition $5.15Na_2O\ Al_2O_3\ 4SiO_2\ xH_2O$

Run No.	Moles H_2O	%X	% Pl	k/min^{-1}	Growth period/min	Induction period/min
3.2	240	92	-	0.077±0.009	62±8	36±4
3.13	315	90	-	0.041±0.007	114±20	40±10
3.14	350	96	-	0.024±0.002	195±16	31±8
3.15	400	96	-	0.027±0.002	178±16	70±8

reactions contained the same amount of nuclei initially. However, for the most dilute reaction the induction period was 70±8 minutes. This suggests that nuclei must grow via collision breeding and in the very dilute system the number of collisions will be smaller and therefore the induction period will be longer. The growth periods increase with increasing dilution although for the most dilute reactions (3.14, 3.15) they are approximately the same.

A scanning electron micrograph (Plate 3) for the product of reaction 3.15 was obtained and the particle size was calculated to be 0.83×10^{-6} m compared with 2.51×10^{-6} m for Linde 13X.

It is interesting to note that although growth was slow in reaction 3.15 no zeolite P1 formation was observed.

3.6.4 EFFECT OF DILUTION ON REACTIONS WITH KS300 AS THE MAJOR SILICA SOURCE

Figure 3.8 shows the effect of varying the water content of the reaction mixture on the growth of zeolite X. Four different compositions were used: $5.15Na_2O.Al_2O_3.4SiO_2.xH_2O$, where $x = 240$, 315, 350 and 400. The results are shown in table 3.9. Each reaction was duplicated and the results obtained for each pair were virtually identical. The results for reactions 3.8 and 3.9 have been discussed in section 3.6.2.

The products of reactions 3.16 and 3.17, for which the molar composition was $5.15Na_2O;Al_2O_3.4SiO_2.315H_2O$, were a mixture of zeolites X, A and P1, in approximately equal quantities. Possible explanations for zeolite P1 formation in this type of silica system have been discussed earlier. Zeolite A is normally

FIG. 3.8 EFFECT OF INCREASING THE WATER CONTENT IN REACTIONS WITH KS300 AS THE MAJOR SILICA SOURCE

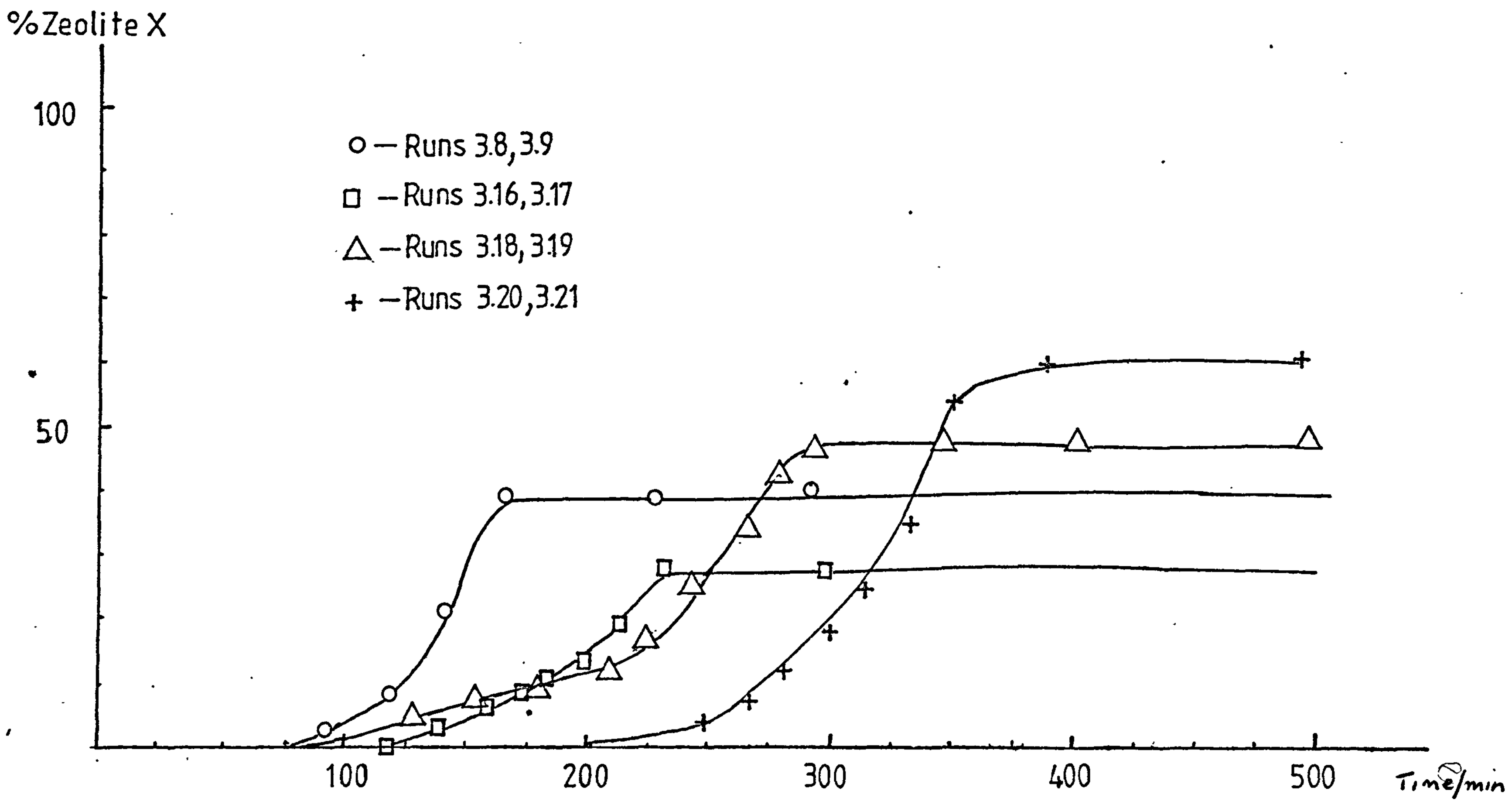

TABLE 3.9 EFFECT OF DILUTION ON REACTIONS WITH KS300 AS THE MAJOR SiO_2 SOURCE

Run No.	Moles H_2O	Product %X	%P1	%A	Rate constant k/min^{-1}	Growth period/ min	Induction period/min
3.8	240	30	66	-	0.023±0.008	150±20	30±18
3.9	240	32	67	-	0.033±0.003	110±10	50±10
3.16	315	28	23	36	0.076±0.002[a] 0.019±0.001	26±4 180±4	134±4
3.17	315	24	23	30	0.086±0.003[a] 0.024±0.003	22±8 60±8	148±4
3.18	350	36	56	-	0.018±0.001	210±8	60±8
3.19	350	48	45	-	0.022±0.001	180±10	142±10
3.20	400	58	nd	33	0.030±0.001[a] 0.018±0.001	98±4 60±4	202±4
3.21	400	62	28	17	0.018±0.001	220±10	150±10

[a] In these reactions two rates of growth were observed.

formed in systems in which the solution phase is aluminate rich, and it is probable that this situation exists in the initial stages of this reaction, since the silica will dissolve more slowly in the less alkaline system. It was not possible to measure separately, the growth curves for each zeolite by absorption measurements, in this ternary product system. However, from x-ray analysis it was found that zeolite A had begun to grow before either zeolite X or zeolite P1. The results are shown in table 3.10

TABLE 3.10 X.r.d. ANALYSIS OF SAMPLES FROM REACTION 3.16

Time/min	%X	%P1	%A
60	-	-	-
120	-	-	8
180	15	-	15
240	34	23	36

In reactions 3.16 and 3.17 (H_2O = 315 moles) the initial growth rate of zeolite X was faster than observed for standard reactions such as those described in section 3.6.1; this was then followed by a much slower growth rate. It is reasonable to expect fast growth of zeolite X initially, since active metasilicate was used in the reaction. The much slower rate observed in the later stages of the reaction probably arises from competition between the zeolite A and zeolite X for the available nutrients.

In the more dilute system of reactions 3.18 and 3.19, molar composition $5.15Na_2O.Al_2O_3.4SiO2.350H_2O$ the products were zeolite X and P1, in equal quantities. No zeolite A formation was observed.

It is possible that zeolite A may have been formed in the initial stages of this reaction and subsequently converted to zeolite P1. (This conversion is known to occur under specific sodium hydroxide concentrations[104]). It is of course possible that the system was too dilute to allow zeolite A nucleation, since zeolite A is known to nucleate via collision breeding. However, this seems unlikely since in the most dilute system, reactions 3.20 and 3.21, molar composition $5.15Na_2O.Al_2O_3.4SiO_2,400H_2O$, zeolite A formation was observed. A more reasonable explanation is that it is the alkalinity of the system which determines whether zeolite A or zeolite P1 is formed.

The rate of growth of zeolite X in reactions 3.20 and 3.21 was similar to that observed in reactions 3.18 and 3.19. However, in these reactions zeolite X was the major component of the product. In reaction 3.20 (H_2O = 400 moles) zeolite A was the minor component and a trace of zeolite P1 was also observed. In reaction 3.21 (H_2O = 400 moles) zeolite A and zeolite P1 were both present as minor components. It follows then that the slower the rate of growth of zeolite, the more zeolite X there will be in the final product. This is not unreasonable since the growth is slow and the concentration of colloidal silica will be low at this high dilution.

Figure 3.9 shows a plot of percentage zeolite formed against the number of moles of water in the reactions. Average amounts of zeolite for the duplicate reactions have been plotted. It can be seen that, as the system becomes more dilute, zeolite X formation is favoured. It seems likely that this is related to the alkalinity of the system. Also, it must be influenced by the concentration of colloidal silica available for incorporation into the gel. This concentration will decrease with increasing water content; thus zeolite P1 formation will be less favoured.

FIG. 3.9 PERCENTAGE ZEOLITE FORMED VERSUS THE NUMBER OF MOLES H_2O IN THE REACTION MIXTURE

3.3.5 EFFECT OF REPLACING Na^+ WITH K^+ IONS

It is known that the zeolite species which crystallises from an aluminosilicate gel is highly dependent on the cation present in the parent gel. For example, the total replacement of Na^+ by K^+ ions in an aluminosilicate gel which would give zeolite Y gives zeolite L. However, partial replacement does not have such a drastic effect. Recently it was reported[105] that the replacement of 30% of the Na^+ ions by K^+ ions in an aluminosilicate gel, which would normally give zeolite A, resulted in the redirection of the reaction to give zeolite X with a low SiO_2/Al_2O_3 ratio.

In this work 25% of the Na^+ ions in the initial reaction mixture, molar composition $5.15M_2O.Al_2O_3.4SiO_2.xH_2O$ were replaced by K^+ ions. The reactions were seeded with active metasilicate and the major silica source was KS300. The results are shown in Table 3.11

TABLE 3.11 EFFECT OF REPLACING Na^+ IONS WITH K^+ IONS

Run No.	Moles H_2O	% K^+ ions	Time/h	%X	%Pl
3.22	240	25	3	-	-
			8	7	47
3.23	300	25	7	-	-

The product of reaction 3.22 (molar composition $1:3K_2O.3.9Na_2O.Al_2O_3.4SiO_2.240H_2O$) was amorphous after 3 hours and after 8 hours the product was zeolite Pl (47%) with traces of zeolite X (7%). This should be compared with reaction 3.8 (pure Na^+ system) in which the product after 4 hours was a mixture of zeolite Pl (66%) and zeolite X (31%). Obviously the addition of

K^+ ions has kinetically hindered the reaction, but not redirected it.

The product of reaction 3.23 (molar composition $1.3K_2O.3.9Na_2O.Al_2O_3.4SiO_2.300H_2O$) was still amorphous after 7 hours, and further analysis was not carried out. Comparison with the pure Na^+ system (reactions 3.16 and 3.17) shows that crystallisation was complete within 4 hours and zeolite A formation had started within 2 hours. Therefore, the effect of dilution together with the presence of 25% K^+ ions in the system kinetically hinders the formation of zeolites X, P1 and A. This is in agreement with work carried out by Meise and Schwochow[84].

The work to study the effect of replacement of Na^+ ions by K^+ ions was discontinued at this stage as the reaction took place over such a long period of time. It is, however, considered that a thorough investigation of the partial replacement of Na^+ ions by K^+ ions would yield some interesting information and should be carried out.

3.7 THE USE OF ^{27}Al N.m.r. IN FOLLOWING THE ZEOLITE REACTION

It is possible to record n.m.r. spectra for ^{29}Si and ^{27}Al. Therefore it should be possible to follow the course of the zeolite reaction by observing the n.m.r. spectra. Since observation of ^{29}Si is a slow process due to the low concentration present in the solution phase of the reaction it was decided to use ^{27}Al to follow the course of a zeolite X reaction.

The existence of two aluminate species, the octahedral ion $Al[H_2O]_6^{3+}$ found in solutions of low pH and the tetrahedral ion $Al[OH]_4^-$ found in alkaline solutions is well established. Aluminium is a relatively convenient nucleus to observe since the common isotope, ^{27}Al, has a nuclear spin with quantum number I = 5/2.

Since I is $>\frac{1}{2}$, the nucleus of ^{27}Al has a quadrupole moment which can interact with unsymmetrical electric field gradients, permitting very efficient nuclear relaxation with consequent n.m.r. line broadening. Thus, sharp ^{27}Al resonances are generally only observed when the nucleus is present in a symmetrical electrical field and the width of the resonance can give useful information about shapes of species[106,107].

In a zeolite reaction, the aluminium is in the form of the tetrahedral aluminate ion $Al[OH]_4^-$. The resonance was observed at δ = 76.2 ppm, to high frequency of the standard $Al[H_2O]_6^{3+}$. An external lock signal was used and this probably accounts for the discrepancy in the resonance observed here for the $Al[OH]_4^-$ ion, from the resonance value of δ = 80.0 ppm reported in the literature[108].

Samples were taken from a zeolite X reaction mixture, every 30 minutes up to 90 minutes, then every 10 minutes for the next hour. The solution phase was separated, by filtration, from the solid phase. Measurements were made at 25.2 MHz by use of the probe normally used for observation of ^{13}C spectra.

The peak heights of the $Al[OH]_4^-$ peaks were measured, and, since peak height is directly proportional to concentration for ^{27}Al spectra, the concentration of aluminate present was calculated. A plot of concentration of aluminate versus time is shown in figure 3.10. (The point at t=o was taken immediately after the silicate solution was added). The concentration of aluminate drops rapidly in the initial stages of the reaction until gel formation is complete. It then remains constant until the end of the induction period and drops again as zeolite crystallisation proceeds. This can be directly related to the course of the zeolite crystallisation.

FIG. 3.10 CONCENTRATION OF ALUMINATE IONS IN THE SOLUTION PHASE OF THE REACTION MIXTURE CALCULATED FROM ^{27}Al N.m.r. MEASUREMENTS VERSUS TIME

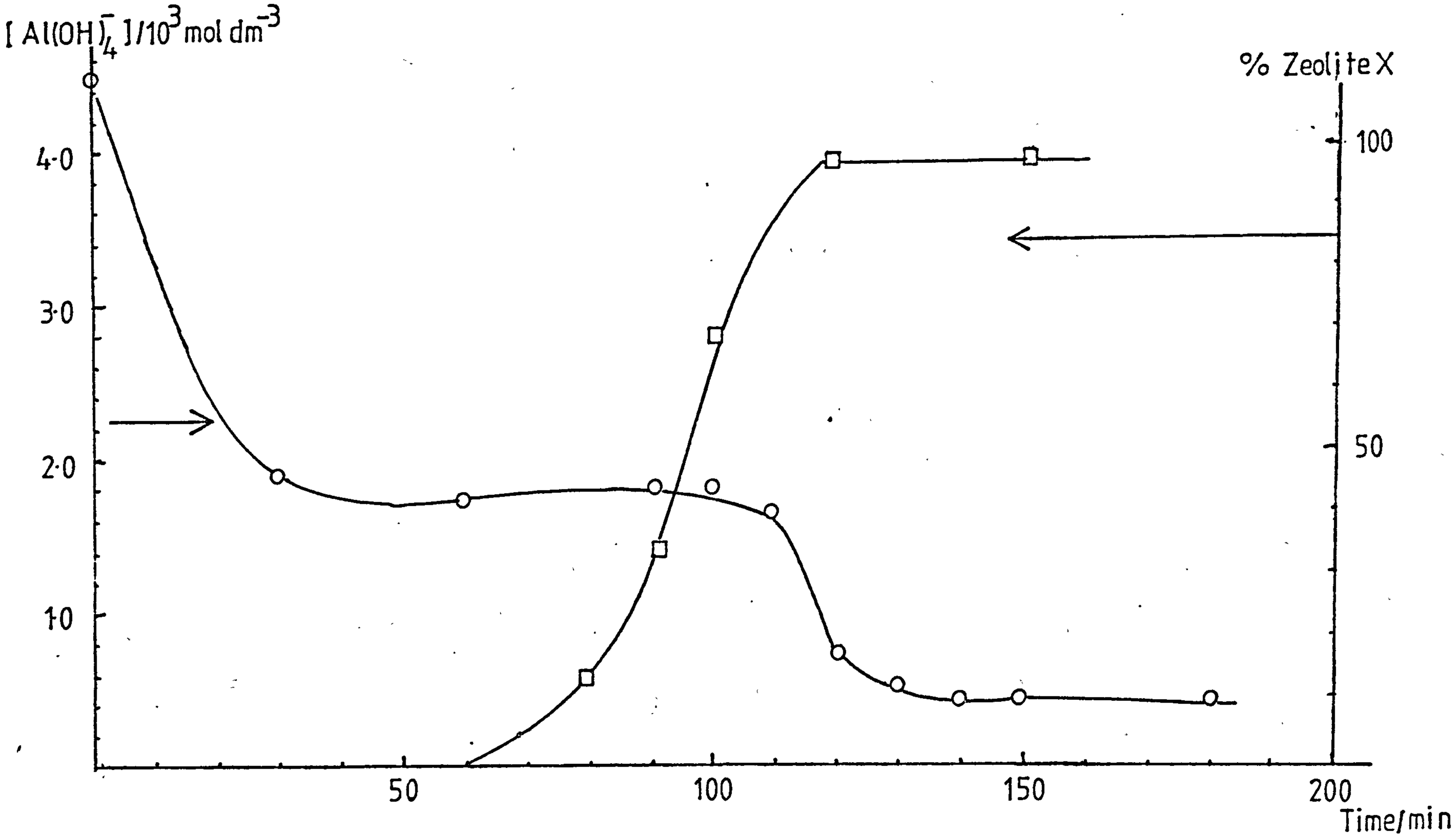

3.8 CONCLUSION

The work described in chapters 2 and 3 has shed some light on the mechanism of zeolite X and P1 formation. It has been shown conclusively that silicate species which are present in the solution and provide nutrients for co-precipitation with aluminate ions have a major influence on the product of the reaction. In particular, in the absence of active metasilicate it has been shown that when high surface area silicas are allowed to dissolve in the presence of aluminate ions, these materials direct the reaction to give zeolite X. It has been suggested that this may be due to the formation of a highly ordered reactive gel which is constructed such that the formation of zeolite X building blocks is favourable. In contrast, when low surface area silicas are used, these materials dissolve to give small colloidal particles which can be trapped in the gel structure and thus act as nucleation sites for zeolite P1 formation.

In the presence of active metasilicate, which is believed to incorporate nucleation centres which can promote zeolite X formation, the influence of low surface area amorphous silicas can override the effect of the active material giving zeolite P1 as the product. When sodium silicate solutions with $SiO_2/Na_2O > 2$ are used, the influence of the higher polymeric silicate species known to be present in these materials can also be seen. The mechanism in this case is probably different from that which operates with amorphous silicas, in that it is not the presence of colloidal particles in the gel which promotes zeolite P1 formation. It is more likely that incorporation of polymeric silicates into the gel leads to a structure which has few alternating Al, Si units but has polymeric silicate chains which are not favourable for the formation of the zeolite X building blocks.

CHAPTER 4

INVESTIGATION OF SOLID/LIQUID SLURRIES

4.1 INTRODUCTION

The use of low water solid/liquid slurries of sodium aluminate and sodium silicate to promote crystallisation of zeolite X has been investigated by MacGilp[67]. The patent literature[109] also describes techniques whereby slurries are prepared containing 'nucleation centres'. These nucleation centres are added to reaction mixtures in order to promote the crystallisation of faujasitic type zeolites. Although the solid/liquid slurries may contain crystalline material, the nucleation centres are amorphous to x-rays either because they are non-crystalline or because the crystallites are extremely small. The slurries prepared by the patent method have a much higher water content than those prepared by the MacGilp method. Both methods involve aging the slurry before addition to the reaction mixture. The period of aging depends on the temperature. At high temperatures, approximately 60°C, the aging period can be as short as one hour, aging at room temperature, ~20°C, can take as long as 24 hours before the slurry is suitably active. MacGilp studied in detail the effect of adding the slurries to reaction mixtures. He noted that slurries which contained crystalline solids were more conducive to the formation of active species, and that the product zeolite did not depend on which slurry component formed the solid phase. However, he observed that activation was more rapid when sodium aluminate was the solid phase.

The active species was thought to be either four or six unit rings, or possibly β cages, since only zeolites which contained the

β cage as its basic unit were found to crystallise. In the slurries themselves zeolites A, X and hydroxysodalite crystallised but never zeolite P1. When the slurry was added to a $5.15Na_2O.Al_2O_3.4SiO_2.240H_2O$ system, the only product formed was faujasite.

Several questions were posed by this work. Was this method only useful in the sodium synthesis field or could it be extended to other synthesis fields e.g. those of potassium and lithium zeolites? If these slurries were allowed to crystallise, which zeolites would form and how would they grow?

The work described here was an attempt to answer these questions. Initially, a preliminary investigation was carried out with solid/liquid slurries prepared in the sodium, sodium + potassium and sodium + lithium fields observing only the post crystallisation products. Using the information from this investigation, a more detailed study of the kinetic growth of zeolites in these mixtures in the sodium field was undertaken.

4.2 PRELIMINARY WORK

4.2.1 EXPERIMENTAL DETAILS

4.2.1.1 MATERIALS

Material	Source
$Na_2SiO_3 5H_2O$ (technical grade)	BDH Ltd.
$1.3Na_2O\ Al_2O_3$ (" ")	"
KOH (" ")	"
$LiOH.H_2O$ (" ")	"
Crystal violet (" ")	"
Pure silica type KS300	AKZO Ltd.

4.2.1.2 APPARATUS

Reaction mixtures were prepared in either 500 cm^3 polypropylene bottles or 50-100 cm^3 glass bottles fitted with air-tight lids. The bottles were placed in an oven in which the temperature was maintained at 57±1°C. The mixtures were not stirred. A 7 cm Büchner filter funnel fitted with Whatman no. 1 paper was used for filtration and washing of the product. Analysis was carried out using an x-ray powder diffractometer (Phillips type PW1051). Products were dried in an oven at 120°C and left to equilibrate with the atmosphere for at least four hours before analysis.

4.2.1.3 PROCEDURE

Except for a few reactions (see table 4.1) the overall composition of the mixtures was

$$(5.74 - x)\ Na_2O\ xM_2O\ Al_2O_3\ 4.44SiO_2\ 82H_2O$$

where M = K or Li. The solid phase was always sodium aluminate ($1.3Na_2O.Al_2O_3$) and consequently x was never more than 4.44. The potassium and lithium ions were always introduced in the solution phase.

The mixtures were made up in the following way. Dry solid sodium aluminate was placed in the reaction vessel. In the pure sodium system, sodium metasilicate was dissolved in water with heating to give a clear, super-saturated solution. This was cooled to room temperature and the lost water replaced. The silicate solution was then added to the solid sodium aluminate, with shaking, until a slurry was formed. This was then placed in the oven at 57±1°C.

In the mixed cation systems, either potassium or lithium hydroxide was dissolved in some of the water, and heated to give a clear solution. Silica was then added with the remaining water and boiled until a clear silicate solution was obtained. For lithium at high concentrations it was not possible to form a clear silicate solution. The rest of the procedure for the mixed cation system was then the same as for the pure sodium system.

The reaction mixtures were sampled using a 5 cm^3 pipette and not more than 10 cm^3 was taken for any one sample. Difficulty was encountered in obtaining a homogeneous sample though in most cases this was overcome by shaking the reaction mixture for a period of five minutes. However, in some cases two layers had formed one of which was a hard solid and the other a liquid, in these cases parts of each layer were extracted.

4.2.2 RESULTS

The results of the preliminary investigation are shown in table 4.1. For the pure sodium system, experiment 4.1, zeolite X formed within one day. Within six days, hydroxysodalite had begun to replace zeolite X, and after 30 days there were only traces of zeolite X and some zeolite P1 was also present. After 189 days all the zeolite X had disappeared and only hydroxysodalite and zeolite P1 remained. Thus the general sequence of product formation in the sodium system was:

$$\text{reaction mixture} \xrightarrow{1d} X \xrightarrow{6d} X+HS \xrightarrow{30d} X+HS+P1 \xrightarrow{189d} HS+P1$$

In the sodium-potassium system, the product depended on the Na_2O/K_2O ratio. In experiment 4.5, Na_2O/K_2O = 12.0, the product

TABLE 4.1 SOLID/LIQUID SLURRIES: RESULTS OF PRELIMINARY INVESTIGATIONS

Expt[a]	Na_2O/Al_2O_3	M_2O/Al_2O_3	Na_2O/M_2O	Zeolites in sample after (N) days at 57°+1°C
Na system				
4.1	5.74	0.00	-	X(1)→X+HS(6)→X+HS(13)→HS+trX+trPl(30)→HS+trPl(189)
4.2[b]	5.74	0.00	-	X(1)→HS+Pl(140)
Na+K system				
4.3[c]	1.30	3.80	0.30	Am[d](1)→Am(6)→trH(13)→H(30)→Q+tr(Na,K)Pt(189)
4.4	1.74	4.00	0.43	Am(16)→H(42)→trQ+(Na,K)Pt(146)
4.5	5.30	0.44	12.00	X(17)→X(42)→X+HS(175)
4.6	3.52	2.20	1.60	E(16)→E(37)→E(175)
4.7	1.30	4.44	0.29	sl.tr.E(15)→H(27)→(Na,K)Pt(174)
4.8[b]	1.30	4.44	0.29	Am(16)→H(27)→(Na,K)Pt(174)
Na+Li system				
4.9	1.30	4.40	0.29	Li_2SiO_3(2)→Li_2SiO_3+HS(17)→Li_2SiO_3+trHS(176)
4.10	5.30	0.44	12.00	X+HS(17)→HS(27)→HS(v.s.)(175)
4.11	4.40	1.34	3.4	X(16)→X+Pl+HS(30)→HS(v.s.)(175)

[a] Overall composition $(5.74-x)Na_2O.xM_2O.Al_2O_3.4.44SiO_2.82H_2O$

[b] Mixture contained crystal violet (1.0 g)

[c] Composition of mixture $1.3Na_2O.3.78K_2O.Al_2O_3.4.44SiO_2.86H_2O$

[d] Am = Amorphous.

was analysed after 17 days and 42 days and found to contain zeolite X and amorphous aluminosilicate. After 175 days, the product was a mixture of zeolite X and hydroxysodalite. This result suggests either than potassium ions in some way stabilise zeolite X, or alternatively that they slow down or block formation of zeolite P1. For experiment 4.6, Na_2O/K_2O = 1.6, zeolite E[110], a zeolite of unknown structure was formed. Zeolite E has only been synthesised in the Na+K mixed base system[111]. Its formation in the present system is not unexpected, since the overall composition is close to that of the patented[110] synthesis mixture ($0.75K_2O.0.75Na_2O.Al_2O_3.2SiO_2.30H_2O$).

Na_2O/K_2O ratios less than one (expt. 4.3, 4.4 and 4.7), all gave zeolite H[112] or zeolite Q[113], which were replaced by zeolite (Na,K)P in the tetragonal form, which is a more thermodynamically stable zeolite in this field[111]. The structures of zeolites H and Q have not been reported. According to Breck, zeolite H usually forms from a pure potassium system, although it has been reported to form in the mixed base system. Although very little is known about zeolite Q it appears from these results (expt. 4.3 and 4.4, table 4.1) that it is more thermodynamically. stable than zeolite H.

The sodium-lithium system presented a problem, in that for Na_2O/Li_2O ratios less than one it was not possible to form a soluble silicate solution. In experiment 4.9, the initial product was lithium orthosilicate[114] and after 17 days traces of hydroxysodalite had formed. For Na_2O/Li_2O ratios greater than one (expt. 4.10 and 4.11), the products were very similar to those obtained in the pure sodium system.

For those experiments (4.2 and 4.8) to which crystal violet was added, the products were virtually identical to those

obtained when no dye was added to the system, i.e. experiments 4.1 and 4.7 respectively.

4.2.3 DISCUSSION

The pure sodium mixture used in experiment 4.1 has been shown[67] to promote the growth of zeolites X when added to suitable reaction mixtures. This ability developed very quickly, e.g. within 70 minutes at 60°C, and certainly before any crystalline products could be detected in the mixture itself. However, the zeolite which does form initially in this mixture is zeolite X, and it could be argued that the zeolite initially formed in the mixture is that which it will nucleate from reaction mixtures of quite different composition. By analogy, it appears from experiments 4.3, 4.4, 4.6 and 4.7 that these Na+K mixed systems could be used to nucleate growth of zeolites E and H. Whereas in the pure sodium field the structure of the nucleated zeolites are known, this is not so for zeolites E and H, and it is not possible to speculate on the nature of the initial building units formed in these mixtures.

The result of experiment 4.5 suggests that small additions of potassium ions either stabilise the formation of zeolite X or possibly block the formation of zeolites A, HS and P1. This theory is supported by results recently reported by workers at Mobil[105], who found that addition of small amounts of potassium ions to a zeolite A synthesis reaction mixture, redirected the reaction such that the product was zeolite X.

The insolubility of lithium silicate makes the study of the Na+Li system very difficult. No lithium containing zeolites were formed. It appears that lithium ions had no influence on the course

of the reaction (expt. 4.10 and 4.11) the products being similar to those observed in the pure sodium system.

4.2.4 CONCLUSION

The conclusions drawn from this preliminary investigation were:-

1) No further investigation of the Na+Li system should be undertaken.

2) Although the Na+K system looked potentially interesting, the zeolites formed were of little commercial interest and there was insufficient knowledge of their structures. Consequently, study of systems in which they nucleate is unlikely to be rewarding.

The sodium system, however, presented a much more interesting case. As mentioned previously, the pre-crystallisation phase of these mixtures had proved to be very useful in directing zeolite reaction mixtures. It was therefore decided to undertake a detailed study of crystallisation products in solid/liquid salt mixtures in the sodium field. In this study, the samples were analysed both before and after zeolite crystallisation had started.

4.3 KINETIC STUDY OF THE GROWTH OF ZEOLITES IN SOLID/LIQUID SLURRIES

4.3.1 INTRODUCTION

As discussed in the previous section, the sodium field seemed the most interesting to study in detail. It was already known that faujasite type crystallites were formed in these systems.

However there was little information on the other silicate or aluminate crystalline solids which may have been present and perhaps more important; the composition of the solution phase was completely unknown.

This study was divided into two parts. The first part involved the analysis of the solids by x-ray powder diffraction using a Guinier-Hagg camera, and determination of quantities of material present by x-ray diffractometry. The other part was concerned with the analysis of the composition of the solution phase, using ^{29}Si Fourier transform n.m.r.

For this study the mixture composition was

$$5.15Na_2O\ Al_2O_3\ 3.98SiO_2\ 80H_2O$$

This composition is identical to that for a typical zeolite X reaction, except that it has a much lower water content.

4.3.2 EXPERIMENTAL DETAILS

The materials and apparatus were as described in sections 4.2.1.1 and 4.2.1.2. All reactions were done in 500 cm^3 polypropylene bottles. The procedure was as described previously, but in some experiments, the solid phase was anhydrous sodium metasilicate or amorphous silica. In these experiments the aluminate solution was made from sodium hydroxide and alumina trihydrate (BACO Ltd.).

4.3.2.1 SAMPLING PROCEDURE

Reaction vessels were removed from the oven and shaken until the contents were homogeneous. In most cases, the mixtures were too thick to be pipetted and so samples were taken with a spoon

spatula. Three spoonfuls were taken and placed on filter paper, and this sample was then sucked dry on a filter pump but was not washed. It was then allowed to dry properly in the atmosphere. It was known that during this drying period, the sample would inevitably pick up carbon dioxide from the atmosphere, and thereby form some sodium carbonate. This did not,however, create a significant problem, as it could be easily recognised in the x-ray diffraction pattern. Another three spoonfuls of reaction mixture were taken, and these were placed in a beaker containing 1000 cm^3 of water. The slurry was stirred thoroughly before filtering to ensure that only insoluble materials were left. This sample was then filtered, washed until the wash water had a pH of about 10 and dried in an oven at 100°C. The sample was then allowed to equilibrate in the atmosphere before being analysed. After sampling, the reaction vessel was returned to the oven as soon as possible. X.r.d. analysis of products was carried out as described in chapter 2.

4.3.3 RESULT

4.3.3.1 EFFECT OF SOLID PHASE ON PRODUCTS

MacGilp[67] observed that, when solid dry sodium aluminate was used, activation was more rapid than when a solid sodium silicate was used. However, the solid phase present in the initial stages made no difference to the product of the reaction to which the slurry was added. Variation of the solid phase and its effect on the crystallisation product of the slurry was investigated in experiments 4.12, 4.13, 4.14 and 4.15. The results are shown in table 4.2 and figures 4-1 - 4.4.

TABLE 4.2 PRODUCTS FROM SOLID/LIQUID SLURRIES

Expt[a]	Solid phase	Solution phase	Zeolites in sample after (N) days at 60°C	Non-zeolite crystalline materials in sample after (N) days
4.12	Na_2SiO_3	$NaAlO_2$	A(1)→A+X(2)→A+X+Pl(4)→X+Pl(5)	Na_2SiO_3(1)
4.13	$NaAlO_2$	Na_2SiO_3	A(1)→X+A+Pl(3)→X+Pl(4)	Na_2SiO_3(1)
4.14	$Na_2SiO_35H_2O$	$NaAlO_2$	X(0.25)→X+HS(2)	-
4.15	$NaAlO_2$	$Na_2SiO_35H_2O$	A+trHS(1)→A+X+HS(2)→X+HS+Pl(19)	-
4.16	CAB-O-SIL	$NaAlO_2$	A+X(1)→X+Pl(28)	$Na_2SiO_38H_2O$(0.25)
4.17	Precipitated SiO_2	$NaAlO_2$	A(0.25)→A+X(1)→A+X+HS(19)→X+HS+Pl(28)	$Na_2SiO_38H_2O$(2)
4.18	-	$Na_2SiO_35H_2O$ $NaAlO_2$	X(1)→X+HS(2)→X+HS(28)	$Na_2SiO_38H_2O$(4)
4.19[b]	$NaAlO_2$	$Na_2SiO_35H_2O$	A(1)→X+A+Pl(3)→X+Pl(23)	-
4.20[c]	$NaAlO_2$	$Na_2SiO_35H_2O$	HS(0.25)→HS(28)	-
4.21[d]	CAB-O-SIL	$NaAlO_2$	X+HS(1)→X+HS(23)	-

[a] Overall composition $5.15Na_2O.Al_2O_3.3.98SiO_2.80H_2O$

[b] Overall composition $5.15Na_2O.Al_2O_3.3.98SiO_2.160H_2O$

[c] Overall composition $5.15Na_2O.Al_2O_3.3.98SiO_2.40H_2O$

[d] Mixture contained methylene blue (1.0 g).

FIG. 4.1 ZEOLITE GROWTH IN SLURRY CONTAINING Na_2SiO_2 (SOLID PHASE) AND $NaAlO_2$ (SOLUTION PHASE) EXPT. 4.12

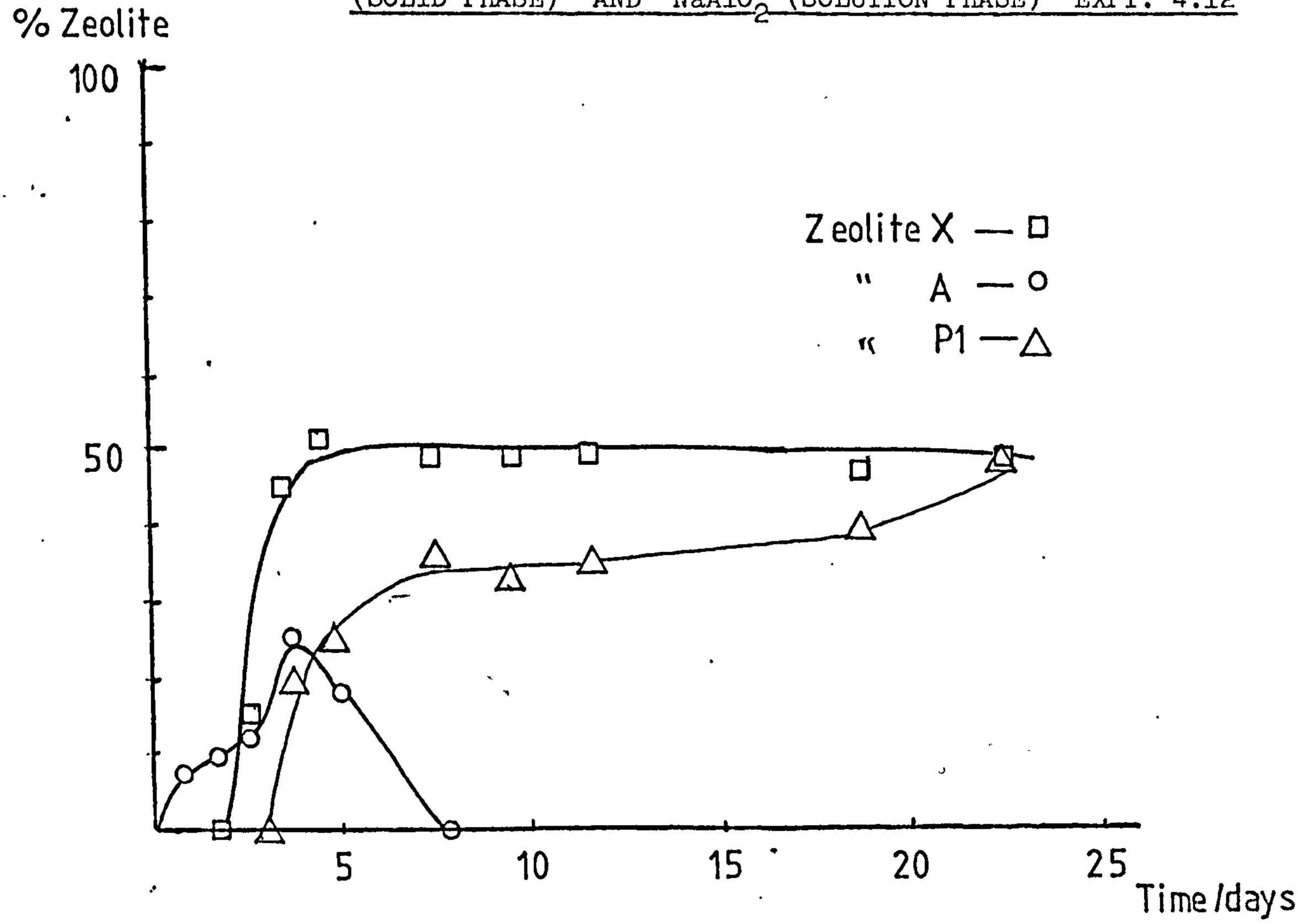

FIG. 4.2 ZEOLITE GROWTH IN SLURRY CONTAINING $NaAlO_2$ (SOLID PHASE) AND Na_2SiO_3 (SOLUTION PHASE) EXPT. 4.13

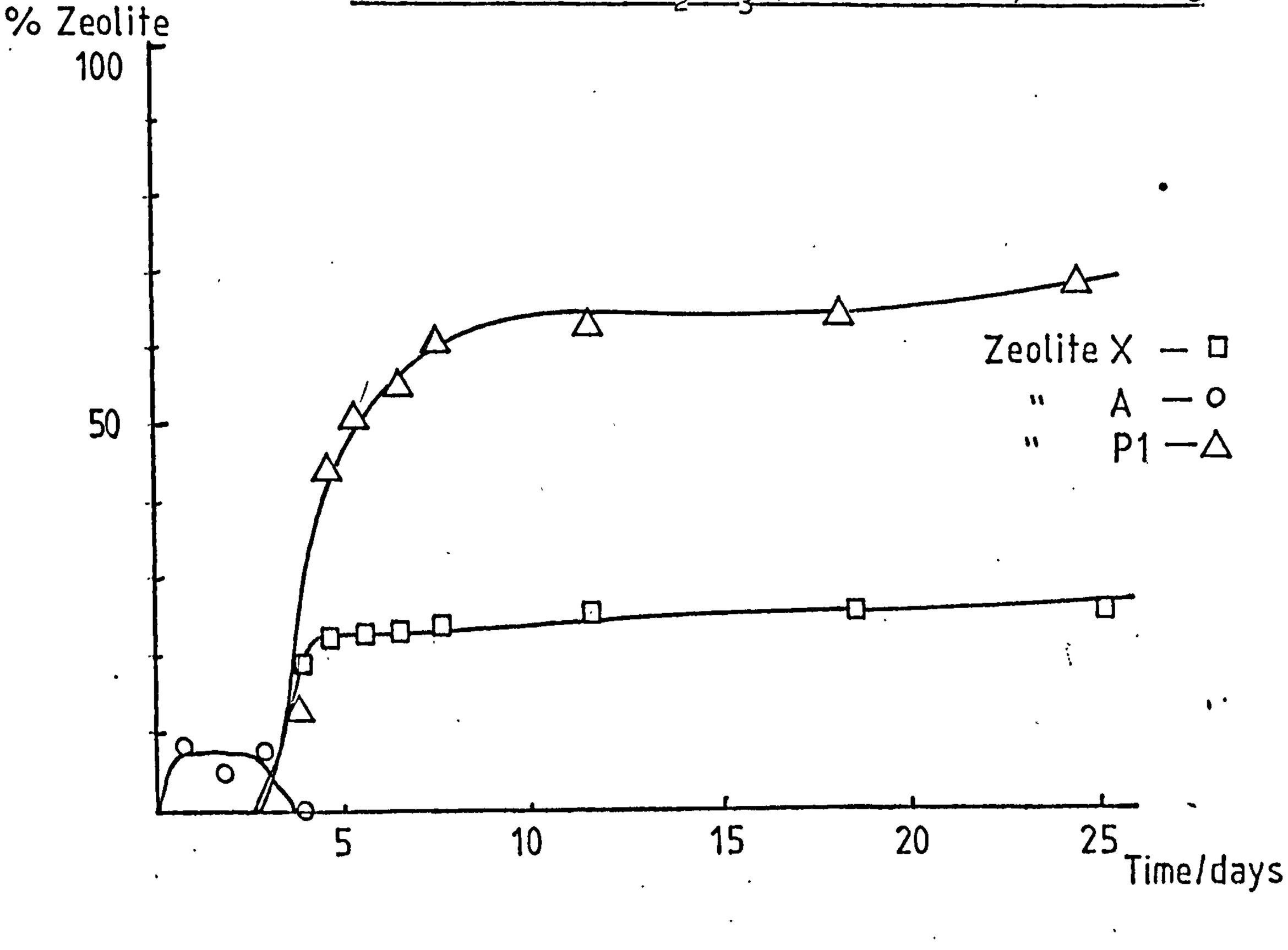

FIG. 4.3 ZEOLITE GROWTH FROM SLURRY CONTAINING $Na_2SiO_25H_2O$ (SOLID PHASE) AND $NaAlO_2$ (SOLUTION PHASE) EXPT. 4.14

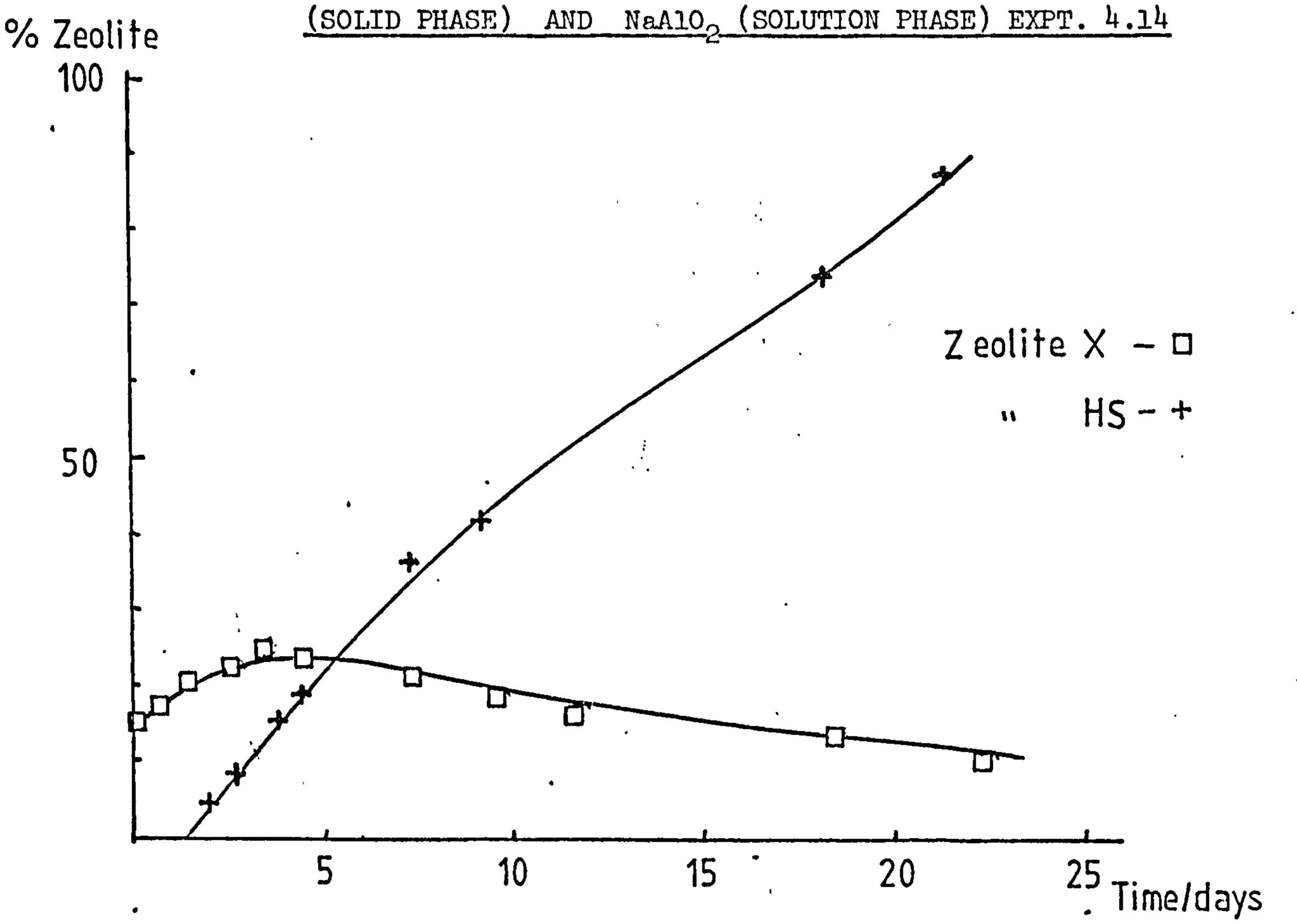

FIG. 4.4 ZEOLITE GROWTH IN SLURRY CONTAINING $NaAlO_2$ (SOLID PHASE) AND $Na_2SiO_25H_2O$ (SOLUTION PHASE) EXPT. 4.15

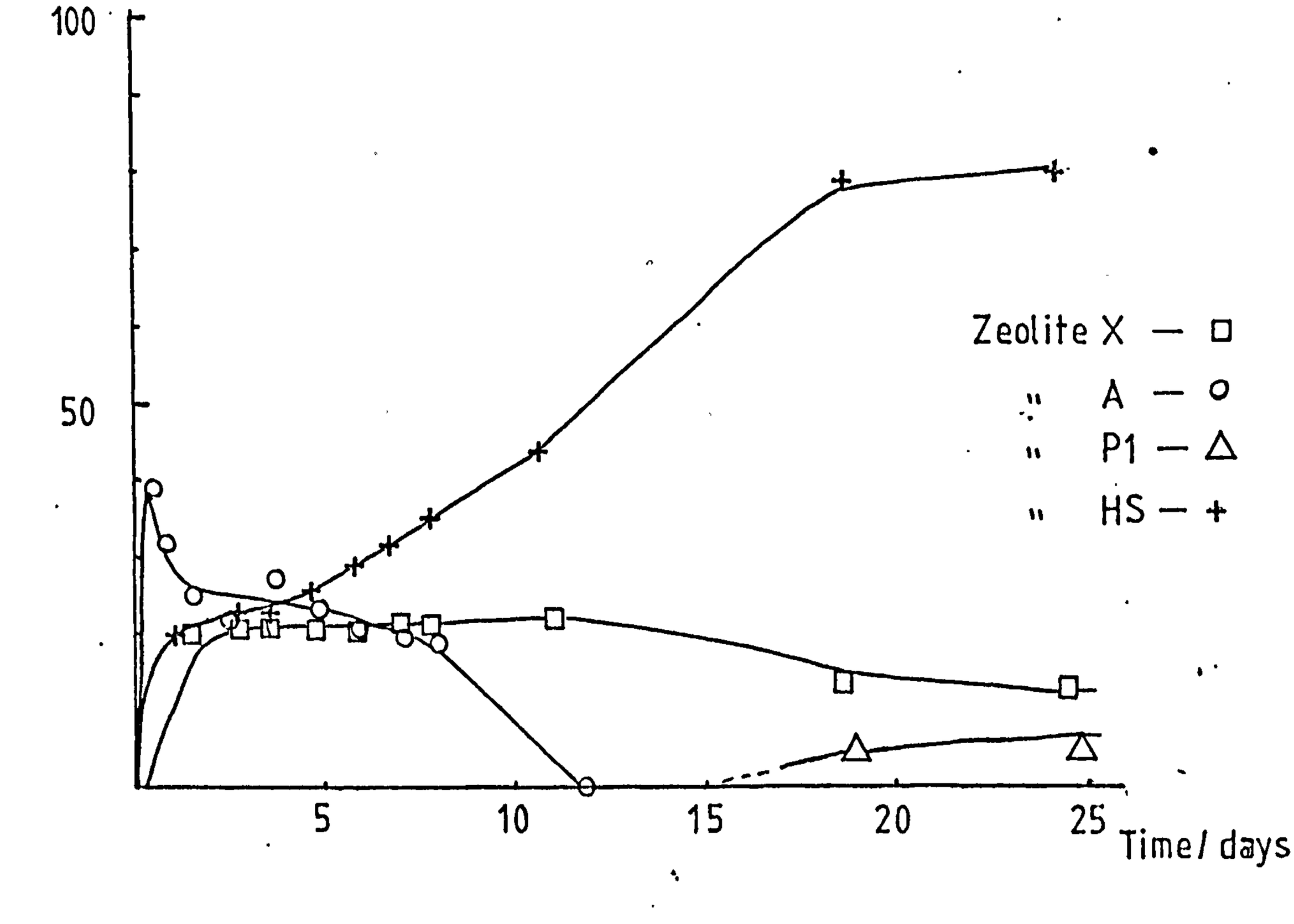

In experiment 4.12 the reactants were solid anhydrous sodium silicate and a sodium aluminate solution. The first zeolite which crystallised was zeolite A, within 1 day. In the sample taken after two days there were traces of zeolite X and after three days there was a significant amount of zeolite X (12%). It was observed that the amount of zeolite A in the system began to decrease after four days and zeolite P1 began to grow. Zeolite P1 grew rapidly while zeolite A disappeared (5d). It seems likely that this is due to the direct transformation of zeolite A to zeolite P1 rather than nucleation of zeolite P1 in the system. Zeolite X continued to grow during this transformation and finally constituted ∿48% of the total crystalline product, the remainder being zeolite P1 (47%).

In experiment 4.13 (figure 4.2) the solid phase was dry sodium aluminate, and the intended solution phase was prepared using anhydrous sodium silicate. An attempt to dissolve the anhydrous sodium silicate proved unsuccessful, but in spite of this, it was decided to go ahead with the experiment. Initially, then, there were two solid phases in the presence of excess sodium hydroxide. As with experiment 4.1 the first zeolite product observed was zeolite A. This formed to the extent of about 10% of the dry product in under one day. No subsequent growth of zeolite A was observed and after four days zeolite A disappeared completely from the system and the presence of zeolites X and P1 was observed. Zeolite X did not continue to grow above the level at which it was initially observed whereas zeolite P1 continued to grow. The final product after 28 days contained zeolite X (20%) and zeolite P1 (80%). Therefore, for the system in which anhydrous sodium metasilicate was the silica source, similar trends of zeolite growth and disappearance were observed, regardless of whether the

sodium aluminate was solid or in solution. It appears, then, that the limiting factor is dissolution of the anhydrous sodium silicate which was present as solid in both experiments 4.12 and 4.13.

For experiments 4.14 (figure 4.3) and 4.15 (figure 4.4) the silica source was an inactive sodium metasilicate pentahydrate. In experiment 4.14, in which the solid phase was sodium silicate, the first zeolite to crystallise was zeolite X (6h). Within two days hydroxysodalite had also started to crystallise. Continued growth of zeolite X was observed up to 5 days and after this the amount of zeolite X in the product declined. However, hydroxysodalite continued to grow throughout the period of the reaction (23d) and the final product contained zeolite X (12%) and hydroxysodalite (85%). It is possible that the decline in the amount of zeolite X is caused by transformation of this zeolite into hydroxysodalite.

In experiment 4.15 in which the solid phase was sodium aluminate, the first products observed were zeolite A and traces of hydroxysodalite. This is a surprising result, since zeolite A normally crystallises from gels in which the solution phase is rich in aluminium. In fact, subsequent growth of zeolite A was not observed. The amount of zeolite A in the product steadily decreased while the amount of zeolite X remained at a constant level up to 12 days, after which the amount of zeolite X decreased and formation of zeolite P1 was observed. The amount of hydroxysodalite increased steadily throughout the reaction. The final product of this reaction contained hydroxysodalite (85%) and zeolite X (15%) and traces of zeolite P1.

The general trends of zeolite growth were similar for experiments 4.14 and 4.15, the main difference being the crystallisation of zeolite A in the system which contained solid sodium aluminate. As mentioned above, this is surprising, since

zeolite A normally grows in systems which are rich in aluminate in the solution phase. A possible explanation of this behaviour is that as the sodium aluminate dissolves, discrete aluminate ions are then rapidly co-precipitated with the silicate ions to give aluminosilicate building units in which Al and Si alternate. Such units would favour the formation of zeolite A, in which this type of alternation is observed.

4.3.3.2 EFFECT OF SILICA SOURCE ON PRODUCTS

It has been known for many years that the silica source used in a zeolite reaction is one of the most important factors in determining the product of the reaction. Experiment 4.12, 4.14, 4.16 and 4.17 were carried out to find out the effects of varying the silica source in solid/liquid slurries. The results are shown in table 4.2 and figures 4.1, 4.3, 4.4 and 4.6. In all these experiments, either the silica or the sodium silicate was the solid phase.

The results of experiments 4.12 and 4.14 have been discussed in the previous section. The silica sources in experiments 4.16 (figure 4.5) and 4.17 (figure 4.6) were CAB-O-SIL M5 and a precipitated silica (BDH Ltd.) respectively. CAB-O-SIL M5 has a much higher surface area (208 $m^2\ g^{-1}$) than the precipitated silica (80 $m^2\ g^{-1}$). Initially the products from the two reactions were very similar, both giving zeolites X and A. However, in experiment 4.17, after 8 days, hydroxysodalite had started to crystallise. The amount of zeolites X and A in the product remained constant up to 19 days, while the amount of hydroxysodalite continued to increase steadily. After 28 days, zeolite A had

FIG. 4.5 ZEOLITE GROWTH IN SLURRY CONTAINING CAB-O-SIL (SOLID PHASE) AND $NaAlO_2$ (SOLUTION PHASE) EXPT. 4.16

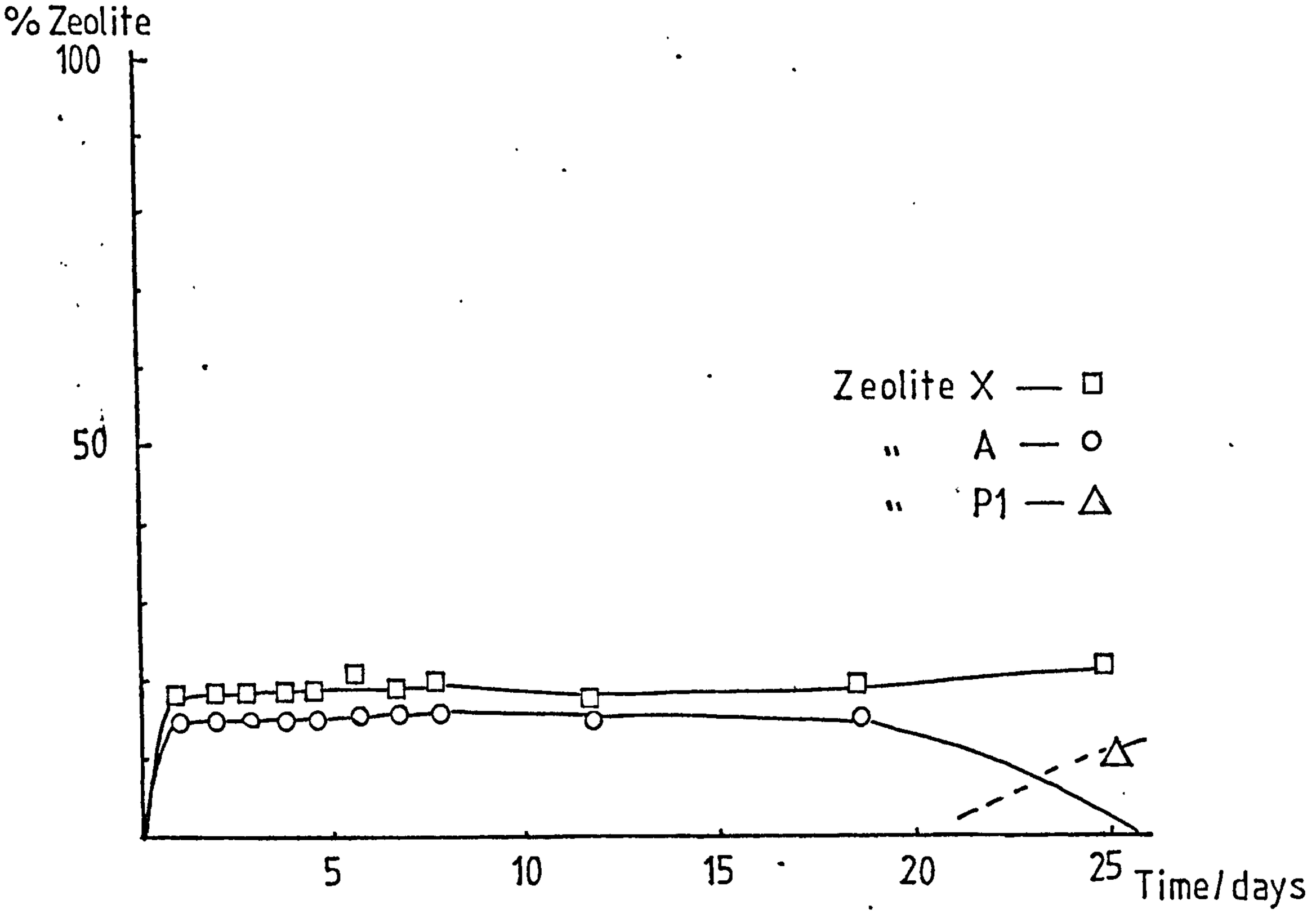

FIG. 4.6 ZEOLITE GROWTH IN SLURRY CONTAINING Ppt SiO_2 (SOLID PHASE) AND $NaAlO_2$ (SOLUTION PHASE) EXPT. 4.17

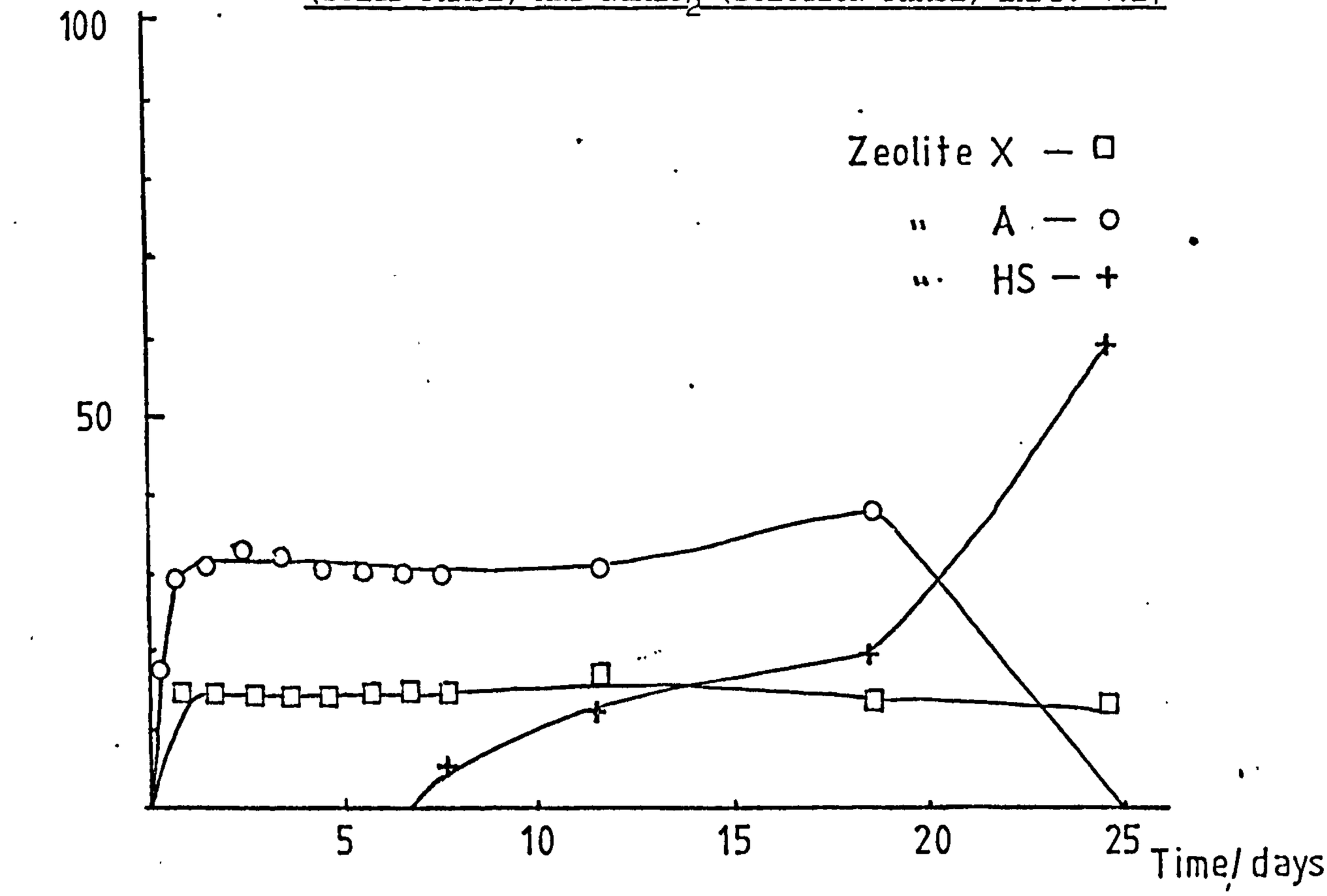

completely disappeared and the rate of growth of hydroxysodalite had increased. The product after 28 days contained zeolite X (20%) and zeolite HS(62%). From figure 4.6 it can be seen that the disappearance of zeolite A is the mirror image of the growth of hydroxysodalite, suggesting transformation of zeolite A into hydroxysodalite. In contrast to this, in experiment 4.16 there was no change in the product until 19 days and no hydroxysodalite was observed. After 28 days, zeolite A had disappeared and a small amount of zeolite P1 (11%) was observed with zeolite X (23%).

A possible explanation of this behaviour can be based on the rate of solubility of the amorphous silicas in these very alkaline systems. For experiment 4.16 in which the silica source was CAB-O-SIL-M5, it is likely that this material will dissolve rapidly, giving a silica-rich solution phase, which will favour zeolite X formation. In contrast, in experiment 4.17, the lower surface area precipitated silica will probably dissolve up more slowly and hence zeolite X will not start to grow. In experiment 4.17 it was noted that the total amount of zeolite formed was less than in experiment 4.16, and since zeolites take up water, the final water content is lower in experiment 4.17. This highly alkaline system favours hydroxysodalite formation which begins to form as an alternative to zeolite A. In experiment 4.16 there is a more dilute solution phase, rich in silica, and hence hydroxysodalite is not formed. Eventually, transformation of zeolite A to zeolite P1 is observed.

In both experiments, sodium metasilicate octahydrate was crystallised in the early stages, and it is probable that this had the effect of lowering the water content in the system but it disappeared very rapidly and likely had no influence on the reaction products.

4.3.3.3 LIQUID/LIQUID SLURRIES

It was decided to investigate the growth of zeolites from a liquid/liquid slurry, which gave an amorphous aluminosilicate as the solid phase and a solution phase rich in silica. In experiment 4.18 (figure 4.7) the mixture was prepared from a solution of sodium aluminate and a solution of sodium metasilicate pentahydrate. Initially the product of this reaction was zeolite X, which was as expected, since the solution phase was silica-rich. After 2 days, hydroxysodalite was observed. This suggested that the reaction mixture was low in water at this stage. It is unlikely that enough zeolite X has grown to significantly lower the water content.

It is therefore necessary to consider the non-zeolitic crystalline product of this reaction; sodium metasilicate octahydrate. Apparently this highly hydrated crystalline silicate lowers the water content of the solid/liquid slurry enough that hydroxysodalite is formed.

It is interesting to note that of all the experiments (4.12 - 4.18) carried out with the exception of 4.14 and 4.18, the first zeolite product observed was zeolite A, whereas for 4.14 and 4.18 it was zeolite X. A likely explanation for this can be based on the dissolution characteristics of the sodium metasilicate used in these experiments. In experiment 4.18 the sodium silicate was dissolved prior to addition to the sodium aluminate solution, and, therefore, it is unlikely that aluminosilicate building units which contain alternating Al and Si atoms will form in this system. In experiment 4.14 although the sodium silicate was added as a solid it is likely that it will dissolve very rapidly to give a similar amorphous

FIG. 4.7 ZEOLITE GROWTH IN SLURRY CONTAINING $Na_2SiO_25H_2O$ (SOLID PHASE) AND $NaAlO_2$ (SOLUTION PHASE) EXPT. 4.18

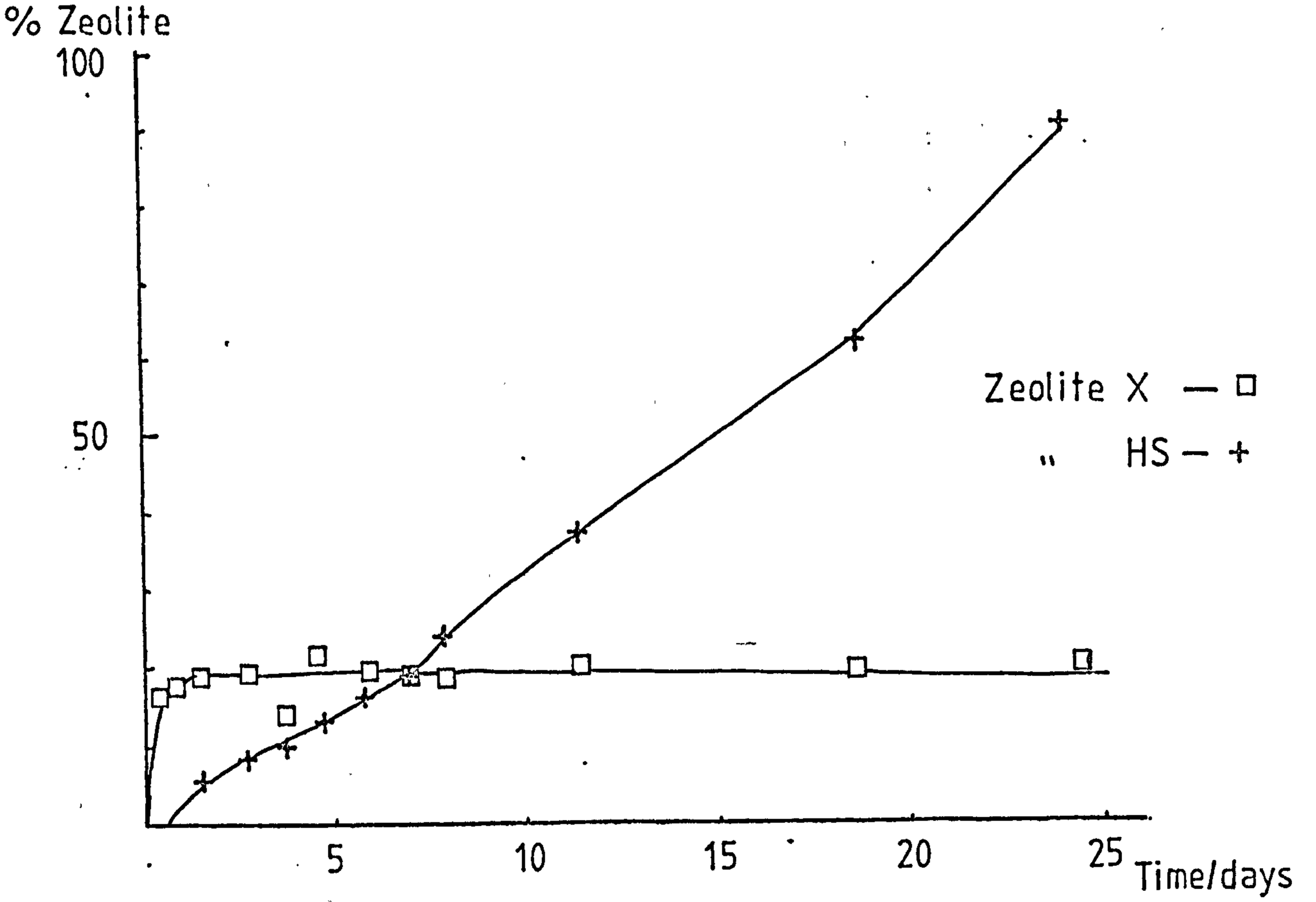

FIG. 4.8 ZEOLITE GROWTH IN SLURRY CONTAINING $NaAlO_2$ (SOLID PHASE) AND $Na_2SiO_35H_2O$ (SOLUTION PHASE) EXPT. 4.19

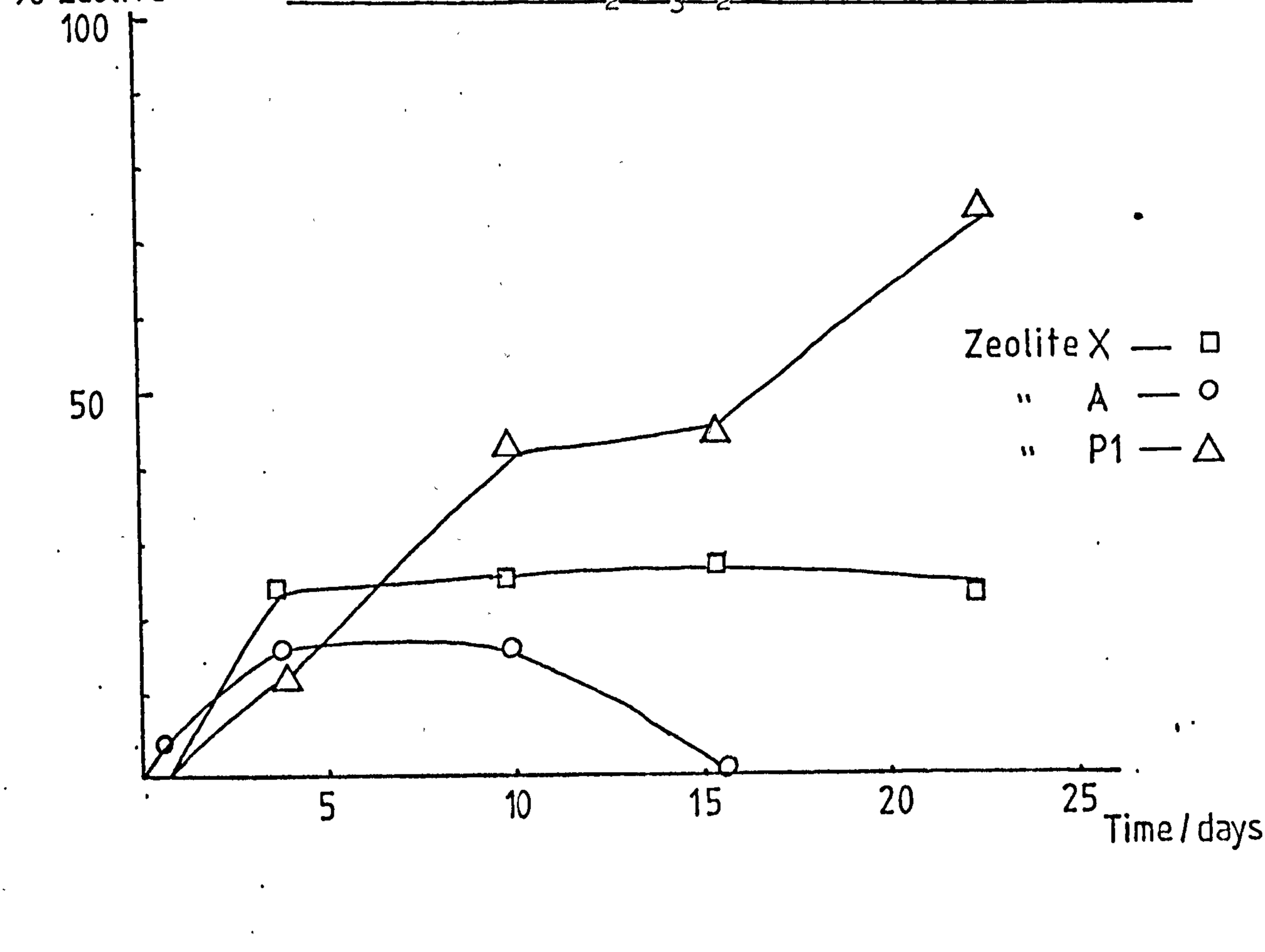

aluminosilicate to that formed in experiment 4.18.

The formation of zeolite A in all the other mixtures is likely to be the result of the formation of aluminosilicate units in which Al and Si alternate favouring the formation of zeolite A.

4.3.3.4 EFFECT OF DILUTION ON SOLID/LIQUID SLURRIES

All of the experiments discussed so far (4.1 - 4.18) were carried out with an H_2O/Al_2O_3 ratio of 80. In an attempt to investigate the role of water in the solid/liquid slurries, experiments 4.19 and 4.20 were carried out. In these, the H_2O/Al_2O_3 ratio was 160 and 40 respectively. The reactants used in experiments 4.19 and 4.20 were sodium aluminate as the solid phase and sodium metasilicate pentahydrate as the solution phase. The results are shown in table 4.2 and figures 4.8 and 4..9.

In experiment 4.19 (figure 4.8) the product formed initially was zeolite A. After 3 days both zeolite X and P1 had formed. The growth of zeolite P1 was reflected by a decrease in the amount of zeolite A, which disappeared after 16 days, suggesting transformation of zeolite A to zeolite P1. The amount of zeolite X in the product remained at the same level as it was initially observed. The product after 23 days contained zeolite X (22%) and zeolite P1 (75%).

On lowering the water content, experiment 4.20 (figure 4. 9), the only product of the reaction was hydroxysodalite. This was not surprising as hydroxysodalite is known to form from sodium rich systems. These results must be considered together with the results of experiment 4.15 for which H_2O/Al_2O_3 was 80. The products of this reaction were described in section 4.3.3.1.

In summary then, if the water content is very low (expt. 4.20) then hydroxysodalite is formed in preference to zeolites X and A.

FIG. 4.9 ZEOLITE GROWTH IN SLURRY CONTAINING $NaAlO_2$ (SOLID PHASE) AND $Na_2SiO_3 5H_2O$ (SOLUTION PHASE) EXPT. 4.20

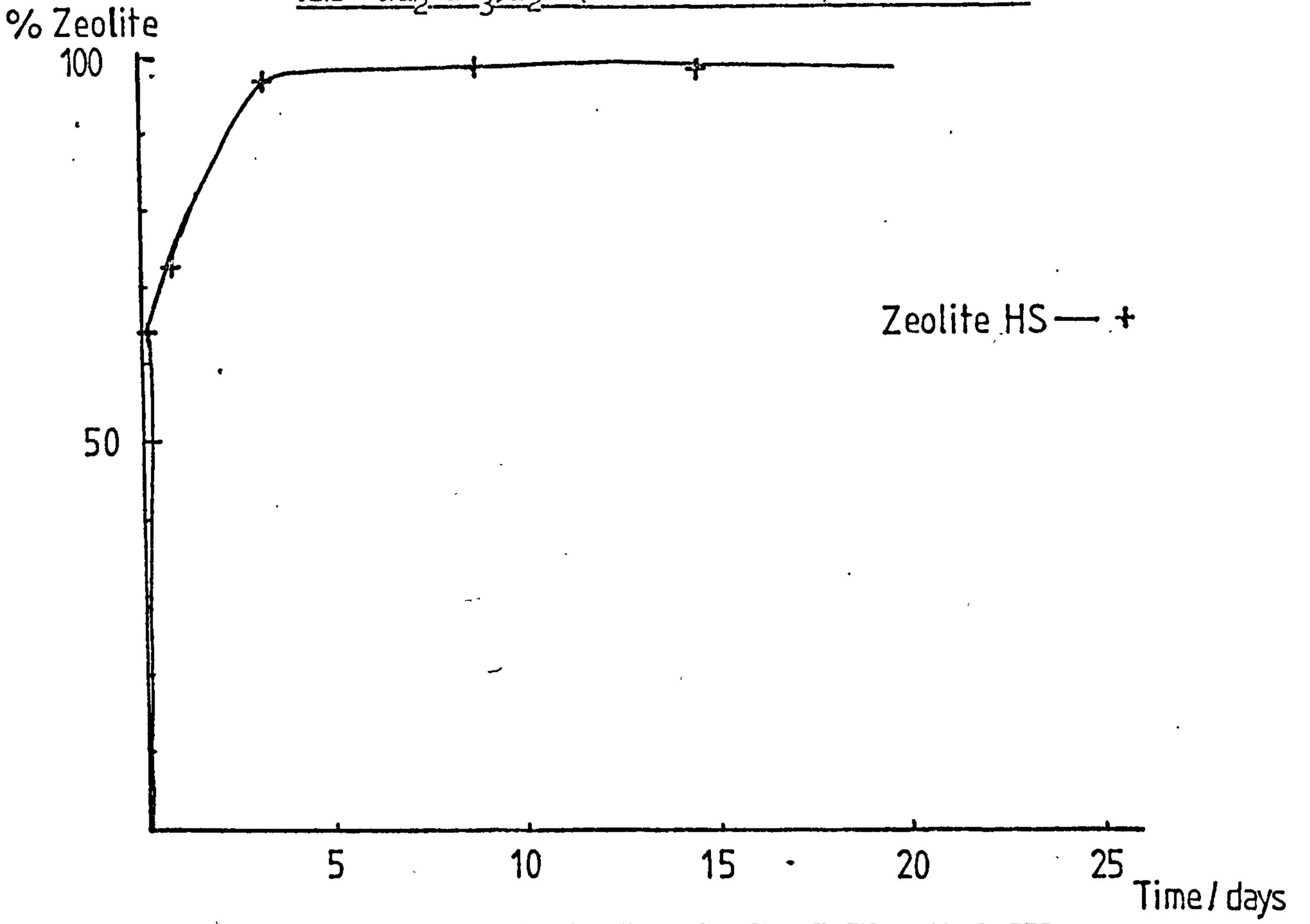

FIG. 4.10 ZEOLITE GROWTH IN SLURRY CONTAINING CAB-O-SIL (SOLID PHASE) AND $NaAlO_2$ (SOLUTION PHASE) + METHYLENE BLUE (1.0 g) EXPT. 4.21

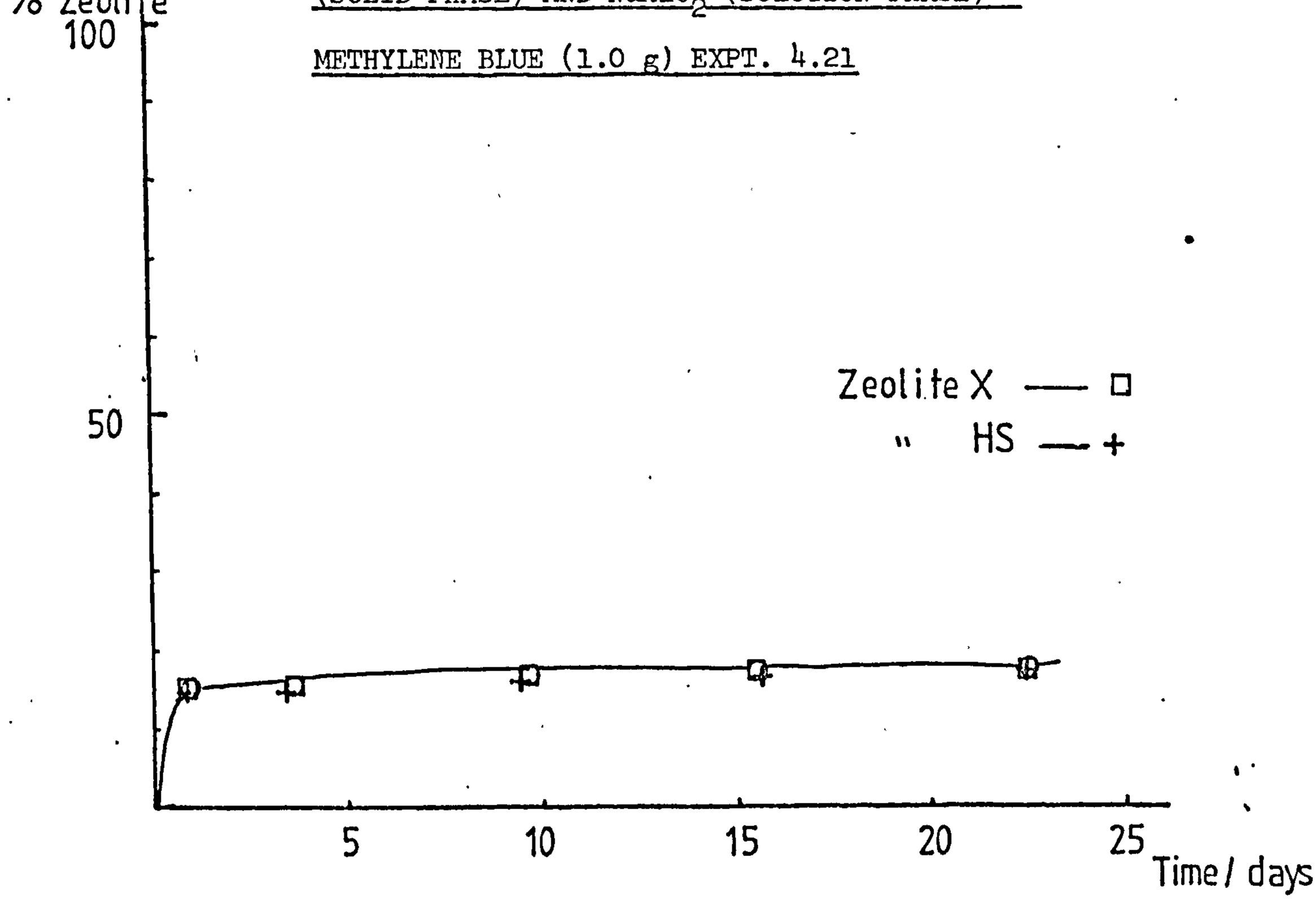

Conversely, if the water content is high (expt. 4.19) hydroxysodalite is not formed at all. Initial formation of zeolites X and A appears to be favoured by an intermediate water content. It appears that if the water content is high (H_2O/Al_2O_3) = 160, then transformation of zeolite A to zeolite Pl occurs rather than transformation of zeolite A to hydroxysodalite, which was observed for H_2O/Al_2O_3 = 80.

4.3.3.5 METHYLENE BLUE ADDITION TO SOLID/LIQUID SLURRIES

The effects of dye addition on zeolite reactions are discussed fully in chapter 5. However, it seems appropriate to include this result at this stage. The reaction mixture for experiment 4.21 was similar to that of experiment 4.16. The methylene blue (1.0 g) was dissolved in water (30 g) and the solution was added to the solid CAB-O-SIL-M5. This silica/dye slurry was aged for 15 minutes with stirring, prior to addition of the sodium aluminate solution. The result is shown in table 4.2 and figure 4.10. The products of the reaction were zeolites X and hydroxysodalite, in contrast to the products of experiment 4.16; zeolites X and A. Apparently, the dye has suppressed the formation of zeolite A and hydroxysodalite has grown in its place. However, it has also inhibited the growth of hydroxysodalite. In all other reactions in which hydroxysodalite has formed, it has grown rapidly to ~80% of the total product, whereas in experiment 4.21 after 23 days, the product contains only 20% hydroxysodalite and zeolite X (20%). A possible explanation is that the dye has adsorbed strongly on the surface of the silica so that there are no more raw materials available for zeolite formation.

4.3.3.6 ADDITION OF SOLID/LIQUID SLURRIES TO ZEOLITE REACTION MIXTURES

As discussed earlier (section 4.1) the addition of solid/liquid slurries, at their pre-crystallisation stage, to zeolite reaction mixtures produces a directing effect on the reaction such that the product is a faujasite type zeolite. This section describes the experiments carried out on the addition of solid/liquid slurries to reaction mixtures. The results are shown in table 4.3.

Experiment 4.22 was carried out to find out if simple addition of water to a solid/liquid activation mixture, to give the same molar composition as that of reactions in chapters 2 and 3, would produce zeolite X. A solid/liquid activation mixture was prepared with solid sodium aluminate, a sodium di-silicate (C100) and sodium hydroxide. This mixture was stirred at 60°C for 2 hours. During this stage it was important to ensure that the sodium aluminate did not stick to the bottom of the flask. After 2 hours, the flask was transferred to a water bath at 95°C or, alternatively, the temperature of the original water bath was increased to 95°C. Excess water to give the same molar composition as the standard reaction was then added and the reaction mixture stirred for another hour. The product of the reaction was pure zeolite X. This reaction might be put to use on an industrial scale. The advantages are two-fold: firstly, it uses a very cheap commercial silicate source, and secondly it does not involve the transfer of caustic liquor.

Experiments 4.23, 4.24 and 4.25 were carried out in a similar fashion to those investigated by MacGilp[67]. Solid/liquid mixtures were prepared as for experiments 4.14 and 4.17 in which the solid silica sources were sodium metasilicate pentahydrate and precipitated SiO_2 respectively and these were then added to reaction

TABLE 4.3 ADDITION OF SOLID/LIQUID SLURRIES TO ZEOLITE REACTION MIXTURES

Expt	Solid/liquid slurry	Aging at 60°C	Product on addition of solid/liquid slurry to zeolite reaction mixture[a]
4.22	(C100+NaOH)+solid $NaAlO_2$	2h	X(100%)
4.23	as 4.14	1h	X(100%)
4.24	as 4.17	1h	trX
4.25	as 4.17	2h	X(100%)

[a] In all cases the slurry was added such that the overall reaction composition was $5.15Na_2O.Al_2O_3.3.98SiO_2.240H_2O$.

mixtures after an aging period. The solid/liquid slurries were prepared such that when added to a reaction mixture the silicate component contributed one-ninth of the total silica in the mixture (cf. reaction mixtures in chapter 3).

For experiments 4.23 and 4.24, the slurries were aged for one hour. A 4.14 type slurry was added in experiment 4.23, and after 3 hours the product was pure zeolite X. When a 4.17 type slurry was added in experiment 4.24, the product contained only trace amounts of zeolite X after 3 hours but aging a 4.17 type slurry for 2 hours prior to addition to the reaction mixture (4.25) gave pure zeolite X in 3 hours.

The initial products (6 h) of experiments 4.14 and 4.17 were zeolite X and zeolite A respectively, yet when either slurry was added to zeolite reaction mixtures, it directed the reaction such that zeolite X was the product. This indicates that the building blocks for zeolite A and zeolite X are similar. For that slurry (4.17) which gave zeolite A, however, it was necessary to age it for a longer period of time before zeolite X formed. This is most likely related to the fact that, in experiment 4.14, small seed nuclei of zeolite X were already present, whereas in experiment 4.17, although building blocks for zeolite X were present, the seed nuclei were zeolite A, and it was necessary to age this slurry for longer until more building blocks formed.

4.4. ^{29}Si F.T. N.m.r. OF SOLID/LIQUID SLURRIES

4.4.1. INTRODUCTION

It has been suggested that the product of a zeolite reaction is dependent on the silicate species present in the solution phase of the gel. Techniques which have been used to identify silicate species in solution include Raman and phosphorescence spectroscopy[82], paper

chromatography[124], infra red spectroscopy[83], trimethylsilylation[116], and reaction with molybdic acid[117]. However, the situation is complex and a detailed knowledge of the species present in the various solutions is not yet available. The technique of ^{29}Si n.m.r. has recently achieved prominence for studying silicate solutions with the introduction of pulsed methods involving Fourier transforms (pulsed F.T. n.m.r.). The use of Fourier transform (F.T.) techniques makes it possible to study ^{29}Si using natural isotope abundance. The magnetically active isotope of silicon ^{29}Si, has a nuclear quantum spin number $I = \frac{1}{2}$, and is present at 4.7% natural abundance. However, it is a difficult nucleus to observe and its relative sensitivity is approximately one half that of ^{13}C.

This technique has given more information about silicate species in solution than any of the other techniques mentioned. The wide range of chemical structures formed have been identified by several workers in this field. It is now possible to assign certain lines in the n.m.r. spectrum obtained with sodium silicate solutions to particular species with some confidence, and it is also possible to determine the relative amounts present.

In view of the advantages of ^{29}Si F.T. n.m.r. over the other techniques for investigating silicate solutions, it was decided to apply this technique to the examination of the solution phase of zeolite reaction mixtures. It was hoped that it would be possible to identify the silicate species present in the solution phase of the gel and their relative amounts. In addition it was hoped to relate the species present in solution to the zeolite which formed.

4.4.2 EXPERIMENTAL DETAILS

The solid/liquid slurries described in section 4.3.2 were used. Since it was suspected that separation of the solid and liquid phases of the slurry may cause, re-equilibration of the silicate species in the liquid phase, it was decided to examine the slurries themselves. The spectra were recorded at approximately 26°C using a 10 mm outside diameter delrim (polyformaldehyde) n.m.r. tube fitted with a delrim insert. This tube was made specifically for use in recording ^{29}Si spectra, since resonance from the glass of a normal n.m.r. tube can cause confusion over line assignments in that region. The spectrometer was a Varian XL-100 operating in the Fourier transform mode. Measurements were made at 19.9 MHz and the sample was given enough pulses to ensure a reasonable signal to noise ratio. Typical conditions used were pulsing to give a 90° tip angle with 0.8 s accumulation time. In most cases, a good spectrum was obtained within one hour. All resonances were measured relative to an external T.M.S. ($(CH_3)_4Si$) signal obtained using pure T.M.S. in a 5 mm outside diameter tube. All chemical shifts are defined as positive to high frequency (low field) of the standard resonances i.e. anti cartesian on the XL-100 traces.

4.4.3 NOTATION

The abbreviated notation used here to describe silicate structures follows that used by Engelhardt[118,119]. In this, all of the O-Si-O structural units in the silicate anions are described as 'Q-units'. The number of Q units directly attached to the one under consideration is indicated by a superscript, the extent of ionisation being ignored e.g.

$Q^1Q^2Q^1$

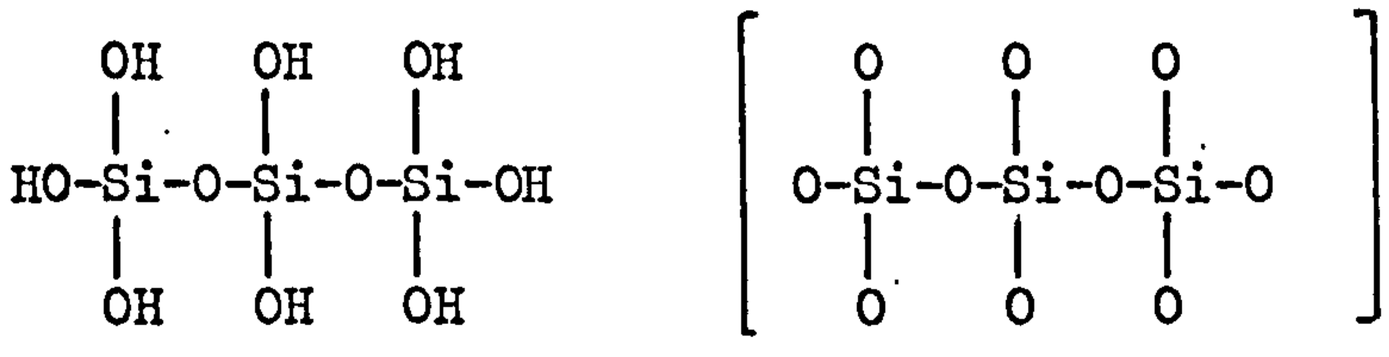

or

$Q^1Q^3Q^2Q^2$

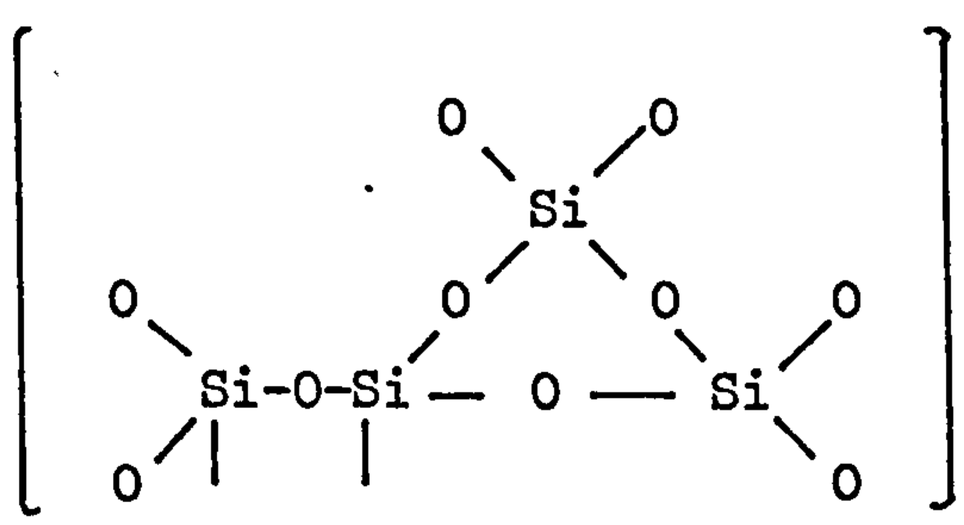

or

$Q^2Q^2Q^2$

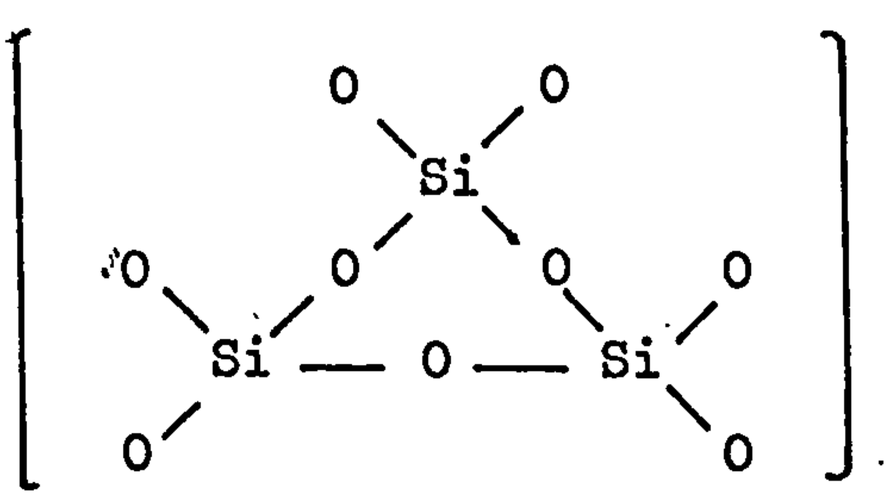

4.4.4 ASSIGNMENT OF RESONANCES

A typical ^{29}Si n.m.r. spectrum of a 1.0 mol dm^{-3} aqueous sodium metasilicate solution is shown in figure 4.11. It is worth noting at this stage that the distribution of silicate anions in the spectrum is influenced[67] more by the SiO_2/Na_2O ratio than the actual concentration of the silicate solution e.g. for low values of SiO_2/Na_2O the predominant species is the monomer whereas high values of SiO_2/Na_2O favour the more condensed, polymeric species.

FIG 4.11 TYPICAL ^{29}Si F.T. n.m.r. SPECTRUM OF 1.0M Na_2SO_3

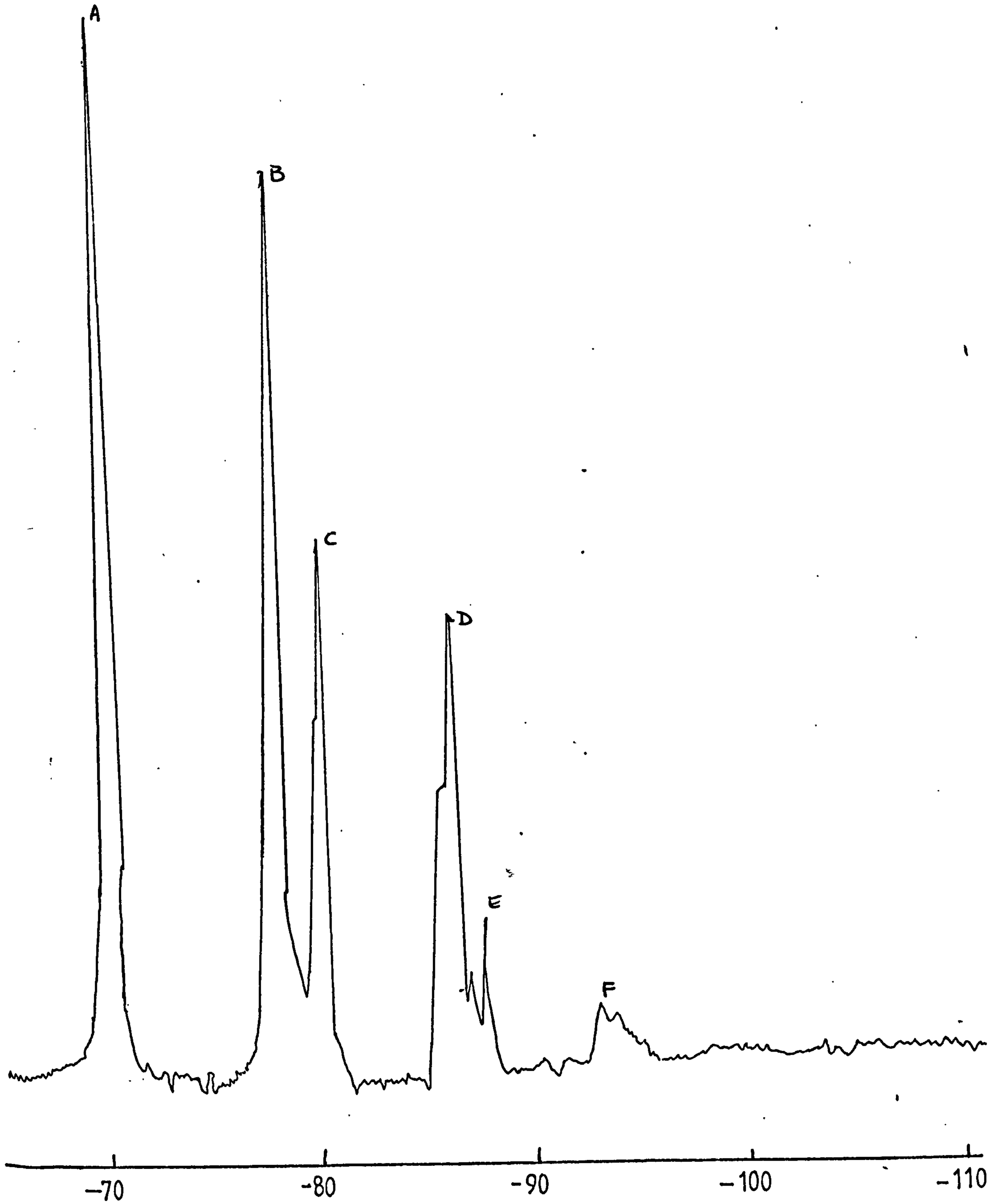

Marsmann[120] labelled the principal feature of the spectrum alphabetically, A-F, and this notation has been adopted by Harris[121]. These labels are used in preference to those used by Lowe[122] and co-workers since they involve no assumptions about the assignment of the resonances. The assignments of bands A to F to certain silicate species are shown in table 4.4.

TABLE 4.4 SILICATE SPECIES CORRESPONDING TO BANDS A-F SHOWN IN FIGURE 4.12

Resonance	Silicate Species
A	$\underline{Q}^0$
B	$\underline{Q}^1\underline{Q}^1$; $\underline{Q}^1[Q^2]_n\underline{Q}^1$; $\underline{Q}^1\overline{Q^3Q^2Q^2}$
C	$Q^1\overline{Q^3\underline{Q}^2\underline{Q}^2}$ $\overline{\underline{Q}^2\underline{Q}^2\underline{Q}^2}$
D	$Q^1\underline{Q}^2\underline{Q}^2Q^1$ $Q^1\underline{Q}^2Q^1$
E	$Q^1\underline{Q}^3\overline{Q^2Q^2}$
F	Q^3 Branched

The original overall assignment[119] of bands A and F to mononuclear (Q^0) and branching units (Q^3) has not been disputed. However, the assignment of the other bands B-E is still the subject of discussion. The assignment of bands B and D to Q^1 and Q^2 units respectively in

acyclic structures and possibly large rings appear to be agreed by most workers in the field. Bands C and E have been assigned to Q^2 and Q^3 units respectively in structures based on the cyclic trinuclear species. In summary then, bands A, B, D and F form a regular sequence assigned to Q^0, Q^1, Q^2 and Q^3 units respectively. However there is some doubt about the assignment of band C, since at various times, the dinuclear species[122] and end groups other than in the dinuclear species[118] have been suggested for this resonance. Harris[121], however, has rejected the suggestion that resonance C is due to end groups, since the total intensity in bands B and C is often too large to be fully explained by end groups. He suggests that band C could be due to the tetranuclear species, but on further consideration he rejects this in favour of the cyclic trinuclear species, in agreement with Engelhardt. There is as yet no certainty about the assignment of this resonance.

4.4.5 RESULTS

The chemical shifts and relative intensities of the n.m.r. signal measured for each sample are shown in table 4.5. The resonances observed are typical of aqueous silicate solutions and tentative assignments to bands A-F has been made. Table 4.6 shows a comparison of the resonances observed in this work and the resonances observed by other workers, together with the silicate species postulated by these workers. Comparison of the resonances observed in this work with those observed by Harris shows reasonable agreement although all the resonances observed in the present work are systematically higher than those reported by Harris. This may be due to the probable difference in silicate concentration: in

TABLE 4.6 COMPARISON OF RESONANCES OBSERVED AND SPECIES ASSIGNED

This work[a]		Engelhardt[118,119]		Harris	
Resonance (-ppm)	Species[b]	Resonance[a] (-ppm)	Species	Resonance (-ppm)	Species
0.00	A	0.00- 2.00	A	0.00	A
7.5 - 8.5	B	7.5 -10.7	B	7.3 - 7.5	B
10.00-10.8	C	10.0 -12.3	C	9.6 - 9.8	C
15.0 -17.0	D			15.27-15.46	D
		18.0 -20.5	E	17.41	E
		22.6 -28.2	F		

[a] These values are rounded to 1 decimal place for easy comparison

[b] See table 4.4

TABLE 4.5 DETAILS OF ^{29}Si SPECTRA RECORDED FOR SOLID/LIQUID SLURRIES

Expt	Age/d	Composition		Spectrum observed (-δ/ppm) and peak intensities (I)[a]			Zeolite product in sample
		Solid phase	Solution phase				
4.12	61	Na_2SiO_3	$NaAlO_2$	70.31(10)	78.19(8) 80.26(8)	86.11(5) 94.0(1) 87.15(2)	X+Pl
4.13	30	$NaAlO_2$	Na_2SiO_3	73.10(10)	81.60(12)	89.5(3)	X+HS
4.14	1	$Na_2SiO_3 5H_2O$	$NaAlO_2$	72.79(10)	-	82.83(4)	X
4.14	61	"	"	72.23(10)	80.24(2.5) 80.53(2)	83.05(3)	X+HS
4.15	1	$NaAlO_2$	$Na_2SiO_3 5H_2O$	72.54(10)	-	82.71(4)	A+trHS
4.15	30	"	"	72.39(10)	80.94(2.5)	83.08(3)	X+Pl+HS
4.16	30	CAB-O-SIL	$NaAlO_2$	73.28(10)	80.73(5)	83.01(1)	X+Pl
4.17	1	Precipitated SiO_2	$NaAlO_2$	73.16(10)	-	-	X+A
4.17	30	"	"	73.45(10)	80.70(1)	83.22(1)	X+Pl+HS
4.18	30	-	$Na_2SiO_3 5H_2O$ $NaAlO_2$	72.23(10)	80.77(3)	83.07(4)	X+HS
4.19	1	$NaAlO_2$	$Na_2SiO_3 5H_2O$	72.77(10)	81.26(3)	83.60(3)	A
4.19	3	"	"	72.77(10)	81.09(3) 81.34(3)	83.66(2)	A
4.20	1	$NaAlO_2$	$Na_2SiO_3 5H_2O$	71.49(10)	79.41(5) 79.65(5)	82.42(9)	HS
4.20	2	"	"	71.67(10)	-	82.44(7)	HS

[a] Since monomer peak was usually most intense this is set =10 and the other peaks are relative to this.

Harris's work it was about 3.0 mol dm^{-3}, whereas for the solid/liquid slurries, the concentration of free silicate anions is likely to be much lower than this. It was noted by Marsmann that the resonance observed for the mononuclear species could vary over a range of ∿5 ppm, from -68.0 ppm to -73.0 ppm depending on the alkalinity of the system: the lower the resonance observed, the higher the alkalinity. This could also explain the lack of consistency within the chemical shifts shown in table 4.5, which vary over ∿3.5 ppm. Comparison with the values reported by Engelhardt shows better agreement. However it should be noted that these comparisons may not be strictly correct since it is possible that the presence of aluminate ions may have an influence on the spectrum observed.

There is no doubt that the peaks observed in this work at -72.4±2.00 ppm are due to the monomeric silicate species Q^0. Also, there seems little doubt that the peaks observed at -80.4±0.7 are due to end groups either in the dimer $\underline{Q}^1\underline{Q}^1$ or end groups of a polymer chain $\underline{Q}^1(Q^2)_n\underline{Q}^1$. The assignment of the peaks observed at -82.9±0.8 is more difficult.

Other workers[118,121] have assigned this peak to the cyclic trinuclear species, but the possibility that this resonance may be due to a cyclic tetranuclear species cannot be disregarded.

An attempt has been made to relate the silicate species observed with the zeolites formed and each sample will be discussed in turn.

In experiment 4.12 the silicate species observed after 61 days were monomers, end groups, cyclic species and branched species. In this experiment, there was no amorphous solid remaining

after 61 days, so it is reasonable to assume that the zeolites X and P1 exist in equilibrium with a sodium silicate solution. The presence of the higher, more condensed polymeric branched species is not surprising, as the solid phase was anhydrous sodium silicates, containing long chain silicates which are not easily depolymerised.

For experiment 4.13, the resonances observed after 30 days have been assigned to monomers, end groups and branched species. Again, as in experiment 4.12, the branched chain species are likely to be due to the use of anhydrous sodium silicate. The zeolite products in this sample (30 d) were zeolites X and P1.

Initially in experiment 4.14, only two peaks were observed, corresponding to monomeric silicate species and a cyclic species. The product at this stage of the reaction was zeolite X, and it seems likely that these species could be important building blocks for zeolite X formation. If this is correct, then it seems reasonable to infer that the cyclic species could be the tetranuclear cyclic species ($Q^2Q^2Q^2Q^2$) since this is considered[75] to be a secondary building unit for zeolite X. After 30 days, two additional peaks which have been assigned as end groups were observed. At this stage, the product was a mixture of zeolites X and hydroxysodalite, and no amorphous aluminosilicate was present. Therefore the silicate species observed are probably a function of the Na_2O/SiO_2 ratio in solution.

In experiment 4.15, the species present after 1 day were similar to those found in expt. 4.14 after 1 day, and the product at this stage was mainly zeolite A. This supports the idea that

the building blocks for zeolite A and zeolite X are the same. The factors which may influence which zeolite forms have been discussed in section 4.3.3.1. After 30 days, the products of expt. 4.15 were zeolites X, P1 and hydroxysodalite, and the silicate species observed now included end group species in addition to the monomers and cyclic species observed after 1 day.

The silica source in experiments 4.16 and 4.17 were amorphous silicas, and it is reasonable to assume that the peaks observed, and the species assigned, relate to the way in which the silica dissolves. Initially in experiment 4.17 (1 day) the only silicate species present was the monomer unit (Q^0). This result suggests that the precipitated silica is dissolving up slowly, i.e. SiO_2/Na_2O is low, which is as expected for a low surface area material.

The products formed at this stage of the reaction were zeolites X and A. After 30 days there were three peaks in the spectrum corresponding to monomers, end groups and cyclic species and the products at this stage were zeolites P1, X and hydroxysodalite. For experiment 4.16 after 30 days, there were three peaks in the spectrum, corresponding to monomers, end groups and cyclic species, and the products were zeolites P1 and X.

For experiment 4.18, the silicate species observed after 30 days were monomers, end groups and cyclic species and the zeolite products at this stage were zeolites X and HS. No amorphous aluminosilicate was present, and therefore the silicate species observed are likely to be a function of the SiO_2/Na_2O ratio.

Experiment 4.19 contained more water in the initial reaction mixture than all the others discussed. The initial product was zeolite A (1 day), and the silicate species present were monomers,

end groups and cyclic species. After 3 days zeolite A was still the only product. However, the spectrum observed contained one additional peak, at -81.09 ppm corresponding to an end group species and one day later it was observed that zeolites X and P1 had started to form. This suggests that the appearance of this anionic species may have had an influence on the formation of these zeolites.

Experiment 4.20 was unique in that it gave a single product, hydroxysodalite. This reaction mixture contained less water than experiments 4.12 - 4.18. After 1 day, five resonances were observed corresponding to the monomer species, end groups (3 peaks) and cyclic species. However, 24 hours later these end groups appeared to have condensed and only two peaks were observed corresponding to monomer species and cyclic species. It is almost certain that the cyclic species observed was a building unit for growth of hydroxysodalite, since this zeolite continued to grow rapidly. It seems likely therefore that this cyclic species could be the cyclic tetranuclear anion, as it is one of the principal building units for hydroxysodalite together with the monomer species.

In summary, then, this type of study of silicate species in solution during slow zeolite reactions shows much promise. It is possible to identify species which can be postulated as building blocks for zeolite growth and to some extent to relate these species to the zeolite which has grown. This study is necessarily limited due to lack of readily available facilities for recording ^{29}Si n.m.r. spectra. However, it is a very interesting field of study and more work should be carried out.

CHAPTER 5

EFFECT OF ORGANIC DYES ON ZEOLITE CRYSTALLISATION

5.1 INTRODUCTION

MacGilp[67] discovered that certain basic dyes adsorbed more strongly on active forms of sodium metasilicate than on inactive forms. The active form, as discussed previously, has very positive directing properties in zeolite reactions, whereas the inactive form appears to have no definite directing tendencies.

The preferential adsorption of crystal violet on active metasilicate led to the idea that the adsorption of appropriate dyes on the components to be employed in zeolite synthesis, or perhaps on the alkali alumino silicate precursor, might give a means of controlling the direction of the zeolite reaction. The ideal was to find a dye which adsorbed on unwanted zeolite nuclei, inhibiting subsequent crystal growth. The use of dyes as crystal growth inhibitors was not a new idea. Marc[123] had shown as early as 1909 that the action of methylene blue inhibited crystal growth of barium sulphate. However, this was not attributed to adsorption on the seed crystals, but to an increased level of supersaturation, due to the presence of the dye.

Whittam[97] carried out a detailed study of dye addition to zeolite Y reactions. He found that certain basic dyes adsorb very strongly on specific zeolites, or only on zeolites having related framework structures. Furthermore, he discovered that some dyes could be used to suppress the formation of unwanted zeolite materials during the synthesis of more desirable zeolites. Since crystal violet adsorbs very strongly on zeolite P1 and on inactive metasilicate, it was the obvious choice for attempts to suppress zeolite P1 formation

in zeolite Y reactions. The results of this study showed (a) that conversion of zeolite Y to zeolite P1 (over-run) was blocked by crystal violet and (b) that any sodium metasilicate pentahydrate can be used in the presence of crystal violet. Thus, for reaction mixtures which included this dye the activity of the metasilicate is of no importance, whereas it is vitally important in the absence of the dye. However, crystal violet was only 100% effective in controlling the zeolite Y reaction when at least part of the silica used was a hydrated sodium metasilicate. When anhydrous sodium metasilicate or water glass was used as the sole silica source, crystal violet could only partially prevent the formation of zeolite P1 and the overall reaction time was trebled.

The addition of zeolite Y seeds to a zeolite Y reaction was found to accelerate the reaction but unfortunately this also accelerated over run since some of the Y seeds convert to zeolite P1 and since this zeolite grows more rapidly than zeolite Y, high yields of zeolite P1 were obtained. Addition of crystal violet to seeded Y reactions was found to suppress zeolite P1 formation and in this way it is possible to reduce the reaction time by seeding and still obtain pure zeolite Y as the product.

In the work described by Whittam, it was found that zeolite P1 formation can be suppressed not only by crystal violet, but also by methyl violet, nuclear fast red, methylene blue, toluidine blue, malachite green, magenta, acriflavine, and salts and esters thereof.

The aim of the work described in this chapter was to find a dye or several dyes which would suppress formation of zeolite P1 in the zeolite X reaction, and also to obtain further information about the way in which addition of dyestuff affected the mechanism of zeolite X formation.

5.2 QUALITATIVE DYE ADSORPTION

5.2.1 INTRODUCTION

Prior to the present investigation there was very little information available on the adsorption of organic dyes on zeolites. It was therefore decided to make a preliminary qualitative investigation of dye adsorption on zeolites X, A, HS, P1 and on silica at three different pH levels. This was followed by a more detailed quantitative study of methylene blue adsorption on zeolites X, A, P1 and silica which is described in chapter 6. For the qualitative study, a range of 37 dyes, including cationic or basic dyes, anionic or acidic dyes and zwitterionic dyes was used.

5.2.2 EXPERIMENTAL DETAILS

5.2.2.1 MATERIALS

Zeolite 13X and zeolite 4A were Linde molecular sieves, in the powder form, supplied by BDH Ltd. Zeolite P1 was prepared from an over run zeolite X reaction (70h). Zeolite HS was also synthesised in the laboratory. The silica was BDH colloidal powder, low in iron. Those dyes which were not BDH standard stains were supplied by Gurr. All experiments were carried out using laboratory distilled water. The salts used to make up buffer solutions were all BDH analar reagent grade.

5.2.2.2 PROCEDURE

Dye (0.5 g) was dissolved in water (1000 g) to give solutions containing 500 ppm of dye. These solutions were adjusted to pH 10 by addition of sodium hydroxide (0.5 mol dm^{-3}), to pH 8 by addition of a phosphate buffer and to pH 4.8 by addition of an acetate buffer.

The phosphate buffer was prepared by dissolving di-sodium hydrogen orthophosphate (28.39 g) and sodium di-hydrogen orthophosphate (7.8 g) in water (1000 cm^3). The acetate buffer was prepared by making up a solution of sodium acetate (10 g) in water (500 cm^3).

The zeolite solid (0.5 g) was stirred with the dye solution (10 cm^3) for 10 minutes, filtered and washed until no more dye could be removed. The zeolite solids were then allowed to dry at room temperature before they were examined to find out the extent of dye adsorption.

5.2.3 RESULTS

The results are shown in table 5.1. In compiling this table the degree of coloration was taken as an approximate measure of the strength of adsorption. Many of the dyes were found to be pH sensitive and faded or precipitated in alkaline solutions.

At pH 10, only cationic dyes adsorbed on all the zeolites and silica. The anionic dyes did not adsorb on zeolites X and A. However, although no adsorption was observed on zeolites X and A for the zwitterions 35-37, weak adsorption was observed on zeolite P1. This specificity was considered to be significant.

At pH 8, all the cationic dyes adsorbed on zeolite X with the exception of methyl green. However, several of these dyes did not adsorb on zeolite A. The difference in adsorption on these two zeolites is almost certainly due to the basicity of the zeolite surface at this pH. No adsorption was observed for the anionic or zwitterionic dyes.

At pH 4.8 all the cationic dyes were adsorbed on zeolite X. Strong adsorption was only observed for brilliant green

TABLE 5.1 QUALITATIVE STUDY OF DYE ADSORPTION ON ZEOLITES[a]

		PH = 10					PH = 8		PH = 4.8	
		X	A	B	HS	SiO_2	X	A	X	A
1.	Azur A	S	S				S	S	S	W
2.	Azur B	N	N				W	W	W	N
3.	Azur C	S	W	S			S	S	S	W
4.	Methylene blue	S		S		S	S	N	S	N
5.	Toluidine blue	S	S		S	S	S	S	S	N
6.	Crystal violet	S	W	S	SF		S	W	W	N
7.	Fuchsin	S	S			S	S	S	S	N
8.	Malachite green	P	P		SPF		W	W	S	N
9.	Brilliant green	PF	PF				S	W	S	S
10.	Methyl violet	S	S		SPF	S	S	W	S	N
11.	Ethyl violet	PF	PF				S	S	S	W
12.	Methyl green	F	F				N	N	S	N
13.	Acriflavine	S	N	S	S		S	W	S	N
14.	Acridine orange	P	P	S			W	N	S	W
15.	Acridine red	P	P				W	N	S	W
16.	Phenosafranine	W	W	S	W	S	W	W	S	N
17.	Safranine AB	W	W			S	W	W	S	N
18.	Neutral red	P	P				S	N	S	N
19.	Janus green	S	S				S	S	S	W
20.	Rhodamine 6G	W	W	S	S	S	W	W	W	W
21.	Nile blue	P	P				S	S	S	W
22.	Quinaldine red	W	W			W	W	N	W	N
23.	Cyanine acid blue	N	N			N	N	N	N	N
24.	Ethyl red	N	N			N				
25.	Methyl red	N	N			W			P	P
26.	Ponceau brilliant	N	N			W				
27.	Naphthol blue black	N	N			W				
28.	Noir naphthalene	N	N			W				
29.	Benzopurpurine	N	N			W	N	N	N	S
30.	Astrazon yellow	P	P							
31.	Acridine	I	I						I	I
32.	Naphthol yellow	N	N			W				
33.	Tartrazine	N	N			W				
34.	Nuclear fast red	N	N		N	S	N	N	W	S
35.	Xylene cyanol FF	N	N	M	N	S	N	N	N	N
36.	Wool fast blue	N	N	W	N					
37.	Alkali blue	N	N	W	W		N	N	N	S

[a] The letters in this table have the following significance:- S, strongly adsorbed; W, weakly adsorbed; N, no adsorption; F, dye fades; P, precipitates; I, insoluble.

on zeolite A, all the other cationic dyes either adsorbed weakly or not at all. Nuclear fast red, an anionic dye, adsorbed weakly on zeolite X and strongly on zeolite A. This adsorption of anions can be attributed to the change in basicity of the surface of the zeolite in the low pH environment. Thus at pH 4.8 the surface of zeolite X is still negatively charged whereas that of zeolite A (which dissolves slowly at this pH) is positively charged.

It seemed obvious, then, that anionic dyes would not be effective in controlling zeolite crystallisation, since they did not adsorb on any of the zeolites or on silica. It was therefore decided not to investigate these materials any further. However, Whittam[97], had reported that nuclear fast red, an anionic dye, adsorbed strongly on zeolite P1 and inhibited the growth of this zeolite, in a zeolite Y reaction and it was therefore decided that this particular dye should be included in further experiments.

It would seem that those dyes which precipitated in alkali could not be used. However, crystal violet precipitates in alkaline solution and Whittam[124] had found it to be the most effective dye for inhibiting zeolite P1 growth in zeolity Y reactions. Therefore, those dyes which precipitated were also retained for further investigation.

No evidence was found to suggest that some dyes adsorbed only on zeolites having related structures, as found by Whittam[124].

The conclusions which were drawn from this investigation were:

1) Only dyes which were cations in alkaline solution adsorbed on the zeolite surfaces at pH = 10 and pH = 8.

2) The strength of adsorption depended on the number of sites on, and probably the structure of, the surface e.g. stronger adsorption was observed on zeolite X than zeolite A. (The adsorption sites are probably ionised silanol groups; because of its higher Si/Al ratio, zeolite X will have more sites).

The dyes which were used in the reactions in the following section were chosen because,

a) They had been used with low activity pentahydrate in Whittam's work.

b) They were soluble in hot alkali, were strongly adsorbed on zeolite X and could not be removed by washing with strong alkali.

5.3 ADDITION OF DYES TO THE ZEOLITE X REACTION

5.3.1 INTRODUCTION

The standard zeolite X reaction described in chapter 3 was carried out with three different sources of sodium metasilicate and several dyes. The metasilicates used were sodium metasilicate pentahydrate, sodium metasilicate.nonahydrate and anhydrous sodium metasilicate.

5.3.2 EXPERIMENTAL DETAILS

5.3.2.1 MATERIALS

The sodium metasilicate pentahydrate used was supplied by Joseph Crosfield Ltd. and was tested and shown to be active. The sodium metasilicate nonahydrate and anhydrous metasilicate were prepared in the laboratory.

5.3.2.1.1 Preparation of sodium metasilicate nonahydrate

The technique used to prepare pure $Na_2SiO_3 9H_2O$ was that of crystallisation from a supersaturated aqueous solution of sodium metasilicate. A hot saturated solution of sodium metasilicate was prepared from either stoichiometric amounts of silica and sodium hydroxide or from sodium metasilicate pentahydrate. This solution was clarified by repeated ultrafiltration through a 200 nm filter. It was then cooled to room temperature and seeded with a few nonahydrate crystals. The crystals were then filtered in the absence of carbon dioxide and dried over sodium metasilicate pentahydrate until they contained exactly nine molecules of water per metasilicate group. This metasilicate was shown to be weakly active giving approximately equal quantities of zeolite X and P1 in a standard zeolite X reaction.

5.3.2.1.2 Preparation of anhydrous sodium metasilicate

A pure solution of sodium metasilicate containing stoichiometric amounts of silica and sodium hydroxide was prepared. The anhydrous sodium metasilicate was then obtained by careful evaporation of this solution at around 100°C. This material was shown to be inactive.

5.3.2.2 PROCEDURE

The zeolite X synthesis reaction described in chapter 3 was used for this work. For those zeolite X reactions in which metasilicates other than the pentahydrate form were used, the sodium metasilicate pentahydrate (4.7 g) was replaced by equivalent quantities of the nonahydrate (7.3 g) and the anhydrous metasilicate (2.7 g). In these two cases the additional amount of water was

adjusted so that the overall stoichiometry was maintained. The reaction procedure was otherwise identical for each metasilicate material.

The dye (0.4 g) was added to the sodium metasilicate solution since addition to the sodium aluminate solution would have resulted in complex formation between the dye and the aluminate ion. The silicate solution with the dye was stirred on a magnetic stirrer for approximately 2 hours at room temperature. These solutions were then filtered using a Gelman filter equipped with Metricel filter discs which enabled particles larger than 0.2 μm to be removed from the solution. The amount of dye was chosen to give a concentration of 1600 ppm in the reaction mixture, however, in some cases (e.g. Malachite green) most of this was removed in the filtration.

5.3.3 DYE ADDITION TO REACTIONS WITH ACTIVE SODIUM METASILICATE PENTAHYDRATE

The results are shown in table 5.2. The only dye which clearly suppressed the formation of zeolite X and led to the formation of zeolite P1 was safranine AB (5.20). This was, of course, an unfavourable effect, but it would be of interest to examine how this dye redirects the course of the reaction. Unfortunately this was not possible, as the actual structure of safranine AB could not be found and subsequent examination of safranine O and safranine T (which were thought to be related dyes) did not show a similar effect. Suppression of zeolite X formation was also observed with acriflavine, but in this case no zeolite P1 was formed.

TEXT BOUND INTO THE SPINE

TABLE 5.2 EFFECT OF DYES ON REACTION WITH ACTIVE METASILICATE PENTAHYDRATE

Run No.	Dye	%X(2θ=23.4)	%X(2θ=26.9)	%X(Average)[a]	H_2O(g/g)[b]	Remarks
1	Absent	83	90	87		
2	"	81	83	82		
3	"	85	89	87	0.304	
4	Crystal violet	75	76	76		
5	Janus green	80	83	82	0.307	tr Pl
6	Janus green	71	76	74		
7	Malachite green	70	81	76		tr Pl
8	Xylene cyanol	100	75	88	0.309	
9	Xylene cyanol	104	93	99		
10	Methylene blue	98	94	96		
11	Azur C	74	72	73		
12	Rhodamine 6G	81	81	81		
13	Acriflavine	48	74	61	0.207	
14	Patent blue	84	87	86	0.314	
15	Lissamine rhodamine	75	77	76		
16	Fast acid violet 10B	62	65	64		
5.17	Naphthalene Green	62	67	65		
5.18	Lissamine blue BF	98	89	94	0.314	
5.19	Fast acid violet 2C	73	76	75		
5.20	Phenosafranine	64	64	64	0.313	
5.21	Safranine AB	26	23	25		45% Pl
5.22	Acid fuchsin	75	85	80		
5.23	Sulphanilic acid	90	98	94	0.304	
5.24	Ethanol	108	100	104	0.314	
		89	98	94		Rpt. x-ray
5.25	Triethylamine	79	86	83		
	Linde 13X (1)				0.303	
	(2)				0.286	

[a] Amount of zeolite X based on average of x-ray peak heights at 2θ = 23.4° and 26.9°. A standard sample of zeolite X (Linde 13X) was taken to be 100% zeolite X and used as a basis for the yields reported in this table. The products identified in this table were those obtained after 3 hours.

[b] Water absorption reported as weight of water absorbed per gram of dry zeolite placed over saturated $Ca(NO_3)_2$ at 25°C (H_2O v.p. = 12 mm Hg).

Since xylene cyanol, a zwitterion, was selectively adsorbed by zeolite P1 (table 5.1), it was expected that the zwitterionic dyes used in runs 5.14 to 5.19 might also be selectively adsorbed by this zeolite. This selective absorption of xylene cyanol is clearly supported by the fact that zeolite X was obtained in a very good, pure crystalline form, in reaction 5.8 and 5.9. However it appears that two zwitterionic dyes, fast acid violet 10B (5.16) and naphthalene green (5.17), have a tendency to suppress zeolite X formation.

It was observed for many of the dyes that there is a colour change during the zeolite reaction. This may be due to the breakdown of the dye caused by the action of the strong alkali. Therefore, the effect on the reaction of three of the possible breakdown products, ethanol, triethylamine and sulphanilic acid, was investigated. No significant effect was observed for any of these materials, although the use of ethanol appeared to give a very good sample of zeolite X.

Of the other dyes investigated in this reaction system, none appeared to have a significant effect on the product of the reaction, although it is possible that the kinetics may be affected.

It appears that the ability of active sodium metasilicate to direct the course of the reaction dominates any effects caused by the dyes.

5.3.4 DYE ADDITION TO REACTIONS WITH ANHYDROUS SODIUM METASILICATE

The products obtained from the standard X reaction using inactive anhydrous sodium metasilicate in place of the active pentahydrate are shown in table 5.3. With no dye present the

TABLE 5.3 EFFECT OF DYES ON THE STANDARD REACTION USING INACTIVE ANHYDROUS METASILICATE[a]

Run No.	Dye	Product
5.26	Absent	Amorphous
5.27	"	"
5.28	Crystal violet	-Pl(55%)
5.29	Janus green	-Pl(75%)
5.30	Malachite green	-Pl(75%)
5.31	Xylene cyanol FF	-Pl(70%)
5.32	Azur C	-Pl(70%)
5.33	Rhodamine 6G	-Pl(80%)
5.34	Acriflavine	(1) Amorphous+trace Na-Pl
		[b](2) Na-Pl (90%)

[a] Reaction time: 3h; reaction temperature: 95°C

[b] Reaction time: 4h.

product obtained after a reaction time of 3 hours was completely amorphous. However, with the possible exception of acriflavine, when dye was present the product obtained after 3 hours was zeolite P1. None of the dyes suppressed zeolite P1 formation - in fact all gave more zeolite P1 than obtained in their absence. Crystal violet did not promote the formation of zeolite P1 to quite the same extent as the other dyes, the product containing only 55% P1, whereas the other dyes gave over 70% P1. The tendency to encourage zeolite P1 was weakest for acriflavine, which gave only a slight trace of P1 after 3 hours.

Thus it appears that the presence of cationic dyes helps to speed up the formation of zeolite P1 from this type of reaction mixture.

5.3.5 DYE ADDITION TO REACTIONS WITH SODIUM METASILICATE NONAHYDRATE

The products obtained from the standard X reaction using sodium metasilicate nonahydrate in place of the active metasilicate are shown in table 5.4. The sodium metasilicate nonahydrate, prepared as described in section 5.3.2.1.1, showed low activity; when it was used in place of active metasilicate in a zeolite X reaction, the product obtained after 3 hours was a mixture of zeolite X and P1, together with some amorphous material. A repeat of this reaction confirmed the low activity of this metasilicate, only 30% zeolite X being formed within 3 hours. Of the seven dyes investigated two, Janus green and Malachite green, appeared to have no effect on the reaction. In the case of xylene cyanol, more zeolite P1 than zeolite X was formed, which is surprising since it had been observed that xylene cyanol adsorbed preferentially on

TABLE 5.4 EFFECT OF DYES ON THE STANDARD REACTION USING METASILICATE NONANHYDRATE[a]

Run No.	Dye	Product
5.35	Absent	X(52)+Pl(20)+Am[b]
5.36	"	X(30)+Am
5.37	Crystal violet	X(73)
5.38	Janus green	X(57)+Pl(30)
5.39	Malachite green	X(31)+Pl(46)
5.40	Xylene cyanol	X(28)+Pl(74)
5.41	Azur C	X(56)+Am
5.42	Rhodamine 6G	X(27)+Am
5.43	Acriflavine	Pl(52)

[a] Reaction time: 3h; reaction temperature: 95°C

[b] Am = Amorphous material

zeolite P1 (see table 5.1) Crystal violet, azur C, and rhodamine 6G all gave only zeolite X, although some amorphous material was detected in the reactions with azur C and rhodamine 6G. It was noted in section 5.3.5 that acriflavine appeared to suppress the formation of zeolite X, and this is supported by the fact that in reaction 5.43, it completely suppressed the formation of zeolite X and allowed only zeolite P1 to grow. Because of the marked effects obtained in these reactions, (table 5.4) it was considered that further investigations would be worthwhile, and in the following section some kinetic measurements are described.

5.4 KINETIC STUDY

5.4.1 INTRODUCTION

The reaction mixture chosen for this kinetic study was that in which the metasilicate component was provided by the weakly active nonahydrate. This mixture was chosen because it gave a final product which contained almost equal amounts of zeolite X and zeolite P1. Furthermore, the most marked effects of dye addition had been observed in this system, and it was therefore considered that it was most sensitive to effects caused by the addition of dyes. The dyes chosen for this study were crystal violet, acridine orange, and acriflavine.

5.4.2 EXPERIMENTAL DETAILS

The method used for following the kinetics of the reactions was the absorption method described in chapter 3. It was shown that adsorbed dye did not affect the extent of absorption (table 5.5). The method of calculating the amounts of zeolite X-

TABLE 5.5 EFFECT OF ADSORBED DYE ON WATER ABSORPTION

Run No.	Dye used in reaction	Product of reaction[a]	Wt H_2O absorbed g/g after 240 h
5.8	Xylene cyanol	X	.307
			.311
5.13	Patent blue	X	.312
			.316
5.17	Lissamine blue BF	X	.313
			.315
5.5	Janus green	X	.314
			.307
5.19	Phenosafranine	X	.317
			.320
5.12	Acriflavine	[b]X	.206
			.209

[a] Two samples of each product were used in each case.

[b] From x.r.d. this sample contained only 61% X and amorphous aluminosilicate - so this absorption value corresponds well with that analysis.

in a sample is described in chapter 3, however, for this work it was necessary to analyse for both zeolites X and P1. A method for carrying out this calculation was devised and is described in the following section.

5.4.3 CALCULATION OF THE COMPOSITION OF MIXTURES OF ZEOLITE X, ZEOLITE P1 AND AMORPHOUS GEL

For a reaction in which both zeolite X and zeolite P1 are formed, the absorption of a sample taken during a run is due to both these materials and to the amorphous gel, i.e.

$$A = x_X A_X + x_P A_P + x_{Am} Am \qquad (5.1)$$

where $$x_X + x_P + x_{Am} = 1 \qquad (5.2)$$

Since there are now three unknowns x_X, x_P and x_{Am} it is necessary to carry out absorptions with two absorbates which show significantly different behaviour with zeolites X and P1. The procedure adopted for these measurements was to equilibrate the sample first with water (as described in section 3.5.4), and then, after repeating the drying procedure, with cyclohexane. The weight of the sample bottle + dry zeolite (WBS2) was redetermined between the absorption measurements and the two dry weights (WD1 and WD2) were usually found to be in good agreement.

The water absorption of the sample A_H is given by -

$$A_H = WH/WD1 = (WBSH - WBS1)/(WBS1 - WB)$$

and the cyclohexane absorption A_C is given by

$$A_C = WC/WD_2 = (WBSC - WBS1)/(WBS1 - WB)$$

The water absorption capacity is given by -

$$A_H = x_X A_{X,H} + x_P A_{P,H} + x_{Am} A_{Am,H} \qquad (5.3)$$

and the cyclohexane capacity by -

$$A_C = x_X A_{X,C} + x_P A_{P,C} + x_{Am} A_{Am,C} \qquad (5.4)$$

in which $A_{X,H}$, $A_{P,H}$ and $A_{Am,H}$ are the absorption capacities of the pure materials for water and $A_{X,C}$, $A_{P,C}$ and $A_{Am,C}$ are the corresponding values for cyclohexane.

In principle, solution of the simultaneous equations 5.1, 5.2 and 5.3 makes it possible to obtain values x_X, x_P and x_{Am}. However this approach does not always give sensible values, primarily, because of the uncertainties involved in the choice of the values of A for the pure materials. For example, any uncertainty in $A_{X,H}$ and $A_{X,C}$ as discussed in section 3.3.6 can give rise to nonsensical values for x_P and x_{Am} as well as x_X. As previously described A_{Am} varies during the nucleation stage of the reaction and it was decided that for both water and cyclohexane the best estimate of A_{Am} was the minimum value of A which occurred just before the x-ray detectable onset of crystallisation. Again it should be realised that the structure of the amorphous gel may vary during the crystallisation, and A_{Am} obtained in this way is probably a maximum value.

Because it was difficult to obtain reliable A values, the mixture composition was determined by the following procedure, which was used in preference to the simple solution of the simultaneous equations. The procedure was carried out as follows:-

1) An estimate of x_P was made using equation (5.5)

$$Ex_P = \frac{[(A_{X,C}-A_{Am,C})(A_H-A_{Am,H})-(A_{X,H}-A_{Am,H})(A_C-A_{Am,C})]}{[(A_{X,C}-A_{Am,C})(A_{P,H}-A_{Am,H})-(A_{X,H}-A_{Am,H})(A_{P,C}-A_{Am,C})]} \qquad (5.5)$$

and then x_P was set equal to Exp

2) A similar procedure was used to estimate x_X

$$Ex_X \quad \frac{[(A_{P,C}-A_{Am,C})(A_H-A_{Am,H})-(A_{P,H}-A_{Am,H})(A_C-A_{Am,C})]}{[(A_{P,C}-A_{Am,C})(A_{X,H}-A_{Am,H})-(A_{P,H}-A_{Am,H})(A_{X,C}-A_{Am,C})]} \qquad (5.6)$$

and finally x_X was set equal to Ex_X

3) x_{Am} was estimated from

$$x_{Am} = 1.0 - Ex_X - Ex_P \qquad (5.7)$$

Additional constraints were applied. In particular:-

a) in all cases in which x_{Am} was calculated to be >1, x_{Am} was set equal to one and x_P and x_X equal to zero

b) likewise if x_{Am} was calculated to be <0, x_{Am} was set equal to zero.

Since the sample of zeolite P1 which was used as a standard was a sample synthesised in the laboratory it had values for $A_{P,C}$ and $A_{P,H}$ close to those expected for the zeolite P1 in typical mixtures. However for zeolite X it was necessary to use a correction factor f, as described in section 3.3.7 such that

$$A_{X,C} = A_{13X,C} f_C$$

and

$$A_{X,H} = A_{13X,H} f_H .$$

A computer program was written in FORTRAN to carry out the calculations.

5.4.4 RESULTS

Figure 5.1 shows growth curves obtained for zeolite X and zeolite P1 growth in the reaction using sodium metasilicate nonahydrate. The growth curves obtained for this reaction when crystal violet, acriflavine and acridine orange were added (1600 ppm) are also shown in figure 5.1. The percentage of zeolite X formed in these reactions was 69%, 62% and 70% respectively and was higher than that formed in the blank reaction (51%). Zeolite P1 was formed in all the reactions.

The induction period for zeolite P1 formation was 190±5 minutes and was independent of the dye added. The induction period for zeolite X formation was slightly reduced by the addition of dyestuff. It was observed that once zeolite P1 had started to grow, the growth of zeolite X stopped. Figures 5.2 - 5.5 show log (%X) versus time for each of the reactions. By examination of these plots a crude rate constant can be estimated. It can be seen that for the dyes the rate constants are approximately equal

FIG. 5.1 GROWTH CURVES FOR ZEOLITE X AND ZEOLITE P1

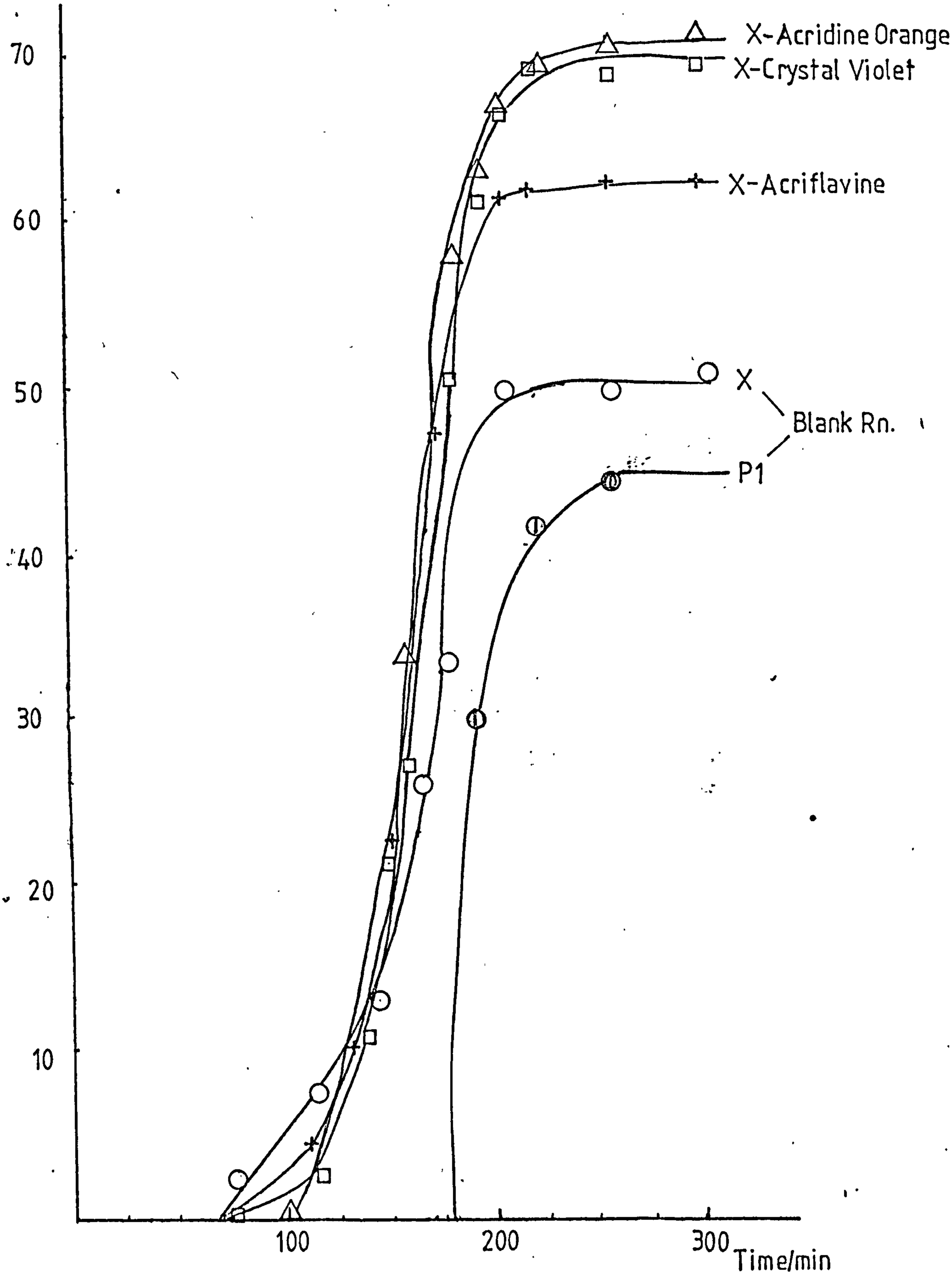

FIGS. 5.2 - 5.5 LOG (%X) VERSUS TIME FOR REACTION WITH NO DYE ADDED, WITH CRYSTAL VIOLET, ACRIDINE ORANGE AND ACRIFLAVINE

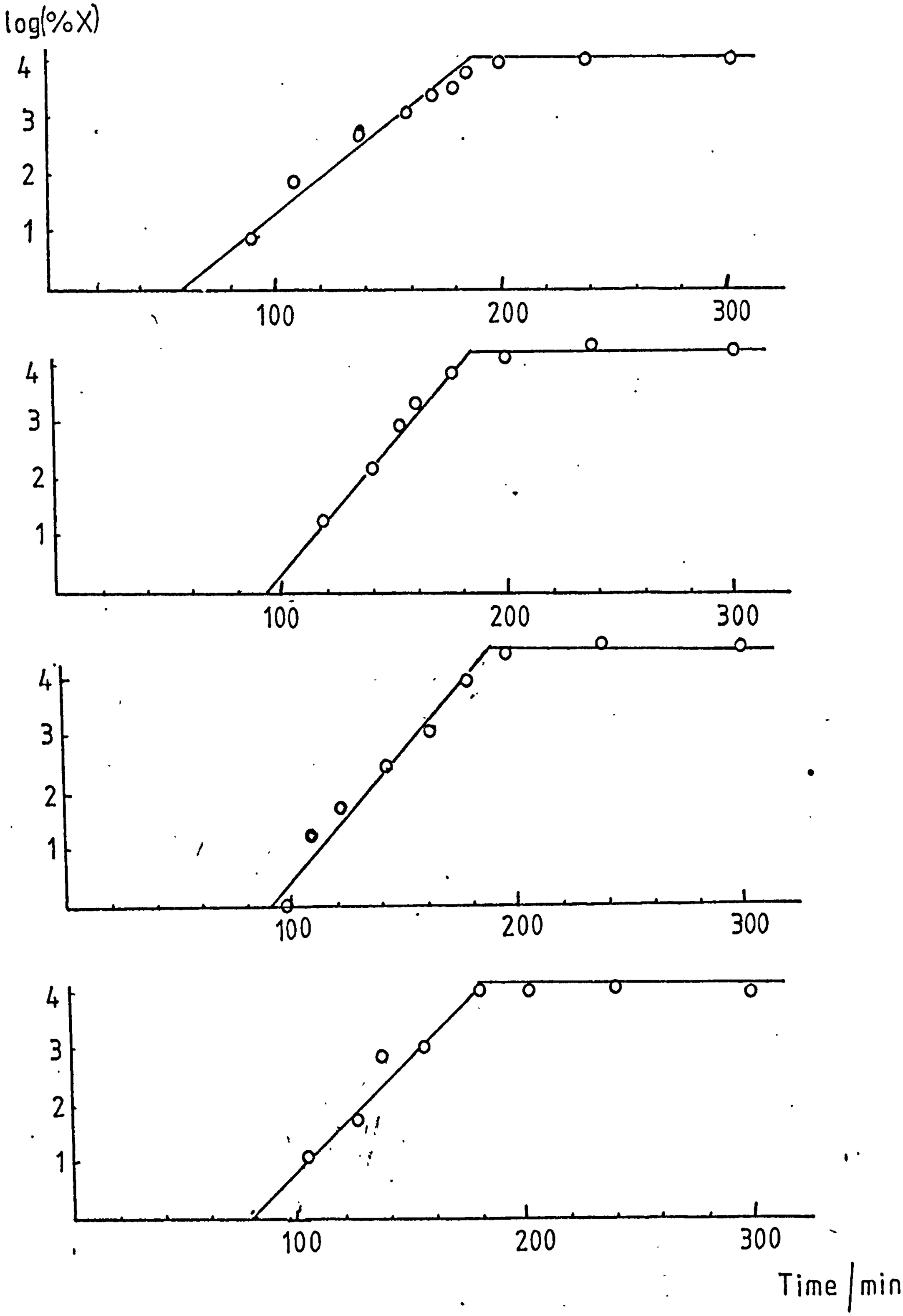

and are greater than in the blank reaction. Thus, it appears that the chief cause of the increased amount of zeolite X formed in the presence of dyes is an increase in its growth rate, rather than the suppression of zeolite P1.

5.5 DYE ADDITION TO THE ZEOLITE P1 REACTION

5.5.1 INTRODUCTION

Since the aim of this work was to find a dye which would inhibit or suppress the formation of zeolite P1 it was decided to test the effect of dye addition to a reaction which was designed to give zeolite P1, rather than zeolite X. This reaction in fact had the same stoichiometry as the zeolite X reaction, but was prepared from a reaction mixture in which all the silica was provided by a sodium disilicate waterglass type C100. It was designated the zeolite P1 reaction in order to distinguish it from those reactions in which part of the silica was provided by a metasilicate component.

5.5.2 ZEOLITE P1 SYNTHESIS

This reaction was set up in the following way. Pure sodium hydroxide (12.8 g) was dissolved in distilled water (12.8 g) and technical grade alumina trihydrate (7.8 g) was added. The mixture was boiled until a clear solution was obtained, then cooled to room temperature, and the lost water was replaced. Sodium disilicate waterglass type C100 (43.1 g) was added to distilled water (50.0 g). This silicate solution was stirred rapidly with an electric mixer while the previously prepared aluminate solution was slowly added to form a stiff gel. Distilled water (124.5 g) was then added and the mixture was stirred until a white homogeneous liquid

was obtained. This mixture was then placed in the reactor and stirred under reflux at 95°C for a fixed period of time.

5.5.2.1 ANALYSIS

The zeolite P1 reaction was followed using x-ray powder diffraction, differential thermal analysis and ^{23}Na F.T. n.m.r. Samples were taken from the reaction at 30 minute intervals for the first 2 hours and then at 20 minute intervals for the next 3 hours and finally at 30 minute intervals up to 3 hours.

X-ray powder diffraction patterns for each of the dry equilibrated solid samples were obtained. All samples up to 2 hours 20 minutes were completely amorphous after which pure zeolite P1 was observed. The quantity of zeolite P1 present was calculated by measuring the peak height of the diffraction line at $2\theta = 28.2^{\circ}$ (d = 3.08) and comparing this with the peak height obtained for a sample of pure zeolite P1. The final sample obtained was calculated to be 105% zeolite P1 relative to the standard sample. The results are shown in table 5.6 and the growth curve for zeolite NaP1 is shown in figure 5.6.

The line width of the ^{23}Na n.m.r. signal was measured throughout the course of the zeolite P1 reaction. The results are shown in table 5.6 and figure 5.7. These measurements were made on complete samples of reaction mixture, however, the observed n.m.r. signal is that of the sodium ions in the liquid phase. The

FIG. 5.6 X.r.d. ANALYSIS OF THE ZEOLITE P1 REACTION

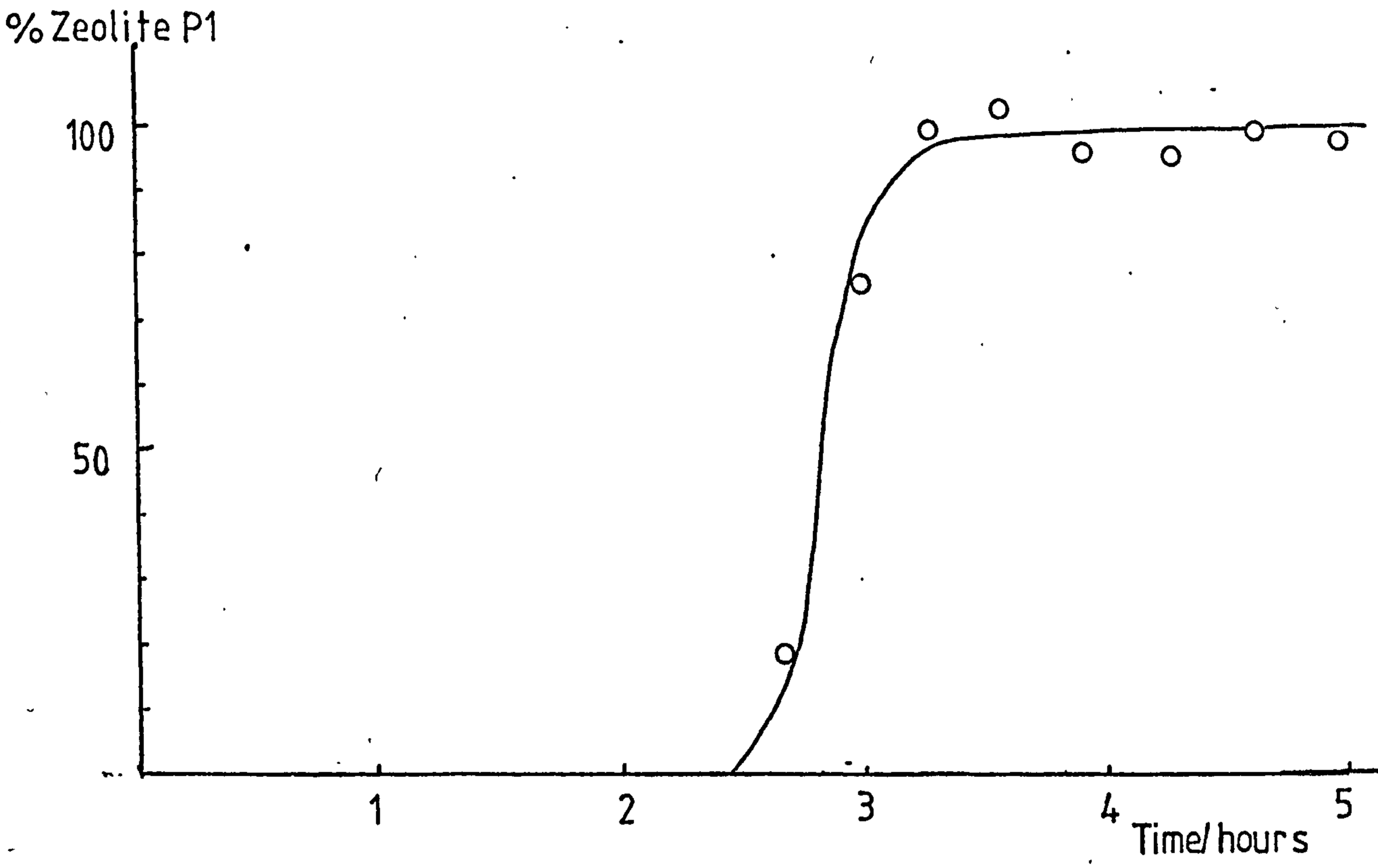

FIG. 5.7 ^{23}Na n.m.r. OF THE ZEOLITE P1 REACTION

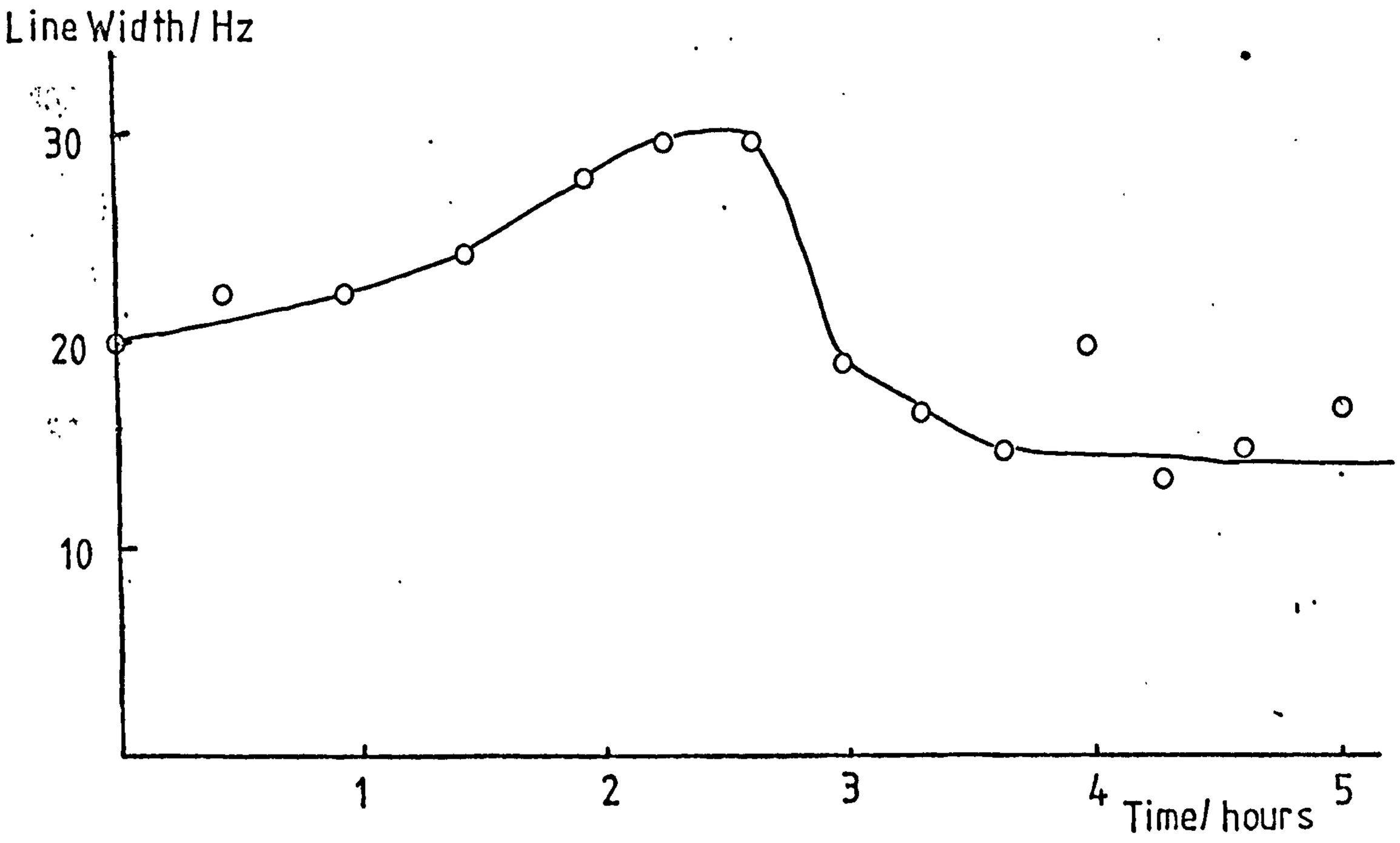

TABLE 5.6 X.r.d., d.t.a. AND ^{23}Na ANALYSIS OF THE ZEOLITE P1 REACTION[a]

Time/h	X.r.d. (%P1)	D.t.a.	^{23}Na n.m.r. line width/Hz
0	0	w,85,118; vw,90	20
0.5	0	none	22
1.0	0	none	22
1.5	0	m,45; 50	23
2.0	0	vw,75	26
2.3	0	vw,79	28
2.7	19	m,75; 80	28
3.0	77	s,80; 105; w,35	18
3.3	103	s,80; 115; m,35,43	15
3.7	111	s,80; 116	14
4.0	102	s,80; 118	20
4.3	103	s,80,112; w,38	13
4.7	98	s,75; 108	15
5.0	106	s,85,113; m,35,45	16
5.5	106	s,80,115; w,42	14
6.0	105	s,85,118; vw,40	16

[a] The symbols used in this table are as follows:- w = weak, m = medium, s = strong
the first temperature is that of the peak onset and the second is that of the peak maximum

line width depends, in part, on the extent to which the sodium ions are complexed with the silicate species in solution. It is therefore possible that the observed increase in line width may reflect an increase in complex formation. The sharp drop during crystallisation would then correspond to the release of Na^+ ions as the silicate is used up. It is of interest to note that this sharp drop also corresponds to the point at which zeolite Na-P1 starts to grow (figure 5.6).

Differential thermal analysis measurements were made on all the dry equilibrated solids obtained from the reaction. The results are shown in table 5.6. A typical d.t.a. trace for zeolite P1 is shown in figure 5.8. The peak observed for zeolite P1 starts at $\sim 80^{\circ}C$ and has its maximum at around $115^{\circ}C$. The most significant observation was the detection of a small zeolite P1 peak at 2 hours and 2 hours 20 minutes although both samples were amorphous to x-rays.

5.5.3 ADDITION OF CRYSTAL VIOLET AND ACRIFLAVINE TO THE ZEOLITE P1 REACTION

5.5.3.1 METHODS OF DYE ADDITION

Two methods of dye addition were employed. The dye was either dissolved in water (50 g) from the reaction mixture and then added to the reaction mixture after gel formation had occurred or the dye was added as a solid to the gel. In both cases the gel plus dye was stirred for 5 minutes before being placed in the reaction vessel.

5.5.3.2 RESULTS

The results of adding crystal violet and acriflavine to the zeolite P1 reaction are shown in table 5.7. It appears that crystal

TYPICAL d.t.a. TRACE FOR ZEOLITE P1

FIG. 5.8

TABLE 5.7 ADDITION OF CRYSTAL VIOLET AND ACRIFLAVINE TO THE ZEOLITE P1 REACTION

Run No.	Dye	Wt dye in 250 g	ppm dye	PRODUCT (N%) 2h	3h	4h
5.43	Acriflavine	0.1	400	Am	P1(105)	P1(110)
5.44	"	0.4	1600	Am	P1(20)+trX	P1(105)+trX
5.45	"	1.0	4000	Am	P1(25)+trX	P1(100)+trX
5.46	"	5.0	20000	Am	C	P1(110)
5.47	Crystal violet	0.1	400	Am	P1(100)	P1(100)
5.48	"	0.4	1600	Am	P1	P1(100)
5.49	"	1.0	4000	Am	P1(100)	P1(105)
5.50	Crystal violet[a] + acriflavine	1.0 1.0	4000 4000	trX	X(55)+P1(30)	X(65)+P1(35)
5.51	Crystal violet[a]	1.0	4000	trX	X(33)+P1(7)	X(30)+P1(50)
5.52	Acriflavine[a]	1.0	4000	Am	X(24)+Am	X(24)+P1(60)

[a] Added as solid

violet has no effect on the zeolite P1 reaction, when added in solution, even at loadings of 4000 ppm dye. In contrast, it was observed that loadings of 1600 and 4000 ppm of acriflavine (added in solution) reduced the amount of zeolite P1 formed in 3 hours (25% compared to 100%) and also, slight traces of zeolite X were produced.

Low loadings (400 ppm) of acriflavine had no effect on the reaction. However, for very high loadings (20,000 ppm) of acriflavine, zeolite C was observed after 3 hours. It is difficult to say how much significance should be placed on the formation of this zeolite, if any, since it is often formed in zeolite synthesis, but is metastable, and always transforms to zeolite P1 with time.

The most significant effect was observed when a mixture of crystal violet (1600 ppm) and acriflavine (1600 ppm) was added as a solid mixture to the zeolite P1 gel. Within two hours, a trace of zeolite X was observed and after 3 hours 55% zeolite X had formed. Thus it appeared that the combination of crystal violet and acriflavine suppressed zeolite P1 formation and allowed zeolite X to grow, although possibly it was the adding of the materials as solids which caused the effect observed. It was therefore decided to find out the effect of adding crystal violet and acriflavine individually as solids to reaction gels. The results are shown in table 5.7. For both crystal violet and acriflavine, substantial amounts of zeolite X were formed.

Thus it appeared that these dyes when added as solids had a different effect to that which they had when added in solution. It was not clear why this should be the case, so it was decided to carry out an investigation of the effect of alkaline solutions on crystal violet and acriflavine at 95°C.

5.5.4 EFFECT OF ALKALINE SOLUTIONS ON CRYSTAL VIOLET AND AND ACRIFLAVINE AT 95°C

The effect of solutions, of sodium hydroxide, sodium silicate and sodium aluminate, all at the same concentrations as those encountered in a zeolite synthesis reaction, on acriflavine and crystal violet were investigated and the results are shown in table 5.10.

The solution of sodium silicate was prepared using waterglass type C100 and sodium hydroxide and the sodium aluminate solution was prepared using alumina trihydrate and sodium hydroxide.

The dye was added as a solid to the alkaline solutions in the cold and then stirred, under reflux at 95°C, for the duration of the investigation.

Reaction of acriflavine with sodium hydroxide gave a brown crystalline compound CI, which was not identified. Similarly, the reaction of crystal violet with sodium hydroxide gave a deep purple crystalline product CII which was not identified.

The reaction of acriflavine with sodium silicate solution produced traces of zeolite P1 after 17 hours with traces of CI still apparent, however, after 6 days no CI was present and the product was zeolite P1 and zeolite Pt. However, it was found that heating sodium silicate solution at 95°C for 2 days produced analcite, so it appears that the presence of dye suppresses the formation of analcite.

In the reaction of crystal violet with sodium silicate the product after 6 days showed traces of a mixture of zeolite P1 and zeolite C, here again the dye appears to have suppressed the formation of analcite. It was thought that the zeolites formed by leaching aluminium from the glass reaction vessels and from

TABLE 5.8 EFFECT OF ALKALINE SOLUTIONS ON CRYSTAL VIOLET AND ACRIFLAVINE AT 95°C [a]

Solution composition	No dye	Acriflavine	Crystal violet
$5.15Na_2O$ $242H_2O$		CI(17h)	CII(17h)
$5.15Na_2O$ $4SiO_2$ $242H_2O$	Analcite+Pl(2d)	CI+Pl(17h)	CII(3h)
	Analcite+Pl(5d)	Pl+Pt(6d)	Pl+C+unknown(6d)
$5.15Na_2O$ Al_2O_3 $242H_2O$	HS(2d)	CI(3h)	CIII(3h)
	HS(2d)	HS+CI(3d)	HS(3d)

[a] CI, CII and CIII are crystalline compounds derived from dyes

The d spacings of their major lines are

CI	6.42,	4.98,	4.75,	4.31,	3.44
CII	10.05,	7.26,	5.07,	4.51,	3.29
CIII	7.63,	5.34,	4.80,	4.42,	3.66

aluminium impurities in the silicate starting material.

The reaction of acriflavine with sodium aluminate produced hydroxysodalite as did the blank reaction. The reaction of sodium aluminate with crystal violet produced a crystalline compound CIII, after 3 hours, which was not identified. After 3 days, however, hydroxysodalite had formed and CIII had disappeared.

5.5.5 EFFECT OF SOME OTHER DYES ON THE ZEOLITE P1 REACTION

Since it had been found that the addition of crystal violet and acriflavine as solids redirected the zeolite P1 reaction to give considerable amounts of zeolite X, it was decided to investigate the effect of some other dyes. The results are shown in table 5.9. Of all these dyes only acridine orange showed any effect. It was decided to repeat the reaction with crystal violet and it was found that the previous result could not be reproduced. The conclusion drawn from this was that the original reactions, which had looked very promising, had in fact been seeded by zeolite X, possibly contaminants from previous reactions in the same vessels. After this finding all vessels were washed out with concentrated HCl after each reaction.

5.6 CONCLUSIONS

There is little doubt from the work done by Whittam that the addition of certain basic organic dyes can influence the products of the zeolite Y reaction in as much as they suppress the formation of the undesirable zeolite P1. From the work reported here it is obvious that a similar suppression of the undesirable zeolite P1 in zeolite X reactions is not possible. The most likely cause for the observed difference is the difference in alkalinity of the two reactions.

TABLE 5.9 EFFECT OF ADDITION OF SOME OTHER DYES TO THE ZEOLITE P1 REACTION

Run No.	Dye	PRODUCT (N%) 2h	3h	4h
5.53	Acridine orange	trX	X(12)+P1(50)	X(17)+P1(90)
5.54	Lissamine rhodamine	Am	P1(90)	P1(110)
5.55	Malachite green	Am	P1(40)	P1(100)
5.56	Nuclear fast red	Am	P1(95)	P1(105)
5.57	Alizarin	Am	P1(100)	P1(100)
5.58	Ethyl violet	Am	C	P1(90)
5.59	Brilliant green	trP1	P1(90)	P1(100)
5.60	Methyl green	trC	P1(100)	P1(100)
5.61	Methyl violet	Am	P1(80)	P1(90)
5.62	Azur C	Am	P1(90)	P1(95)
5.63	Toluidine blue	Am	P1(90)	P1(100)
5.64	Proflavine	Am	P1(90)	P1(100)
5.65	Crystal violet	Am	P1(90)	P1(95)

Zeolite Y reaction mixtures are much higher in silica content and consequently much less alkaline than zeolite X reaction mixtures, therefore the dye cations have a much better chance of survival in the zeolite Y reaction environment. In the zeolite Y system, the dyes can remain in such a form that this will be adsorbed on negatively charged surfaces. Thus, in zeolite Y reaction mixtures, it seems probable that the dye is preferentially adsorbed on surfaces which lead to zeolite P1 formation and consequently the growth or the nucleation of this zeolite is depressed. This is not the case in the much more alkaline environment of the zeolite X reaction mixture, where the dyes cannot survive for long periods in their cationic form. It has been shown in the present study that both crystal violet and acriflavine form insoluble crystalline compounds in alkaline solution.

It does seem that acriflavine can exert some degree of growth suppression on both zeolites X and P1. However, it seems unlikely, in the light of the results shown in section 5.5.4, that the mechanism of suppression is that of dye adsorption on negatively charged surfaces.

If a dye can be found which is stable at high pH, this would possibly exert some influence on the product of the zeolite X reaction. Methylene blue was found to be stable at pH 12 and it was decided to study this dye in some detail. Chapter 6 describes an investigation of the adsorption of this dye on zeolite and silica surfaces.

CHAPTER 6

METHYLENE BLUE ADSORPTION ON ZEOLITES A, X AND P1 AND SiO_2

6.1 INTRODUCTION

Since it is known[97] that the products of some zeolite reactions can be influenced by the addition of certain cationic dyes, it was considered of interest to investigate, in detail, the adsorption of a cationic dye on the surfaces of zeolites A, X and P1 and on silica. The dye chosen for this study was methylene blue principally because of its stability at high pH values (∿12). The structure of methylene blue is shown below

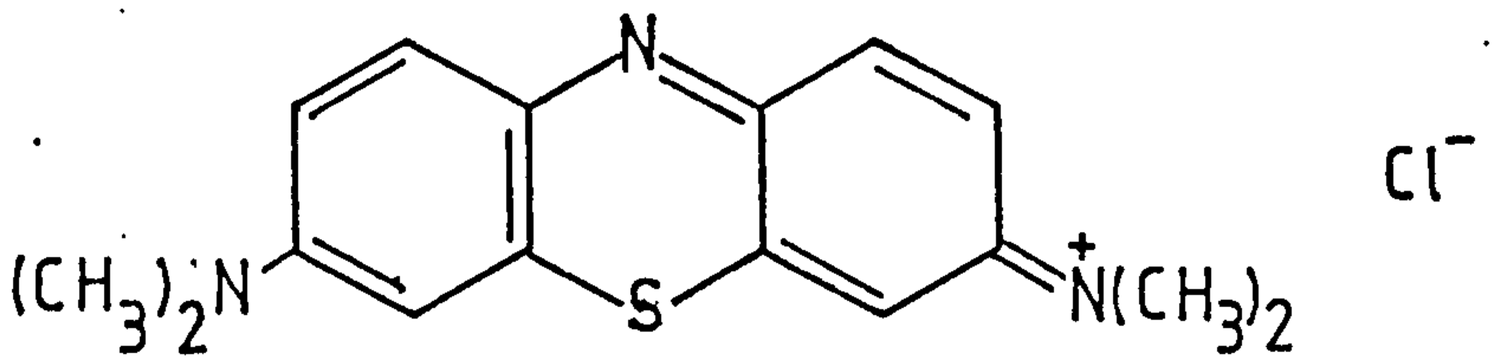

This molecule has three resonance forms, one of which is shown.

In solution there is also a dimeric species in which two methylene blue molecules lie parallel to one another. This species is particularly evident in concentrated solutions. Some evidence has been put forward for a trimeric species, but, spectrophotometrically it is difficult to detect.

In addition to the fact that methylene blue is relatively stable in alkaline solution, it has the advantage of having been widely used in dye adsorption studies on clay minerals. Therefore,

there was considerable information available on it prior to this investigation.

Dye adsorption on ionogenic surfaces has been extensively studied by several workers. The types of materials which have been used are clay minerals[125], kaolinite[126,127,128], silicas[129,130,131], aluminas[132], graphite[133] and many other solids[134] which are capable of taking dye on to their surface from solution. However, only three studies of dye adsorption on zeolites have been reported. These have been almost entirely restricted to zeolite A, and no work on zeolite P1 has been reported.

Schuger and Smolka[135] studied the adsorption of methylene blue on zeolite A. They compared this with the adsorption of benzopurpurine, an anionic dye, and found that methylene blue was much more strongly adsorbed.

Susic[136] and co-workers, in their investigation of the adsorption of methylene blue on occluded and non-occluded synthetic zeolites, studied the base catalysed demethylation of methylene blue on a denitrated zeolite A. They found that the adsorption of methylene blue on zeolite A was of the Langmuir type. They also showed that demethylation of methylene blue occurred in the presence of the denitrated zeolite and concluded that the demethylation is base catalysed by the activity of the strongly electronegative surface of the denitrated zeolite.

Studies of the adsorption of dyes on synthetic zeolites 13X, 4A and 5A have been carried out by Levina[137] and co-workers. The dyes used were acridine orange, methylene blue and crystal violet. These workers concluded that the adsorption of basic dyes from aqueous solutions was irreversible i.e. they could not be desorbed. They also stated that, the quantity of dye adsorbed was a function of the size of

the zeolite crystal, and adsorption on these three zeolites only occurred on the external surface. Furthermore, they stated that the dye was adsorbed by an ion exchange reaction which involved only those Na^+ ions located on the crystal surface.

It is generally agreed that the mechanism of dye adsorption on ionogenic surfaces takes place by two distinct mechanisms operating simultaneously:- 1) an irreversible ion exchange process and 2) a physical adsorption process which operates in the presence of excess dye in solution. However, although the adsorption of cationic dyes on clays is primarily an ion exchange process, it is complicated by many other factors e.g. molecular size, molecular geometry, dye-dye interaction and the surface characteristics of the sorbent.

In this work, the adsorption of methylene blue on zeolites X, A and P1 and on silica has been measured. In a more detailed study of zeolite X, adsorption has been measured while varying the Na^+ ion concentration, and the weight of solid/volume of solution (w/v) ratio, together with an attempt to measure adsorption under circumstances close to those encountered in a zeolite X reaction mixture. Qualitative studies of desorption from zeolite A, P1 and SiO_2 have been carried out. Finally, the use of dye adsorption in the determination of surface areas is discussed.

6.2 EXPERIMENTAL DETAILS

6.2.1 ANALYSIS OF METHYLENE BLUE

A detailed examination of three methylene blue materials (A) BDH redox indicator (B) BDH technical grade and (C) BDH standard stain was carried out.

Bergmann and O'Konski[138] have reviewed the absorbancy values reported for methylene blue in the literature, and have concluded

that the wide range of values arises from the use of impure materials. For the present work the values found by Bergmann and O'Konski were considered to be correct. The purity of the three methylene blue samples A, B and C were estimated spectrophotometrically. The spectrum of methylene blue was taken at neutral pH and such low concentrations that very little dimer was present. Absorption curves for A, B and C are shown in figure 6.1. From the heights d and e of the peak and the inflection point of the absorption curve respectively, the ratio R (= d/e) was calculated. The results are shown in table 6.1. Since all the demethylation products, which would be the expected impurities, have absorption peaks at lower wavelengths than methylene blue, demethylation tends to decrease R [138]. Also, in the presence of demethylation products, the peak is shifted towards lower wavelengths, but this shift is not as sensitive to impurities as the change in R. The R value for the methylene blue redox indicator sample A, was 2.00 for $c = 6.32 \times 10^{-6}$ mol dm^{-3} which compared favourably with the value found by Bergmann and O'Konski for their pure sample in which R = 2.01 for $c = 5.7 \times 10^{-6}$ mol dm^{-3}.

The effective molar absorption coefficient ε is given by

$$\varepsilon = \frac{A}{lc}$$

where A is the absorbance, l is the path length which is equal to 1 cm for this work and c is the concentration of methylene blue.

For sample A, $\varepsilon = 7.9 \times 10^{4}$ dm^{3} mol^{-1} cm^{-1}, for $c = 6.32 \times 10^{-6}$ mol dm^{-3} which is in reasonable agreement with the values quoted by Bergmann and O'Konski, $\varepsilon = 9.5 \times 10^{4}$ dm^{3} mol^{-1} cm^{-1}, for $c = 5.7 \times 10^{-6}$ mol dm^{-3}.

FIG. 6.1 ABSORPTION CURVES FOR MATERIALS A, B AND C

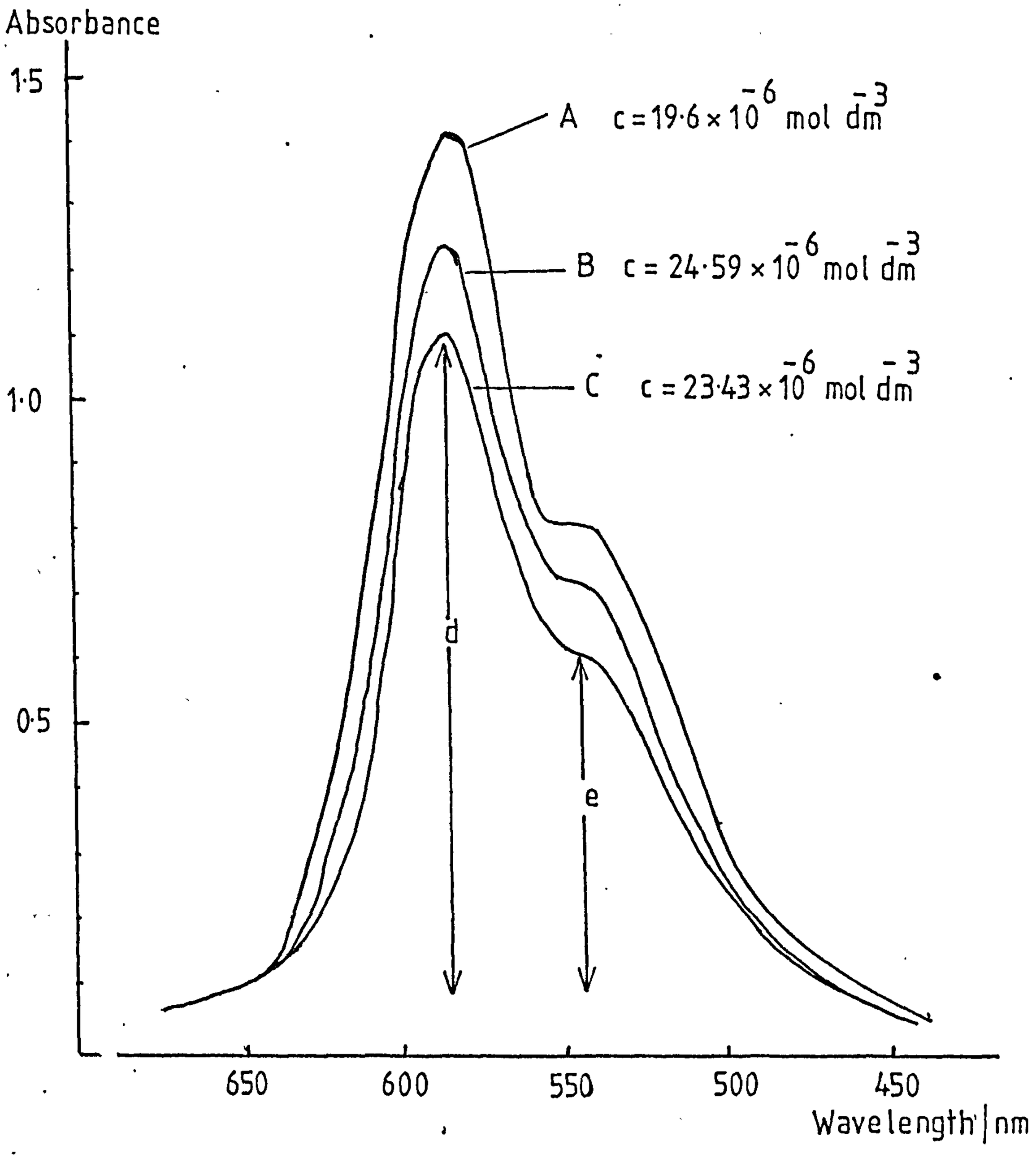

TABLE 6.1 SPECTROPHOTOMETRIC DATA FOR MATERIALS A, B AND C

Methylene blue

Material	Concentration 10^6 c/mol dm^{-3}	Absorbance	R(d/e)	Extinction coefficient ε 10^4 ε/dm^3 mol^{-1} cm^{-1}
A (Redox indicator)	19.20	1.40	1.72	7.29
	18.09	1.30	1.75	7.19
	12.34	0.94	1.88	7.62
	6.32	0.50	2.00	7.91
B (Technical grade)	24.59	1.24	1.79	5.04
	18.87	1.02	1.84	5.40
	12.88	0.71	1.92	5.51
	6.59	0.37	1.95	5.61
C (Standard stain)	23.43	1.11	1.85	4.74
	17.98	0.92	1.91	5.11
	12.27	0.66	1.94	5.38
	6.28	0.35	2.05	5.57

Although the R values for samples B and C were in reasonable agreement with the literature values, the effective molar absorption coefficients were very low, suggesting the presence of impurities. These samples were not used for adsorption studies and were not subjected to further analysis.

Gravimetric analysis of the methylene blue redox indicator was carried out by the Ferrey[139] method, in which the dye is precipitated as its dichromate, $(MB)_2Cr_2O_7$. Methylene blue (0.2 g) was dissolved in distilled water (100 cm^3) and the solution was added to a solution (50 cm^3) of potassium dichromate (0.1 mol dm^{-3}), a further 50 cm^3 of distilled water was then added, and a precipitate was formed. The precipitate was then heated to 75°C and maintained at that temperature for 5 minutes. The precipitate was then filtered on a sintered glass crucible (porosity 3) and dried at 100°C for one hour, and no further loss occurred on heating for a further two hours. The precipitate was then weighed and the percentage anhydrous methylene blue was calculated.

The percentage of anhydrous methylene blue in the redox indicator was found to be 81.67%. From a weight loss measurement, the amount of water present in the sample, was 17.08%. The discrepancy of ~1% could not be accounted for by experimental error and suggested the presence of an impurity. Analysis of the MB dichromate precipitate gave:-

	%C	%H	%N	C/N
Calculated	48.98	4.59	10.71	4.57
Found	48.55	4.48	10.38	4.68

The agreement between the theoretical and experimental values is good, and it is therefore unlikely that an organic impurity had been precipitated by the dichromate.

Titration of a solution of methylene blue (0.005 mol dm^{-3}) against sodium hydroxide (0.1 mol dm^{-3}) was carried out, in order to find out if there was an acid impurity. The pH of the initial methylene blue solution was 4.0 and 0.2 cm^3 of the sodium hydroxide solution was necessary to neutralise this. Therefore it was concluded that there was a strong acid impurity of $\sim 2 \times 10^{-5}$ mol dm^{-3} H^+ ions/mol methylene blue. However this could not account for the observed discrepancy. It was thought that the impurity was probably a heavy metal and could be considered negligible.

As a final check on the purity, the redox indicator sample was submitted to a chromatographic test. The technique used was thin layer chromatography (t.l.c.). A silica plate was used and a mixture of MeOH and CH_3CO_2H in the ratio 9:1, was the eluent. No separation was observed.

On the basis of the results of the three analytical methods used, it was concluded that the redox indicator sample of methylene blue was sufficiently pure to be used in dye adsorption studies on zeolites. It was not considered necessary to re-crystallise the dye.

6.2.2 OTHER MATERIALS

Zeolites X and A were BDH Linde molecular sieves which were equilibrated with water by being spread over filter paper and allowed to stand for at least 3 days at room temperature and humidity.

Zeolite P1 was synthesised in the laboratory from a reaction mixture which used an inactive sodium silicate as the only source of silica. The silica was BDH colloidal silica, and the amorphous aluminosilicate was taken from a gel mixture at zero reaction time, filtered and washed thoroughly.

The cetyl trimethyl ammonium bromide (CTAB) and the dimethyl-dichloro-silane solution were both supplied by BDH Ltd. The sodium salts used were all BDH analar grade reagents. Laboratory distilled water was used in all experiments.

6.2.3 PREVENTION OF DYE ADSORPTION ON GLASSWARE

A major source of error in the measurement of dye adsorption on solids is the spurious adsorption of dye on glassware. Previous workers[126-128] considered the use of pyrex glass vessels, to which the dye did not readily adhere, sufficient to minimise the problem. Initially in this work, pyrex glass vessels which were soaked in concentrated dye solution and rinsed thoroughly were used. However, it was observed that significant dye adsorption on the glass vessels had occurred, and a more effective method of minimising the errors was necessary.

Allingham[130] et al used a cationic surface-active agent, Lissolamine A, (cetyl trimethyl ammonium bromide) to avoid errors due to adsorption of dye on the glass and so it was decided to try this method. A solution of cetyl trimethyl ammonium bromide (CTAB) was used to rinse all the glassware and then it was rinsed once with cold water before use with methylene blue solutions. This appeared to work very well initially, however, following an overnight adsorption run, bubbles were observed at the air/water interface of the solution after the slurry had been centrifuged. On investigating this surface activity a Tyndall beam was observed indicating the presence of a colloidal dispersion. A possible explanation of this phenomenon was that CTAB had desorbed from the glass surface, stabilising a colloidal dispersion and consequently not all the zeolite could be removed by centrifuging at 4000 r.p.m.

In an attempt to find out if this was the case, two flasks, one coated with CTAB, the other untreated, were filled with a zeolite/water slurry and shaken for 4 hours. The slurries were then transferred to centrifuge tubes and centrifuged for 20 minutes at 4000 r.p.m. The liquid phase of the slurry from the treated flask showed a Tyndall beam and an absorbance of 0.05 was recorded which corresponded to light scattering throughout the visible region of the spectrum.

In contrast, the liquid phase from the untreated flask showed no Tyndall beam, and no light scattering was observed. Therefore this method of preventing dye adsorption on the glassware had to be abandoned.

The problem was finally solved by treating all glassware with a 20% solution of dimethyl-dichloro-silane in trichloro ethane. This procedure proved extremely effective and no recurrences of the previous effects were observed.

6.2.4 APPARATUS AND PROCEDURE

For each run, eight 50 cm^3 pyrex flasks with B19 Quickfit stoppers were used. Zeolite was weighed directly into the flask. Distilled water was added by pipette and this was made up to 25 cm^3 by adding a predetermined amount of methylene blue for a stock solution of known concentration to give a range of dye concentrations. The flasks were stoppered and parafilm wound round the neck of the flask and stopper to prevent leakages when shaking. Each flask was wrapped in aluminium foil to ensure the dye solution did not fade by the action of light. Likewise, the stock solution of dye was kept in a flask wrapped in aluminium foil. The eight flasks containing zeolite plus dye solution were then shaken by a wrist action

mechanical shaker for two hours. The slurry was then transferred to a 40 cm^3 centrifuge tube and centrifuged for 20 minutes at 4000 r.p.m. The supernatant liquid was extracted, and the visible spectrum was recorded on a Perkin-Elmer 402 UV-visible spectrophotometer or on a Unicam SP-500 spectrophotometer. The spectrophotometers were calibrated using eight methylene blue solutions of known concentration.

Since a plot of absorbance A against concentration was not linear, it was necessary to plot A/c against concentration, c. This gave a straight line, the equation of which was

$$\frac{A}{c} = \varepsilon_1 + \varepsilon_2 c$$

The two constants ε_1 and ε_2, obtained as the intercept and slope of the line were used to calculate the final dye concentration from the absorbance A, in experimental runs. The values obtained for ε_1 and ε_2 were 8.94×10^6 and -6.43×10^8 respectively.

pH measurements were made using a Philips PW9409 digital pH meter fitted with a Pye-Unicam glass electrode Cal. No. 405-60. Sodium concentrations were determined by means of an 'EEL' flame photometer.

It was discovered that the methylene blue in solution interfered with sodium determination causing readings which were too low. It was therefore necessary to calibrate the instrument at several different methylene blue concentrations.

6.3 RESULTS

6.3.1 CALCULATION OF RESULTS

The amount of dye adsorbed (x) was calculated according to

the relation

$$x = \frac{(C_1 - C_2)\ V}{W_z}$$

where C_1 is the initial dye concentration (g/l) which was calculated from the known concentration of the stock dye solution, C_2 is the final concentration of the dye (g/l) which was found from spectrophotometric measurements described in section 6.4. V is the volume of the dye solution in litres and W_z is the weight of the zeolite in grams. Calculation of x and C_2 was carried out with the aid of a computer.

6.3.2 ERRORS

The sources of error which have to be considered are

1) Measurement of the initial concentration
2) Calibration of spectrophotometer
3) Weighing of solid adsorbent (negligible)
4) Dilution of solution at high concentrations, when measuring optical density
5) Adsorption of dye on surfaces other than zeolite.

The estimated error in initial concentration (C_1) of the dye was 0.1%. The error in final concentration (C_2) of the dye solution depends on the error in the initial concentration, and the error in the calibration of the spectrophotometer together with the error incurred by dilution. The calibration of the spectrophotometer was repeated on three occasions and the error in the values of the constants ε_1 and ε_2 was estimated to be $\pm$1.0%. In those cases where it was necessary to dilute the solution before measuring optical density, i.e. $c > 40 \times 10^{-6}$ mol dm^{-3} an additional error of $\pm$3% was incurred.

The relative error in the extent of adsorption was then estimated at ±1% for final dye concentrations less than 40×10^{-6} mol dm^{-3} and ±2% for dye concentrations greater than 40×10^{-6} mol dm^{-3}.

6.3.3 EFFECT OF EQUILIBRATION TIME

Prior to this adsorption study, there was little agreement in the literature concerning the time taken for solid-liquid adsorption systems to reach equilibrium. Table 6.2 shows a list of workers, the solids they used and the method and time of equilibration.

In order to investigate fully a range of equilibration times, adsorption was measured over a period of 21 days. Eight flasks containing the same amount of zeolite, and the same concentrations of dye were used. The progress of adsorption with time was determined by taking flasks at fixed time intervals and measuring the extent of adsorption. The results are shown in table 6.3 and figure 6.2. It appears that two equilibrium phases exist.

TABLE 6.3 INVESTIGATION OF EQUILIBRATION TIME

Time of equilibration	Adsorption 10^5 x/mol g^{-1}
30 min	0.906
1 h	0.862
3 h	0.857
6 h	1.000
1 d	1.233
4 d	1.432
21 d	1.592

TABLE 6.2 COMPARISON OF TIME AND METHOD OF EQUILIBRATION USED IN DYE ADSORPTION STUDIES BY OTHER WORKERS

Workers	Solid Material	Time and method of equilibration
Levina et al[137]	Zeolites 4A, 5A, 13X	1 h shaking, allowed to stand 4-10 days
Susic et al[136]	Zeolite A	24 h, with agitation
De et al[125]	Bentonite, vermiculite, kaolinite, asbestos and feldspar	agitated 2 h, allowed to stand overnight then shaken 2 h
De et al[126,127,128]	Kaolinite, bentonite	24 h
Kipling et al[133]	Carbon black, graphite	3 d or 1 d, with agitation
Singh[132]	Alumina	8-10 min
Bergmann et al[138]	Montmorillonite	30 min - 1 h
Allingham et al[130]	Silica	a few minutes
This work	Zeolites X, A, Pl and SiO_2	2 h, with agitation

FIG. 6.2 ADSORPTION VERSUS EQUILIBRATION TIME

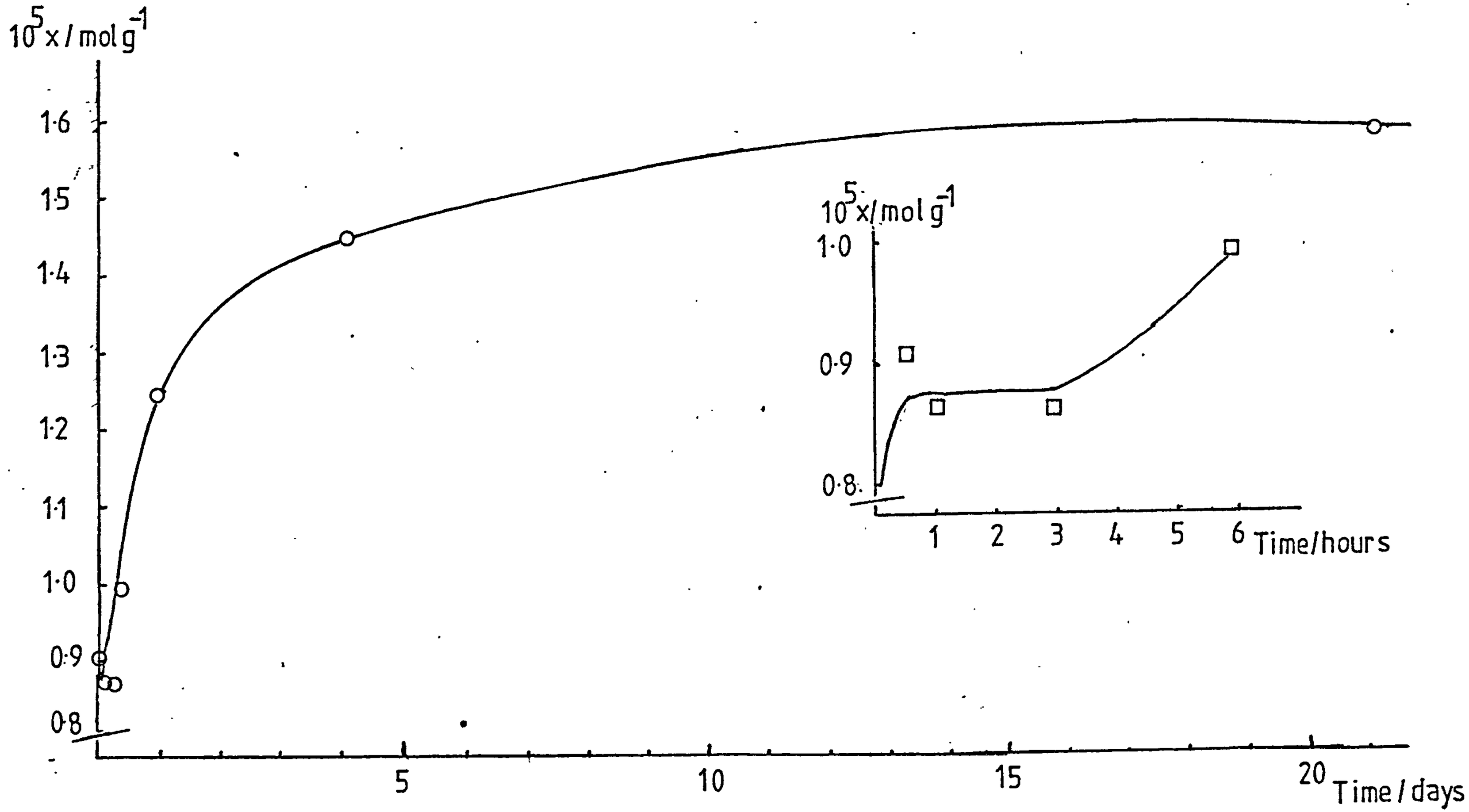

For the first three hours the extent of adsorption remained virtually constant; this was followed by an increase in adsorption which tailed off after 4 days. However, no constant value was reached, and after 21 days no further measurements were made.

It is possible that the first equilibrium phase observed was a metastable equilibrium and that true equilibrium is not reached until much later. However, this is unlikely to be the case. A more reasonable explanation is that the first equilibrium, reached within a few minutes, is the true one. The subsequent increase in adsorption could be due to aggregation of the dye on the surface or adsorption by some other mechanism, not responsible for the initial rapid equilibration. The continued slow increase could perhaps be due to increasing surface area of the zeolite caused by etching or by loss of dye to other surfaces rather than the zeolite which would give the same effect.

In view of the possible factors discussed above which may affect adsorption after 6 hours, it was decided to choose an equilibration time in the first plateau region of the adsorption against time curve. An additional and perhaps more important reason for choosing an equilibration time of 2 hours, was that this related more closely to the time scale of a zeolite synthesis reaction. For all the work which follows, the equilibration time was 2 hours, during which the slurry was shaken.

6.3.4 EFFECT OF TEMPERATURE ON DYE ADSORPTION ON ZEOLITE X

In order to establish if variation in temperature had an effect on the extent of adsorption, experiments 6.1 and 6.2 were

FIG. 6.3 EFFECT OF TEMPERATURE ON ADSORPTION

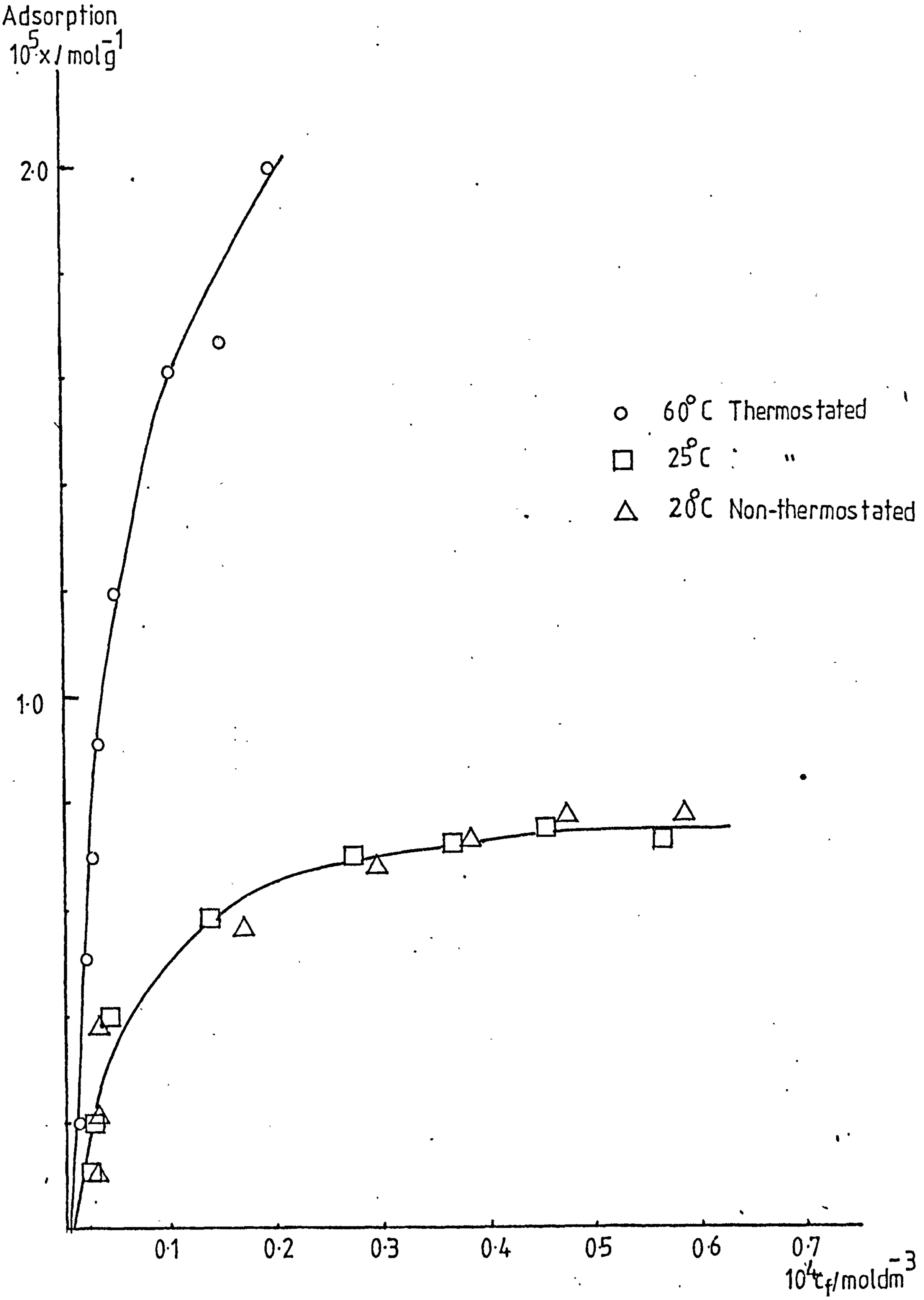

carried out under thermostat (25°C) and non-thermostat (RT ~20°C) conditions respectively. The results are shown in figure 6.3 and comparison shows no significant differences. Therefore, throughout this work the experiments were carried out unthermostatted at room temperature.

However, when dye is added to a reaction mixture (see Chapter 5) the temperature is generally 95°C. It was therefore interesting to study the adsorption of methylene blue at an elevated temperature (experiment 6.3). The temperature chosen was 60°C since this was convenient and relatively easy to control. The results are shown in figure 6.3. The extent of adsorption appears to be much higher at 60°C than at room temperature. However, it had been observed previously[133] that methylene blue solutions faded if held at 80°C for an appreciable time and it seems likely that this also applies at 60°C. This then would explain, at least in part, the apparent high adsorption at 60°C.

6.3.5 ADSORPTION ISOTHERMS FOR ZEOLITES X, A AND P1

Typical adsorption isotherms for methylene blue adsorption on zeolite X, A and P1 are shown in figure 6.4. These isotherms appear to be of the simple Langmuir type,

$$\frac{x}{x_m} = \frac{Kc}{1+Kc} \qquad (6.1)$$

in which x is the amount of dye adsorbed in mol g^{-1}, c is the molar concentration of the dye in equilibrium with the zeolite, x_m is the monolayer capacity and is related to the maximum number of adsorption sites available and K is an equilibrium constant which is related to the strength of the interaction between the dye and the adsorption site.

FIG. 6.4 ADSORPTION ISOTHERMS FOR ZEOLITES X, A AND P1

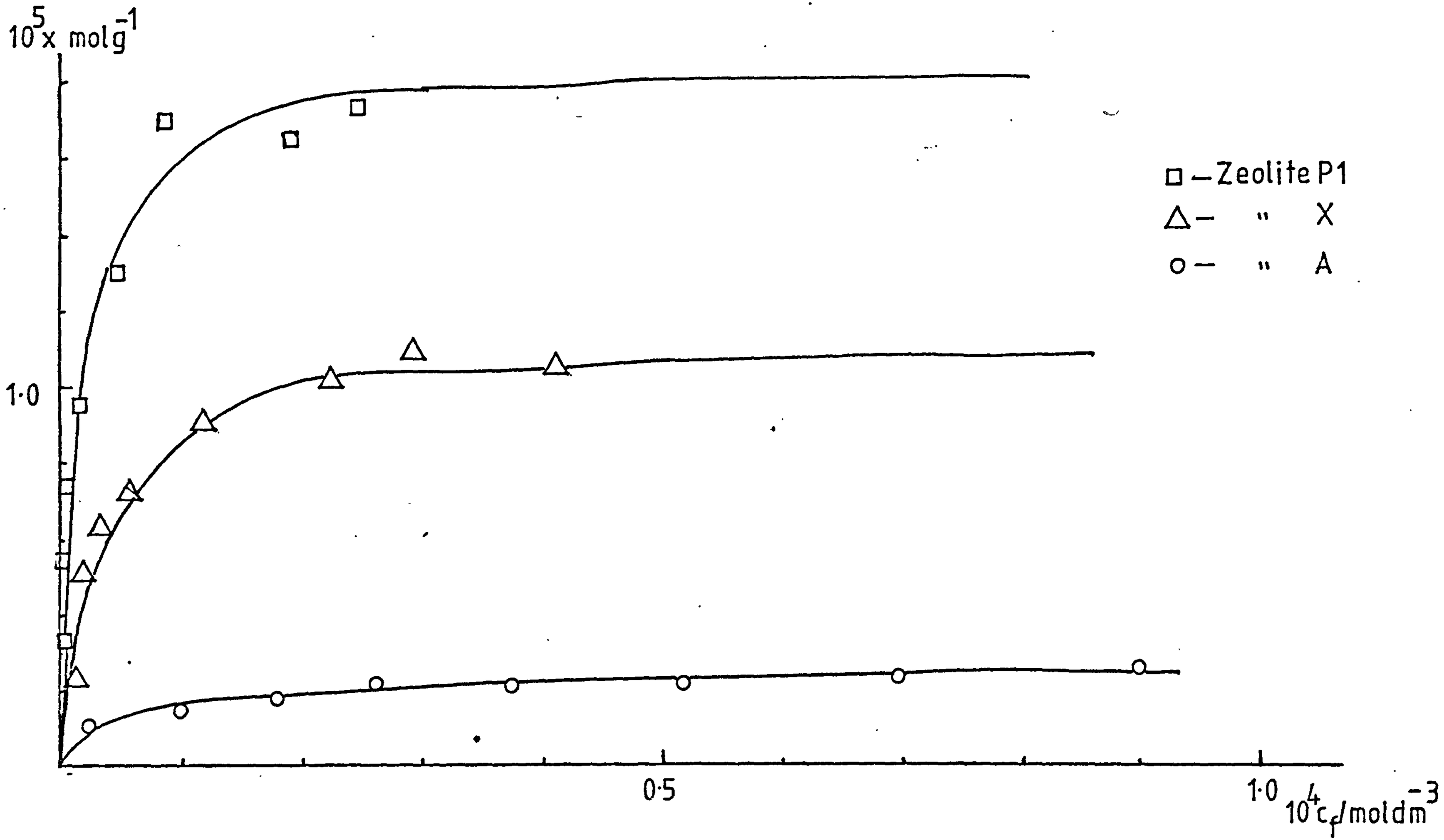

To test whether the isotherms fitted the Langmuir equation, equation (6.1) was rearranged in the form

$$\frac{c}{x} = \frac{1}{x_m K} + \frac{c}{x_m} \qquad (6.2)$$

Figure 6.5 shows typical plots of $\frac{c}{x}$ against c which are linear and can be used to find x_m and K. A computer program was written to carry out these calculations of x_m and K from the experimental results. Typical values for x_m and K are given in table 6.4.

TABLE 6.4 TYPICAL x_m AND K VALUES FOR ZEOLITES X, A AND P1

Run. No.	Zeolite	Y[a]	10^5 x_m/mol g^{-1}	10^5 K/g mol^{-1}
6.4	X	500	1.06±0:04	4.2±1.4
6.5	A	125	0.21±0.02	1.8±0.6
6.6	P1	500	1.81±0.04	6.4±1.2

[a] Y = volume/weight ratio where volume always equals 25 cm^3

The values of K increase in the order P1>X>A. Since the Langmuir constant is directly proportional to the strength of adsorption, the higher value indicates stronger binding of the dye to the adsorbent. Therefore, the dye is more strongly bound to zeolite P1 than to zeolite X.

From the x_m values in table 6.4 it can be seen that the monolayer capacity on zeolite A is much lower than on zeolite X, which is, in turn, lower than on zeolite P1. To discuss these results properly it is necessary to consider the zeolite surface.

FIG. 6.5 TYPICAL PLOTS OF c/x VERSUS c FOR ZEOLITES A, X AND P1

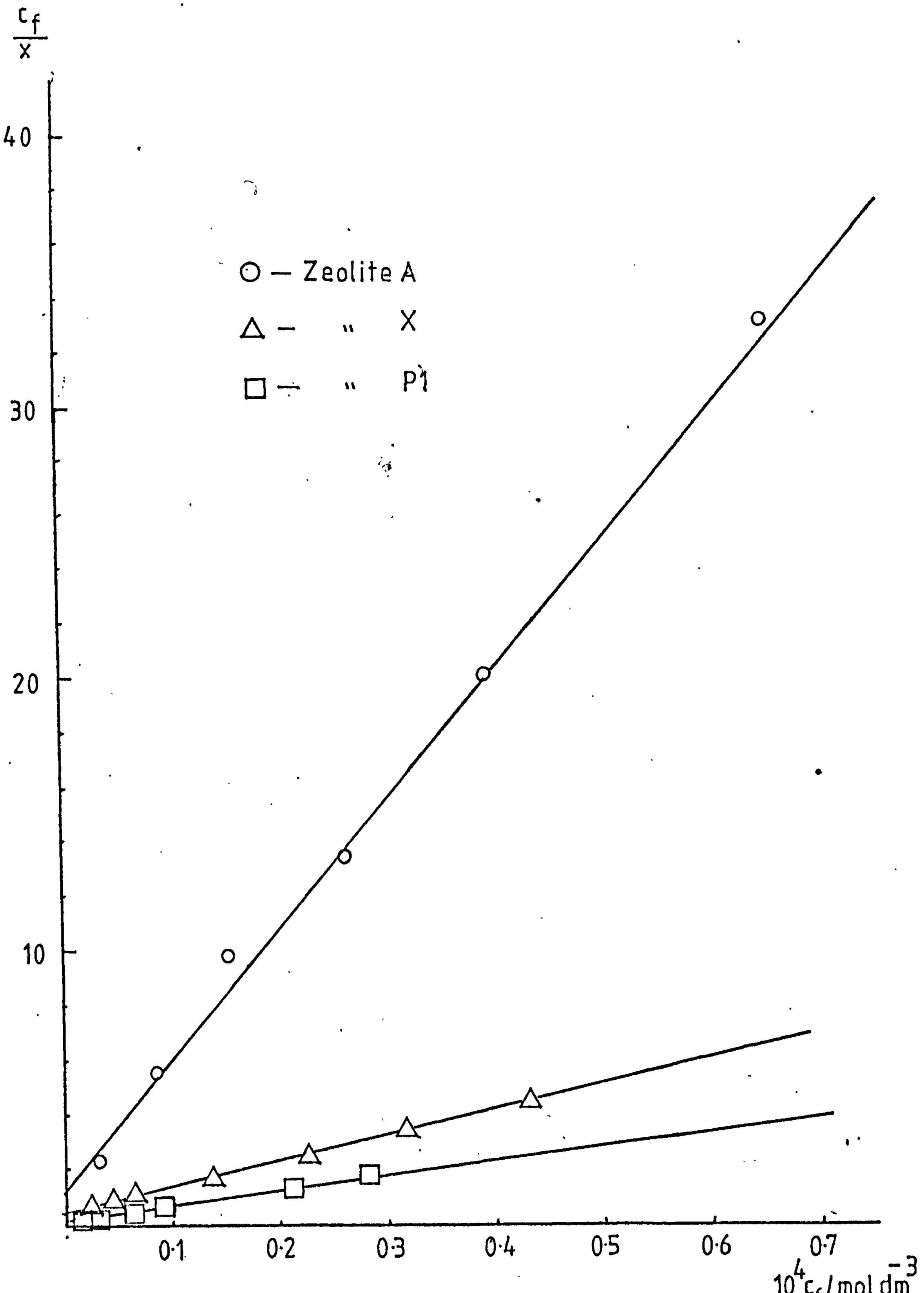

Models of the zeolite surfaces are shown in figure 6.6. As discussed in the introduction, it is known that adsorption of dyes on ionogenic surfaces is primarily an ion exchange process, and in the case of zeolites the sites involved are probably the $Si\text{-}O\ Na^+$ groups at the surface. Therefore, since at pH=10 these silanol groups will be dissociated giving $Si\text{-}O^-$ sites, it can be seen that the zeolite with the highest Si/Al ratio will have the greatest surface exchange capacity. Thus, the following order $x_m(Pl)>x_m(X)>x_m(A)$ would be expected since the Si/Al ratio for zeolite Pl can be between 1.1 and 2.5, for zeolite X it is normally 1.2, and for zeolite A it is normally 1.0. This order was observed.

Although the isotherm for dye adsorption on zeolite X shown in figure 6.4 obeys the Langmuir equation very well, it was observed in those instances in which the weight of zeolite was greater than 0.05 g this was not the case. The isotherm did not pass through the origin and the amount of dye adsorbed decreased with increasing weight of zeolite. It was therefore decided to study this effect in some detail and this is described in section 6.3.7.

6.3.6 DYE ADSORPTION ON AMORPHOUS SILICA

The adsorption of methylene blue on silica was measured at pH=10.4 and the results are shown in figure 6.7.

The adsorption increases sharply over the range of concentrations investigated and no plateau was observed. At this pH value it is likely that the silica surface has become ionised to give $Si\text{-}O^-$ groups which will act as ion exchange sites for the methylene blue. The surface area of the amorphous silica used was 174 $m^2\ g^{-1}$ (cf. zeolite X $\sim 4 m^2\ g^{-1}$) and it is therefore likely that the monolayer capacity has not been reached in this experiment.

FIG. 6.6 MODELS OF THE ZEOLITE SURFACE

AT pH = 10

zeolite A

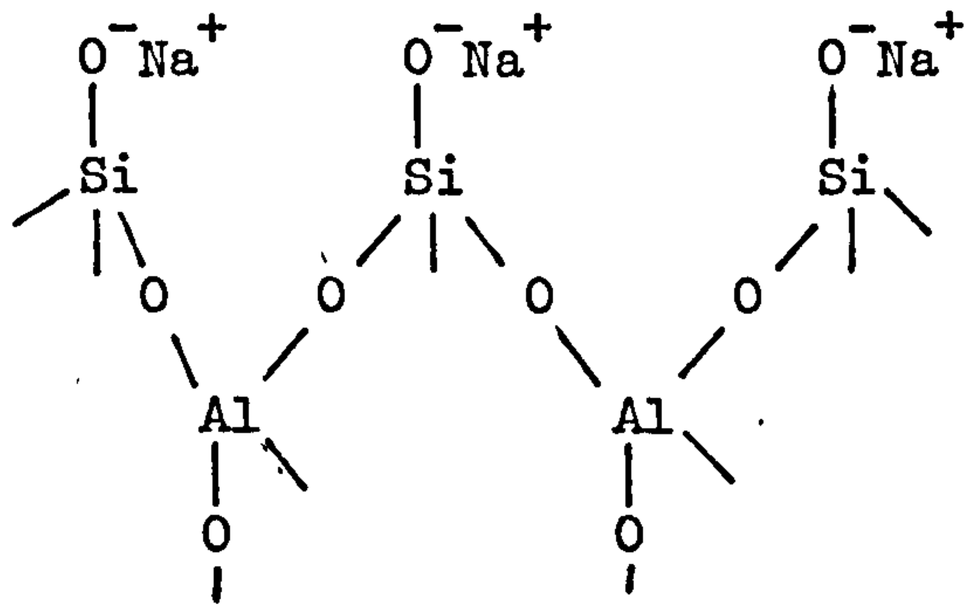

zeolite X

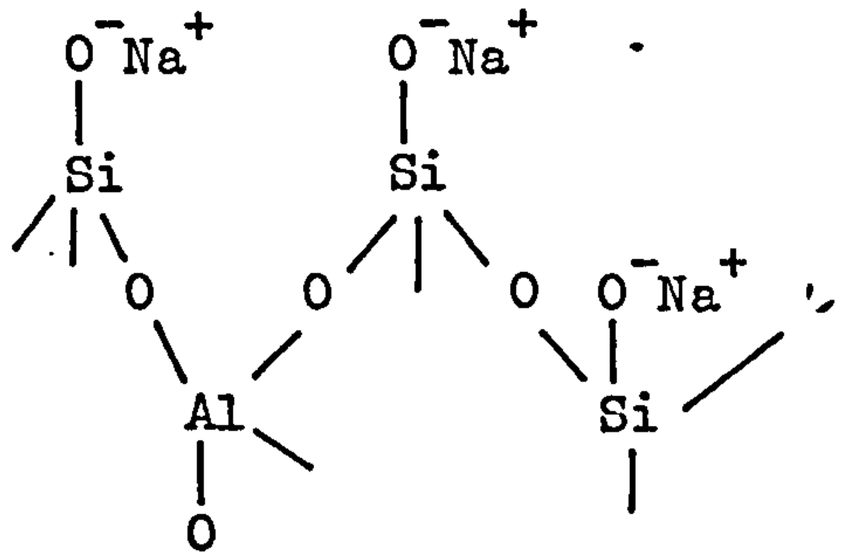

zeolite P1

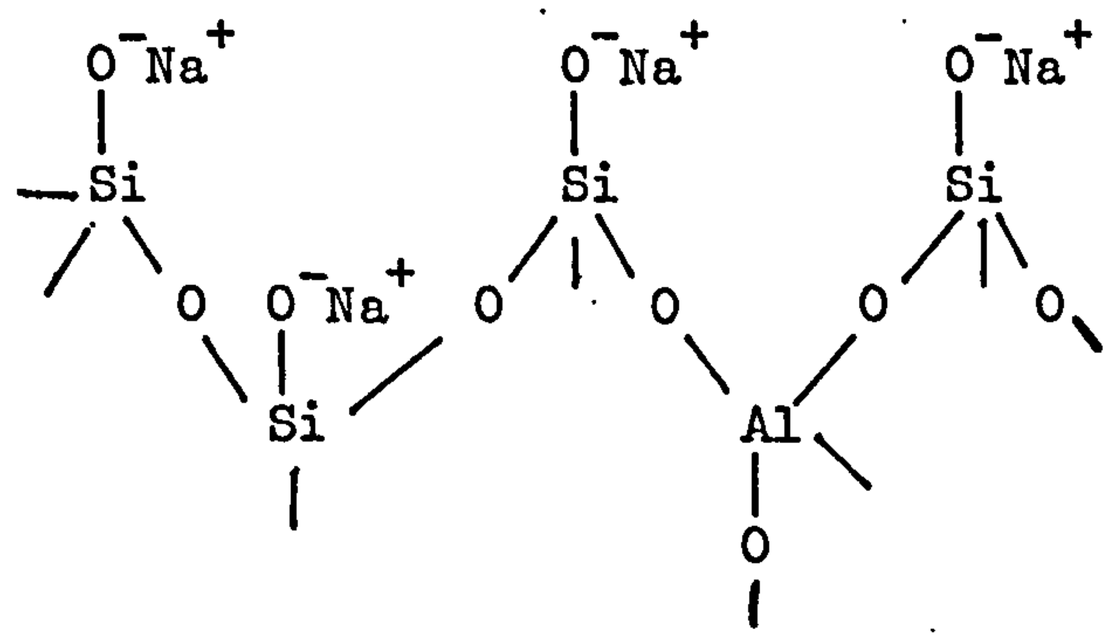

FIG: 6.7 ADSORPTION OF METHYLENE BLUE ON SILICA

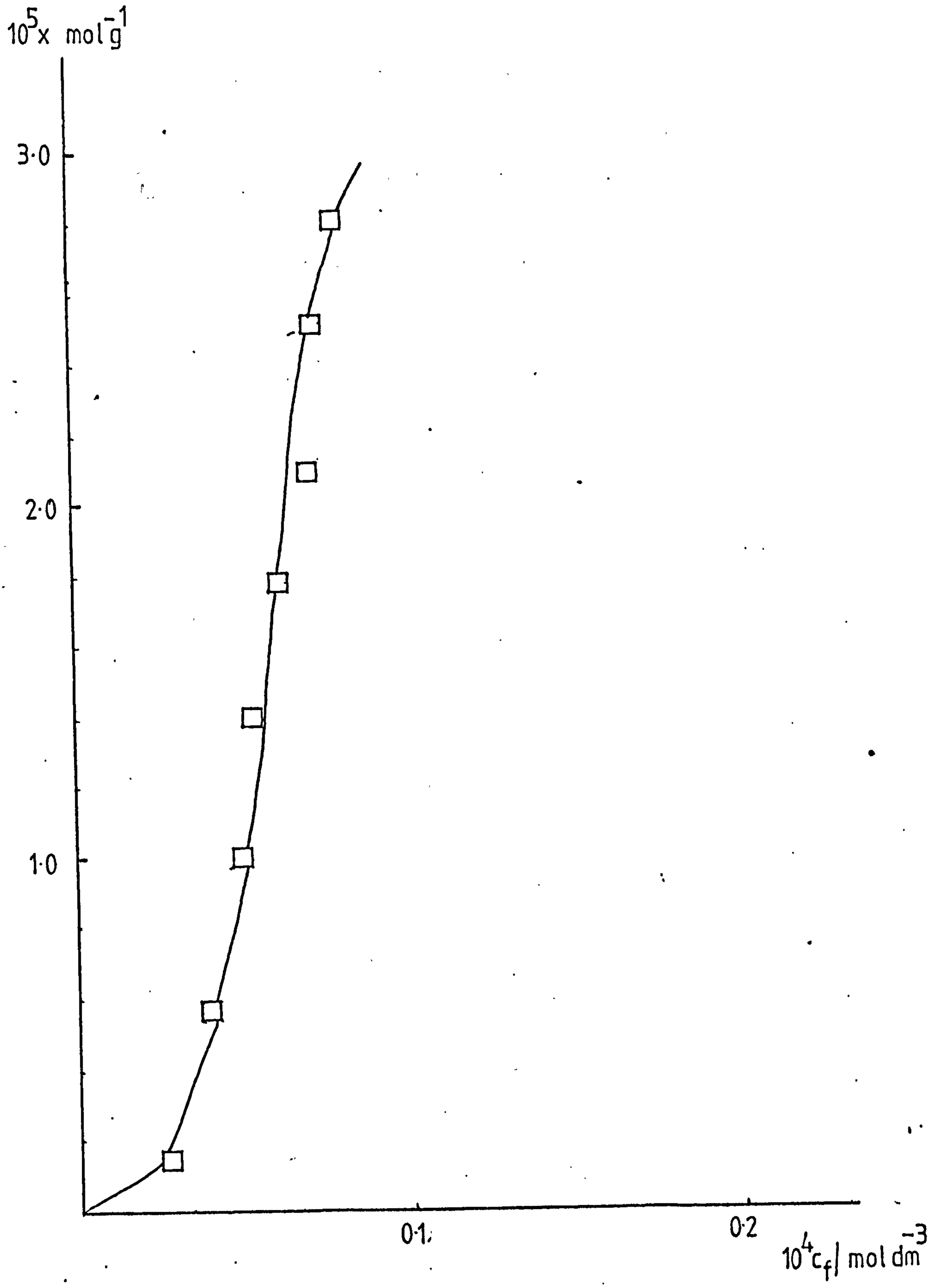

6.3.7 EFFECT OF WEIGHT/VOLUME RATIO ON DYE ADSORPTION ON ZEOLITE X

In theory, the amount of solute adsorbed should be independent of the volume of the solvent and amount of solvent present:- it should depend only on the equilibrium concentration of the solution in contact with the zeolite surface. However, if we consider the zeolite surface as an ion exchanger, then each dye cation D^+ requires one sodium ion to exchange, i.e. takes one site on the surface. Therefore at equilibrium:

$$Na^+_{(z)} + D^+_{(aq)} \rightleftharpoons D^+_{(z)} + Na^+_{(aq)}$$

$$K = \frac{[D^+_{(z)}][Na^+_{(aq)}]}{[Na^+_{(z)}][D^+_{(aq)}]}$$

Now let $[Na^+]_{aq} = c$ and $[D^+]_{aq} = d$

The monolayer capacity $x_m = [Na^+]_z + [D^+]_z$ mol g^{-1}

and the amount adsorbed $x = [D^+]_z$ mol g^{-1}

It follows then that

$$K = \frac{x}{x_m - x}\ \frac{c}{d}$$

$$\text{and} \qquad x = x_m\ \frac{K\frac{d}{c}}{1+K\frac{d}{c}}$$

Thus, the difference between this case and the simple Langmuir case is the replacement of d by $\frac{d}{c}$.

If, now, we consider the situation in the dye adsorption experiments carried out in this work in which

Weight of zeolite = w

Volume of solution = V

Initial dye concentration = d^o

Final dye concentration = d

Initial $[Na^+]$ concentration = 0

Final $[Na^+]$ concentration = c

Then

$$x = \frac{V(d^o-d)}{w} \qquad \text{and} \qquad c = (d^o-d)$$

Hence:- $$x = x_m \frac{K\,c}{1+K\,\frac{d}{c}}$$

becomes $$x = x_m \frac{Kd}{(d_o-d)+Kd}$$

but $$(d_o-d) = \frac{xw}{V}$$

and so $$x = x_m \frac{Kd}{\frac{xw}{V} + Kd}$$

Therefore, the curves observed for adsorption of dye on a zeolite surface should depend on the weight/volume ratio and this was as found in the experiments carried out. The results are shown in figure 6.8. This effect of weight/volume ratio on the adsorption capacity of the adsorbent was also observed by Allingham et al [130]

FIG. 6.8 ADSORPTION ISOTHERMS FOR METHYLENE BLUE ON ZEOLITE X FOR VARYING WEIGHT/VOLUME RATIOS

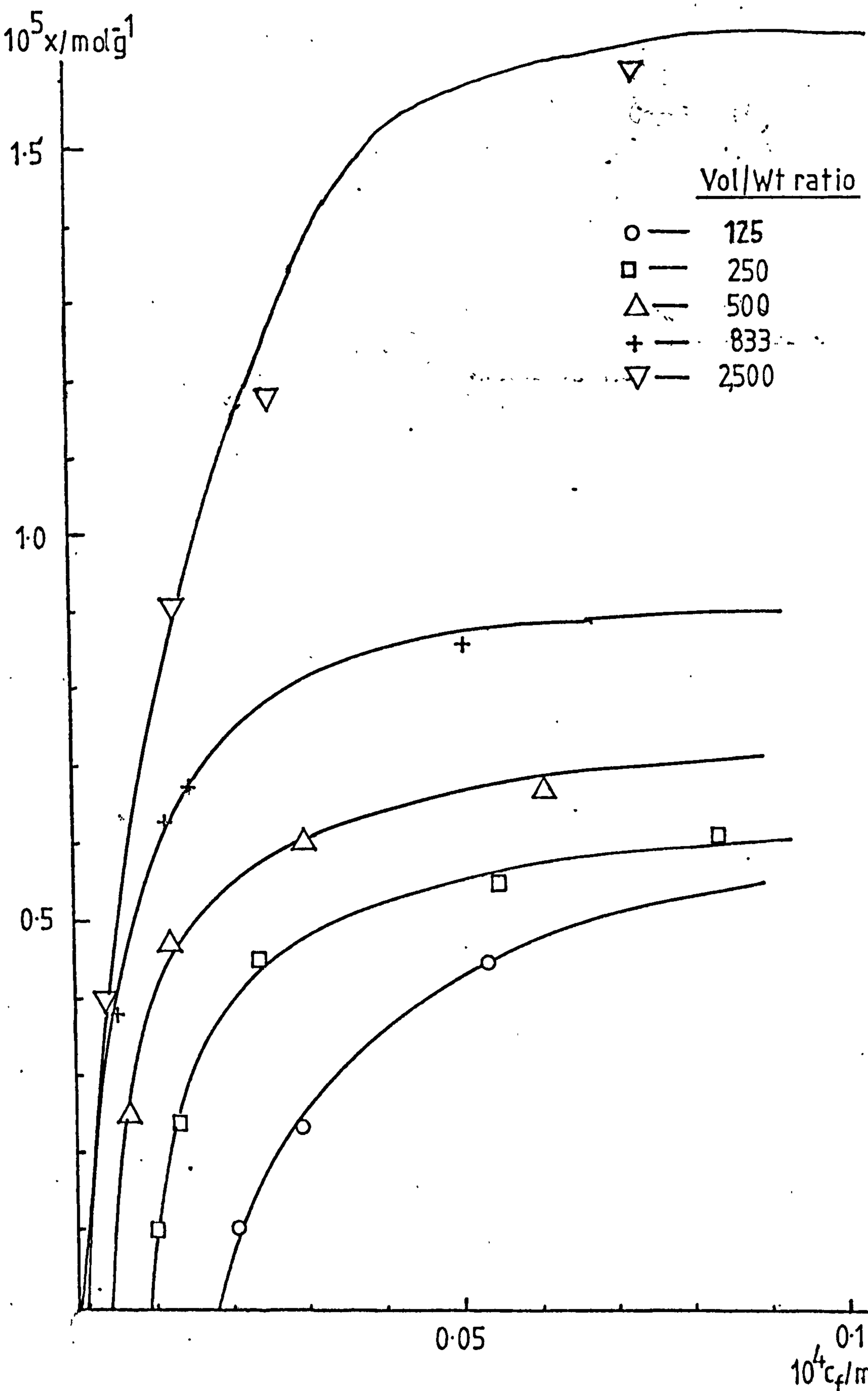

in their work on silica. However, in their system they explained the results in terms of solubility of the adsorbent silica.

Although the above explanation deals with the observation of increased adsorption capacity on decreasing the weight/volume ratio, it does not explain why the curves do not pass through the origin. It seems likely that the explanation lies in the effect of the sodium ion concentration on the adsorption. In this treatment it has been assumed that the initial sodium ion concentration in solution was equal to zero. However, this is known to be incorrect, and an investigation of the sodium ion concentration in the zeolite slurry was therefore carried out.

6.3.8 SODIUM ION CONCENTRATION IN ZEOLITE X SLURRY

When zeolite X is added to water sodium ions are released and the slurry is alkaline. There are two sources of these Na^+ ions, 1) sodium ions on the surface which have not been replaced by hydrogen ions when the zeolite was washed after preparation and 2) as the counter ion of some other anion which has been occluded in the zeolite lattice during preparation, usually aluminate.

On the basis of pH measurements it was estimated that the sodium ion concentration was ca. 5 ppm or (2.2×10^{-4} mol dm^{-3}). However, on measuring the sodium ion concentration it was found to be 32 ppm (1.4×10^{-3} mol dm^{-3}) for zeolite X (0.2 g) in water (25 cm^3). To obtain further information a series of zeolite 'washing' experiments were carried out as follows. Zeolite (0.2 g) and water (25 cm^3) was shaken in a plastic bottle for 15 minutes and then the slurry was transferred to a centrifuge tube and

centrifuged for 5 minutes. The supernatant liquid was decanted and the sodium ion concentration was measured using a flame photometer. A further 25 cm^3 of water was added to the remaining wet solid and the process was repeated six times. The results are shown in table 6.5. After the fifth washing the slurry was allowed to stand for 64 hours. The subsequent increase in sodium ion concentration is probably due to sodium ions in less accessible positions being exchanged for H_3O^+ ions. The decrease in pH is probably due to some dissolved CO_2 rather than a peculiarity of the system. On considering the results obtained after wash 5, which represents more correctly the final well-washed system, it is found that $[Na^+] \simeq [OH^-]$ as follows.

From the results in table 6.5:-

Wash 5 - pH = 9.6

$[Na^+] = 9.2$ ppm

For pH = 9.6 $[H^+] = 10^{-9.6}$

i.e. $[OH^-] = 10^{-3.4}$

$= \underline{4 \times 10^{-4} \text{ mol kg}^{-1}}$

Now for $[Na^+] = 9.2$ ppm $[Na^+] = \frac{9.2}{23} \times 10^{-3}$ mol kg^{-1}

$= \underline{4 \times 10^{-4} \text{ mol kg}^{-1}}$

This is consistent with silicate or aluminate ion impurities in the initial zeolite slurry.

It is evident, then, that zeolite slurries used in the adsorption experiments had sodium ion concentration of about 40 ppm,

TABLE 6.5 INVESTIGATION OF SODIUM ION CONCENTRATION IN ZEOLITE SLURRY

		Wash 1		Wash 2		Wash 3		Wash 4		Wash 5		Wash 6	
V/cm^3	Wt zeolite (w)/g	$[Na^+]$/ppm	pH	$[Na^+]$/ppm	pH	$[Na^+]$/ppm	pH	$[Na^+]$/ppm	pH	$[Na^+]$/ppm	pH	$[Na^+]$/ppm	pH
25	0.2	39.8	10.8	18.8	10.4	12.9	10.1	10.8	9.8	9.2	9.6	16	8.6
25	0.2	37	10.8	18	10.3	13.1	10.1	10.6	9.8	9.2	9.6	15	8.6

and that they contained a small quantity of another anion besides OH^-. This anion is likely to be silicate or aluminate which could arise either because the original zeolite had not been washed thoroughly, or, at low pH values it could be a breakdown product of the zeolite lattice.

From this work it has been shown that the initial $[Na^+]$ in the system is higher than would be expected. Therefore the amount of dye taken up will be reduced and this will be more evident as the amount of zeolite is increased which is consistent with the observations reported in section 6.3.5.

However, this does not account for the observation that the curves do not pass through the origin. A possible explanation is that the methylene blue stabilises a colloidal dispersion of the zeolite similar to the way in which CTAB has been shown to. This would account for the observation since the spectrophotometer would give an apparent reading caused by the light scattering of the colloidal particles. This would be more evident with increasing weight of zeolite in the system.

6.3.9 EFFECT OF ADDING SODIUM IONS

When dyes are added to zeolite reactions it is likely that they are constantly in competition with the sodium ions in the system for the available adsorption sites. Therefore it is important to study the effect of varying the sodium ion concentration on the adsorption capacity of the zeolite, while maintaining a constant dye concentration i.e. varying the $[Na^+]/[D^+]$ ratio. Five $[Na^+]/[D^+]$ ratios in which $[D^+]$ was 53.54×10^{-6} mol dm^{-3} were investigated and the results are shown in table 6.5 and a plot of

log [NaCl] versus adsorption is shown in figure 6.9. This experiment was repeated for an initial dye concentration of 85.66×10^{-6} mol dm^{-3} and the results are shown in table 6.6 and figure 6.8. The curves obtained for both dye concentrations were parallel. It was observed for those mixtures in which $[Na^+]$ was particularly low i.e. 5×10^{-6} mol dm^{-3} that the adsorption was lower than expected from extrapolation of the curves. This observation is difficult to explain and may possibly be related to the rate at which equilibrium is achieved.

It can be concluded that these results confirm beyond doubt that there is in fact competition between Na^+ ions and D^+ ions for the available sites on the zeolite surface.

6.3.10 DYE ADSORPTION AT $[Na^+]/[D^+]$ RATIOS SIMILAR TO THOSE IN ZEOLITE REACTION MIXTURES

Since the main objective of this work was to find out how the dyes behaved in zeolite reaction mixtures, it was decided to study the adsorption of methylene blue at $[Na^+]/[D^+]$ ratio found in typical zeolite X reaction mixtures to which dye had been added.

Since the reaction mixture can produce either zeolite X or P1 and must at some stage contain an amorphous aluminosilicate and frequently contains amorphous silica, it was decided to study the adsorption on these four substrates.

The adsorption of methylene blue on each of the four materials was studied at four different dye concentrations while maintaining a constant $[Na^+]/[D^+]$ ratio of 492. The absolute $[Na^+]$ concentrations were lower than those in a typical reaction mixture, and, to prevent decomposition of the dye due to high pH, sodium

FIG. 6.9 EFFECT OF VARYING THE $[Na^+]/[D^+]$ RATIO ON THE ADSORPTION CAPACITY OF ZEOLITE X

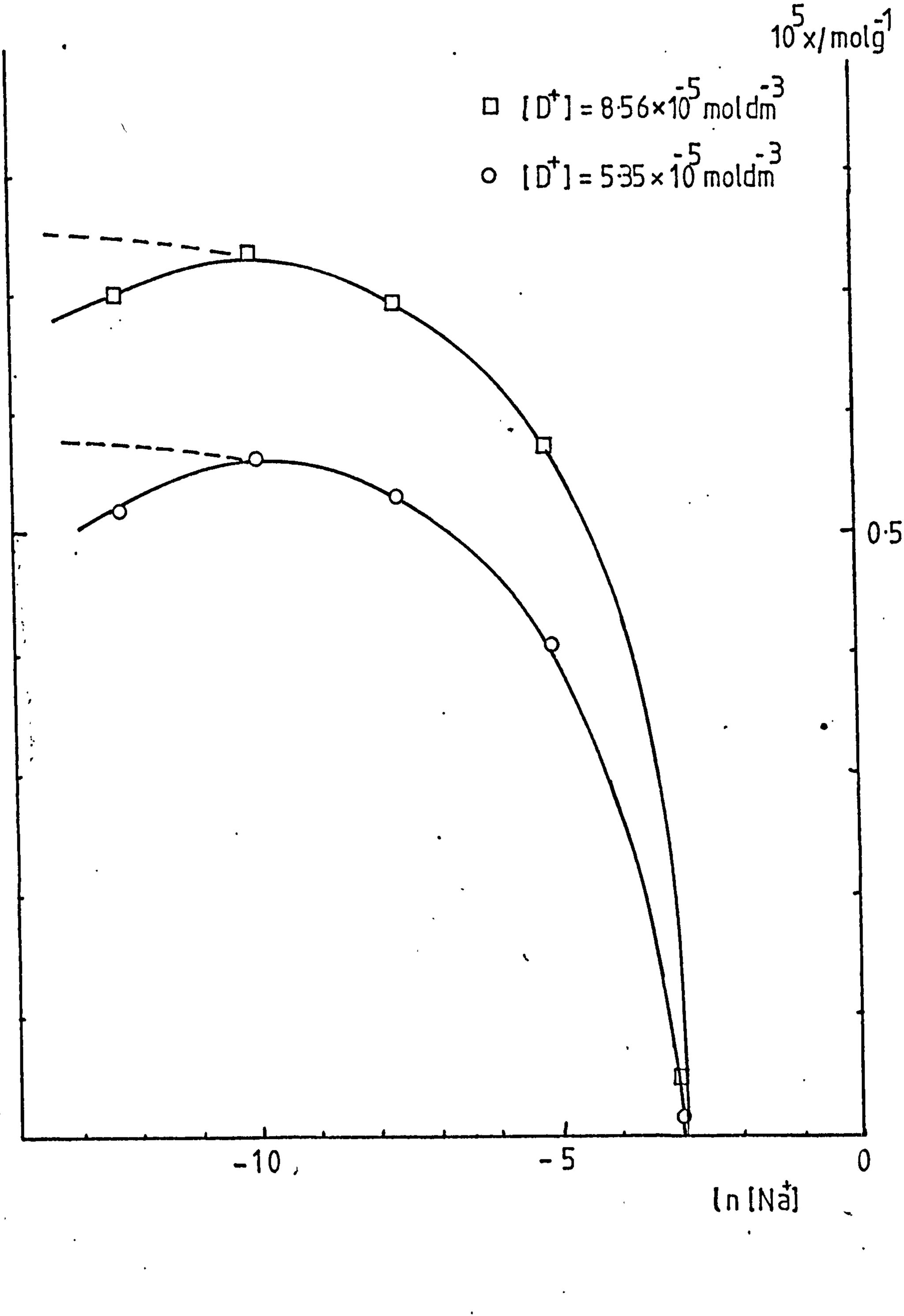

TABLE 6.6 EFFECT OF ADDING SODIUM IONS ON DYE UPTAKE ON ZEOLITE X

$[Na^+]$/mol dm^{-3}	$[D^+]=5.35\times10^{5}$ mol dm^{-3}	$[D^+]=8.56\times10^{-5}$ mol dm^{-3}
	10^5 x/mol g^{-1}	10^5 x/mol g^{-1}
5×10^{-2}	~0.020	0.058
5×10^{-3}	0.425	0.587
5×10^{-4}	0.528	0.696
5×10^{-5}	0.552	0.740
5×10^{-6}	0.504	0.695

carbonate was used in preference to sodium hydroxide. The results are shown in table 6.7 and figure 6.10.

The adsorption of methylene blue on silica increased with increasing dye concentration. This was as expected, since adsorption on silica can be attributed almost entirely to ion exchange at this pH, as discussed in section 6.3.6.

For zeolites X and P1 the adsorption remained almost constant over the range of dye concentrations. However, a decrease in adsorption on zeolite X, was observed as the dye concentration, and consequently the sodium concentration increased. A slight increase in adsorption on the amorphous aluminosilicate material was observed when the dye concentration was increased to 31.64×10^{-6} mol dm^{-3} and the sodium ion concentration increased to 0.0156 mol dm^{-3}. Thereafter the adsorption remained constant.

The difference in extent of adsorption on the amorphous colloidal silica and on zeolite X was of interest. It has been suggested previously (Chapter 2) that zeolite P1 formed when colloidal particles were incorporated in the amorphous aluminosilicate gel. If, now, methylene blue is used in a reaction, in which an amorphous silica was the silica source, the methylene blue should adsorb on the SiO_2 preventing it taking part in the reaction and allowing zeolite X to grow.

6.3.11 SIMULATION OF DYE ADSORPTION IN A ZEOLITE X REACTION MIXTURE

The adsorption of dye on a zeolite surface was investigated under conditions similar to those encountered in a zeolite reaction. An attempt was made to simulate as closely as possible the conditions met in a reaction mixture.

TABLE 6.7 DYE ADSORPTION AT $[Na^+]/[D^+]=492$ ON ZEOLITE X AND P1, AMORPHOUS SiO_2 AND AMORPHOUS ALUMINOSILICATE

Material	$[D^+]=2.11\times10^{-5}$ mol dm^{-3}	$[D^+]=3.16\times10^{-5}$ mol dm^{-3}	$[D^+]=4.21\times10^{-5}$ mol dm^{-3}	$[D^+]=5.27\times10^{-5}$ mol dm^{-3}
	10^5 x/mol g^{-1}	10^5 x/mol g^{-1}	10^5 x/mol g^{-1}	10^5 x/mol g^{-1}
Zeolite X	0.93	0.90	0.55	0.74
Zeolite P1	1.66	1.46	1.52	1.76
Amorphous SiO_2	3.85	5.75	5.53	6.31
Amorphous aluminosilicate	1.01	1.67	1.23	1.68

FIG: 6.10 DYE ADSORPTION AT $[Na^+]/[D^+] = 492$ ON ZEOLITE X, P1, AMORPHOUS SiO_2 AND AMORPHOUS ALUMINOSILICATE

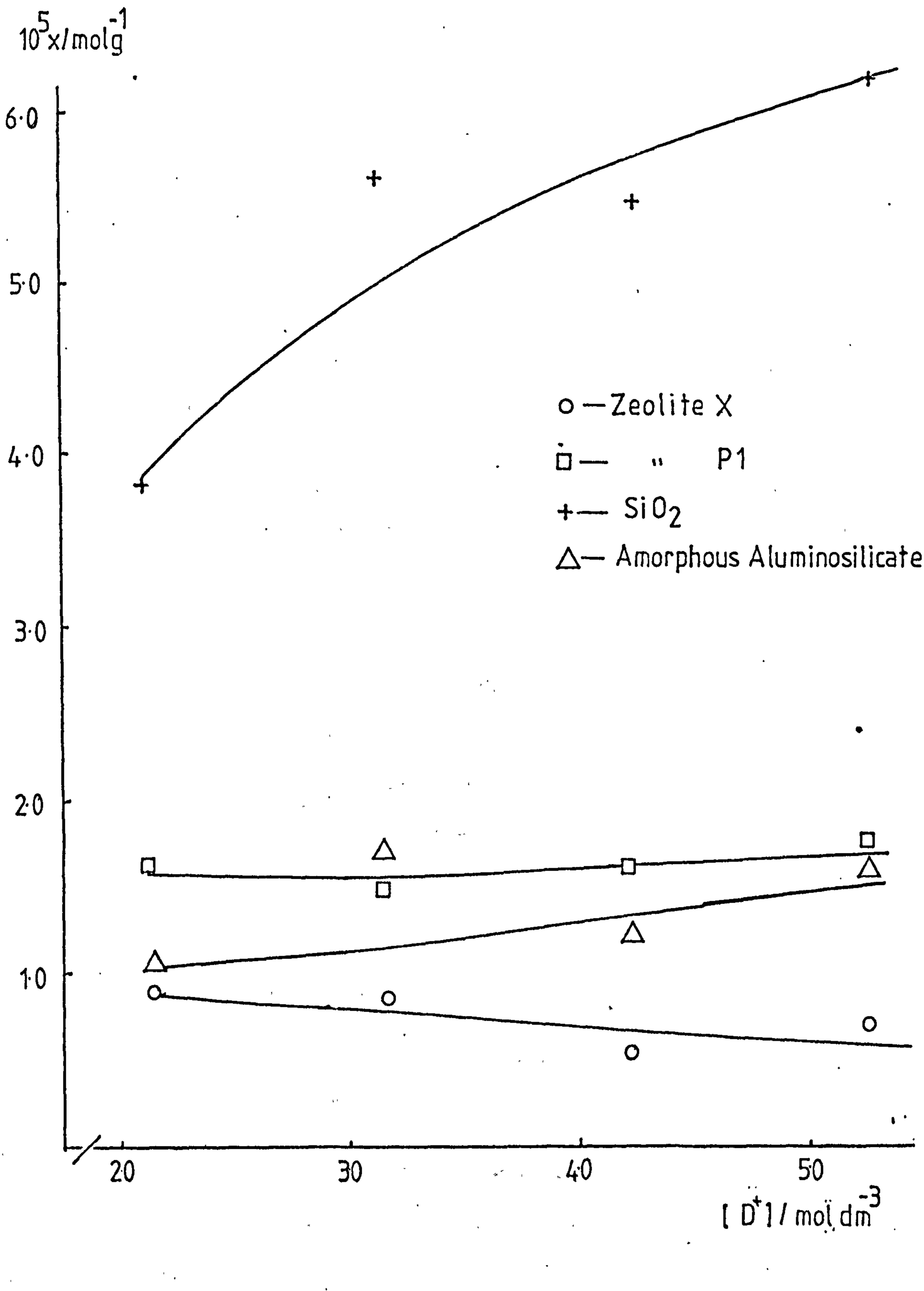

In setting up this experiment, it was necessary to consider the final composition of a reaction mixture e.g.

Initially $5.15Na_2O\ Al_2O_3\ 4SiO_2\ 242H_2O$

Finally $4.15Na_2O[Na_2O\ Al_2O_3\ 4SiO_2]242H_2O$

solid zeolite

Therefore a close approximation was chosen as

	Solution		Solid
	$4.15Na_2O$	: $242H_2O$	$Na_2O\ Al_2O_3\ 4SiO_2$
Mol wt	257.22	: 4356	404.26

Although under real reaction conditions the final solution is sodium hydroxide, for the reasons described previously it was decided to use sodium carbonate.

Thus a solution of Na_2CO_3 (0.95 mol dm^{-3}) was prepared in which methylene blue (0.0369 g) was dissolved with shaking over a period of 2 hours and zeolite X (2.3 g) was added. The mixture was then allowed to equilibrate for 2 hours with agitation. The solution was intensely coloured, and it was necessary to dilute it 100 times to observe an optical density within the scale of the spectrophotometer. The results are shown below -

Wt zeolite X/g	Amt MB adsorbed $10^5\ x/mol\ g^{-1}$
2.3073	0.104

It should be noted that the figure quoted above is subject to a large error caused by dilution. It was interesting to note that

there appeared to be two layers of coloured solid, the lower one being more strongly coloured. This could possibly be due to a difference in particle size.

Similar experiments were carried out using silica and zeolite P1 as the solid. The results are shown below -

	Wt of solid/g	Amt MB adsorbed 10^5 x/mol g^{-1}
(1)	SiO_2	4.03
(2)	Zeolite P1	2.42

Again the results are probably subject to large errors, however it is obvious that methylene blue adsorbs much more strongly on SiO_2 than on zeolites X and P1. Also, it appears that methylene blue is adsorbed more strongly by zeolite P1 than by zeolite X.

6.3.12 DESORPTION OF METHYLENE BLUE - QUALITATIVE STUDY

The solid zeolite X, zeolite P1 and amorphous silica, on to which dye had been adsorbed (section 6.3.10) were used for this desorption study. The supernatant liquid from the zeolite X slurry was decanted and some pure distilled water was added. The solid plus water was shaken for a few minutes and then centrifuged for 5 minutes. At this stage most of the dye had been desorbed and the solution was intensely coloured. This liquid was decanted and 25 cm^3 of a solution of Na_2CO_3 (1.5 mol dm^{-3}) was added. The procedure was similar to that described above, and after centrifuging all dye had been desorbed from the solid.

For the zeolite P1 sample, the supernatant liquid was decanted and the solid was washed twice with pure distilled water.

At this stage all the dye had not been desorbed. The solid was then washed twice with 25 cm^3 of a sodium carbonate solution (1.5 mol dm^{-3}) and still the dye was not totally desorbed.

This contrasts with the findings of Levina[137] and co-workers who concluded that basic dyes adsorbed from solution could not be desorbed. The dye was not completely desorbed from zeolite P1 as it was from zeolite X. It had been observed that the dye on zeolite P1 appeared to have changed colour slightly. It was possible that the dye had undergone a reaction, possibly demethylation[136] due to the basicity of the surface. If this is the case, then the binding forces may be quite different from those on the surface of zeolite X.

In an attempt to desorb the dye from the silica the solid was washed twice with pure distilled water. However, the solutions were only faintly coloured, indicating that no desorption had taken place. It is important to know whether the dye could be desorbed from silica by the use of Na_2CO_3. Sodium carbonate solution (25 cm^3 of 1.5 mol dm^{-3}) was added to the solid. This mixture was shaken and then centrifuged. A significant amount of dye was desorbed, but the solid silica was still very deeply coloured. This washing with sodium carbonate was repeated twice. Each time, significant desorption was observed, but the solid remained very dark blue.

From this qualitative study it is possible to conclude that desorption from the solids, zeolite X, zeolite P1 and amorphous silica, occurred but with increasing difficulty in the order,

$$X < P1 < SiO_2$$

6.4 DYE ADSORPTION AS A METHOD OF DETERMINING SURFACE AREA

There are many methods by which surface area can be determined, the most widely used being adsorption of gases. The B.E.T. method is usually employed and the results are reliable, but it requires complex apparatus and is tedious and lengthy. The solution adsorption method is much simpler but not always so reliable.

Dyes are normally used because of the ease with which they can be analysed spectrophotometrically. However, since aggregation of the dye molecules occurs, the true cross sectional area of the adsorbed species is then indeterminate. Even so, the method can be used as a rough guide, so long as the user is aware of its limitations. Kipling and Wilson[133] have used methylene blue in the determination of the surface area of a carbon black and a synthetic graphite. In their work three possible cross sections of the methylene blue molecule are considered: flat 1.35 nm^2, edgewise 0.75 nm^2 and end on 0.395 nm^2. These areas were calculated considering a 'raft-like' methylene blue cation. Brooks[140], however, quotes different values for the methylene blue molecule, flat (1.12 nm^2) edgewise (0.64 nm^2) and end on (0.28 nm^2).

In this work, specific external surface areas estimated from the monolayer capacities for zeolite A, X and Pl have been calculated, for each of the possible orientations of the molecule and using the values given by Kipling et al[133] and Brooks[140]. The results are shown in table 6.8 together with surface areas measured from scanning electron micrographs. It seems likely that the areas of methylene blue given by Brooks are correct.

Comparison of the measured surface area of zeolite X with those estimated suggests that the methylene blue molecule is adsorbed end on. However, comparison of the surface area of

TABLE 6.8 SURFACE AREA AS DETERMINED BY DYE ADSORPTION AND S.E.M.

		Surface area (s.a.)/m^2 g^{-1}					
		Brooks[140]			Kipling[133]		
Zeolite	s.a. from s.e.m.	Flat	Edgewise	End On	Flat	Edgewise	End On
		Am[a] = 1.12	Am = 0.64	Am = 0.28	Am = 1.35	Am = 0.75	Am = 0.395
X	1.46	7.15	4.08	1.79	8.61	4.78	2.52
A	1.57	1.54	0.88	0.39	1.87	1.03	0.547
P1	0.483	12.2	6.97	3.05	14.7	8.17	4.3

[a] Am = cross sectional surface area of methylene blue.

zeolite A with those estimated suggests that the molecule is adsorbed flat. This difference in orientation of the molecule on different solids is not surprising, since the most probable orientation must be governed primarily by the distribution of the cation exchange sites on the surface.

None of the estimated surface areas agrees with the measured surface area for zeolite P1. It must be assumed that the maximum coverage on zeolite P1 does not agree with monolayer coverage.

6.5 Conclusion

This work has demonstrated convincingly that the adsorption of methylene blue on synthetic zeolites A, X and P1 and silica occurs to differing degrees depending on the surface of the adsorbent. The type of binding mechanisms which operate on zeolite P1 appear to be different from those on zeolites X and A. The primary mechanism on zeolites X and A is ion exchange, although some physical adsorption probably occurs. However, on zeolite P1, the adsorption is much greater than would be expected if only ion exchange were occurring. The simple explanation would be that physical adsorption is occurring. However, the observation that a colour change of the dye takes place when it is adsorbed on zeolite P1 must be considered. This suggests that a reaction has taken place on the surface of the zeolite, possibly demethylation. This is likely to affect the adsorption in some way.

Adsorption on silica takes place via an ion exchange process at the pH investigated and the adsorption capacity is high due to the high surface area.

This work suggests that in zeolite X reaction mixtures the methylene blue would preferentially adsorb on zeolite P1 and silica

rather than zeolite X, which from Whittams work would suggest that the formation of zeolite P1 would be inhibited and zeolite X would grow. However, this was not observed in those reactions carried out using methylene blue.

CHAPTER 7

THIN LAYER CHROMATOGRAPHY

7.1 INTRODUCTION

As explained in chapter 6, the adsorption experiments were difficult to control and it was decided that a simpler and quicker way of studying dye zeolite interaction was necessary. For this purpose, the use of thin layer chromatography (t.l.c.) was considered.

Thin layer chromatography is a method of chromatographic separation which uses a thin, adsorbent, layer held on a rigid support, (normally a glass plate) as the stationary phase. Usually, the mobile phase in t.l.c. is an organic solvent, and the stationary phase is activated silica or alumina. The technique is mainly used for separation of organic mixtures. The separation achieved in this way depends on the partition of the organic molecules between the stationary phase and the product. Hence, if a zeolite is used as the stationary phase, the extent to which the organic molecules moves relative to the solvent, the R_f value

$$R_f = \frac{\text{distance moved by organic molecule}}{\text{distance moved by solvent front}}$$

will depend in part on the interaction between the organic molecule and the zeolite. In this way, it should be possible to examine the interaction between a dye and a zeolite surface. If a cationic dye is used, the binding of the dye to the surface is likely to be due, at least in part, to an ion-exchange process. For ion-exchange chromatography it is usually desirable to use a

simple salt in a polar solvent as the mobile phase.

Prior to this work, only one study of dye separation on zeolites by t.l.c. had been reported. This study was carried out by Grba[141] and his co-workers, who investigated the possibility of using synthetic zeolites A and X as the stationary phase and attempted in this way to separate mixtures of organic dyes. Mixtures of three types of dyes were used: water soluble dyes, ethanol soluble dyes and benzene soluble dyes. They found that separation of mixtures of water soluble dyes was possible with simple developers such as water and ethanol, but good separation was achieved only with three component systems such as n-butanol-water-acetic acid. These separations were achieved on both zeolites A and X. Separation of mixtures of ethanol soluble dyes was achieved on both zeolites A and X, but the separation was not as good as for water soluble dyes, the spots being more diffuse. The third group, the benzene soluble dyes, could not be separated on either zeolite. Attempts to separate all groups of dyes on amorphous aluminosilicate layers were unsuccessful. From this study, Grba et al concluded that good, homogeneous thin layers can be made from crystalline forms of synthetic zeolites A and X without the addition of a binder. Moreover, it is possible to separate water soluble organic compounds on these layers, if neutral solvents or solvent systems containing a weak acid as the developer are used. In addition, they found that the activation of the thin layer, i.e. length of time at 100°C, was an important feature affecting separation.

From this work it seemed likely that t.l.c. could indeed give useful information about adsorption of dye on zeolites and that the R_f value obtained for a certain dye would give a rough measure of the extent to which that dye was adsorbed by a particular zeolite.

Grba and his co-workers did not consider the possibility of ion exchange of the dyes with cations on the zeolite surface and it seems likely that in consequence they made a poor choice of mobile phase. It was therefore decided to investigate the use of t.l.c. to study dye adsorption on zeolites A, X and P1 and on silica, and in particular to look at the contribution of ion exchange to the adsorption process.

7.2 EXPERIMENTAL DETAILS

7.2.1 MATERIALS

For this work five dyes were used. Methylene blue, acriflavine and crystal violet were BDH technical grade standard stains, while acridine orange and azur C were Hopkin and Williams technical grade dyes. The structures of these dyes are shown in Table 7.1. Zeolites X, 3A, 4A and 5A were Linde molecular sieves obtained from BDH Ltd. Zeolites P1 and Y were synthesised in the laboratory. Scanning electron micrographs of most of the materials were obtained and are shown in plates 1-5. The silica plates were prepared using Merck silica "G". The silica used for mixing with zeolite X was Akzo pure silica type KS300. All solvents were prepared using BDH analar reagents.

7.2.2 PREPARATION OF THIN LAYERS

Slurries of the zeolites in water were made up in the ratios shown below:

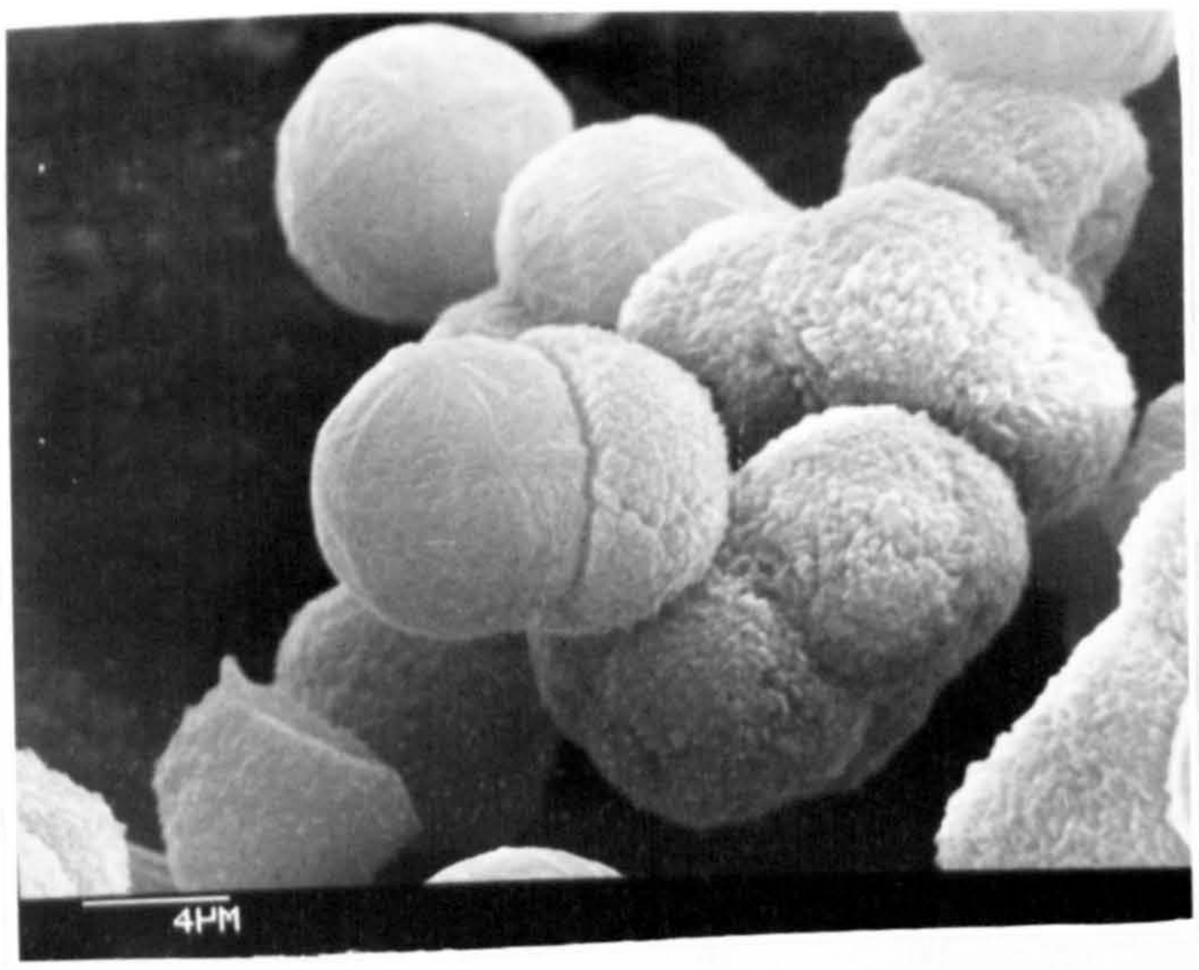

PLATE 4 —
Zeolite P1.

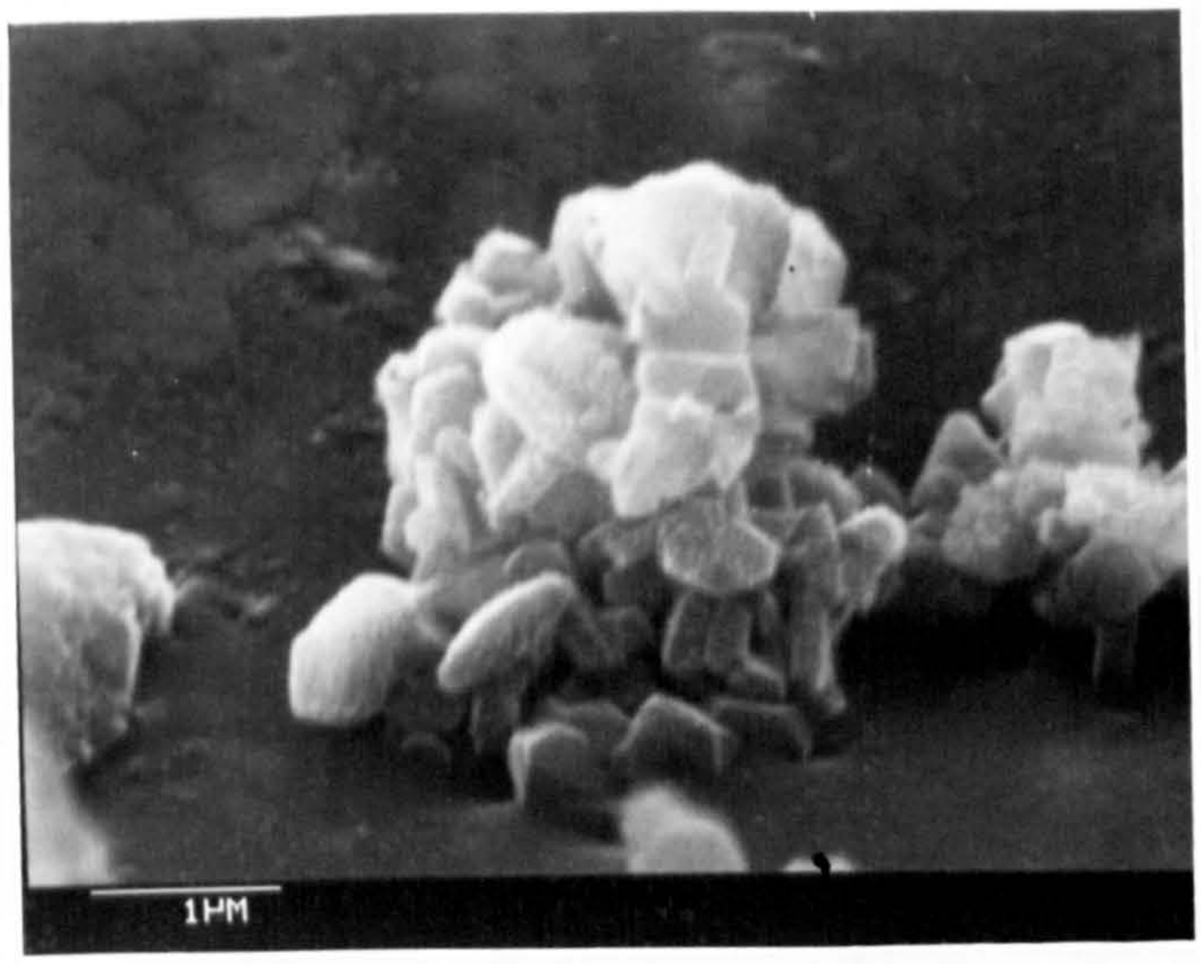

PLATE 5 —
Zeolite Y

TABLE 7.1 DYES USED IN THIS WORK

Dye	Structure
Methylene blue (MB)	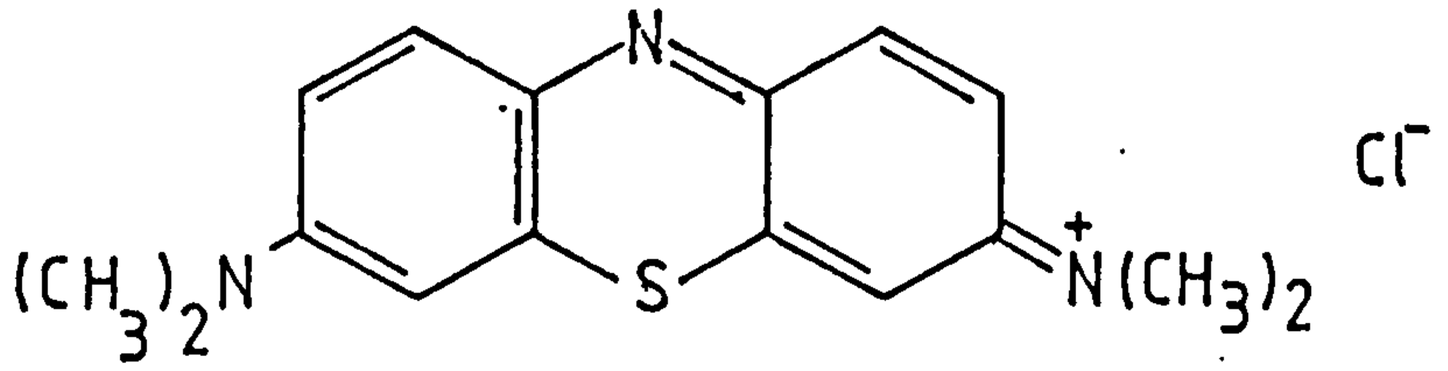
Acridine Orange (AO)	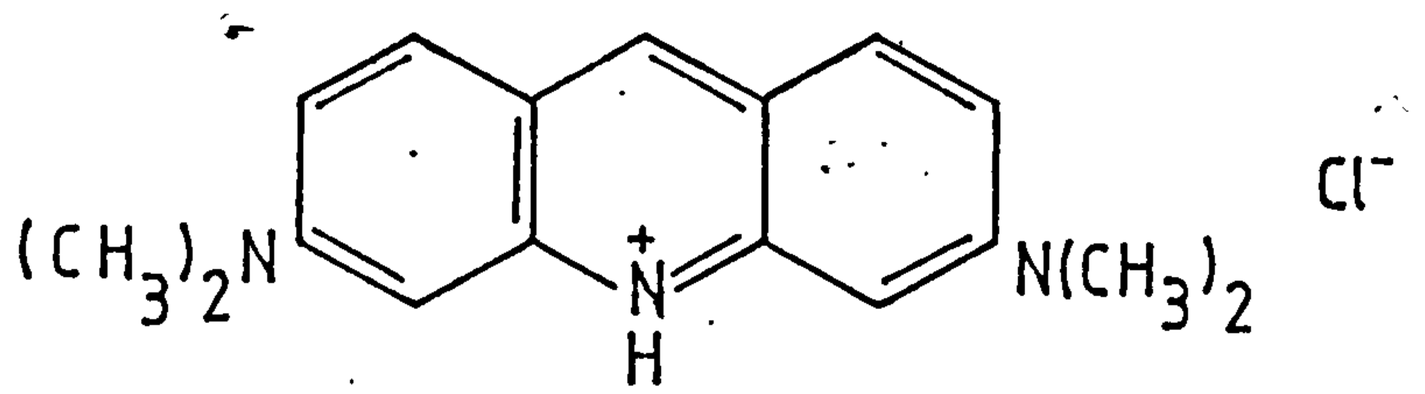
Crystal Violet (CV)	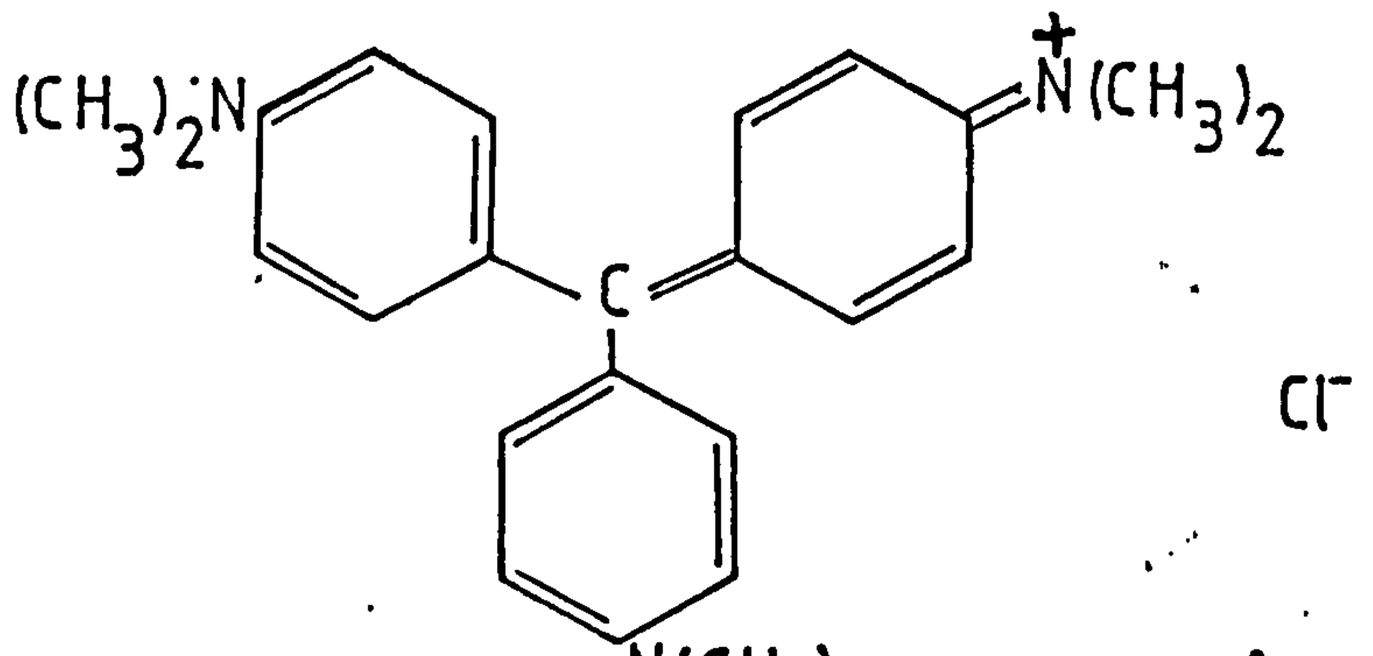
Acriflavine (AC)	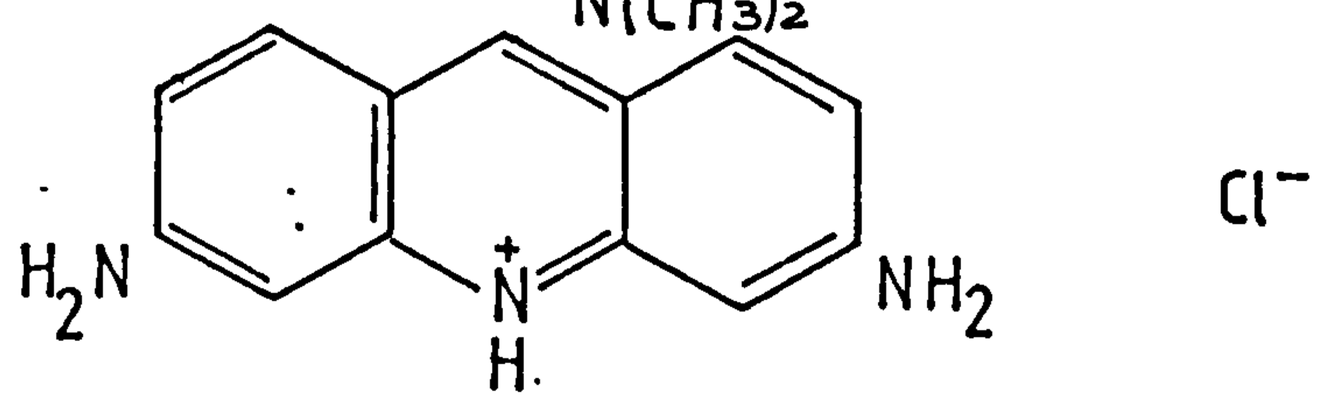
Azur C (AZC)	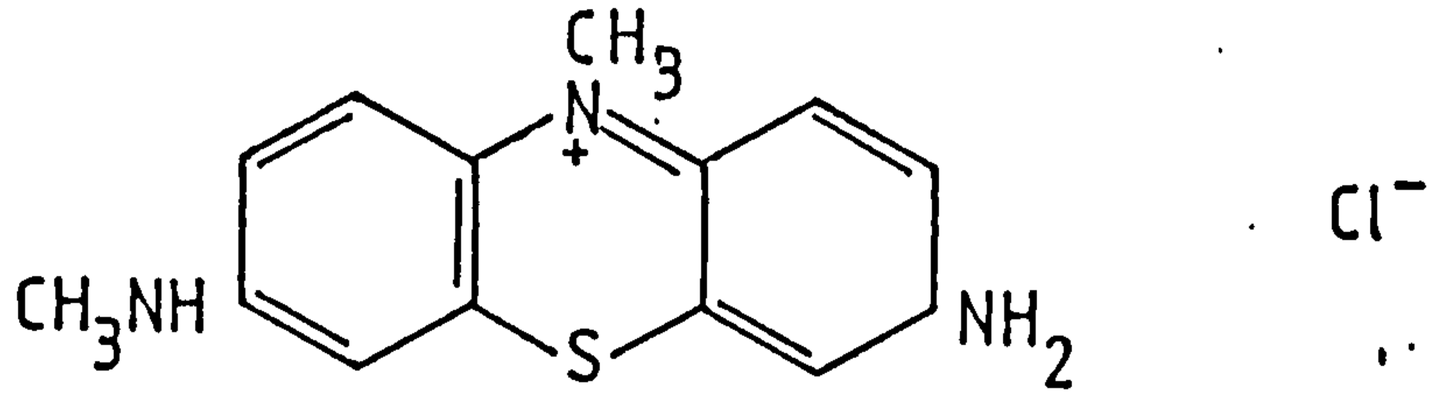

zeolite type	H_2O/zeolite (w/w)
X	1.2
3A	1.0
4A	1.2
5A	1.0
Pl	1.2
Y	2.0

Glass plates 5x20 cm were cleaned thoroughly before use, washed with water and detergent, drained, dried and finally washed with acetone. It was very important to avoid touching the surface of the plates with the fingers, as any grease marks prevented the zeolite from adhering at that place on the surface. The plates were then spread to a wet thickness of 0.25 mm using a Shandon Southern Ltd. adjustable spreader type SAB2818 of the moving spreader type. After drying at room temperature for 15 minutes, the layers were activated at 100°C for one hour. All the zeolites adhered well to the glass surface; however, with the exception of zeolites 3A and 5A, all layers were gritty. The use of a calcium sulphate binder might have helped to overcome this problem but this was thought inadvisable as it is slightly soluble in water. The results obtained on the gritty plates were reproducible within reasonable error limits and so it was decided that they were acceptable.

7.2.3 DEVELOPMENT AND DETECTION

Development was by the ascending technique in a 20x15x10 cm chamber. Since equilibration with solvent vapour is known to be important in thin layer chromatography, it was essential that the

tank had a lid which fitted properly and that this vessel was as small as possible. Saturation of the atmosphere in the tank, was assisted by lining the walls with filter paper soaked in solvent. With these precautions it was not necessary to allow any equilibration time prior to the start of the run. All runs were carried out at room temperature. R_f values were not affected by changes in temperature of up to $\pm 10^{o}C$.

Standardisation of the geometrical parameters of the plate was desirable. The length of run was always 10.0 ± 0.5 cm. The spots were situated 2 cm from the startline and the distance between spot centres was at least 1 cm. 75 ml of solvent was used. Dyes could be easily identified by the colour of the spots.

7.2.4 PROCEDURE

A solution of the dye in water was applied using a capillary tube to give a loading of $\sim$1 µg. It was important that only the drop emerging from the tube should touch the surface; if the tube itself touched the zeolite surface a hole was formed, and this caused a major obstruction to the solvent flow. Irregularity of solvent flow around a hole can cause the moving spot to be completely distorted. When the spot had dried, the plate was placed vertically in the tank with its lower edge immersed in the selected mobile phase to a depth of 0.5 - 1.0 cm. Two plates were usually run simultaneously. At the end of the run, the solvent was allowed to evaporate and the R_f value was measured. For all dyes tailing was observed, so the R_f value was defined as the distance from the initial spot position to the front of the streak divided by the distance travelled by the solvent front. To check that this method gave reproducible results, each experiment was repeated at least once and usually three times in the case of

methylene blue. R_f values were reproducible to within ±10% and frequently to within ±5%.

For experiments at pH ∿7, aqueous sodium chloride solution was used as the mobile phase for sodium containing zeolites and silica. For experiments at pH ∿11 and pH ∿13, aqueous sodium carbonate and sodium hydroxide solutions were used. For the potassium containing zeolite 3A, the solutions were prepared from potassium chloride, potassium carbonate and potassium hydroxide.

7.3 RESULTS

7.3.1 R_f VALUES FOR DYES ON ZEOLITES 4A, X, Y, P1 AND ON SILICA

R_f values were determined for each of the five dyes (see table 7.1) using sodium carbonate solutions as the mobile phase, and the results are shown in figures 7.1 -·7.5 (all figures will be found at the end of this chapter) and tables 7.2 - 7.6. In the absence of sodium carbonate these cationic dyes were bound firmly to the zeolites (R_f=0), whereas an anionic dye, nuclear fast red was very weakly bound (R_f∿1). Initially the R_f values of the cationic dyes increase rapidly as the sodium ion concentration is increased, a result which suggests that an ion exchange process is operating at the zeolite surface.

On examination of the R_f concentration curves for acridine orange and crystal violet (figures 7.2 and 7.3 respectively) it can be seen that at sodium carbonate concentrations greater than 0.5 mol dm^{-3} the R_f values decrease with increasing concentrations. This surprising result is possible due to the instability of these dyes in alkaline solutions.

For azur C, the R_f values increase with the sodium carbonate concentration on all of the zeolites except zeolite A. In this case,

TABLE 7.2 R_f VALUES ON ZEOLITE X WITH VARIATION IN Na^+ CONCENTRATION

Dye[a]	Na_2CO_3 concentration/mol dm^{-3} 1.0	0.5	0.25	0.1	0.01
MB	0.93±0.03	0.91±0.05	0.86±0.02	0.69±0.01	0.37
AO	0.28±0.02	0.41±0.06	0.55±0.01	0.44±0.01	0.02
CV	0.44±0.02	0.57±0.03	0.64±0.01	0.64±0.01	0.39
AC	0.86±0.03	0.88±0.06	0.74±0.02	0.57±0.02	0.21
AZC	0.87±0.03	0.79±0.10	0.73±0.04	0.54±0.01	0.24

[a] MB = methylene blue; AO = acridine orange; CV = crystal violet; AC = acriflavine; AZC = azur C

TABLE 7.3 R_f VALUES ON ZEOLITE A WITH VARIATION IN Na^+ CONCENTRATIONS

	Na_2CO_3 concentration/mol dm^{-3}			
Dye[a]	0.5	0.25	0.1	0.05
MB	0.86±0.04	0.87±0.03	0.85±0.02	0.76±0.04
AO	0.32±0.03	0.40±0.04	0.42±0.02	0.37±0.03
CV	0.58±0.03	0.60±0.01	0.60±0.05	0.63±0.06
AC	0.73±0.03	0.86±0.01	0.64±0.04	0.57±0.03
AZC	0.57±0.02	0.70±0.06	0.60±0.04	0.56±0.01

[a] see footnotes to table 7.2

TABLE 7.4 R_f VALUES ON ZEOLITE P1 WITH VARIATION IN Na^+ CONCENTRATIONS

	Na_2CO_3 concentration/mol dm^{-3}			
Dye[a]	1.0	0.5	0.1	0.01
MB	0.62±0.01	0.48±0.01	0.18	0.08
AO	0.37±0.01	0.32	0.22	0.16
CV	0.26±0.01	0.46	0.32	0.15
AC	0.37±0.01	0.41	0.18	0.07
AZC	0.26±0.01	0.21	0.10	0.05

[a] see footnotes to table 7.2

TABLE 7.5 R_f VALUES ON ZEOLITE Y WITH VARIATION IN Na^+ CONCENTRATIONS

	Na_2CO_3 concentration/mol dm^{-3}				
Dye[a]	1.0	0.5	0.1	0.01	0.0
MB	0.24±0.04	0.21±0.02	0.11±0.01	0.00	0.00
AO	0.09±0.02	0.18±0.02	0.13±0.01	0.02	0.00
CV	0.18±0.02	0.32±0.02	0.24±0.01	0.06	0.00
AC	0.11±0.01	0.12±0.01	0.06±0.01	0.04	0.00
AZC	0.20±0.04	0.14±0.01	0.07±0.01	0.00	0.00

[a] see footnotes to table 7.2

TABLE 7.6 R_f VALUES ON SILICA

	Na_2CO_3 concentration/mol dm^{-3}
Dye[a]	1.0
MB	0.05
AO	0.14
CV	0.16
AC	0.19
AZC	0.04

[a] see footnotes to table 7.2

for sodium carbonate solutions with concentrations above 0.25 mol dm^{-3}, two separate spots, one purple and one blue, were observed. As this was not observed for any of the other zeolites, it suggests that a reaction of azur C is catalysed by the zeolite surface. A demethylation reaction of methylene blue on the surface of a NaA-Na_2O zeolite surface has been reported by Susic[136] and co-workers. According to these workers, this is an entirely base catalysed reaction, caused by the presence of localised basicity on the zeolite surface. It seems likely that demethylation also takes place during t.l.c. of azur C on zeolite A as the localised basicity of its surface is probably greater than that of any of the other zeolites. Azur C is the only dye tested which has a methyl group attached to a ring nitrogen and it seems likely that it is this which causes this dye, but not the others, to react on the zeolite surface.

The results for methylene blue and acriflavine are shown in figures 7.1 and 7.4. These two dyes behave similarly on all the zeolites although the R_f values for methylene blue are always higher than those for acriflavine. There are two possible explanations for this behaviour: firstly, that methylene blue may be more soluble than acriflavine and will therefore adhere less readily to the plate, and secondly, that there is a specific interaction between the dye and the zeolite which is possible for acriflavine (e.g. some form of H-bond) but not for methylene blue. It is likely that both these effects are operating to some extent.

7.3.2 R_f VALUES FOR DYES ON ZEOLITE 3A AND 5A

R_f values for each of the five dyes were measured over a range of potassium carbonate concentrations (0.01 mol dm^{-3} - 1.0 mol dm^{-3}) on zeolite 3A and a range of calcium chloride concentrations

TABLE 7.7 R_f VALUES ON ZEOLITE 3A AND K^+ CONCENTRATIONS

	K_2CO_3 concentration/mol dm^{-3}			
Dye	1.0	0.5	0.1	0.01
MB	0.84±0.05	0.94±0.02	0.80±0.05	0.15
AO	0.37	0.45±0.02	0.37±0.03	0.23
CV	0.33±0.02	0.34±0.02	0.38±0.02	0.31±0.03
AC	0.88±0.01	0.93±0.01	0.64±0.03	0.32±0.08
AZC	0.59±0.05	0.60±0.03	0.52±0.01	0.24±0.04

TABLE 7.8 R_f VALUES ON ZEOLITE 5A AND Ca^{++} CONCENTRATIONS

	$CaCl_2$ concentration/mol dm^{-3}			
Dye	1.0	0.5	0.1	0.01
MB	0.88±0.03	0.86±0.02	0.56±0.06	0.07
AO	0.44±0.02	0.39	0.40±0.03	0.08±0.01
CV	0.34±0.01	0.36±0.01	0.50	0.32
AC	0.45±0.02	0.37±0.01	0.24	0.07
AZC	0.51±0.02	0.46±0.01	0.23±0.01	0.07

(0.01 mol dm^{-3} ; 1.0 mol dm^{-3}) on zeolite 5A. The results are shown in figures 7.6 and 7.7 and tables 7.7 and 7.8. Zeolites 3A and 5A are respectively the potassium exchanged and calcium exchanged forms of zeolite 4A. The behaviour observed for methylene blue on both zeolites is similar to that on zeolite 4A and crystal violet and acridine orange also show similar behaviour. The R_f value for azur C, however, does not decrease above potassium carbonate concentrations of 0.5 mol dm^{-3}, or calcium chloride concentrations of 0.5 mol dm^{-3}, as observed for zeolite 4A above sodium carbonate concentrations of 0.5 mol dm^{-3}. Presumably, decomposition of azur C does not take place on the K- and Ca- forms of zeolite A. This may be related to surface basicity.

The R_f value for acriflavine on zeolite 3A is comparable with that recorded on zeolite 4A. However, the R_f value obtained on zeolite 5A with 1.0 mol dm^{-3} calcium chloride is approximately half that on zeolite 4A with 1.0 mol dm^{-3} sodium carbonate. This can probably be attributed to a pH effect.

Comparison of the R_f values for methylene blue measured with 1.0 mol dm^{-3} sodium chloride for zeolite 4A, 1.0 mol dm^{-3} potassium chloride for zeolite 3A and 1.0 mol dm^{-3} calcium chloride for zeolite 5A shows the following order

$$4A < 3A < 5A$$

Since high R_f values imply that the dye cation is weakly bound to the zeolite surface and the inorganic cation is strongly bound, then, for a given dye, the higher the R_f value the more tightly bound is the cation. In this case, the Na^+ ion is the more strongly bound and the order of binding is

$$Na^+ > K^+ > Ca^{2+}$$

7.3.3 EFFECT OF pH ON R_f VALUES

R_f values were determined for each of the five dyes on zeolites X, P1, Y and 3A and on silica at pH = 7 and pH = 11. At pH = 13, only the R_f values for methylene blue and acriflavine on zeolites X, Y and 3A and on silica were determined, as all the other dyes decomposed at this pH. However, R_f values for all the dyes at pH = 13 were determined on zeolite P1. The results are shown in figures 7.8 - 7.11 and tables 7.9 - 7.13. It is difficult to understand why it is possible for all the dyes to survive at pH = 13 on zeolite P1 - possibly the dyes move via a mechanism which allows them to be attached to the zeolite surface at all times and hence decomposition does not occur.

For all the zeolites there is little difference between the R_f values obtained at pH = 7 and pH = 11. However, those R_f values recorded at pH = 13 are markedly different to those obtained at lower pH values. On zeolites X, the R_f values at pH = 13 are considerably lower than those obtained at pH = 11 (for methylene blue 0.70 at pH = 13; 0.93 at pH = 11 and for acriflavine 0.66 at pH = 13; 0.87 at pH = 11). This is also the case for zeolite 3A, although the decrease is less marked. In contrast to this, on zeolites P1 and Y the R_f values at pH = 13 are considerably higher than at pH = 11. The R_f value recorded for methylene blue on silica also increased at pH = 13.

7.3.4 R_f VALUES ON MIXTURES OF ZEOLITE X AND AMORPHOUS SILICA

Mixtures of varying composition of zeolite X and silica were prepared by weight, and R_f values for methylene blue were measured using 1.0 mol dm^{-3} sodium carbonate as the mobile phase. The results are shown in figure 7.12 and table 7.14. The most marked effect is

TABLE 7.9 R_f VALUES ON ZEOLITE X AT VARYING pH LEVELS

	pH		
Dye	7	11	13.5
MB	0.94±0.03	0.93±0.03	0.66±0.04
AO	0.52±0.01	0.48±0.02	
CV	0.44±0.02	0.44±0.02	
AC	0.87±0.01	0.86±0.03	0.66±0.04
AZC	0.88±0.01	0.87±0.03	

TABLE 7.10 R_f VALUES ON ZEOLITE P1 AT VARYING pH LEVELS

	pH		
	7	11	13.5
Dye		(Na_2CO_3=0.5 mol dm^{-3})	
MB	0.72±0.01	0.48	0.73
AO	0.21	0.32	0.59
CV	0.18	0.46	0.40
AC	0.36	0.41	0.53
AZC	0.26	0.21	0.24

TABLE 7.11 R_f VALUES ON ZEOLITE Y AT VARYING pH LEVELS

	pH		
Dye	7	11	13.5
MB	0.17±0.01	0.24±0.04	0.75
AO	0.19	0.09	-
CV	0.28	0.18	-
AC	0.31	0.11	0.42
AZC	0.17	0.20	-

TABLE 7.12 R_f VALUES ON ZEOLITE 3A AT VARYING pH LEVELS

	pH		
Dye	7	11	13.5
MB	0.83	0.84	0.80
AO	0.46	0.37	-
CV	0.40	0.33	-
AC	0.81	0.88	0.82
AZC	0.75	0.59	-

observed when silica makes up less than 30% by weight of the mixture and especially when less than 10% (wt) is silica. It is important to note that the mixtures of zeolite X and silica were made up on a weight basis. The silica, being much less dense than the zeolite, constituted the major part by volume of most mixtures. If a similar mixture was made up by volume and R_f values measured, one would expect to find a curve similar in shape to figure 7.12 but with the points moved to the right.

R_f values were also measured using 1.0 mol dm^{-3} sodium hydroxide as the mobile phase. The results are shown in figure 7.13 and table 7.15. The initial rise in the curve is due to the increased R_f value recorded on silica at pH = 13 (see section 7.3.3). However, the R_f value recorded on zeolite X decreases with an increase in pH. The resultant effect at silica/zeolite X ratios between 0.1-0.9 is an overall increase in the recorded R_f values compared with those observed when sodium carbonate solution was the mobile phase.

7.3.5 R_f VALUES ON MIXTURES OF ZEOLITE X AND ZEOLITE P1

Mixtures of zeolites X and P1 were prepared by weight, and R_f values for methylene blue were measured. The mobile phase was 1.0 mol dm^{-3} sodium carbonate solution. The results are shown in figure 7.14 and table 7.16. It was observed that as the amount of zeolite P1 increased, the R_f value steadily decreased.

The R_f value for methylene blue was measured on a sample (HC172/6h) which had been synthesised in the laboratory and shown by x-ray powder diffraction to contain zeolite X (32%) and zeolite P (68%). From figure 7.14, the predicted R_f value was

TABLE 7.13 R_f VALUES ON SILICA AT VARYING pH LEVELS

Dye	pH	
	11	13
MB	0.05	0.16
AO	0.14	0.11
CV	0.16	0.16
AC	0.19	0.16
AZC	0.04	-

TABLE 7.14 R_f VALUES FOR METHYLENE BLUE ON MIXTURES OF ZEOLITE X AND SILICA AT pH=11

Composition of mixture % SiO_2 (w/w)	R_f
100	0.05
20	0.24±0.04
50	0.28±0.02
30	0.32±0.03
20	0.38±0.02
15	0.42±0.04
10	0.50
5	0.64±0.02
0	0.93±0.03

0.68 and the measured R_f value was 0.71, indicated by a cross on the graph. This measured value is well within experimental error and demonstrates the potential of this technique as an aid to analysis.

7.3.6 R_f VALUES FOR METHYLENE BLUE ON MIXTURES OF AMORPHOUS ALUMINOSILICATE WITH ZEOLITE X

Attempts were made to measure R_f values for methylene blue on mixtures of amorphous aluminosilicate and zeolite X, prepared by weight. The amorphous aluminosilicate was prepared in a reaction designed to make zeolite X in which the silica source was silica sol. The sample was taken after 1 hour when no crystallisation had occurred. For comparison, a chromatoplate was run using an amorphous aluminosilicate obtained from a reaction in which the silica source was active sodium metasilicate pentahydrate. The R_f values obtained for the two amorphous aluminosilicate materials agreed within experimental error. For mixtures of amorphous aluminosilicate (Am.As) and zeolite X in which Am.As was greater than 50% it was not possible to prepare thin layers of the mixture since the amorphous material did not adhere strongly to the glass plate and when dried the layers tended to flake. However R_f values were recorded for mixtures in which Am.As was less than 50%. The results are shown in figure 7.15 and table 7.17. Initially at compositions containing 10% amorphous aluminosilicates, the R_f value decreases, and subsequently, as more amorphous aluminosilicate was added, the R_f value increases.

The cross marked on figure 7.15 shows the R_f value measured for a sample which had been synthesised in the laboratory and

TABLE 7.15 R_f VALUES FOR METHYLENE BLUE ON MIXTURES OF ZEOLITE X AND SILICA AT pH=13.5

Composition of mixture wt % SiO_2	R_f
10	0.68±0.02
30	0.56±0.02
50	0.56±0.02
70	0.46±0.01
100	0.05

TABLE 7.16 R_f VALUES FOR METHYLENE BLUE ON MIXTURES OF ZEOLITE X AND ZEOLITE P1 AT pH=11

Composition of mixture wt % P1	R_f
0	0.93±0.03
10	0.85±0.01
20	0.79±0.05
30	0.75±0.05
50	0.70±0.05
70	0.74±0.05
100	0.62±0.01

TABLE 7.17 R_f VALUES FOR METHYLENE BLUE ON A MIXTURE OF ZEOLITE X AND AMORPHOUS ALUMINOSILICATE

Composition of mixture wt % AmAS	R_f
10	0.66±0.02
30	0.74±0.02
50	0.76±0.02

TABLE 7.18 COMPARISON OF R_f VALUES ON DIFFERENT ZEOLITES AT pH=13

Zeolite	R_f
X	0.70
Y	0.75
P1	0.73
3A	0.80

analysed by x-ray powder diffraction to contain 48% zeolite X, the remaining 52% being amorphous material. The discrepancy between this and the artificially prepared sample of this composition suggests that the structure of the amorphous aluminosilicate changes during the reaction and is quite different after 3 hours. It seems likely that t.l.c. could be used to study the amorphous aluminosilicate materials present in zeolite reaction mixtures.

7.4 INTERPRETATION OF RESULTS

In order to interpret the observations recorded in section 7.3, it is necessary to consider the possible mechanisms by which the dye adsorbs on the zeolite surface and also to have a model of the zeolite surface. There are two possible mechanisms for adsorption on inorganic surfaces (a) physical adsorption and (b) ion exchange. Initially in this t.l.c. work, it was considered that the only mechanism by which the dye was bound to the zeolite surface was ion exchange. If this were the case, then for each dye the R_f value would approach unity as the inorganic cation concentration is increased, and for very high cation concentrations the dye adsorption would be insignificant, and consequently R_f would be 1. However, it was not, and it appears that another mechanism besides ion-exchange, probably physical adsorption, also operates.

For an ion-exchange process involving dye and sodium ions, it is possible to develop a simple theoretical treatment as follows. From the simple theory of partition chromatography

$$\frac{R_f}{1-R_f} = \frac{V_m}{V_s} \cdot \frac{C_m}{C_s} = \frac{V_m}{V_s} \cdot \frac{1}{k'} = \text{const} \frac{1}{k'} \qquad (7.1)$$

where C_m and C_s are the concentration of dye in the mobile and stationary phases and V_m and V_s are the corresponding volumes. It follows that

$$k' = \frac{V_m}{V_s} \cdot \frac{1-R_f}{R_f} \qquad (7.2)$$

The equilibrium constant for the ion-exchange process is given by

$$K_{IE} = \frac{[Na^+]}{[D^+]} \frac{[ZX^-, D^+]}{[ZX^-, Na^+]} \qquad (7.3)$$

and hence the distribution coefficient is given by

$$D_{IE} \alpha \frac{[ZX^-, D^+]}{[D^+]} = \frac{[ZX^-, Na^+]}{[Na^+]} \qquad (7.4)$$

Since concentration of ion-exchange sites is constant and fixed by the structure of the matrix, $[ZX^-, Na^+]$ is effectively constant, and we can write

$$k' = D_{IE} \alpha \frac{1}{[Na^+]} \qquad (7.5)$$

and hence

$$\frac{(1-R_f)}{R_f} \alpha \frac{1}{[Na^+]}$$

This relation has been plotted for the results obtained for methylene blue on zeolite X, and is shown in figure 7.16 It can be seen that the curve does not go through the origin and this confirms that another binding mechanism in addition to ion-exchange is operating.

In addition to knowledge of the exchange mechanism, it is necessary to have a model for the zeolite surface. Several models for the zeolite surface can be envisaged:-

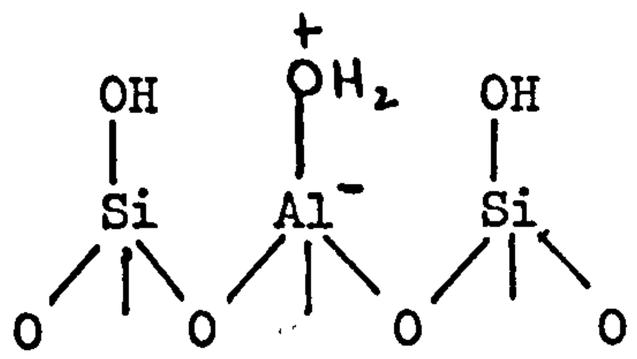

(I) neutral pH - no ion exchange sites

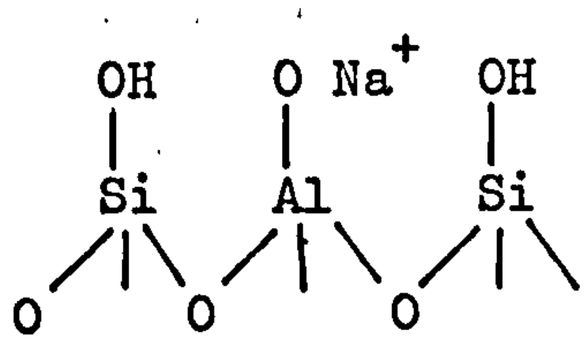

(II) neutral pH ion exchange site

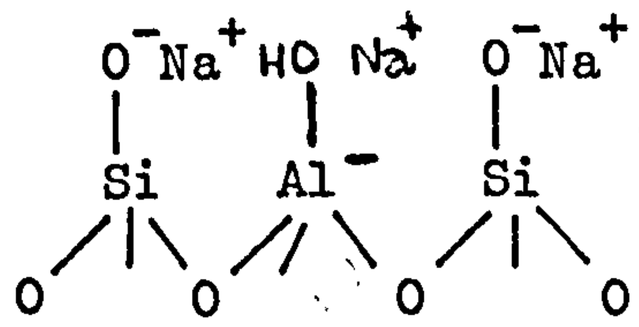

(III) high pH form of I

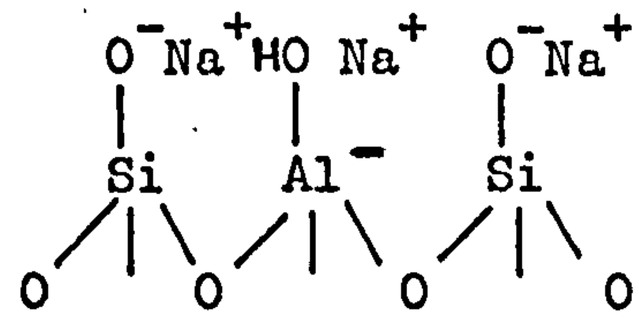

(IV) high pH form of II

Since there is little difference between the R_f values obtained at pH = 7 and pH = 11 (figures 7.8 - 7.11) it seems likely that the ion exchange site operative at these pH values is -

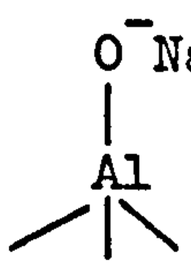

This indicates that structure II is more likely than structure I, and structure IV is the better model for the high pH surface.

For a given dye, the differences between the R_f values obtained on different zeolites at 1.0 mol dm^{-3} sodium carbonate concentration must therefore by explained in terms of the zeolite structure and surface. It is important to realise that the interaction between dye and zeolite takes place on the external surface of the zeolite and not inside the cages, as all the dye molecules are too large to enter the channels.

If pure water is used as the mobile phase, the dye does not move, as there are no inorganic ions which can displace it. However, when an ionic solute such as sodium carbonate is employed, the Na^+ ions are preferentially adsorbed on the ionic sites, and the dye is displaced and moves up the plate. The extent to which the dye moves, i.e. the R_f value, depends on the Si/Al ratio of the zeolite. Comparison of the R_f values obtained for methylene blue on zeolites A, Y and on silica (figure 7.1) demonstrates this most clearly. As the Si/Al ratio increases, the R_f value recorded decreases. It seems reasonable to assume therefore that adsorption sites from which the dye cannot be easily removed by Na^+ ions are made up of adjacent

silicon atoms. It follows, then, that as the Si/Al ratio increases the R_f value should decrease, and this can be seen by comparison of the R_f value for methylene blue on zeolites A, X, P, Y and silica when the mobile phase is 1 mol dm^{-3} sodium carbonate

R_f value for methylene blue	$X \approx A > P > Y > SiO_2$
Si/Al ratio	$X \approx A < P < Y < SiO_2$

As mentioned previously, there is little difference between the R_f values obtained at pH = 7 and pH = 11 on all zeolites. However, marked differences were observed between R_f values obtained at pH = 11 and pH = 13. For zeolites X and 3A, the R_f value for methylene blue decreased with increasing pH. In contrast, for zeolites Y and P the R_f value increased with increasing pH. At high pH values, the zeolite surface is probably as depicted in structure IV, so all zeolites will have a similar surface structure. The physical adsorption sites on zeolites Y and P have been replaced by ionic sites O^-, and so an increase in R_f value is observed since the dyes can now be exchanged for Na^+ ions. On zeolites X and 3A, the number of ion exchange sites has now doubled, and it is reasonable to assume that there are not sufficient Na^+ ions to exchange at all these sites (the number of terminal hydroxyl groups $\sim 0.15 \times 10^{20}$ per gram of 1 micron particle size zeolite), so the methylene blue is more tightly bound to the surface. Comparison of the R_f value recorded for methylene blue at pH = 13 on each of these zeolites (table 7.18) shows reasonable agreement which is consistent with the surface model postulated.

In addition, an increase in R_f value for methylene blue on silica at pH 13 was observed, which is consistent with the formation of O^- sites and an ion-exchange mechanism.

The R_f values obtained for mixtures of zeolite X with zeolite P1 silica and amorphous aluminosilicate can be explained in terms of ion exchange and adsorption sites.

For zeolite X/silica mixtures, the R_f values recorded using sodium carbonate solution (1.0 mol dm^{-3}) as the mobile phase decrease rapidly and continue to fall as the ratio of silica/ zeolite increases. This is due to the increase in non-ion exchange adsorption sites i.e. adjacent silicon atoms. Mixtures of zeolite X and zeolite P1behave similarly, although the decrease is less marked. This is consistent with the fact that zeolite P1 has a smaller number of non-ion exchange adsorption sites than silica. The behaviour observed for mixtures of zeolite X and the amorphous aluminosilicate is more difficult to explain. Since the amorphous aluminosilicate is an ion exchanger, it is not surprising that the R_f value at AmAs/ zeolite X values of 0.3 and 0.5 is relatively high. The initial sharp decrease in R_f value is possibly due to the introduction of non-ion exchange adsorption sites. Since however little is known about the structure of this material it is difficult to be entirely sure of the reasons for this behaviour.

7.5 CONCLUSIONS

This investigation of zeolites as the adsorbent for thin layer chromatography has shown conclusively that ion exchange takes place on the zeolite surface and that on zeolites whose

framework structure contains at least two adjacent silicon atoms other adsorption sites are also present.

In addition, this work has demonstrated convincingly the usefulness of this technique in differentiating between zeolites of similar structure but different Si/Al ratios e.g. zeolite X and zeolite Y. Thus, using a calibration curve of R_f versus Si/Al ratio it should be possible to make a rapid estimate of the Si/Al ratio of a zeolite X or Y sample from an R_f measurement.

This work has shown that using similar procedures it is possible to determine the amount of amorphous silica in an impure zeolite (e.g. in X or A), and the rough composition of a binary zeolite mixture (e.g. X and Pl). For all these procedures to work satisfactorily it is necessary that the dye is stable under the alkaline conditions present on the zeolite surface, and the present work has shown that methylene blue meets these requirements.

As described in section 7.3.2, t.l.c. also provides a method whereby selectivity between cations e.g. K^+, Na^+ and Ca^{++} on zeolite A surface can be deduced. This is a very important observation, since it gives a very direct, quick method to obtain information about affinities of inorganic cations for zeolite surfaces.

This work has shown that t.l.c. provides a very promising technique for a wide variety of investigations related to zeolites and their synthesis. For example, it could be used to investigate the solid phase of the alumino-silicate gels from which zeolites are crystallised. This technique also opens up the possibility of studying ion exchange in the internal cavities and external surface of zeolites independently. Further work on all these aspects should be carried out.

Fig. 7.1 R_f versus $[Na_2CO_3]$ for methylene blue on zeolites X, A, Pl, Y and silica.

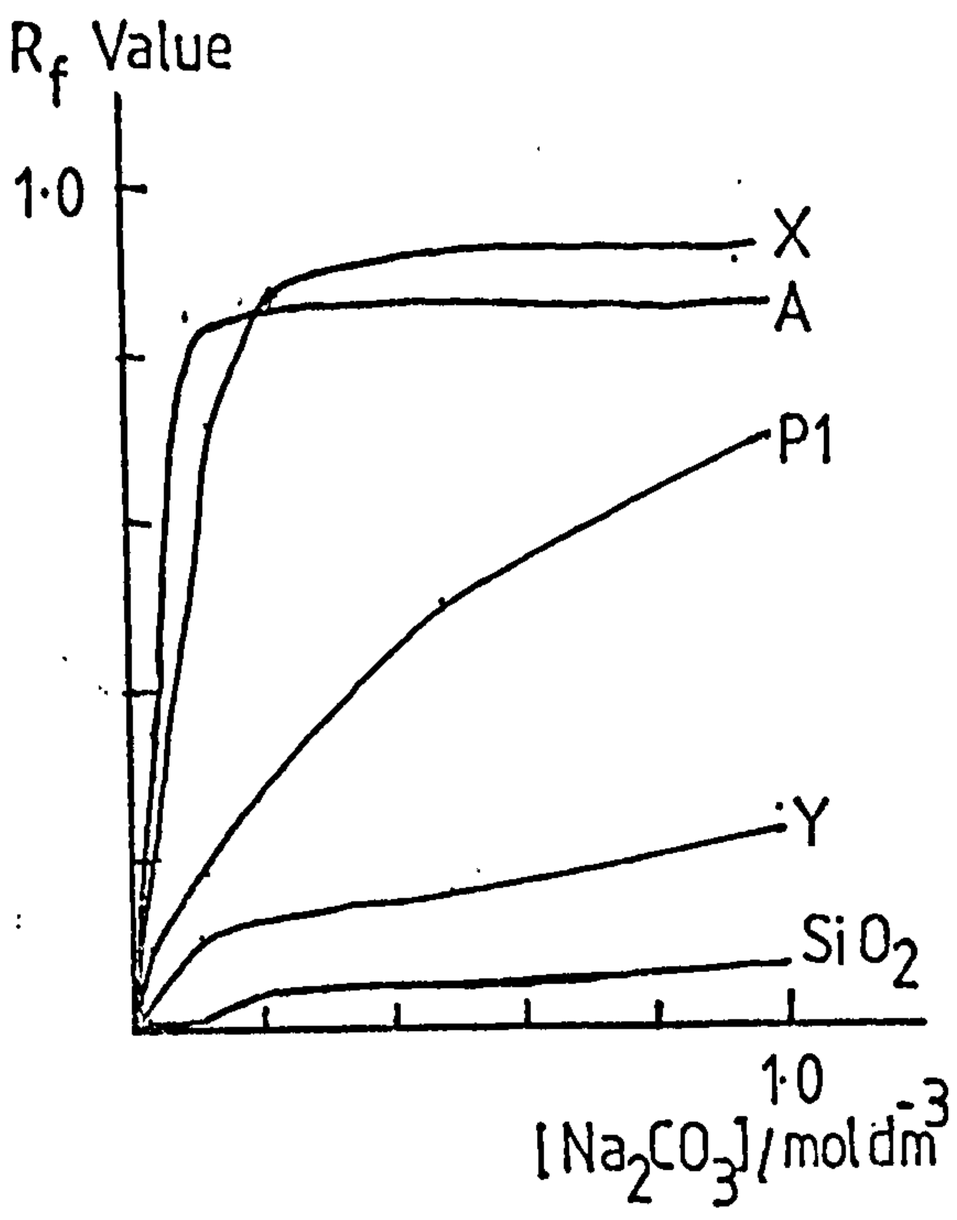

Fig. 7.2 R_f versus $[Na_2CO_3]$ for Acridine Orange on zeolites X, A, Pl, Y.

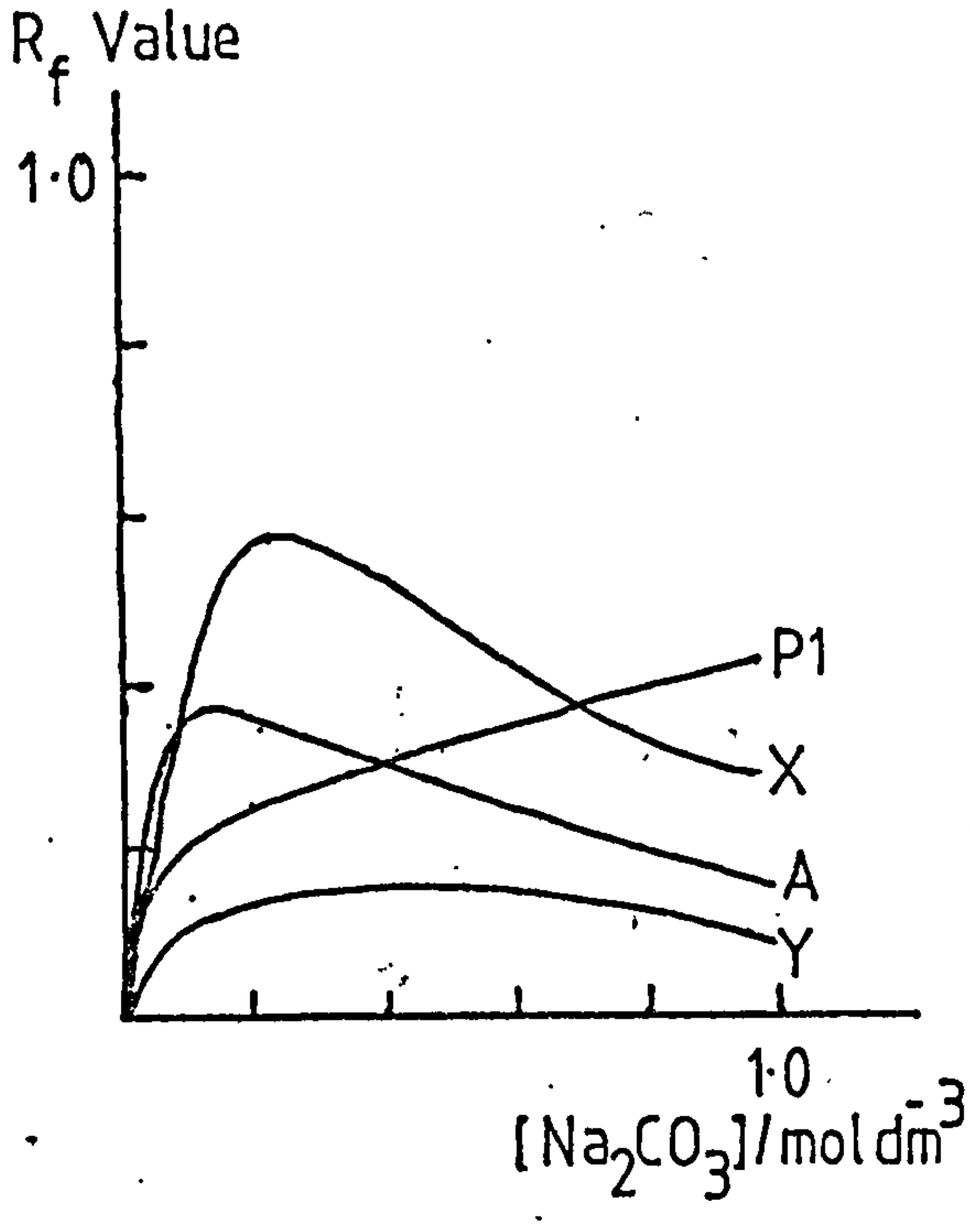

Fig. 7.3 R_f versus $[Na_2CO_3]$ for Crystal Violet on zeolites X, A, Pl, Y.

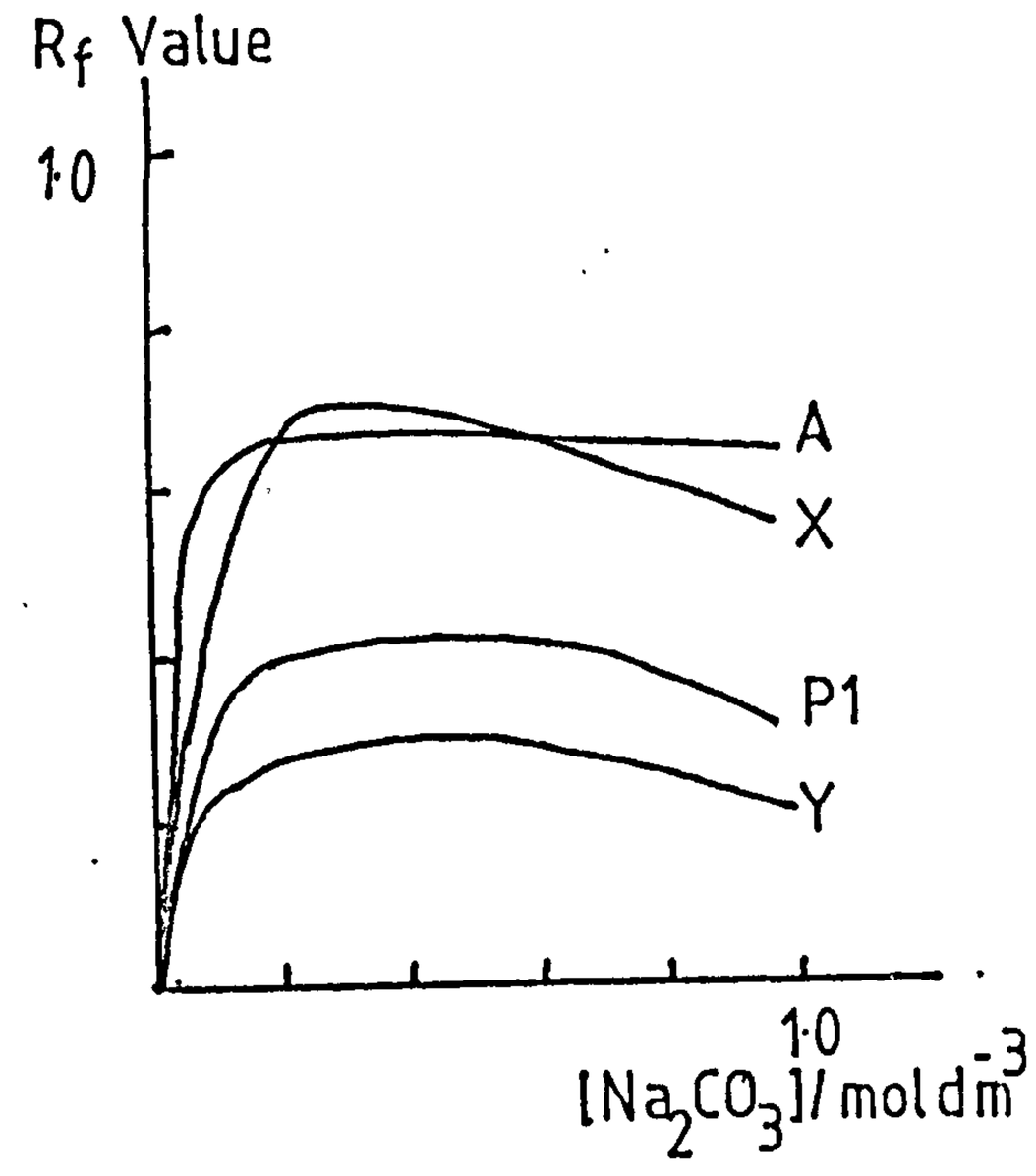

Fig. 7.4 R_f versus $[Na_2CO_3]$ for Acriflavine on zeolites X, A, Pl, Y.

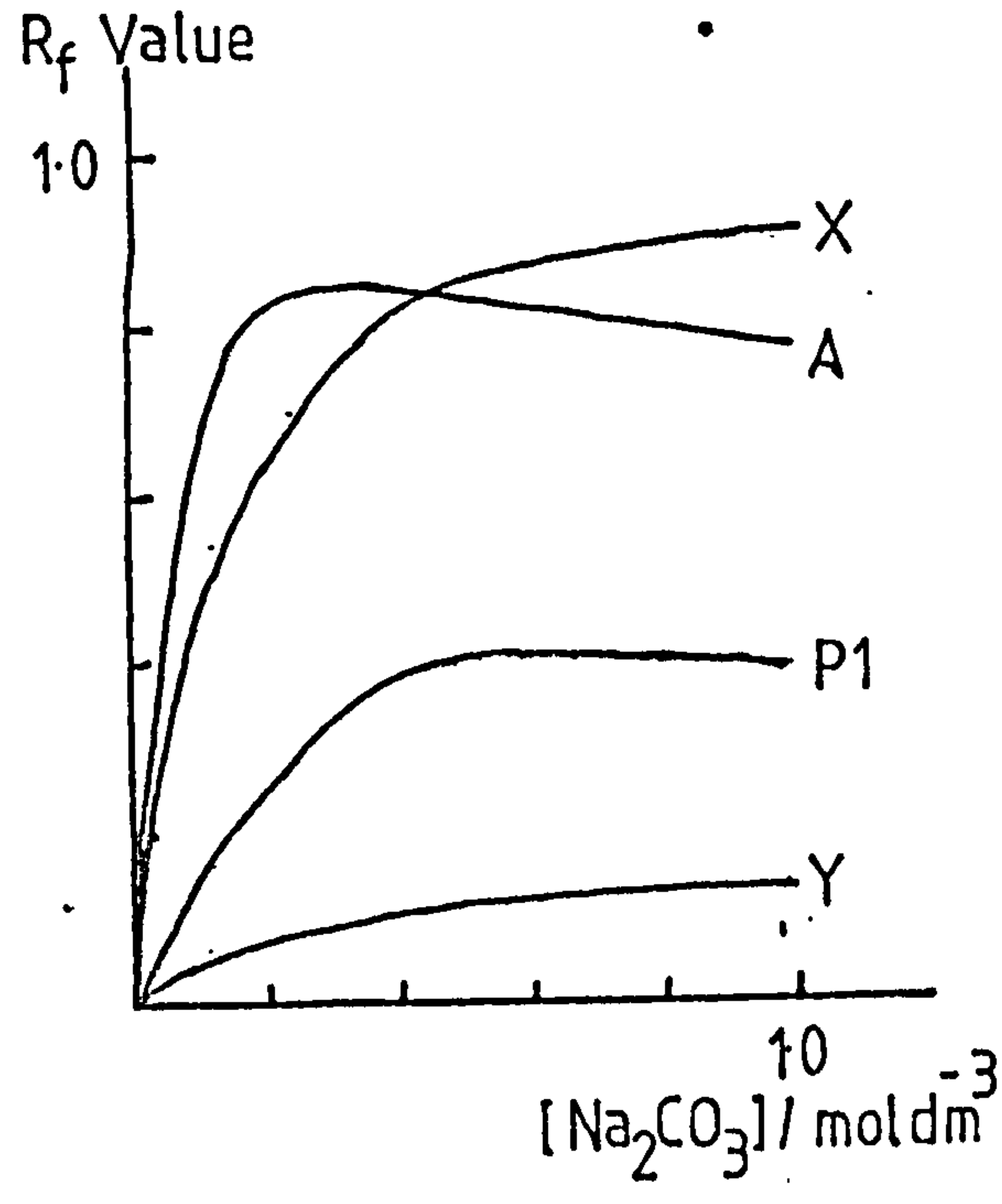

Fig. 7.5 R_f versus $[Na_2CO_3]$ for Azur C on zeolites X, A, P1, Y.

Fig. 7.6 R_f versus $[K_2CO_3]$ for dyes on zeolite 3A.

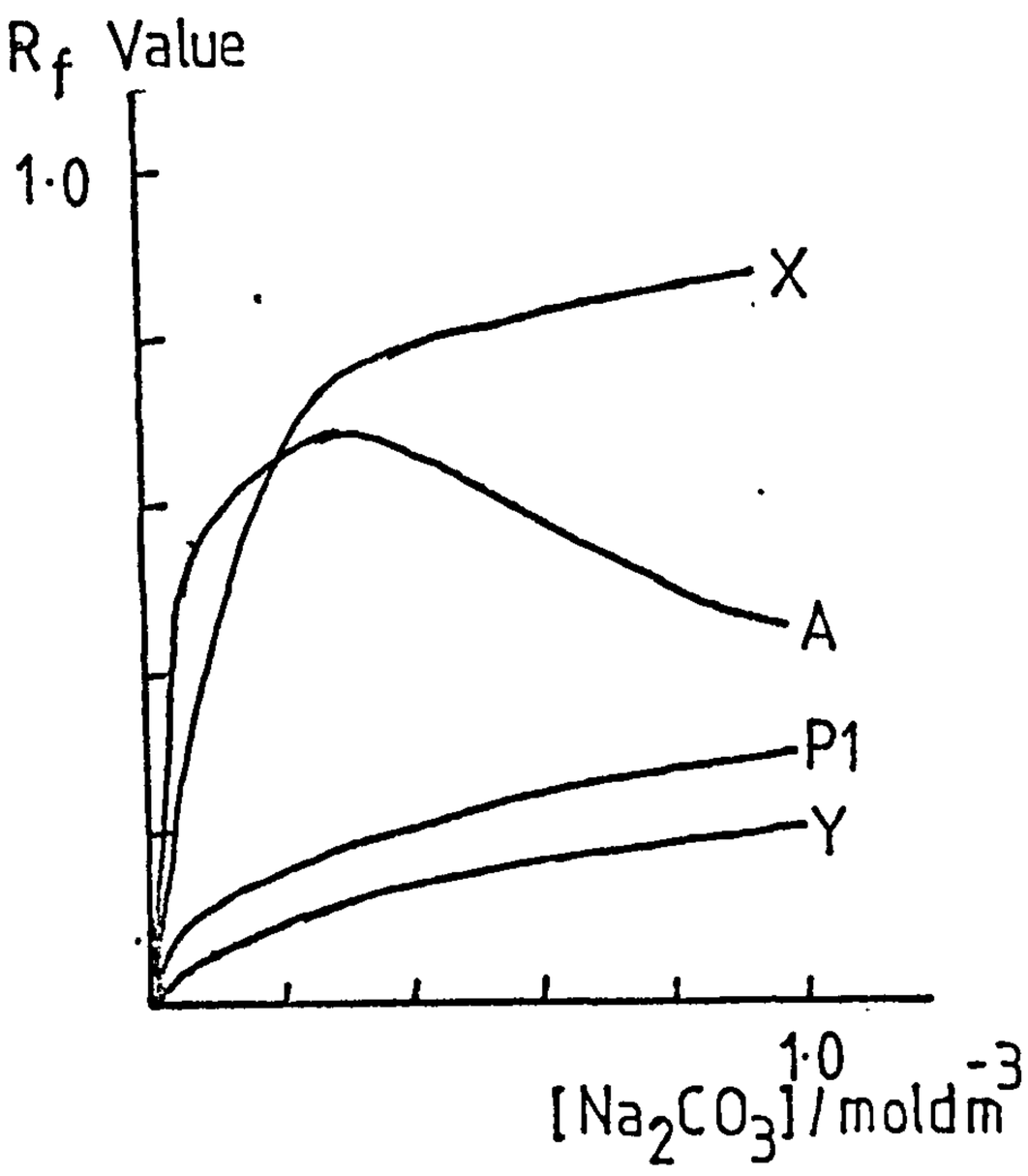

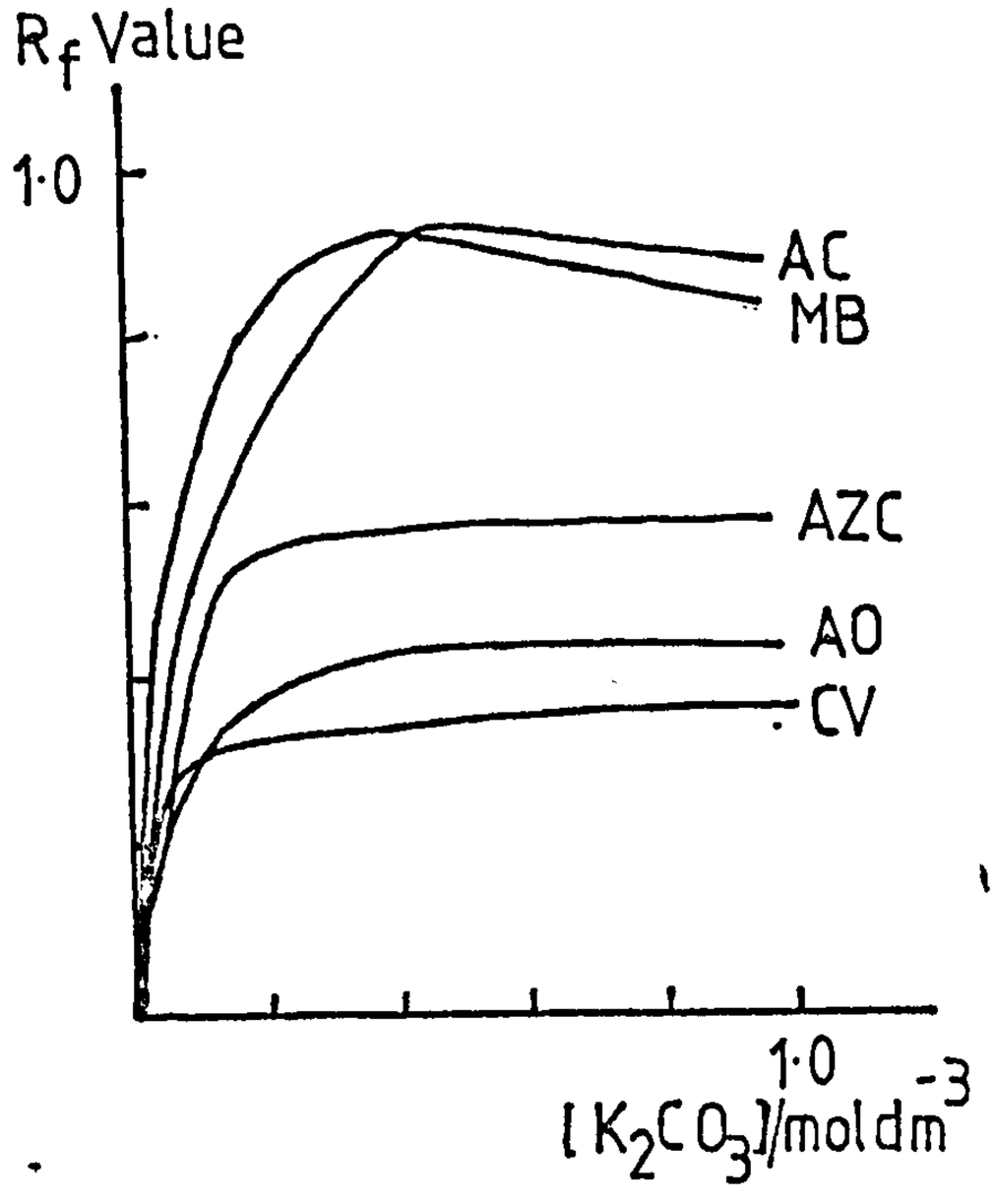

Fig. 7.7 R_f versus $[CaCl_2]$ for dyes on zeolite 5A

Fig. 7.8 R_f versus pH for dyes on zeolite X

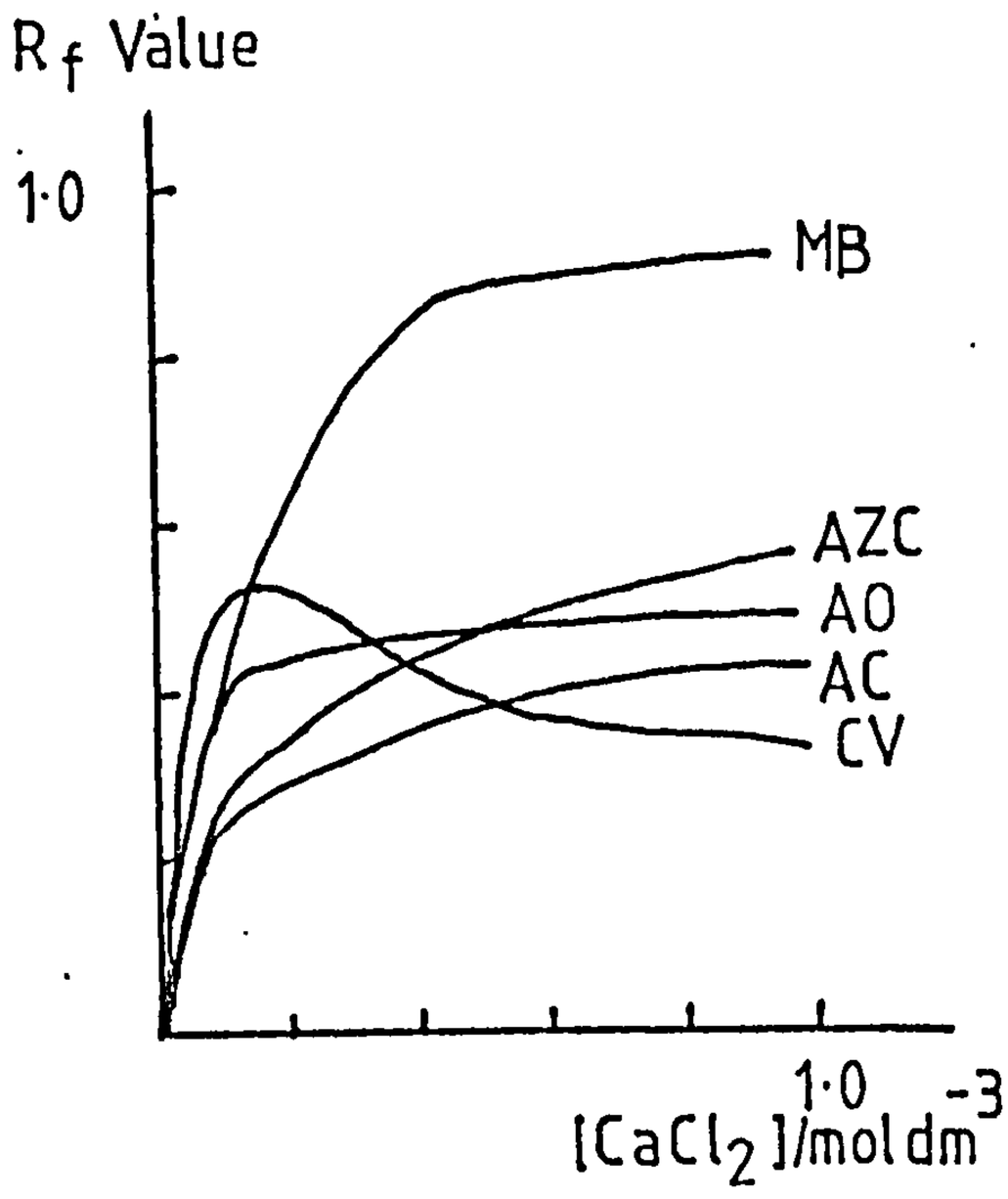

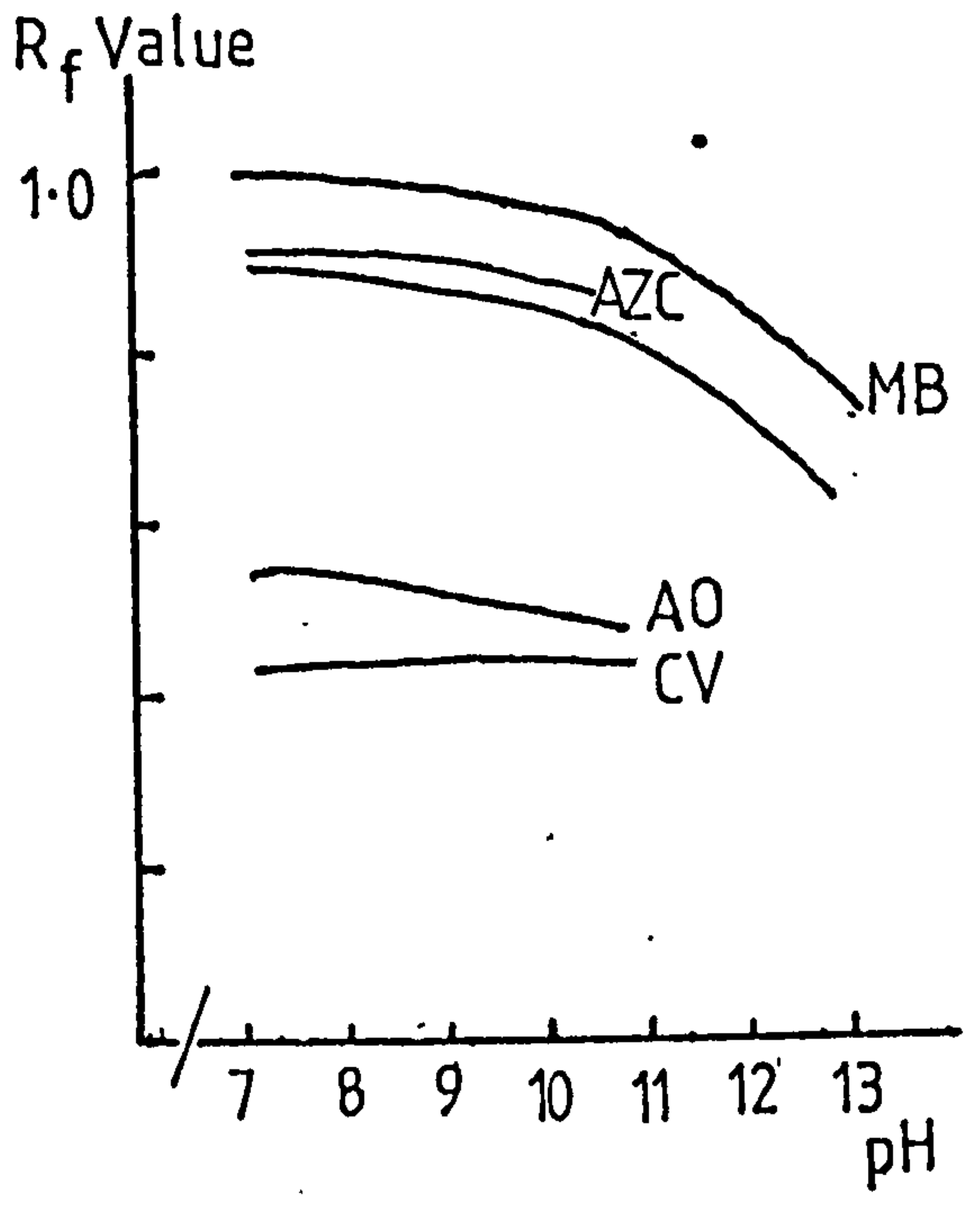

Fig. 7.9 R_f versus pH for dyes on zeolite Y

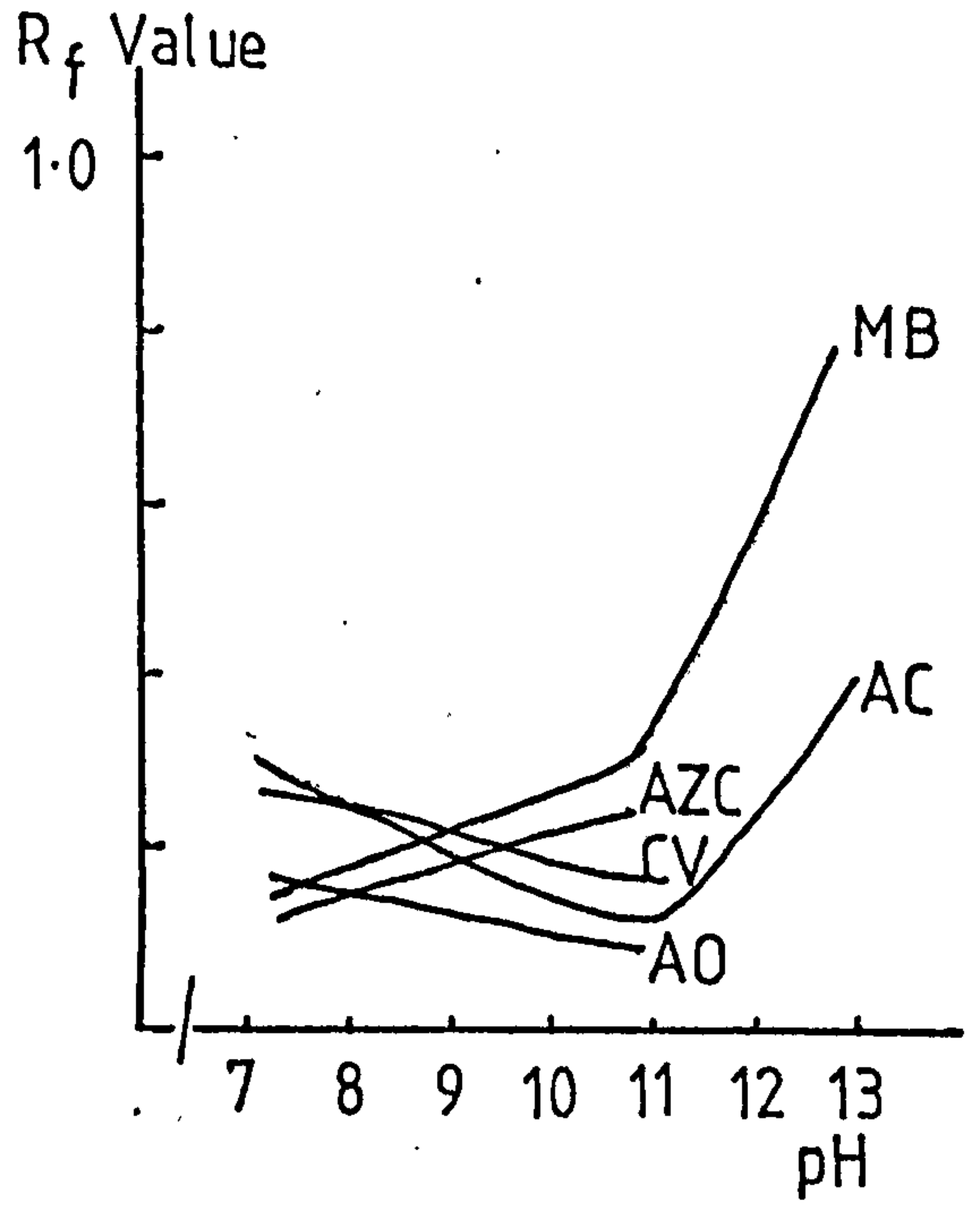

Fig. 7.10 R_f versus pH for dyes on zeolite 3A

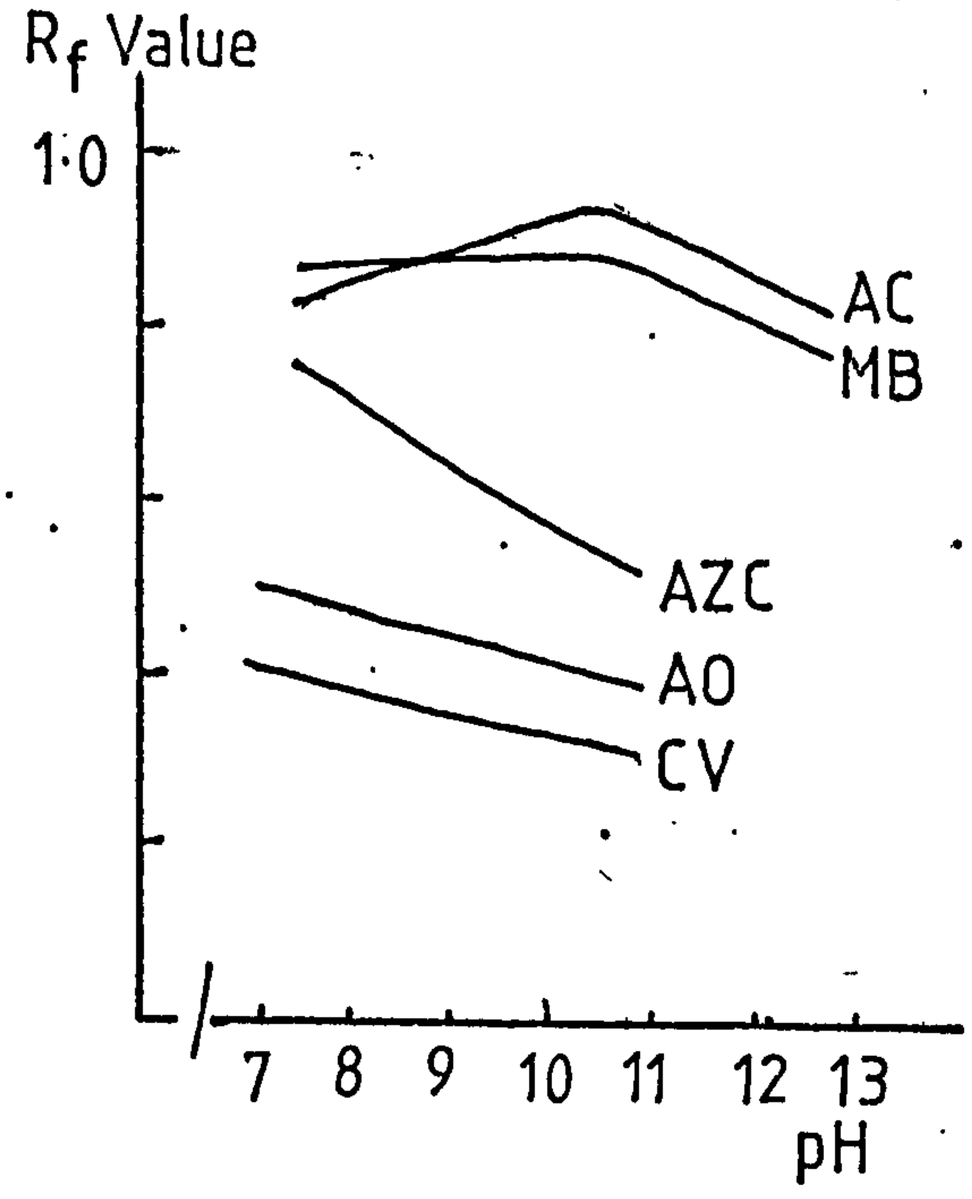

Fig. 7.11 R_f versus pH for dyes on zeolite P1

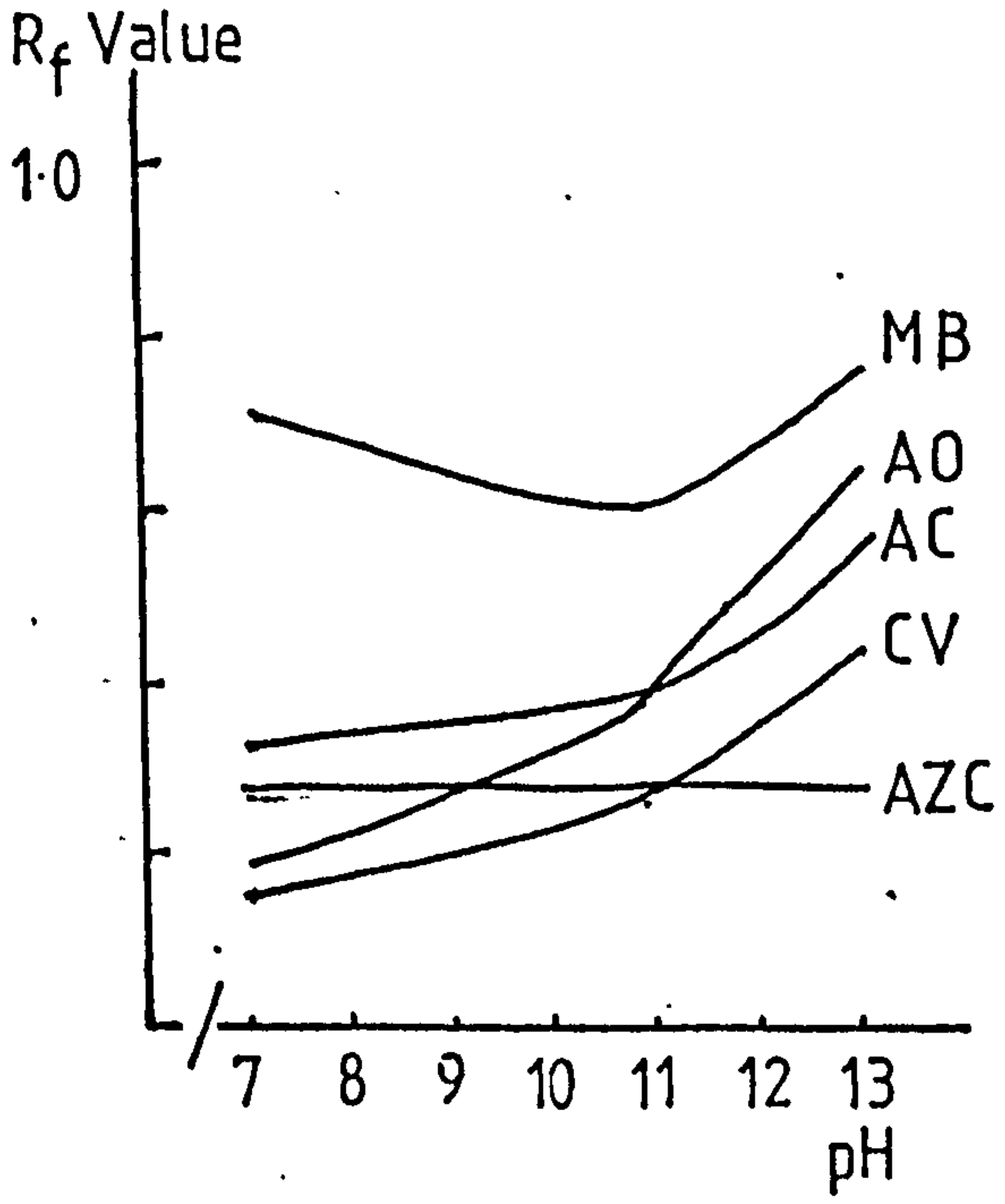

FIG. 7.12 R_f VALUES FOR METHYLENE BLUE ON MIXTURES OF ZEOLITE X AND SILICA AT pH = 11

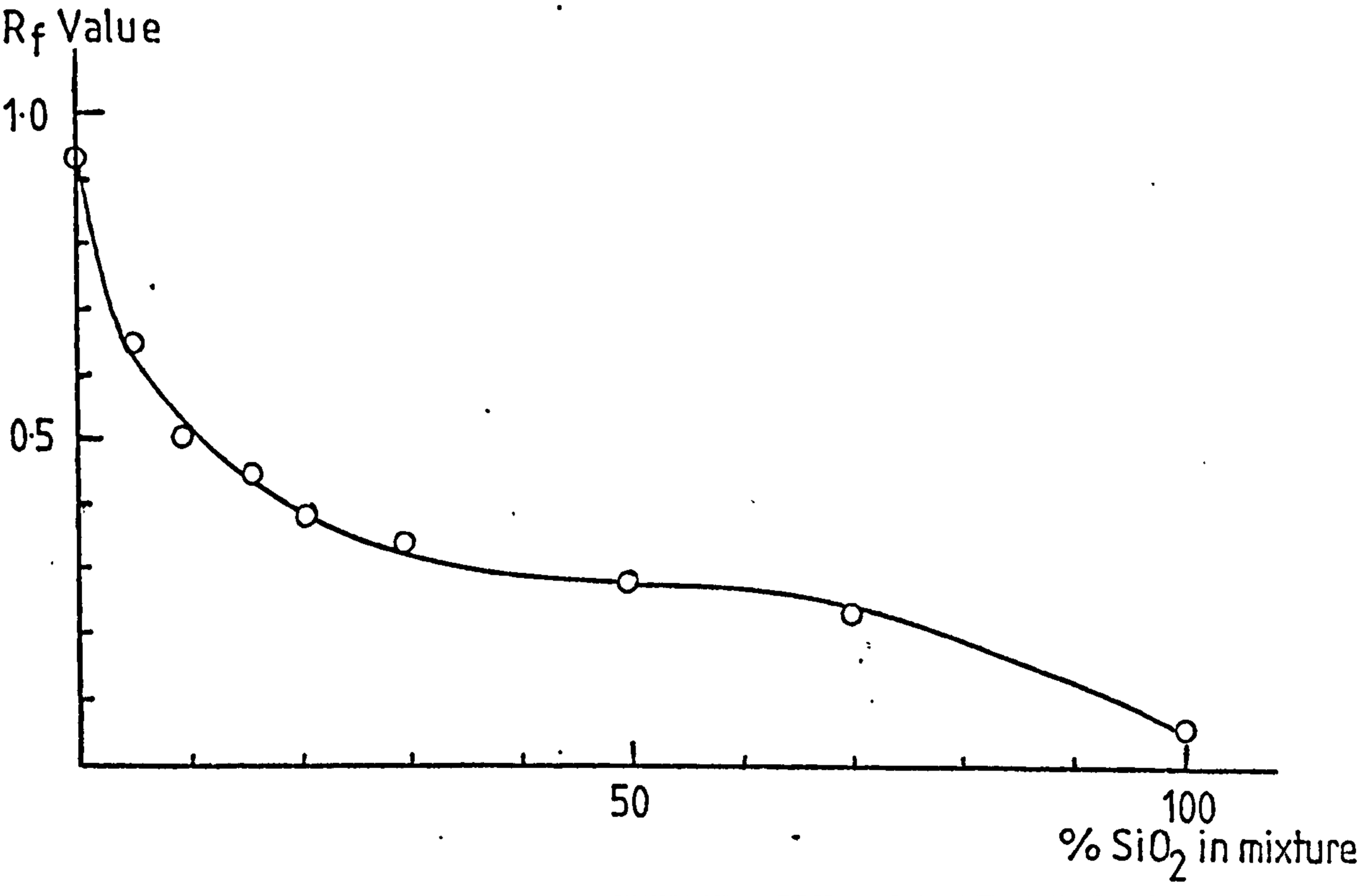

FIG. 7.13 R_f VALUES FOR METHYLENE BLUE ON MIXTURES OF ZEOLITE X AND SILICA AT pH = 13

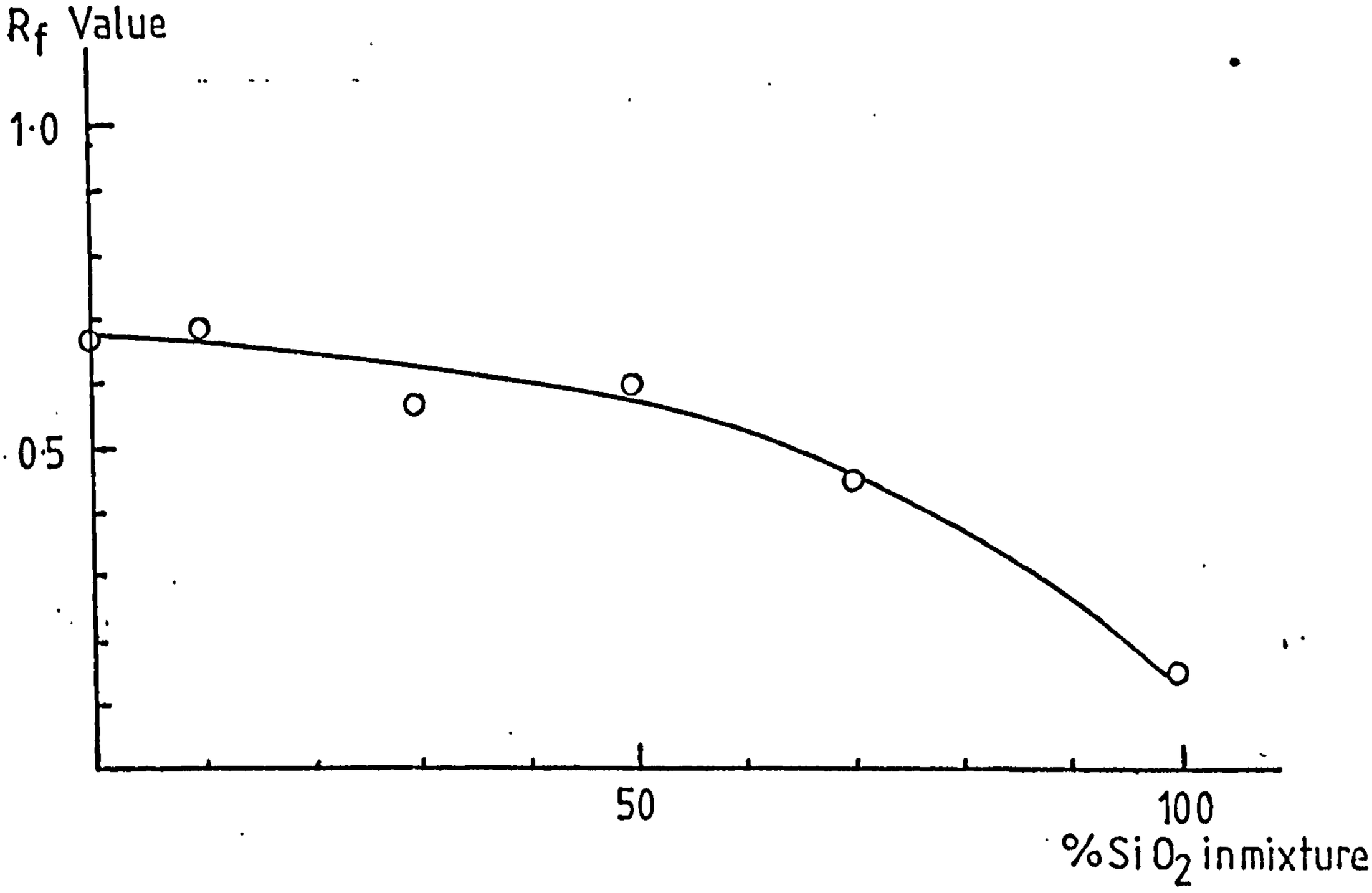

FIG. 7.14 R_f VALUES FOR METHYLENE BLUE ON MIXTURES OF ZEOLITE X AND P1

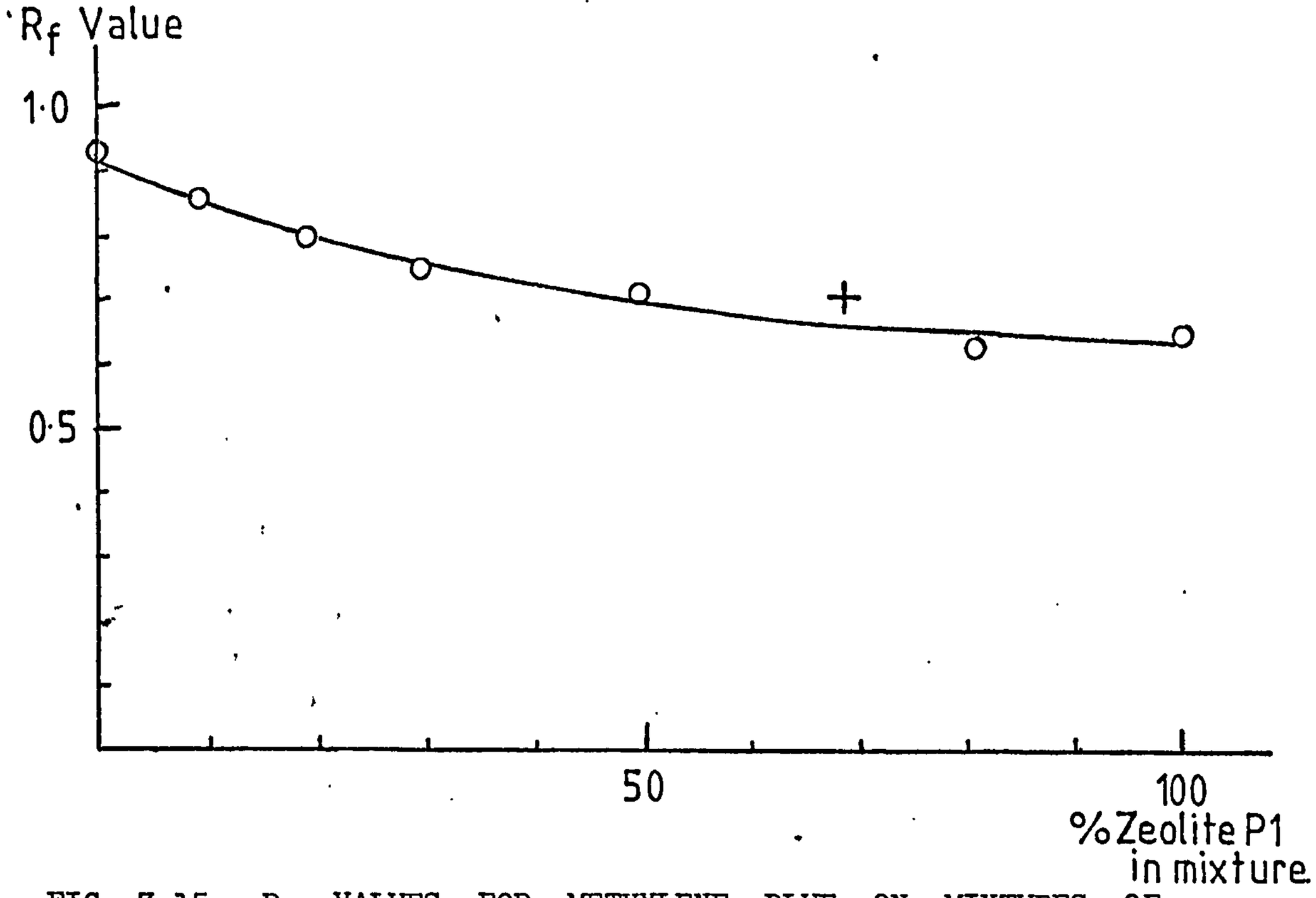

FIG. 7.15 R_f VALUES FOR METHYLENE BLUE ON MIXTURES OF ZEOLITE X AND AMORPHOUS ALUMINOSILICATE

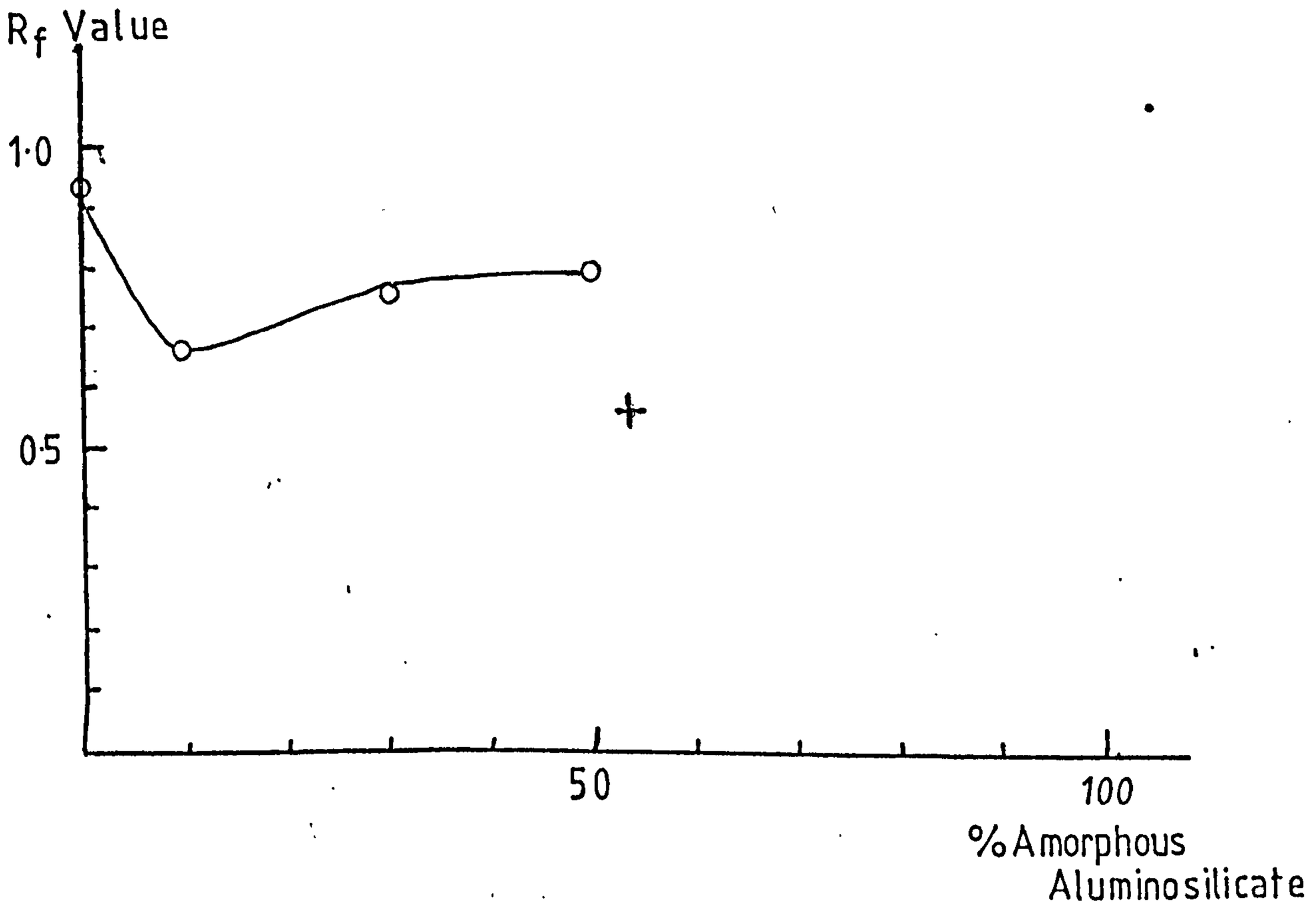

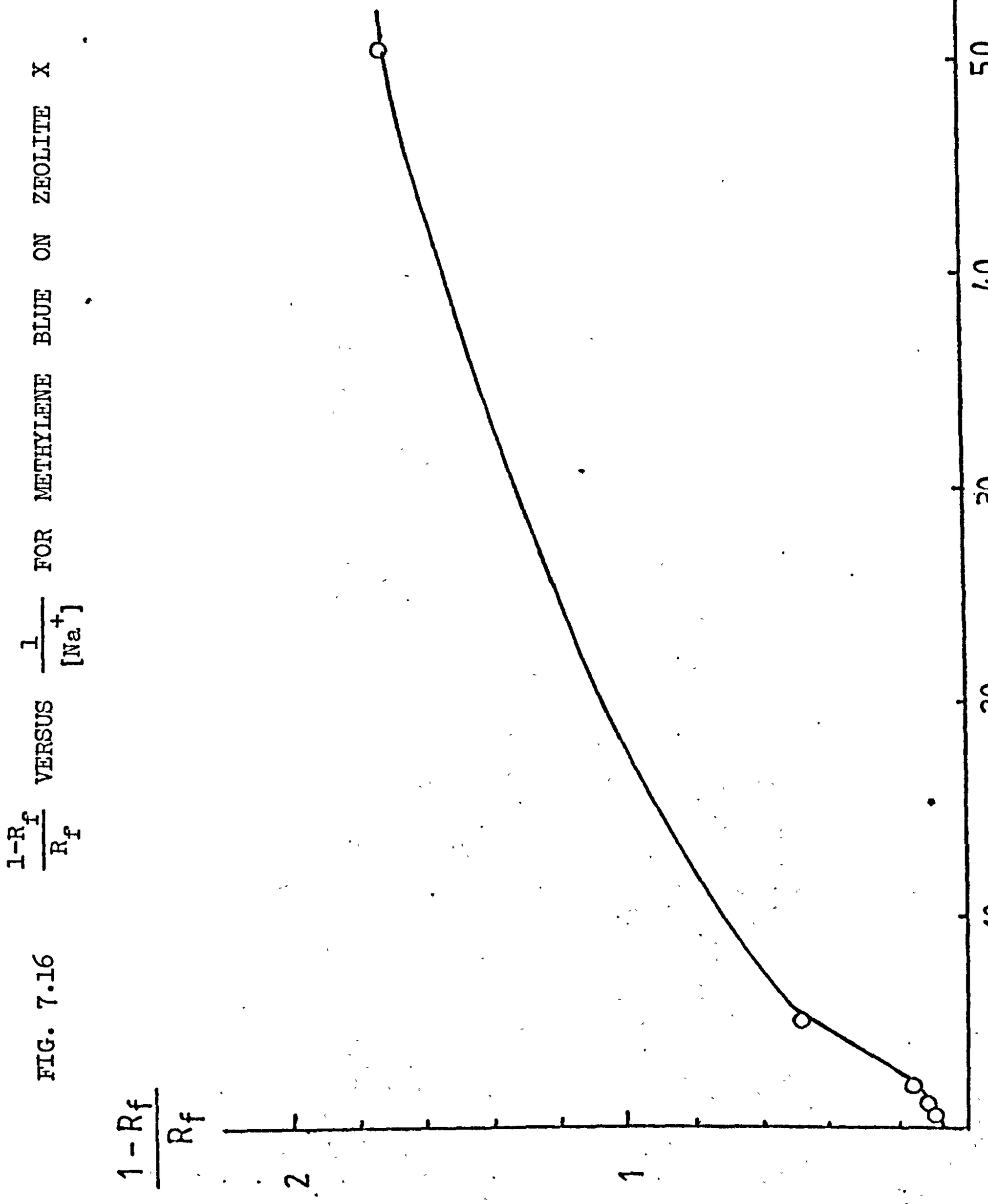

FIG. 7.16 - FOR METHYLENE BLUE ON ZEOLITE X

BIBLIOGRAPHY

1. A. Cronstedt, Akad. Hanal. Stockholm, 1756, 120, 18.

2. J.V. Smith, Mineralogical Society of America Special Paper No. 1, 1963, 281.

3. J.V. Smith, R. Rinaldi, Int. Mineral Soc. Mtg., (Berlin 1974).

4. R.L. Hay, Geological Society of America Special Paper No. 85, New York 1963, 338.

5. D.W. Breck, "Zeolite Molecular Sieves", John Wiley & Sons, 1974, p.207.

6. J.W. McBain, "The Sorption of Gases and Vapours by Solids", Routledge & Sons, London, 1932, Ch. 5.

7. R.M. Barrer, "Zeolites and Clay Minerals as Sorbents and Molecular Sieves", Academic Press Ltd., London, 1978.

8. R.M. Barrer, J. Soc. Chem. Ind., 1945, 64, 130.

9. R.M. Barrer, L. Belchetz, J. Soc. Chem. Ind., 1945, 64, 131.

10. R.M. Barrer, J. Soc. Chem. Ind., 1945, 64, 133.

11. D.W. Breck, W.G. Eversole, R.M. Milton, T.B. Reed, T.L. Thomas, J. Amer. Chem. Soc., 1956, 78, 5963.

12. P. Saha, Am. Mineralogist, 1961, 46, 858.

13. A.J. Regis, L.B. Sand, C. Calmon, M.E. Gilwood, J. Phys. Chem., 1960, 64, 1567.

14. R.M. Barrer, J. Chem. Soc., 1950, 2342.

15. D.W. Breck, J. Chem. Ed., 1964, 41, 678.

16. R.M. Barrer, M.B. Makki, Can. J. Chem., 1964, 42, 1481.

17. A.H. Keough, L.B. Sand, J. Amer. Chem. Soc., 1961, 83, 3536.

18. D.W. Breck, et al. J. Amer. Chem. Soc., 1956, 78, 5963.

19. D.W. Breck, ref. 5, p.570.

20. D.W. Breck, ref. 5, p.192.

21. R.C. Hansford, J.W. Ward, J. Catalysis 1969, 13, 316.

22. H. Otouma, Y. Arai, H. Ukihashi, Bull. Chem. Soc. Japan, 1969, 42, 2449.

23. M. Ihemoto, K. Toutsumi, H. Takahashi, Bull. Chem. Soc. Japan, 1972, 45, 1330.

24. U.S. Patent No. 3,702,866.

25. N.Y. Chen, R.L. Gorring, H.R. Ireland, J.R. Stein, Oil Gas J., 1977, 75, 165.

26. R.E. Grimm, Clay Mineralogy, McGraw-Hill, New York, 1970, 2nd Ed. Ch. 9.

27. I.D. Mikheikin, O.I. Brotikovskii, V.B. Kazanskii, Kinet. Catal. 1972, 13, 481.

28. D.W. Breck, E.M. Flanigen, S.C.I. Conference on molecular sieves, London 1967.

29. J. Lowenstein, Am. Mineral. 1954, 39, 92.

30. J. Selbin, R.B. Mason, J. Inorg. Nucl. Chem. 1961, 20, 222.

31. R.M. Barrer, J.W. Baynham, F.W. Bultitude, W.M. Meier, J. Chem. Soc., 1959, 195.

32. R.M. Barrer, D.J. Marshall, J. Chem. Soc., 1965, 6616 and 6621.

33. G.H. Kuhl, "Molecular Sieves", Soc. Chem. Ind., London, 1968, p.85.

34. G.H. Kuhl, "Molecular Sieve Zeolites", A.C.S. Monograph, 1971, p.63.

35. E.M. Flanigen, R.W. Grose, as ref. 34, p.76.

36. R.M. Barrer, M. Liquornik, J. Chem. Soc. Dalton, 1974, 2126.

37. R.M. Barrer, E.F. Freund, J. Chem. Soc. Dalton, 1974, 19, 2060.

38. J.V. Smith, as ref. 2.

39. K.F. Fischer, W.M. Meier, Fortschr Mineral 1965, 42, 50.

40. W.M. Meier, "Molecular Sieves", Soc. Chem. Ind., London, 1968, p.10.

41. D.W. Breck, "Molecular Sieve Zeolites", A.C.S. Monograph, 1971, p.20.

42. R.M. Barrer, Brit. Chem. Eng., 1959 (May), p.1.

43. U.S. Patent, 3,008,803.

44. U.S. Patent, 3,567,372.

45. E.M. Flanigen, "Molecular Sieves", A.C.S. Monograph, 1973, p.119.

46. U.S. Patent, 3,030,181.

47. U.S. Patent, 3,054,657.

48. R.H. Daniels, G.T. Kerr, L.D. Rollmann, J. Amer. Chem. Soc., 1978, 10, 3097.

49. W. Seiber, W.M. Meier, Helvetica Chimica Acta. 1974, 57, 1533.

50. G.W. Morey, E. Ingerson, J. Econ. Geol., 1937, 32, 607.

51. R.M. Barrer, U.K. Patent 548,905 and J. Soc. Chem. Ind., 1945, 64, 130.

52. R.M. Barrer, L. Belchetz, J. Soc. Chem. Ind. 1945, 64, 132.

53. R.M. Barrer, J. Chem. Soc., 1948, 2158.

54. R.M. Barrer, British Patent 574, 911.

55. R.M. Barrer, J. Chem. Soc., 1948, 127.

56. R.M. Barrer, D.W. Riley, J. Chem. Soc., 1948, 133.

57. U.S. Patent, 2,882,243.

58. U.S. Patents, 2,882,244 and 3,130,007.

59. C. Collela, R. Aiello, Ann. Chim (Rome) 1971, 61, 721.

60. F. Schwochow, H. Weber, G. Heinze, DOS 2,028,163 (1970) Bayer A.G.

61. D.W. Breck, ref. 5, Ch. 4.

62. D.W. Breck, E.M. Flanigen, "Molecular Sieves", Soc. Chem. Ind. London, 1968, p.47.

63. "Sintering and Catalysis" Edited by J. Kuyenski, Ch. 4 ref. 1.

64. United Kingdom Patent Specifications Nos. 1,082,131; 1,145,995, 1,171,462; 1,171,463.

65. F. Schwochow, G. Heinze, H. Weber, DOS 1,812,339 (1968) Bayer A.G.

66. R.M. Barrer, J. Chem. Soc. Dalton Trans. 1977, 10, 1020.

67. N.A. MacGilp, Ph.D. Thesis, University of Edinburgh, 1976.

68. E.F. Freund, J. Crystal. Growth 1976, 34, 11.

69. J.R. Goldsmith, J. Geol., 1953, 61, 439.

70. G.J. Kerr, J. Phys. Chem., 1968, 72, 1385.

71. R.M. Barrer, J.F. Cole, J. Chem. Soc. (A), 1970, 1516.

72. G.J. Kerr, J. Phys. Chem. 1966, 70, 1047.

73. S. Zhdanov, 'Molecular Sieves' A.C.S. Monograph 1970, p.19.

74. D.W. Breck, E.M. Flanigen, "Abstracts of Papers" 137th Meeting, A.C.S., Cleveland, 1960.

75. J. Ciric, J. Coll. Int. Sci., 1968, 28, 315.

76. S. Zhdanov, 'Molecular Sieves' Soc. Chem. Ind. London, 1968, p.62.

77. R. Aiello, R.M. Barrer, I.S. Kerr, 'Molecular Sieves' A.C.S. Monograph 1970, p.44.

78. R. Aiello, C. Colella, Sersale, 'Molecular Sieves' A.C.S. Monograph, 1970, p.57.

79. F.E. Schwochow, G.W. Heinze, 'Molecular Sieves' A.C.S. Monograph, 1970, p.102.

80. P.K. Migal, S.V. Nelyubov, Sb. Nauch. Statei Kishinev. Gos. Univ., Estesto Mat. Nauk, 1969, 105.

81. B.D. McNicol et al. 'Molecular Sieves' A.C.S. Monograph, 1973, p.152.

82. B.D. McNicol, et al. J. Phys. Chem., 1972, 76, 3388.

83. W.C. Beard, 'Molecular Sieves' A.C.S. Monograph 1973, p.162.

84. W. Meise, F.E. Schwochow, 'Molecular Sieves' A.C.S. Monograph 1973, p.152.

85. A. Culfaz, L.B. Sand, 'Molecular Sieves' A.C.S. Monograph 1973, p.140.

86. Y.V. Mirskii, V.V. Pirozhkov, Russ. J. Phys. Chem. 1970, 44, 1508.

87. C.L. Angell, W.H. Flank, 'Molecular Sieves', A.C.S. Monograph 1977, p.194.

88. A. Culfaz, P. Orbey, 'Molecular Sieves', A.C.S. Monograph 1977, p.708.

89. F. Polak, E. Cichocki, 'Molecular Sieves' A.C.S. Monograph 1970, p.209.

90. F. Polak, E. Stobiecka, Zesz. Nauk U.J. 1976, 21, 291.

91. F. Polak, E. Stobiecka, ref. 90, p.309.

92. F. Polak, E. Stobiecka, ref. 90, p.318.

93. M.A. Borowiak, J.M. Berak, Rocz. Chem. 1974, 48, 509.

94. H. Kacirek, H. Lechert, J. Phys. Chem. 1975, 79, 15.

95. H. Kacirek, H. Lechert, J. Phys. Chem. 1976, 80, 12.

96. H. Kacirek, H. Lechert, 'Molecular Sieves' A.C.S. Monograph 1977 p.244.

97. T.V. Whittam, British Patent 1,453,115.

98. F. Schwochow, G. Heinze, H. Weber, U.K. Patent, 1,346,683.

99. R.A. Cournoyer, W.L. Kranich, L.B. Sand, J. Phys. Chem., 1975, 79, 15.

100. Private communication.

101. G.R. Landolt, Analyt. Chem., 1971, 43, 4.

102. A.L. McClellan, H.F. Harnsberger, J. Coll. Int. Sci., 1967, 23, 577.

103. H.S. Lipson, H. Steeple, 'Interpretation of x-ray powder diffraction patterns', MacMillan, London, 1970.

104. Ref. 5, p.272

105. French Patent, 2,333,857.

106. D.E. O'Reilly, J. Chem. Phys., 1960, 32, 1007.

107. H. Haraguchi, S. Fujiwara, J. Phys. Chem., 1969, 73, 3467.

108. R.J. Moolenaar, J.C. Evans, L.D. McKeever, J. Phys. Chem., 1970, 74, 3629.

109. U.S. Patent 1,279,484.

110. U.S. Patent 2,962,355.

111. D.W. Breck, ref. 5, p.289.

112. U.S. Patent 3,010,789.

113. U.S. Patent 2,991,151.

114. A.S.T.M. Index Li_2SiO_3.

115. W. Wieker, D. Hoebbel, Z. Anorg. Chem., 1967, 366, 139.

116. C.W. Lentz, Inorg. Chem., 1964, 3, 574.

117. E. Thild, W. Weiker, H. Stade, Z. Anorg. Chem., 1965, 340, 261.

118. G. Engelhardt, Z. Chem., 1974, 14, 109.

119. G. Engelhardt, Z. Anorg. Chem. 1975, 418, 7.

120. H.C. Marsmann, Zeit. Naturforschung, 1974, 29B, 495.

121. R.K. Harris, R.H. Newman, Trans. Farad. Soc. 1977, 73, 1204.

122. R.O. Gould, B.M. Lowe, N.A. MacGilp, J. Chem. Soc. Chem. Comm., 1974, 693, 720.

123. R. Marc, Z. Physik. Chem. 1909, 67, 470.

124. T.V. Whittam, private communication.

125. D.K. De, J.L. Das Kanungo, S.K. Chakravarti, Ind. Chem., 1974, 12, 1187.

126. D.K. De, S.K. Chakravarti, S.K. Mukherjee, J. Ind. Chem. Soc., 1967, 44, no. 9.

127. D.K. De, S.K. Chakravarti, S.K. Mukherjee, J. Ind. Chem. Soc., 1969, 46, no. 12.

128. D.K. De, S.K. Chakravarti, S.K. Mukherjee, Ind. Jour. Chem., 1974, 12, 165.

129. C.H. Giles, S.N. Nakhwa, J. Appl. Chem. 1962, 12, 266.

130. M. Allingham, J.M. Cullen, C.H. Giles, S.K. Jain, J.S. Woods, J. Appl. Chem., 1958, 8, 106.

131. J.G. Gibb, P.D. Ritchie, J. Appl. Chem. 1954, 4, 473.

132. Raj.Singh, J.R.P. Gupta, B.B. Prasad, Proc. Indian Natl. Sci. Acad. Part A 1975, 41, 163.

133. J.J. Kipling, R.B. Wilson, J. Appl. Chem., 1960, 10, 109.

134. W.W. Ewing, F.W.J. Lui, J. Coll. Sci., 1953, 8, 204.

135. M.J. Schwuger, H.G. Smolka, Colloid & Polymer Sci. 1976, 254, 1062.

136. M. Susic, N. Pejranovic, B. Miocinovic, J. Inorg. Nucl. Chem. 1972, 34, 2349.

137. S.A. Levina, L.N. Malashevich, N.F. Ermolenko, Kolloidnyi Zhurnal 1963, 25, 567.

138. K. Bergmann, C.T. O'Konski, J. Phys. Chem. 1963, 67, 2169.

139. G.W. Ferrey, Quart. J. Pharm. 1943, 16, 208.

140. C.S. Brooks, Koll. Zeit. und Zeit Polym. 1964, 199, 31.

141. V. Grba, Z. Soltic, I.Bican. Chromatographia 1977, 10, 661.

APPENDIX 1

X.r.d. lines observed for reaction 2.22/5 h

Lines observed[a] (d/Å)	Kieselguhr (d/Å)	Zeolite A (d/Å)	Losod (d/Å)
12.26(75)		12.29(100)	
8.73(75)		8.71(69)	
7.62(25)			7.64(35)
7.13(75)		7.11(35)	
6.42(100)			6.42(83)
5.53(50)		5.51(25)	
4.77(25)			4.75(74)
4.12(100)		4.11(36)	
4.08(100)	4.08		
3.81(100)			3.91[c](54)
3.67(100)		3.741[b](53)	3.72[c](80)
3.41(5)		3.41(16)	
3.35(25)	3.35		
3.29(100)		3.29(47)	3.29[d](100)
2.99(100)		2.99(55)	
2.84(25)	2.86		
2.76(25)		2.75(12)	
2.69(5)		2.69(4)	
2.62(75)		2.63(22)	
2.59(25)			2.61(41)
2.12(25)			2.15(34)

[a] Numbers in brackets denote intensity. [b] Apparently absent. [c] Poor agreement. [d] This line also appears in zeolite A - however intensity is reported as 47% and in sample intensity of this line is 100% - additional intensity comes from Losod.

X.r.d. lines observed for reaction 2.23/5 h

Lines observed[a] (d/Å)	Kieselguhr (d/Å)	Zeolite A (d/Å)	Losod (d/Å)	Zeolite HS (d/Å)
12.35(75)		12.29(100)		
11.03(25)			11.106(10)	
8.75(50)		8.71(69)		
7.54(5)			7.64(35)	
7.13(50)		7.11(35)		
6.31(100)			6.43(83)	6.28(80)
5.49(25)		5.51(25)		
4.73(50)			4.75(74)	
4.36(5)				4.44(30)
4.35(5)				
4.26(5)	4.27		4.21(14)	
4.10(50)	4.10	4.11(36)		
4.03(25)			4.07(3)	
3.85(5)			3.91(54)	3.97
3.71(25)		3.71(53)	3.72(80)	
3.66(100)				3.63(100)
3.41(5)		3.42(16)		
3.35(50)	3.35			
3.28(25)			3.29(100)	
3.24(50)			3.22(10)	
3.15(5)	3.16			
2.98(50)		2.98(55)		
2.82(75)				2.81(80)
2.75(25)		2.75(12)	2.79(17)	
2.63(50)		2.63(22)	2.63(41)	
2.57(75)				2.56(80)
2.46(5)		2.46(4)		
2.43(5)			2.43(1)	
2.38(5)		2.37(3)		
2.10(75)				2.09(80)
1.75(50)				
1.74(25)				1.74(80)

[a] Numbers in brackets denote intensity.